THE UNIVERSITY *of* EDINBURGH

Carbon based nutrition of *Staphylococcus aureus* and the role of sugar phosphate transporters in intracellular bacterial replication

John Alexander Bell

PhD

The University of Edinburgh

College of Medicine and Veterinary Medicine

School of Biomedical Sciences

2013

Thesis Declaration

I, John Alexander Bell, hereby certify that this thesis, which is approximately 39,000 words in length, has been written by me, that it is the record of work carried out by me and that it has not been submitted in any previous application for higher degree or qualification.

Signature..... **Date** .....

List of Figures

List of Tables

Abbreviations

58K	Microtubule binding golgi associated protein
8325-4	Laboratory *S. aureus* strain
agr	Accessory gene regulator system (*S. aureus*)
ATP	Adenosine triphosphate
BHI	Brain Heart Infusion bacterial growth medium
C3	3-carbon containing sugars
C6	6-carbon containing sugars
CA-MRSA	Community associated - methicillin resistant *Staphylococcus aureus*
CFU/ml	Colony forming units per ml
DAPI	4',6-diamidino-2-phenylindole
F-1,6-BP	Fructose-1,6-bisphosphate
F-6-P	Fructose-6-phosphate
G-1-P	Glucose-1-phosphate
G-6-P	Glucose-6-phosphate
GCA	Golgicide A inhibitor
glpT	Glycerol phosphate permease gene
GlpT	Glycerol phosphate permease
Gol-1-P	Glycerol-1-phosphate
Gol-2-P	Glycerol-2-phosphate
Gol-3-P	Glycerol-3-phosphate
HHWm*	Hussain Hastings White phosphates modified staphylococcal minimal growth medium
hpt	Listerial hexose phosphate permease gene
Hpt	Listerial hexose phosphate permease
IGC	Intracellular growth coefficient
IgG	Immunoglobulin G antibody isotype
LAMP	Lysosomal associated membrane protein
LB	Luria-Bertani bacterial growth medium
LDH	Lactate dehydrogenase
MIC	Minimum inhibitory concentration
mM	Milimolar concentration
MOI	Multiplicity of infection
NADH	Nicotinamide adenine dinucleotide
OD_{600}	Optical density at 600nm absorbance
P14	*L. monocytogenes* clinical wild type isolate (Serovar 4b)
P14-A	*L.monocytogenes prfA** mutant of P14
PCR	Polymerase chain reaction
PrfA	Listerial transcription factor regulating virulence genes
PTS	Phosphotransferase system
Rab7	Ras- related GTP-binding protein
TCA cycle	Tricarboxylic acid cycle
uhpT	Hexose phosphate permease gene
UhpT	Hexose phosphate permease
USA300 LAC	CA-MRSA strain
WT	Wild type
Δ*agr*	*S. aureus* USA300 LAC *agr* deficient strain
Δ*glpT*	*S. aureus* USA300 LAC *glpT* gene deletion mutant
Δ*hpt*	*L.monocytogenes* P14-A *hpt* gene deletion mutant
Δ*uhpT*	*S. aureus* USA300 LAC *uhpT* gene deletion mutant
Δ*uhpT* Δ*glpT*	*S. aureus* USA300 LAC *uhpT,glpT* double gene deletion mutant

Acknowledgements

I am grateful to Jose Vazquez-Boland and Mariela Scortti for giving me the opportunity to engage in innovative scientific research at The University of Edinburgh.

I am indebted to Aitor des las Heras for providing supervision, support and experience in helping me develop my skills and scientific thinking. Rob Cain has also imparted valuable knowledge, helped sharpen my lab skills and has taught me the critical approach to research.

To Ross Fitzgerald and members of his research group, I appreciate their assistance and advice.

To family, friends and my partner who kept me going through rough times and never ceased to ‘spoil me with laughs’; I couldn’t have done it without you.

Abstract

The Gram positive bacterium *Staphylococcus aureus* is a major cause of human disease in industrialized countries. This multifaceted pathogen is adapted to thrive in a variety of host niches, including the intracellular compartment. *S. aureus* rapidly develops antibiotic resistance, and infections due to resistant clones pose a global threat, calling for novel therapeutic approaches. The ability to exploit host nutrients and efficiently metabolize these resources for growth is paramount for bacterial pathogenesis. Understanding the nutritional and metabolic determinants that underpin bacterial virulence may lead to the identification of novel antimicrobial targets. This thesis investigates carbon nutrition and metabolism of community-acquired methicillin resistant *S. aureus* (CA-MRSA) USA300, a widely spread, hyper virulent multi-resistant strain.

The dependence of *S. aureus* on carbohydrates for growth was considered first. *In vitro* studies in supplemented chemically defined media showed that sugar phosphates, such as hexose phosphates and glycerol phosphates, promote staphylococcal growth more efficiently than glucose. Deletion mutations were introduced to the two putative sugar phosphate transporter genes present in the *S. aureus* genome, *uhpT* (hexose phosphate permease) and *glpT* (glycerol phosphate permease). Phenotypic analysis of USA300 mutants and heterologous expression of the transporters in a previously described *Listeria monocytogenes* Δ*hpt* mutant, totally unable to use sugar phosphates, confirmed that *S. aureus* UhpT and GlpT have different substrate specificities. Whilst both can transport glycerol monophosphate (excluding glycerol-2-phosphate) and the organophosphate antibiotic fosfomycin, hexose monophosphates are only imported via UhpT. Since sugar phosphates are only present in significant amounts inside living tissues, particularly the intracellular compartment, the role of *S. aureus* UhpT and GlpT in pathogenesis was investigated by constructing a double deletion mutant. The Δ*uhpT*Δ*glpT* USA300 mutant was used to infect several relevant mammalian cell lines. In the conditions tested, it was found that UhpT and GlpT played no role in the intracellular replication of *S. aureus*. By contrast, *Listeria* exploits sugar phosphates from the host cell cytosol via the homologous hexose phosphate transporter, Hpt, to maximise replication and enhance virulence. The distinct requirement of sugar phosphates for intracellular

proliferation may reflect intrinsic differences in carbon nutrient dependence between the two organisms. It was confirmed that *S. aureus* can efficiently use other readily available carbon sources for growth, such as amino acids. In contrast, *Listeria* is strictly dependent upon sugar-derived carbon for growth, due to an incomplete tricarboxylic acid cycle. Whilst the double Δ*uhpT*Δ*glpT* mutation had no effect in *S. aureus*, expression of staphylococcal *uhpT* or *glpT* restored wild-type intracellular growth in the *L. monocytogenes* Δ*hpt* mutant. Taken together, the results illustrate that sugar phosphate permeases have a contextual role in bacterial virulence, where the background in which the genes are expressed determine their contribution as a virulence factor.

The intracellular dynamics of *S. aureus* was also explored using immunofluorescence microscopy. It was observed that, during epithelial cell infection, USA300 remains enclosed in a membrane-bound vacuole. This localisation may form a barrier to cytosolic sugar phosphates and potentially explain the absence of effect of the sugar phosphate permease deletions in intracellular proliferation. Preliminary characterisation of the *S. aureus* containing vacuole (SACV) was performed and it was found to be positive for the Rab7 late-endosomal GTPase and for trans-Golgi markers. This suggests that SACVs converge at the Golgi apparatus. Interestingly, a USA300 mutant lacking the global regulatory system *agr* was unable to proliferate intracellularly and did not acquire Rab7 or Golgi markers. Since the Δ*agr* mutation did not cause any impairment in carbon source dependent growth, these preliminary data suggest that modification of the SACV by Agr-regulated effectors may play a key role in modulating cellular processes that control staphylococcal intracellular survival and/or replication.

Evidence presented in this thesis provides a platform for further exploration of *S. aureus* host cell nutrient dependence and the mechanisms that drive replication.

Contents

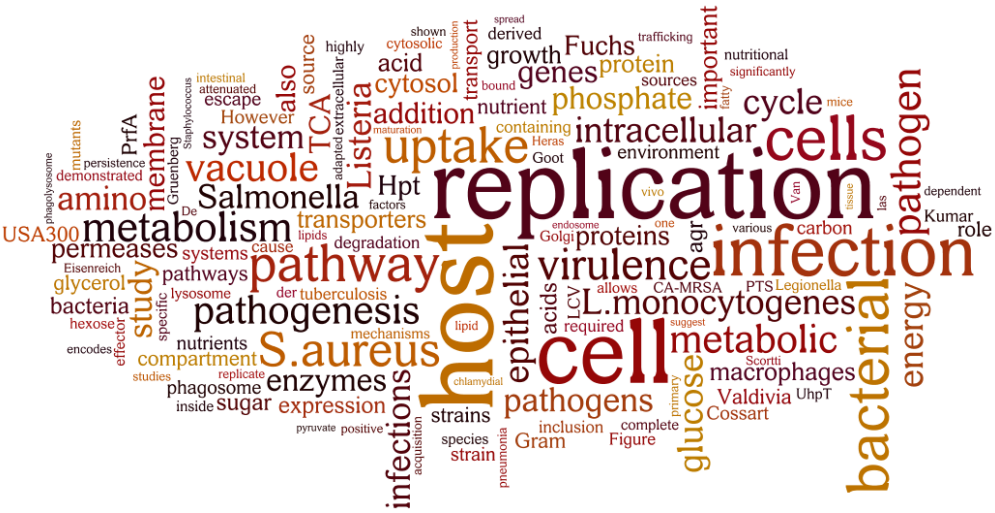

Chapter 1

Introduction

1.1 Host cell bacterial invasion

Pathogenic bacteria have evolved mechanisms to invade and colonise host cells (Cossart & Sansonetti 2004; Pizarro-Cerdá & Cossart 2006; Kumar & Valdivia 2009). Host cell niches provide refuge to pathogens from the hostile extracellular environment. It provides shelter from physical stress, shear stress, complement deposition, antibody labelling and exposure to effectors of the adaptive immune defence system (Hornef *et al.* 2002; Pizarro-Cerdá & Cossart 2006). Protection in this niche can also present bacteria with nutritional supplies for replication (Fuchs *et al.* 2012).

Professional phagocytes, such as macrophages, and non-professional phagocytes, for example epithelial cells, can engulf pathogens via phagocytosis (Rabinovitch 1995). In normally non-phagocytic cells, phagocytosis is actively induced by invasive bacteria by mediating specific protein interactions between host-pathogen membranes. These interactions initiate a molecular response by host cells and bacteria are ingested by endocytosis (Pizarro-Cerdá & Cossart 2006). *Staphylococcus aureus,* for example, induces this event primarily through expression of fibronectin binding proteins A and B (Sinha *et al.* 1999). These surface proteins anchor the extracellular matrix glycoprotein, fibronectin, which forms a bridge connecting to host cell α5β1 integrins. These staphylococcal MSCRAMMs (microbial surface components recognizing adhesion matrix molecules) are integral to efficient internalisation of *S. aureus* by epithelial cells (Dziewanowska *et al.* 1999). Upon internalisation, the majority of pathogens are immediately bound within a membraneous compartment, the phagosome (Pizarro-Cerdá & Cossart 2006; Flannagan *et al.* 2009).

The cellular endosomal pathway acts to traffic vesicles containing lipids, receptors and enzymes to various cell locations. Cell effector proteins are recruited to the endosomal membrane, such as Rab GTPases and phosphoinositides, which regulate protein sorting, trafficking and signalling of these compartments (Gruenberg & Van der Goot 2006). Endosomes

containing lipids and proteins may be trafficking to the trans-Golgi network where they are recycled back to the membrane. However, bacterial containing endosomes (phagosomes) are targeted for maturation and fusion with the cell lysosome to form a phagolysosome (Gruenberg & Van der Goot 2006). The phagolysosome creates a highly acidic, degradative environment in which proteases, nucleases, lipases and superoxide radicals are injected to destroy pathogens (Luzio *et al.* 2007). A summary of the phagosome degradation pathway is illustrated in Figure 1.1. Phagosome maturation is characterised by association of trafficking proteins belonging to the cellular endocytic pathway. Early endosome related proteins, such as EEA1 and Rab5 may integrate with the phagosome membrane to initiate the maturation process (Gruenberg & Van der Goot 2006). Late endosome proteins are recruited, such as Rab7 and cathepsins, which then potentiates the recruitment of lysosomal markers such as lysosomal associated membrane proteins (LAMPs) and V-ATPases which reduce the pH of the phagolysosomal compartment.

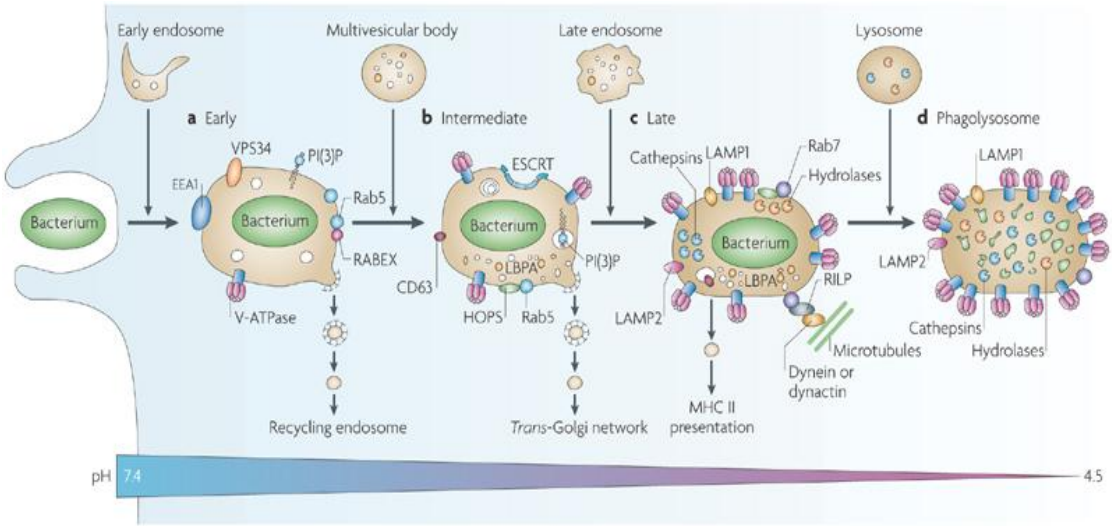

Figure 1.1. Phagosome trafficking to the phagolysosome. Host cell endocytic pathway proteins associate with the bacterial phagosome interface to mediate the transition to lysosome fusion (taken from Flannagan *et al.* 2009).

The risks associated with seeking shelter in the host cell endosome has led to evolutionary pressure to avoid obliteration via phagolysosome entrapment (Gruenberg & Van der Goot 2006). Bacteria have developed mechanisms to bypass this innate host cell defence against microbial invasion (Cossart & Sansonetti 2004; Gruenberg & Van der Goot 2006). Diverse adaptations have arisen among bacterial species which allow modification and manipulation of the phagosomal compartment (Sinai & Joiner 1997; Gruenberg & van der Goot 2006). Unique manipulation of host cell processes by bacterial effectors, allows pathogens to replicate and/or survive in a cellular compartment (Cossart & Sansonetti 2004; Kumar & Valdivia 2009; Saka & Valdivia 2010; Knodler & Steele-Mortimer 2003; Isberg *et al.* 2009). These strategies also allow acquisition of host derived nutrients which are produced by the metabolic and catabolic pathways of the cell (Fuchs *et al.* 2012). Bacteria can process these host cell nutrients via a number of endogenous metabolic pathways.

1.2 Bacterial metabolism

Bacteria may generate energy through 6 known endogenous metabolic pathways; glycolysis, pentose phosphate pathway (PPP), gluconeogenesis, the tricarboxylic acid cycle (TCA), glyoxylate shunt pathway and the Entner-Doudoroff pathway (ED). Figure 1.2 outlines the metabolic pathways, indicating the substrates and intermediates that are integral to their processes. The hexose sugar, glucose, is imported to the bacterial cell primarily via glucose specific phosphotransferase system (PTS) transporters, where import is coupled to phosphorylation, forming glucose-6-phosphate (Postma *et al.* 1993). Glucose-6-phosphate, and other phosphorylated hexoses, can also be directly imported via hexose phosphate transporters (UhpT) (Dietz 1976). Glucose-6-phosphate can be converted to pyruvate via the glycolysis pathway to generate ATP energy. Alternatively, glucose-6-phosphate can be converted to gluconate-6-phosphate where it may be metabolised through the pentose phosphate

pathway or the Entner-Doudoroff pathway. By converting glucose-6-phosphate into ribose phosphates, the PPP generates NADPH, which acts to combat oxidative stress. Ribose phosphates are used to fuel nucleotide synthesis. The interconversion of ribose phosphates synthesizes glyceraldehyde-3-phosphate and fructose-6-phosphate sugars which can feed the glycolysis pathway (Wammelink *et al.* 2008). ED pathway enzymes are encoded mainly by Gram negative bacteria and are essentially used to convert glucose-6-phosphate to glyceraldehyde-3-phosphate in alternate reactions to the energy expending phase of glycolysis (Fuchs *et al.* 2012; Eisenreich *et al.* 2010).

Glycerol uptake facilitator protein, GlpF, is a major intrinsic protein family transporter that non-specifically allows passive uptake of glycerol (Heller *et al.* 1980). Glycerol is phosphorylated inside the bacterial cell to glycerol-3-phosphate, which can also be scavenged directly by glycerol phosphate permeases (GlpT) (e.g. Lemieux *et al.* 2004). Glycerol phosphate is metabolised to glyceraldehyde-3-phosphate which drives glycolysis.

Energy can be generated from non-carbohydrate sources using the TCA cycle, the glyoxylate shunt pathway and gluconeogenesis pathway. The TCA cycle utilises organic intermediates such as pyruvate from carbohydrate metabolism and acetyl Co-A from lipid metabolism to generate energy as well as intermediates for amino acid synthesis. Lipid fatty acids can be degraded by β-oxidation to acetyl CoA, and can be converted into TCA cycle intermediates via the glyoxylate shunt pathway enzymes, which allows simple non-carbohydrate carbon sources to be used for energy (Bishai 2000). Oxaloacetate can also be converted to phosphoenolpyruvate (PEP) which can be metabolised by enzymes in the reverse flux to glycolysis to produce glucose-6-phosphate, known as gluconeogenesis.

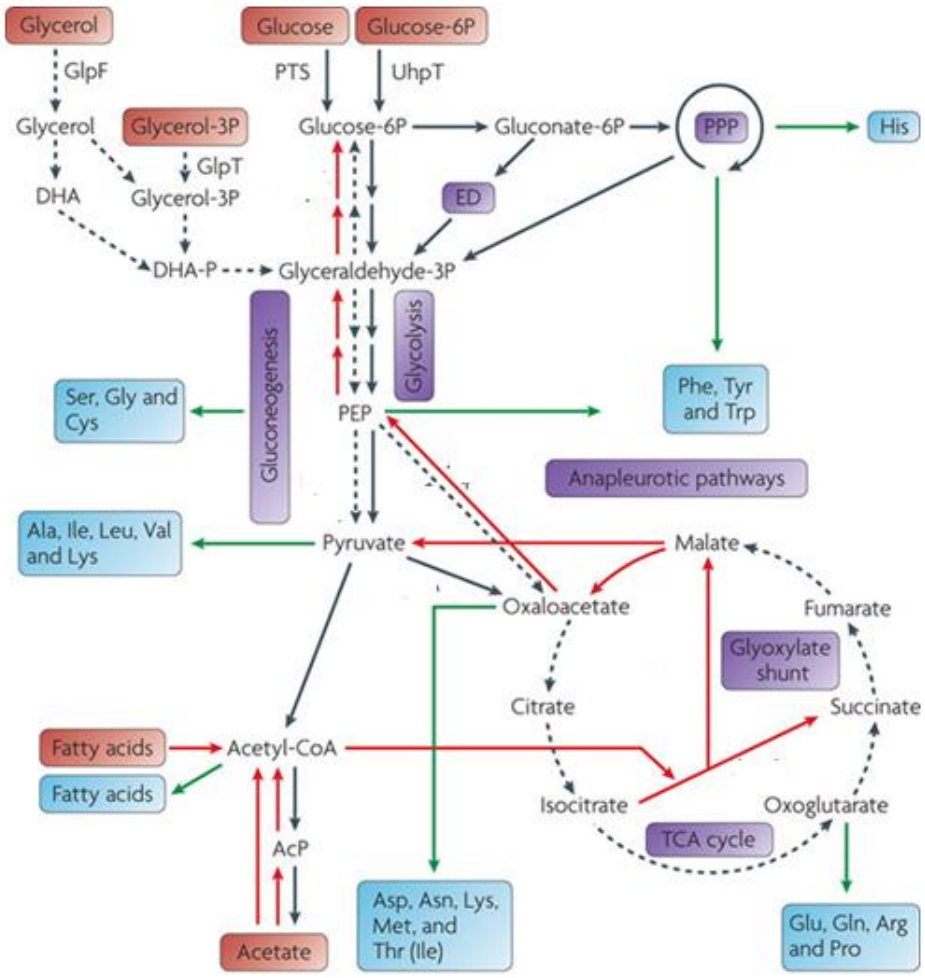

Figure 1.2. Bacterial metabolic pathways. Central metabolic pathways (purple boxes) are summarised by key interconversions. Substrates in red represent major carbon sources that can initiate pathway processes. Metabolic fluxes are shown for glucose / G-6-P (black arrows), glycerol, Gol-P and phosphoenolpyruvate (PEP) (dashed black arrows) and C3/C2 substrates (red arrows). Metabolites are highlighted in blue, showing fatty acids and amino acids (3 letter codes) that can be synthesized from pathway intermediates (green arrows). (Adapted from Eisenreich *et al.* 2010).

1.3 Bacterial metabolism in host cell pathogenesis

Bacterial pathogens can invade host cells using two strategies;

i) Remain inside a vacuole which can be modified to promote survival and replication.

ii) Escape the vacuole to the cell cytosol, where host nutrients are compartmentalised.

The adaptations used in host phagosome modification, mechanisms of nutrient acquisition and metabolic pathways employed are diverse among a range of invasive pathogens. Examples will be illustrated for both strategies of host cell colonisation by bacteria.

1.3.1 Intravacuolar replication

Pathogens that remain within a membrane bound compartment must devise ways to actively acquire the means to replicate. This results in a fine balance between vacuole modification/ host cell protein commandeering and host nutrient scavenging for growth.

1.3.1.1 *Salmonella enterica*

The Gram negative bacterium *Salmonella enterica* is one of the most common food-borne pathogens which penetrate the intestine epithelial cells to cause salmonellosis (Bowden *et al.* 2010). *Salmonella* containing vacuoles (SCVs) have been relatively well characterised. *Salmonella* can escape the degradation pathway to the lysosome through uncoupling of the late endosomal marker Rab7 GTPase from Rab7-interacting lysosomal protein (RILP) using a bacterial effector, SifA (Harrison *et al.* 2004). *S.* Typhimurium mutants defective in SifA fail to replicate in murine macrophages and are highly attenuated *in vivo* (Harrison *et al.* 2004). SCVs depend upon Rab7 recruitment for association with microtubule motor proteins (Méresse *et al.* 1999; Gruenberg & van der Goot 2006). This allows migration of SCVs to the perinuclear region of the cell where extensive

modification of the SCV membrane occurs at the endoplasmic reticulum (ER). The *Salmonella* vacuole is targeted to the trans-Golgi network by an effector protein, SseG, allowing the replication stage of infection to commense, which is thought to be the stage of nutrient acquisition (Salcedo & Holden 2003). Disruption of SCV-Golgi association significantly reduces replication in epithelial cells and macrophages (Salcedo & Holden 2003).

The nutritional requirements of vacuolar *Salmonella* replication appear to be diverse. Screening metabolic gene expression in mice infected with *Salmonella* revealed extensive redundancy in functional metabolic networks (Becker *et al.* 2006). The large majority of metabolic enzymes cited in this study were found to have a non-essential role in *S. enterica* pathogenesis. This may highlight the flexibility of nutrient acquisition in this species during *in vivo* infection. Partial attenuation in mutations for catabolic and transport genes revealed that host cell nucleosides, mannose, ribose and glycerol are likely to be used as nutrition sources during infection (Becker *et al.* 2006). A role for glucose uptake and metabolism in mouse macrophages has been shown for *S.* Typhimurium (Bowden *et al.* 2009). Deletion mutants in enzymes of the glycolytic pathway, in addition to deletion mutants in the major glucose and mannose PTS transporters, decreased replication in the host compartment. In addition, intracellular carbon nutrient analysis revealed that uptake and incorporation of host cell ^{13}C glucose into amino acids was high, citing glucose as the primary carbon source when available in epithelial cells (Götz *et al.* 2010) This would suggest that the SCV is not impervious to host sugars. A separate study failed to see an effect upon replication of S. Typhimurium in human intestinal epithelial cells when glucose PTS, mannose PTS and UhpT systems were all deleted in one strain (Götz & Goebel 2010). Seemingly, growth differences between PTS sugar uptake mutants in epithelial cells and macrophages suggest dependence on sugars may differ according to the host cell environment of *Salmonella*.

S. enterica may rely more heavily upon more alternative nutrient sources for replication. Deletion of high affinity glutamine uptake transporters, *glnH* and *glnQ* , did not significantly affect the virulence of S. Typhimurium in mice (Klose & Mekalanos 1997). However, in a glutamine auxotroph mutant, deletion of either *glnH* or *glnQ* caused significant attenuation of virulence in mice, suggesting that biosynthesis and/or host acquisition of glutamine is important in replication. Strong attenuation in mice was noted in mutants in which biosynthesis of aromatic amino acids is obstructed (Eisenreich *et al.* 2010). The TCA cycle has also shown to be an important energy pathway in *Salmonella* infection. Deletion mutants in TCA enzymes resulted in a marked reduction in replication of S. Typhimurium in epithelial cells and in murine infection models, showing a complete TCA cycle is essential for full virulence (Bowden *et al.* 2010; Yimga *et al.* 2006). By contrast, the gluconeogenesis pathway is not required for *Salmonella* virulence *in vivo* (Yimga *et al.* 2006). In Gram negative bacteria, the TCA cycle is subject to repression during growth in glucose (Nanchen *et al.* 2008). Evidence suggests therefore that metabolism of non-carbohydrate sources by the TCA cycle may provide the primary source of energy for salmonellosis, rather than carbohydrate metabolism pathways. Furthermore, studies have demonstrated that *Salmonella* strains auxotrophic for various amino acids are attenuated in mice and in macrophages (Appelberg 2006).

1.3.1.2 *Mycobacterium tuberculosis*

Mycobacterium tuberculosis is an obligate aerobe and the acid-fast Gram positive causative agent of the pulmonary disease tuberculosis (McKinney *et al.* 2000). Upon infection of lung macrophages, the *Mycobacterium* pathogen vacuole (MPV) acquires typical early endosomal markers such as Rab5 GTPase (Kumar & Valdivia 2009). However, the pathway to degradation is arrested at this early step as the pathogen excretes a mimic of phosphatidylinositol which inhibits the activity of PI(3)Kinase and interrupts the signalling cascade for phagosome maturation (Kumar &

Valdivia 2009). In addition, MPVs require association with Rab 14 GTPase for maintained arrest of phagosome maturation to lysosome fusion (Kyei *et al.* 2006). Rab14 is primarily involved in the recycling endosome pathway, which traffics lipids and receptors back to the cell membrane (Junutula *et al.* 2004). This interaction is also thought to deliver nutrients such as lipids to the MPV for replication (Kumar & Valdivia 2009).

Lipid metabolism is a primary feature of *M. tuberculosis* pathogenesis (Eisenreich *et al.* 2010). A study reports that lipid droplets, which are abundant inside macrophages, are a source of host acquired triacylglycerol for *M. tuberculosis* and are required for fatty acid metabolism contributing to virulence (Daniel *et al.* 2011). A transcriptome analysis of macrophages infected with *M. tuberculosis* revealed that enzymes required for fatty acid degradation, in addition to glyoxylate cycle enzymes, where the most common and highly up-regulated genes (Schnappinger *et al.* 2003). The persistence of *M. tuberculosis* in mice is dependent upon the action of isocitrate lyase (McKinney *et al.* 2000). Isocitrate lyase is an enzyme that catalyses the conversion of TCA cycle isocitrate to glyoxylate, a step which maintains the glyoxylate cycle that provides energy from fatty acid metabolism (Bishai 2000). A study demonstrated that *M. tuberculosis* mutants devoid in enzymes that catalyse β-oxidation of fatty acids to acetyl Co-A were also highly attenuated in virulence (Rengarajan *et al.* 2005). Uptake and catabolism of cholesterol may also play a role in *M. tuberculosis* survival and replication (Pandey & Sassetti 2008). This highlights the strict dependence of vacuole based *Mycobacterium* upon host derived lipids and fatty acid biosynthesis pathways for pathogenesis.

1.3.1.3 *Chlamydia* species

The intracellular metabolic requirements of obligate intravacuolar *Chlamydia* pathogens appear to be more particular. Pathogenic *Chlamydia* spp. most commonly cause infections of the genital epithelium *(*Yasir *et al.* 2011). The chlamydial inclusion, the membrane bound replicative vacuole

of *Chlamydia*, is totally independent of the endocytic pathway and does not fuse with components of the lysosome degradation pathway (Sinai & Joiner 1997; Kumar & Valdivia 2009). The chlamydial inclusion localises at the Golgi apparatus and lies on the exocytic pathway (Saka & Valdivia 2010). From this position, the inclusion subverts exocytic vesicle trafficking by recruiting various specific Rab GTPases and SNARE proteins, which function to allow vesicle fusion (Saka & Valdivia 2010). The secretory vesicles of the Golgi apparatus offer a healthy supply of sphingomyelin and cholesterol to the bacterial inclusion, which are crucial for bacterial replication (Heuer *et al.* 2009). It has also been shown that interference with Rab14 GTPase, significantly reduces the bacterial inclusion sphingolipid uptake and subsequently decreases the replication rate (Capmany *et al.* 2011). Membrane bound lipid droplets localise to and enter the chlamydial inclusion, which supply another host cell derived nutrient that contributes to bacterial metabolism and replication (Kumar *et al.* 2006).

Recently it has been investigated that *Chlamydia* actively implement fragmentation of the Golgi apparatus by cleaving the Golgi matrix protein golgin-84 (Heuer *et al.* 2009). Inhibition of this Golgi restructuring results in markedly reduced delivery of lipid containing vesicles to the inclusion, and causes severe attenuation of bacterial replication. This provides another example of intravacuolar pathogenesis that is heavily reliant upon host cell lipids for efficient replication. Intracellular chlamydial infection is obligate, meaning other than the specific human intracellular niche the pathogen cannot proliferate elsewhere. The reliance upon the host for nutrition can be reflected in the metabolic make-up of the *Chlamydia* genome. This pathogen lacks biosynthetic enzymes for *de novo* synthesis of vitamins, purines, pyramidines, most amino acids and ATP (Fuchs *et al.* 2012). This genus relies upon a multitude of transport systems for amino acid uptake, RNA uptake and ATP intake exclusively dependent upon the host cell supplies (Saka & Valdivia 2010). This would strongly suggest that the

chlamydial inclusion is permeable to a wide variety of host derived nutrients. Lack of a complete TCA cycle, and lack of a glucose uptake system (Fuchs *et al.* 2012) could propose that lipid sources from Golgi derived vesicles may be the most primary source of nutrition for this adapted pathogen.

1.3.1.4 *Legionella pneumophilla*

Legionella pneumophilla is the Gram negative etiological agent of Legionnaires disease, a form of pneumonia contracted by inhaling contaminated water droplets (Robinson & Roy 2006). Upon invasion of macrophages, the *Legionella* containing vacuole (LCV) becomes rapidly dissociated from markers of the early endocytic pathway (Sinai & Joiner 1997). The LCV recruits Sar1, Rab1 and Arf1 to the membrane surface, GTPases which are normally involved in vesicle trafficking from ER to Golgi (Kumar & Valdivia 2009). The fusion of ER derived vesicles leads to remodelling of the LCV. Deposition of ER derived components to the lumen of the LCV may deliver peptides and other nutrients to utilise as growth sources (Robinson & Roy 2006). The modification of the LCV, the manipulation of host cell proteins and the intravacuolar replication is dependent upon a type IV secretion system (Isberg *et al.* 2009). The Dot/Icm translocation complex operates to secrete effector protein substrates across the vacuole membrane into the host cytoplasm (Laguna *et al.* 2006). Without the function of this translocase system, cell pathway targeting ability is lost and the LCV is rapidly tagged for lysosome degradation (Laguna *et al.* 2006). In addition to deletion of specific *dot/icm* genes which impair replication, there are translocated effector substrates that are required for effective persistence (Isberg *et al.* 2009). An example is the SdhA protein which is essential for *Legionella* persistence, but does not influence LCV formation (Laguna *et al.* 2006). This study postulates that SdhA is important in preventing macrophage destruction, allowing prolonged replication inside the vacuole. *Legionella* represents a prime

example for highlighting the importance of vacuole modifying mechanisms that are required to promote effective replication.

Legionella lack a PTS transport system for carbohydrates and a permease for glucose phosphates (Fuchs *et al.* 2012) meaning alternative carbon sources are essential for pathogenesis. *Legionella* are unable to biosynthesize many amino acids, and the abundance of amino acid permeases, proteases and peptidases in addition to a possession of a complete TCA cycle would suggest that these raw materials are the most likely host derived source of growth (Fuchs *et al.* 2012). A study demonstrated that deletion of an amino acid importer, SLC1A5, completely inhibited *Legionella* replication (Wieland *et al.* 2005). In addition, this study also showed that restriction of the amino acid content of host cell media resulted in a substantial inhibition in intracellular LCV replication.

The adaptations of various pathogens for initiating and sustaining vacuole based survival and replication are extremely sophisticated. It would seem that the specific interplay between bacterial effectors and host cell vesicle pathways can support nutritional requirements for growth. Studies have shown that microinjection of intravacuolar pathogens directly into the cytosol of host cells does not lead to effective cytosolic replication in the majority of cases (Goetz *et al.* 2001). Similarly, *Salmonella* expressing *Listeria* pore forming toxin listeriolysin O was able to escape the SCV but was not able to replicate in the cytosol (Gentschev *et al.* 1995). Low percentages of *Salmonella* naturally escape the vacuole to the cytosol, where they are rapidly targeted for ubiquitination and degradation (Kumar & Valdivia 2009). *Salmonella enteric*a encodes genes to complete every available metabolic pathway for energy production in bacteria (Eisenreich *et al.* 2010). In theory, this pathogen should be equipped to capitalize upon nutrients made available in the cytosolic niche, but in practice this pathogen isn't adapted for life outside the *Salmonella* containing vacuole.

1.3.2 Cytosolic replication

In contrast to vacuole based pathogenesis, studies citing nutritional determinants of bacteria that escape the phagosome are less well established.

Enteroinvasive Escherichia coli (EIEC) and *Shigella flexineri* are Gram negative pathogens which cause gastroenteritis via infection of the intestinal epithelium (Van den Beld & Reubsaet 2012). Both of these species rapidly escape the phagosome to increase bacterial numbers inside the cytosolic compartment (Fuchs *et al.* 2012). These pathogens are extensively equipped for scavenging nutrients from the cytosol for growth. They possess a complete set of biosynthetic enzymes for all known bacterial metabolic pathways, in addition to copious transporters for uptake of diverse carbon and nitrogen sources for growth (Fuchs *et al.* 2012, Eisenreich *et al.* 2010). The metabolic adaptability of *E. coli* has been highlighted in the employment of separate metabolic pathways when distinct niches are colonised. During urinary tract infection, this pathogen utilises the gluconeogenic energy pathway and TCA cycle (Alteri *et al.* 2009), By contrast, the glycolysis and Entner-Doudoroff pathways are employed during intestinal epithelial infection (Chang *et al.* 2004). In one study, glucose was determined as the primary carbon source for EIEC strains infecting intestinal cells (Götz *et al.* 2010). However, this study found that when glucose uptake, in addition to hexose phosphate import was abolished, intracellular replication was unaffected suggesting redundant nutrient uptake mechanisms can maintain growth. During macrophage infection, *Shigella flexineri* down regulates expression of glucose and glucose-6-phosphate transport systems and glycolysis enzymes. Instead, carbon metabolism is maintained through uptake of C_3 substrates and the use of the gluconeogenesis pathway (Lucchini *et al.* 2005). Nutritional requisites of pathogens that are adapted to escape to the cytosol appear to be much broader. This may highlight the adaptation of these pathogens to ensure efficient replication in the host cytosol.

Listeria monocytogenes rapidly escapes the phagosome and replicates in the host cell cytosol (Scortti *et al.* 2007). *L. monocytogenes* represents a rare example of a Gram positive human pathogen with well established metabolic determinants of virulence.

1.4 *Listeria monocytogenes* pathogenesis and metabolism

Listeria monocytogenes is an important pathogen of humans. This Gram positive bacterium is ubiquitous in the environment, existing as a saprophyte (Farber & Peterkin 1991). It is transmitted by food contamination and consumption results in the penetration of the intestinal epithelia causing gastroenteritis (De las Heras *et al.* 2011). *L. monocytogenes* can cross the intestinal barrier to the blood, causing bacteraemia and also spread to the central nervous tissue accounting for 10% of community acquired bacterial meningitis (Vázquez-Boland *et al.* 2001). Dissemination of *Listeria*, can frequently lead to colonisation of the liver tissue causing abscesses and hepatitis (Scholing *et al.* 2007). Listeriosis is particularly important in high case fatality neonatal sepsis (De las Heras *et al.* 2011). Serotype 4b strains, for example P14, account for more than 50% of human infections (Vázquez-Boland *et al.* 2001). *Listeria monocytogenes* is still very much at the forefront of infectious diseases and gained notoriety in 2011 when an outbreak of listeriosis spread across America. Consumption of cantaloupe contaminated with *L. monocytogenes* resulted in 147 cases of listeriosis and 33 deaths. According to the Centres for Disease Control and Prevention, this was one of the worst epidemics of foodbourne illness based upon deaths since records began.

1.4.1 *L. monocytogenes* pathogenesis

The intracellular life cycle of *L. monocytogenes* is centred upon cytosolic replication for cell to cell spread. Figure 1.3 depicts a schematic of listerial pathogenesis and virulence factors that determine infection (adapted from Scortti *et al.* 2007).

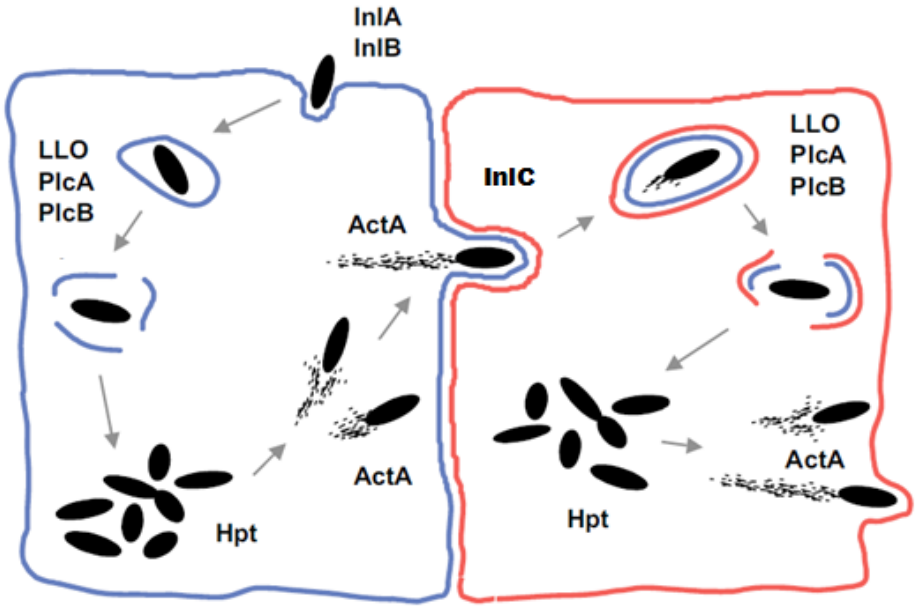

Figure 1.3. Invasive pathogenesis of *L. monocytogenes* depicting PrfA dependent virulence factors affecting the infection lifecycle (adapted from Scortti *et al.* 2007).

L. monocytogenes expresses surface attachment proteins internalin A and internalin B (InlA, InlB) which interact with host cell receptors E-cadherin and c-MET respectively, to induce phagocytosis (Pizarro-Cerdá & Cossart 2006). Upon engulfment, *Listeria* are trapped within a membrane bound compartment that transiently acquires cellular markers of the early endosome (Gruenberg & Van der Goot 2006). However, the maturation process of this vacuole is abruptly impeded almost immediately upon invasion. *Listeria* expresses the pore forming hemolysin toxin, listeriolysin O (LLO), which mediates rupture and escape from the phagosome (Scortti *et al.* 2007). In addition to LLO, phospholipase enzymes A and B (PlcA, PlcB) also contribute to degradation of the vacuole lipid bilayer (Vázquez-Boland *et al.* 2001). Rupture of the phagosome allows the bacteria to enter the cell cytosol where extensive replication occurs. An identified metabolic virulence factor involved in enhancing listerial replication is the hexose phosphate transporter, Hpt (Chico-Calero *et al.* 2002). Cytosolic *L. monocytogenes* can disseminate throughout the cytosol by expression of

the effector protein ActA (De las Heras *et al.* 2011). ActA polymerises cellular actin, in order to propel the bacteria arbitrarily towards the periphery of the cell (Cossart & Sansonetti 2004). Cell to cell spread is mediated by secreted internalin C (InlC), and *Listeria* protrude into neighbouring cells, which results in a double membrane surrounding the invading bacterium (De las Heras *et al.* 2011). The cell infection cycles to culminate in widespread tissue infection (Vázquez-Boland *et al.* 2001).

The virulence factors that are required for efficient pathogenesis, highlighted in Figure 1.2, all are under the control of central virulence regulator PrfA (Scortti *et al.* 2007). PrfA is a member of the Crp/ Fnr family of bacterial transcription factors and activates transcription of virulence genes by binding to a specific palindromic DNA sequence known as the PrfA box (De las Heras *et al.* 2011). In the extracellular environment, PrfA remains weakly active at basal levels of transcription but an allosteric change in conformation occurs when sensing host cells, switching on the activity (Scortti *et al.* 2007). The transition from the extracellular environment to the intracellular host, conferring 'activation' of PrfA initiates a positive feedback loop which up regulates the expression and translation of *prfA*, heightening virulence factor expression (De las Heras *et al.* 2011).

1.4.2 *L. monocytogenes* metabolism

Compared to other cytosolic based pathogens, nutrition driven replication of *L. monocytogenes* is better understood. *Listeria* relies upon glycolysis, gluconeogenesis, the pentose phosphate pathway and pyruvate metabolism for energy production (Eisenreich *et al.* 2010). *L. monocytogenes* is unable to grow on amino acids as a source of energy, due to an incomplete TCA cycle (Joseph & Goebel 2007). *Listeria* is strictly dependent upon the host cell cytosol for cysteine, thiamine, branched chain amino acids, biotin, riboflavin and lipoate due to lack of biosynthetic enzymes (Fuchs *et al.* 2012). The genome of *L. monocytogenes* contains 88

carbohydrate uptake permeases, mostly PTS dependent transporters, which is twice the number encoded by *E. coli* (Glaser *et al.* 2001). Given that *Listeria* infiltrates the rich intracellular milieu, but can only rely primarily upon carbohydrate metabolism pathways for energy, the large redundancy for carbohydrate importers reflects the adaptation of this species. A study demonstrated severely impaired *in vitro* growth in glucose of a *L. monocytogenes* strain mutated in the *ptsG* and *manXYZ* uptake systems (Stoll & Goebel 2010). However, replication of this strain was unaffected in the epithelial cytosol which can underpin the redundancy of sugar transport for replication energy. Indeed, studies highlight glycerol to be an important cellular sugar energy source during infection. Intracellular up regulation of genes specific for glycerol uptake and metabolism was observed in macrophages (Chatterjee *et al.* 2006). In addition, a study showing a mutant strain defective in the same glycerol metabolism genes had an impaired intracellular replication rate and a decreased ^{13}C incorporation into endogenous amino acids (Eylert *et al.* 2008). In addition, a mutant strain lacking glycerol-3-phosphate dehydrogenase, the enzyme responsible for conversion of glycerol monophosphate to glycerone phosphate in glycerol metabolism, was markedly impaired in the ability to replicate inside epithelial cells (Schauer *et al.* 2010). Oxaloacetate is an intermediate of the TCA cycle, and is an important precursor for amino acid biosynthesis in *L. monocytogenes* (Schär *et al.* 2010). The production of oxaloacetate is predominantly due to carboxylation of pyruvate during intracellular infection (Eisenreich *et al.* 2010). Deletion of the enzyme that catalyses this reaction leads to loss of intracellular replication and strongly attenuated virulence in mouse models of infection (Schär *et al.* 2010). Despite having multiplicity of sugar permeases glycerol uptake and metabolism, possibly through the gluconeogenesis pathway, is thought to be one of the main strategies of *Listeria* pathogenesis (Fuchs *et al.* 2012) .

A role for the hexose phosphate transporter, Hpt, has been determined for *Listeria* during infection and is a demonstration of the highly adapted

nature of *L. monocytogenes* to replicate inside the cytosolic compartment. A study noted knock down of PrfA conferred reduced ability to grow upon glucose-1-phosphate as the primary carbon source (Ripio *et al.* 1997). The *hpt* chromosomal locus was identified as a monocistron, under the control of the PrfA promoter (Chico-Calero *et al.* 2002). Mutational analysis showed that hexose phosphates such as glucose-1-phosphate and glucose-6-phosphate were exclusively transported into *L. monocytogenes* through the expressed Hpt, and promoted substantial growth *in vitro* (Chico-Calero *et al.* 2002). Intracellular infection studies in epithelial cells and macrophages found a marked reduction in replication in strains deficient in Hpt. This was also noted *in vivo*, as bacterial replication in mouse liver tissue was attenuated, suggesting that metabolic processing of glucose to glycogen provided favourable intermediates that promoted growth, accessible through Hpt (Chico-Calero *et al.* 2002). Import of sugar phosphates from the host cytosol therefore represents a significant source of nutrition for *Listeria* contributing to pathogenesis.

Figure 1.4 depicts the functionality of Hpt during intracellular infection. Hexose sugars, such as glucose, are phosphorylated inside the host cell compartment which uses ATP energy. Expression of the Hpt protein via activated PrfA allows import of these intermediates into the listerial cytoplasm. An energy expending step is therefore bypassed in *Listeria* metabolism. This strategy provides substrates that can be directly incorporated into the two carbohydrate energy pathways existing in *L. monocytogenes* (glycolysis and pentose phosphate pathway). This mechanism allows scavenging of important usable nutrients from the host cell. Substrates transported through the Hpt protein are considered to be preferable to glucose as an intracellular carbon source (Fuchs *et al.* 2012). Hpt is considered a determinant of *L. monocytogenes* pathogenesis.

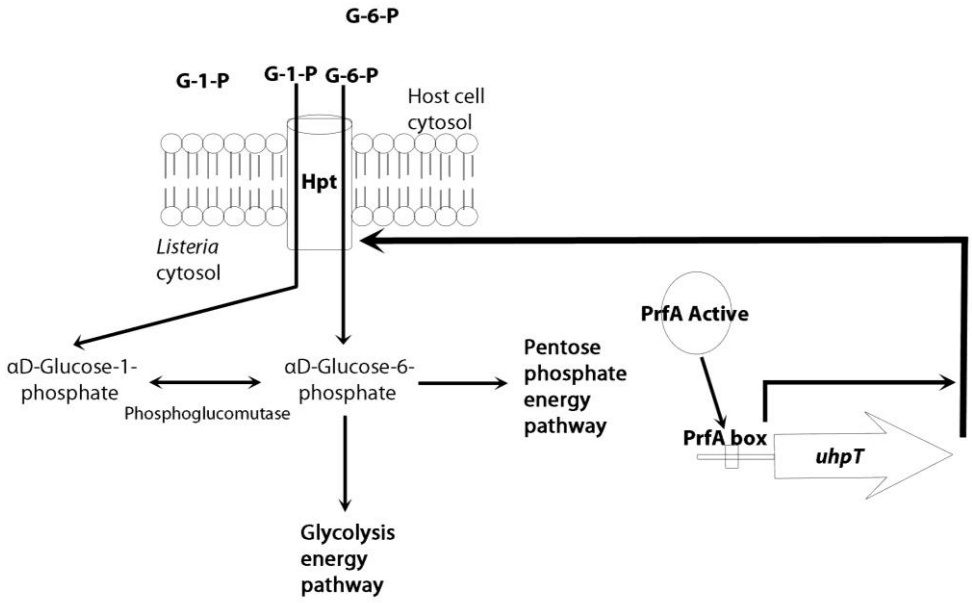

Figure 1.4. Role of listerial Hpt during intracellular infection.

1.5 Hpt related transporters

Putative hexose phosphate transporters are conserved among a host of important Gram positive and Gram negative bacterial species, including *Staphylococcus aureus* and *Escherichia coli* (Winkler 1973). Hexose phosphate transporters, most commonly termed UhpT, belong to the Major Facilitator Superfamily (MFS) of membrane transport systems (Law *et al.* 2008). These permeases are organophosphate: inorganophosphate antiporters which couple the export of inorganic phosphate to the uptake of sugar phosphates (Pao *et al.* 1998). Highly similar to UhpT is the glycerol phosphate permease, GlpT, which falls under the same family of transporters (Pao *et al.* 1998). The structure, topology and functionality of these two transport systems has been best characterised in *E. coli*, which encode both permeases (Lemieux *et al.* 2004; Lloyd & Kadner 1990; Island *et al.* 1992). These proteins consist of 12 transmembrane domains which insert into the bacterial membrane as a monomer in an inverted pyramid conformation (Lemieux *et al.* 2005). In *E. coli*, *uhpT* and *glpT* genes exist in distinct operons in which genes are linked to tightly regulate expression of these permeases through sensory inducible mechanisms (Merkel *et al.* 1995; Lemieux *et al.* 2004). For example, the *uhpABC* genes are situated directly upstream of *uhpT* (Island *et al.* 1992). UhpC acts as a membrane associated sensory receptor for the presence of extracellular glucose-6-phosphate. UhpA and UhpB act as the signal receiver and response regulator unit for UhpC, similar to a two-component system, which then induces expression of UhpT to uptake the sugar phosphates (Merkel *et al.* 1995; Island *et al.* 1992). Despite the characterisation of UhpT and GlpT in *E. coli*, the relevance of these transporters in bacterial infection is poorly established and generally not well researched. In fact, the role of the putative Hpt permease in *L. monocytogenes* infection is the only certifiable example of sugar phosphate permeases having a contributory role in intracellular replication and pathogenesis (Lucchini *et al.* 2005; Götz & Goebel 2010; Chico-Calero *et al.* 2002).

The UhpT and GlpT permeases provide the only entry route for the broad-spectrum organophosphate antibiotic fosfomycin (Popovic *et al.* 2010). In the current climate of increasing antimicrobial resistance, fosfomycin is being revisited as a therapeutic approach, due to the high conservation of UhpT and GlpT throughout important human pathogens (Falagas *et al.* 2008; Popovic *et al.* 2010). In *L. monocytogenes*, for example, PrfA controlled expression of Hpt during *in vivo* infection also confers significant susceptibility to fosfomycin treatment and causes severe attenuation of virulence (Scortti *et al.* 2006).

The therapeutic potential of sugar phosphate permeases makes these systems desirable for research. However, little work has gone into determining a nutritional function for these transporters and the importance that they may carry in bacterial replication during infection. In the case of *L. monocytogenes*, an important role has been established which may be echoed in other bacterial species. As another Gram positive bacterium and a clinically important pathogen of humans, *Staphylococcus aureus* is an appropriate species for investigation.

1.6 *Staphylococcus aureus* pathogenesis and metabolism

Staphylococcus aureus is the foremost cause of septicaemia, lower respiratory tract infections and skin and soft tissues infections (SSTIs) in industrialised countries (Deleo & Chambers 2009). This facultative pathogen is the second leading cause of pneumonia and endocarditis (States *et al.* 2007). Other more serious infections are commonly attributed to this pathogen, such as osteomyelitis, meningitis and toxic shock syndrome (TSS) (Hidron *et al.* 2009). Methicillin resistant *S. aureus* (MRSA) strains are the most frequently isolated bacterial pathogen in hospital acquired infections (World Health Organisation, 2013). In Europe alone, Healthcare Associated MRSA infections account for over 170,000 bacterial infections (almost half of all bacterial pathogen infections), causing 5400 deaths and over a million extra days of hospitalization each year (Gould *et al.* 2012). The ability of *S. aureus* to acquire multiple resistance to mainstream antibiotics and persist in the environment has made this pathogen notoriously difficult to treat (Rice 2006).

In the 21st century, community associated MRSA (CA-MRSA) strains have emerged and prevailed. These hyper-virulent lineages of *S. aureus* can cause serious and invasive infections to otherwise healthy people who have not had contact with the healthcare environment (Thurlow *et al.* 2012). A dramatic increase in CA-MRSA infections has occurred over the last 2 decades and in the USA these strains have reached unprecedented levels (Dukic *et al.* 2013). By far the most dominant CA-MRSA strain that has become endemic in hospitals around America and spread globally is USA300 (Nimmo 2012). USA300 has rapidly become as the most frequently isolated *S. aureus* isolate in infections, and now even represents 98% of all CA-MRSA SSTIs in America (Chadwick *et al.* 2013). In this strain of CA-MRSA resistance to β-lactams and ciprofloxacin is chromosomally encoded, while resistance to tetracycline, macrolides, lincosamides, streptogramin B and

mupirocin is encoded on native plasmids pUSA02 and pUSA03 (Diep *et al.* 2006).

1.6.1 *S. aureus* pathogenesis

USA300 has been recognised as the most virulent CA-MRSA strain in animal models of infection (Li *et al.* 2010; Thurlow *et al.* 2012). This lineage encodes an extensive repertoire of virulence factors that enhance pathogenesis (Watkins 2012). Panton-Valentine leukocidin is a pore forming toxin that has strong epidemiological association with CA-MRSA strains and causes cell lysis (Gordon & Lowy 2008). This secreted toxin has been demonstrated to cause necrotizing pneumonia in animal models and is strongly associated to necrotizing fasciitis (Lehman *et al.* 2010; Labandeira-Rey *et al.* 2007). Pulmonary infections by USA300, in particular, lead to aggressive and often fatal acute haemorrhagic necrotizing pneumonia in young and otherwise healthy people (Thurlow *et al.* 2012; Hidron *et al.* 2009).

USA300 uniquely harbours a DNA transposon known as the arginine catabolic mobile element (ACME) (Thurlow *et al.* 2012). ACME encodes the *arcA* gene, which translates to an arginine deaminase enzyme. Enzymatic modification of host cell L-arginine may deplete the substrate required for nitric oxide production, the antimicrobial toxic metabolite produced by host cells (David & Daum 2010). This mobile genetic element may enhance USA300 virulence by allowing colonisation of skin surfaces, proliferate in low oxygen conditions such as abscesses and evade host defences (Gordon & Lowy 2008). Studies have shown that absence of ACME significantly decreases the *in vivo* fitness of USA300 which suggests a key role in pathogenesis (David & Daum 2010).

Virulence of *S. aureus* is mainly controlled by the accessory gene regulator (*agr),* a global regulatory quorum sensing system. Figure 1.5 illustrates the mechanism of activation of the *agr* system.

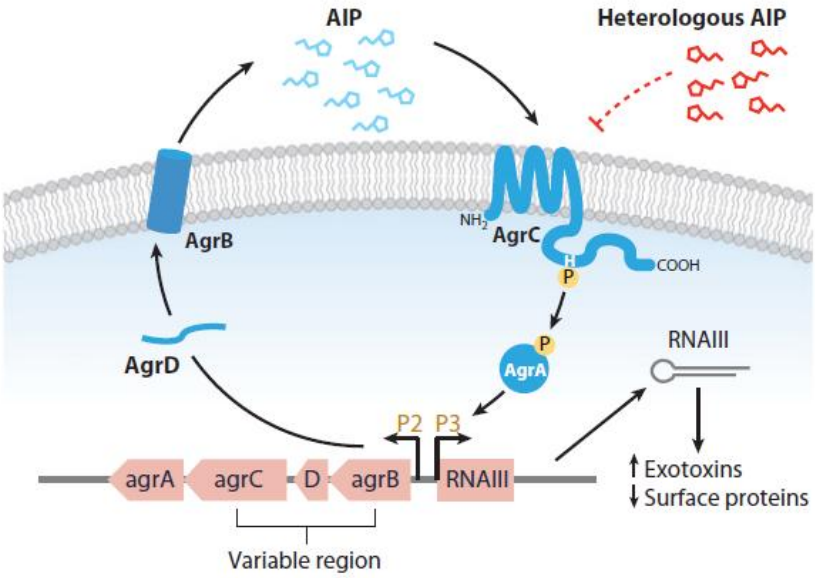

Figure 1.5. The *agr* quorum sensing system of *S. aureus* (taken from Novick & Geisinger 2008). AgrD gene encodes a peptide precursor which is cleaved and secreted by transport protein AgrB to form active auto-inducting peptide (AIP). This extracellular signalling molecule interacts with AgrC receptors of *S. aureus* cells in the locality to initiate upregulation of the *agr* operon.

The *agr* locus encodes genes which ensure autoactivation and quorum sensing to induce activation of neighbouring *S. aureus agr* systems. AgrD encodes a small peptide precursor, which is processed by a transmembrane endopeptidase, AgrB, and secreted. This active autoinducing peptide (AIP) is a signalling molecule that can interact with the extracellular domain of transmembrane protein AgrC. AgrC and AgrA act as a two component system in which AgrA is activated to bind to target DNA. AgrA binds specifically to two promoters, P2 which induces up regulation of this signalling system and P3 which activates transcription of the effector molecule, RNAIII. This RNA transcript acts to induce transcription of a host of virulence genes (Novick & Geisinger 2008). Up regulation of the *agr* system in USA300 induces production of cytolytic

toxins such as phenol soluble modulins, δ-toxin and α-toxin (Cheung *et al.* 2011). These toxins contribute significantly to the severity of mouse skin infections and also in the pathogenesis of necrotising pneumonia (Kobayashi *et al.* 2011, Wardenburg *et al.* 2007). In addition, the *agr* system is responsible for expression of peptidases, proteases and lipases which act to destroy cell tissue and promote dissemination (Gordon & Lowy 2008, Cheung *et al.* 2011). In USA300 in particular, the *agr* system is highly overactive, due to high frequency polymorphisms in the *agr* locus, which promotes overproduction of toxins and proteases, and is one of the primary reasons for extreme virulence (Thurlow *et al.* 2012). USA300 lacking *agr* are highly attenuated in the ability to cause sepsis, skin abscess and pneumonia in animal models of infection (Montgomery *et al.* 2010, Cheung *et al.* 2011, Kobayashi *et al.* 2011).

Staphylococcal infections are most commonly found in the extracellular environment, but research over recent years has determined that *S. aureus* can invade and survive in host cells (Sinha & Fraunholz 2010). Studies have demonstrated intracellular persistence in epithelial cells, endothelial cells, osteoblasts, fibroblasts and keratinocytes (Garzoni & Kelley 2009). Laboratory infection studies have determined that the intracellular fate of various strains of *S. aureus* is extremely variable and this pathogen does not categorically behave as an intravacuolar pathogen nor as a cytosolic bound pathogen (Sinha & Fraunholz 2010). For example, a study investigated the localisation of *S. aureus* RN6390 in tracheal epithelial cells (Jarry & Cheung 2006). In this study, infection of cystic fibrosis tracheal epithelial cells (CFT-1) by RN6390 was characterised by phagosomal escape and replication in the cytosol which caused destruction of cells. However, in the wild type tracheal cell line, the same strain remained within an endosome where it was degraded and cleared from lung cells. It is not clearly defined whether invasive *S. aureus* infections lead to replication or just persistence. *S. aureus* NOVEL invades bovine mammary epithelial cells, escapes the endosome and replicates efficiently (Bayles *et al.* 1998)

whereas *S. aureus* 6390 can invade enterocytes and survive for several days without replication or destruction of cells (Hess *et al.* 2003). Virulent *S. aureus* wild type strains invading endothelial cells neither persisted or replicated and were uniformly targeted to the lysosome for destruction (Schröder *et al.* 2006). Escape from the staphylococcal containing vacuole and bacterial persistence is largely thought to be dependent upon the expression of pore forming toxin α-hemolysin which is under the control of the *agr* virulence regulator system (Sinha & Fraunholz 2010). A study has demonstrated that *S. aureus* lacking α-hemolysin failed to escape from CFT-1 cell phagosomes and became entrapped in acidified lysosomal compartments (Jarry *et al.* 2008).

1.6.2 *S. aureus* metabolism

The metabolic profile of *S. aureus*, in addition to encoded nutrient uptake systems are well characterised (Fuchs *et al.* 2012). *S. aureus* encode enzymes which complete the glycolysis, gluconeogenic, PPP and TCA cycle metabolic pathways. This pathogen encodes a plethora of transport proteins including PTS specific hexose and ribose permeases, iron acquisition transporters, sugar phosphate permeases, glycerol facilitator and amino acid / peptide transporters. In addition, *S. aureus* encode all of the enzymes required for *de novo* biosynthesis of every amino acid (Nuxoll *et al.* 2012).

Despite extensive genome annotation of the membrane proteins that can act to acquire host cell nutrients, investigation of *S. aureus* metabolism during intracellular infection is a poorly studied topic. One publication analysed the transcriptome of *S. aureus* in human lung epithelial cells (Garzoni *et al*. 2007). The glycerol uptake facilitator GlpF and sugar phosphate permeases UhpT and GlpT were significantly up-regulated throughout infection. Intense up regulation of genes encoding transporters of nucleotides, oligopeptides, urea and iron was notable during infection. A transient shutdown of metabolic pathways was apparent, as genes

involved in the TCA cycle, pyruvate metabolism and oxidative phosphorylation were dramatically down regulated. This may highlight a role for the glycolytic pathway in infection metabolism of *S. aureus*, as glucose uptake is associated with strong repression of the TCA cycle (Seidl *et al.* 2009). Mutagenesis studies are crucial to investigate the nutritional and metabolic factors that influence invasive *S. aureus* pathogenesis.

1.7 Justification and Objectives

In the battle between antimicrobial treatment and bacterial resistance, bacteria are rapidly gaining the upper hand. The exhaustion of current antibiotic treatment calls for more rigorous research into bacterial pathogenesis to find alternative therapeutic targets. *S. aureus* is a prolific pathogen which has prevailed in the presence of antibiotic pressures. The evolution and ascendancy of hyper-virulent, multi-resistant lineages, such as CA-MRSA USA300, emphasises the need for novel strategies. Bacterial nutrition underpins the ability to multiply inside host cells. Host cell nutrient scavenging and bacterial metabolism is necessary for energy production needed to fuel virulence factor expression, promoting infection. Better understanding of bacterial mechanisms that drive replication and support pathogenesis can identify important factors that are required for virulence.

Work in this thesis aims to evaluate organic substrates that can be utilised by *S. aureus* USA300 to promote replication. Permease dependent sugar phosphate uptake contributes to replication of *L. monocytogenes* in the intracellular compartment. The significance of sugar phosphate acquisition has not been explored in *S. aureus.* The major objectives addressed in this thesis were;

1. Investigate the ability of *S. aureus* strains to grow on sole carbon nutrient sources which are present inside the cellular compartment, including sugar phosphates.
2. Identify candidate sugar phosphate transport proteins in *S. aureus* USA300 for targeted mutagenesis in order to abolish function and characterise substrate specificity.
3. Complement *hpt* deficient *L. monocytogenes* with staphylococcal sugar phosphate permeases for further substrate analysis and functionality testing relative to the listerial hexose phosphate permease.

4. Standardise and characterise a reproducible model of mammalian epithelial cell infection by *S. aureus* USA300 to measure intracellular replication.
5. Analyse the intracellular replicative ability of permease deficient *S. aureus* USA300 in order to determine the role of sugar phosphate transporters in host cell pathogenesis.
6. Explore the host cell dynamics that predispose *S. aureus* USA300 replication. Direction can be given to research to uncover mechanisms that support staphylococcal growth through host cell interactions with the replication niche.

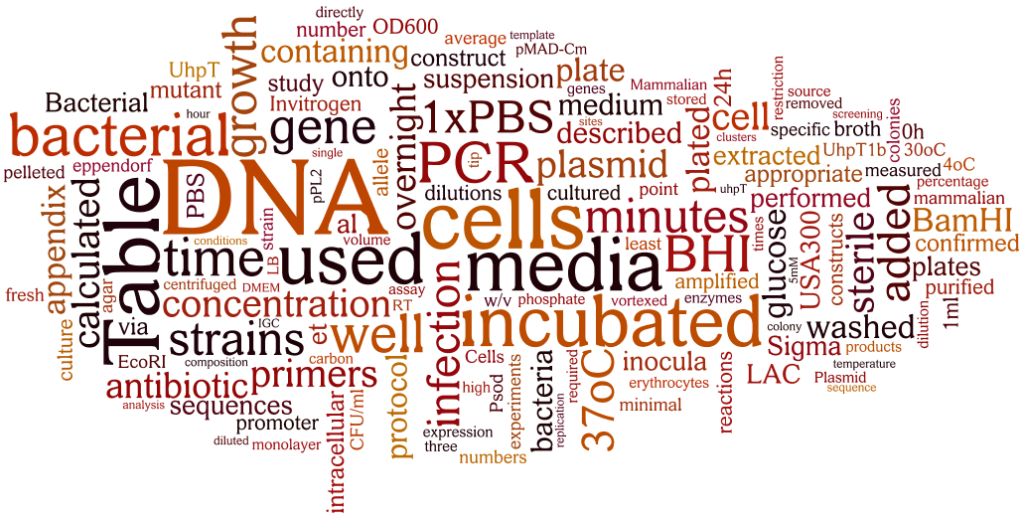

Chapter 2

Materials and methods

2.1 Bacterial strains, plasmids and oligonucleotides

Bacterial strains produced and used in this study are described in the appendix Table A1. Plasmids employed and constructed in this thesis are described in appendix Table A2. Oligonucleotide primers designed and used in this research are illustrated in appendix Table A3. Bacterial strains and plasmids were constructed and handled in accordance with the genetically modified organisms (GMO) regulations of The University of Edinburgh.

2.2 Bacterial culture and antibiotics

E. coli strains were routinely cultured in Luria-Bertani (LB) broth. *L. monocytogenes* and *S. aureus* strains were regularly cultured in Brain Heart Infusion (BHI) broth. Liquid cultures were grown at 37^{o}C (unless otherwise stated) in a shaking incubator at 200rpm. *E. coli* strains were plated on LB agar medium (1.6%(w/v) AgarB (MP Biomedicals) / LB medium). *L. monocytogenes* and *S. aureus* strains were plated on BHI agar medium (1.6%(w/v) AgarB (MP Biomedicals) / BHI medium). Bacterial plates were incubated overnight at 37^{o}C (unless specifically stated). The composition of BHI and LB medium are listed in appendix Table A4 and A5 respectively.

Antibiotics were used to select for plasmid constructs. Table 2.1 describes the antibiotic concentrations used when selecting strain dependent plasmid constructs.

Table 2.1. Plasmid and strain specific antibiotic selection.

Bacterial strains	Plasmid harboured	Antibiotic	Concentration (μg/ml)
E. coli	pTOPO / pCRBLUNT	Kanamycin	50
	pPL2	Chloramphenicol	15
	pMAD-Cm	Chloramphenicol	15
		Erythromycin	250
L. monocytogenes	pPL2	Chloramphenicol	7.5
S. aureus RN4220	pMAD-Cm	Erythromycin	10
S. aureus USA300 LAC	pMAD-Cm	Chloramphenicol	10

2.3 Molecular techniques

2.3.1 DNA extraction

Genomic DNA was extracted from bacteria using the GenElute Bacterial Genomic DNA kit (Sigma). Bacterial DNA was extracted according to the manufacturers' protocol. Plasmid DNA was extracted using the QIAprep Spin Miniprep kit (Qiagen) according to the manufacturers' protocol. In the initial re-suspension of bacterial pellets, *S. aureus* strains required the addition of 5µl (5mg/ml) lysostaphin (Ambi) to the kit buffer solution. The staphylococcal re-suspension was incubated at 37^{o}C for at least 30 minutes to allow the lysostaphin to degrade the cell wall, before continuing with the DNA extraction processes. DNA quality and quantity was assessed using a nanodrop machine. For plasmid transformation, If DNA quantity was less than 100ng/µl, the concentration was increased by using a speed vacuum.

Colony PCR screening of *E. coli* and *L. monocytogenes* required rapid DNA extraction. Single bacterial colonies were collected onto the end of a sterile pipette tip, streaked onto a fresh agar plate and the same tip used to re-suspend the remaining biomass into 50µl sterile pure water (Sigma) in a 1.5ml eppendorf tube. The suspension was boiled at 100^{o}C for 10 minutes in a eppendorf heat block. The lysate was briefly vortexed and 3µl used as template DNA for PCR reactions.

A technique was developed in this study for faster extraction of staphylococcal DNA for colony PCR screening. Staphylococcal colonies were collected onto the end of a sterile pipette tip, streaked onto a fresh agar plate and the same tip used to re-suspend the remaining biomass in 200µl Instagene Matrix Beads (Biorad) containing 5 µl lysostaphin in a 1.5ml eppendorf tube. The eppendorf was vortexed for 20 seconds to physically weaken the cell wall. The suspension was incubated at 56^{o}C for 20 minutes, vortexed for another 20 seconds and then incubated at 100^{o}C for 10 minutes. The matrix beads were pelleted using a table top centrifuge

(8000rpm, 5min) and 3 µl of the suspension was used as template DNA for PCR reactions.

2.3.2 DNA digestion and ligation

Plasmid DNA was digested using restriction endonuclease enzymes (New England Biolabs). High fidelity enzymes were used wherever possible. The recommended optimal conditions for reactions were followed. Plasmid constructs were created through ligation of open ended sequences. This was performed using T4 DNA Ligase (Promega) following the recommended protocol and provided reagents.

2.3.3 Polymerase chain reactions (PCR)

For routine PCR screening reactions, DNA was amplified using Taq DNA Polymerase (Biotools). Reaction compositions for purified template DNA and lysate DNA are described in Table 2.2A and 2.2B respectively. Thermocycling of Taq Polymerase reactions are shown in Table 2.2C.

Table 2.2A. Quantified DNA PCR Reactions

Component	Volume (µl)
Pure water (Sigma)	40
Taq Polymerase 5U/µl (Biotools)	1
5x phusion buffer (Biotools)	5
dNTPs 10mM each (Biotools)	1
Forward primer 10mM	1
Reverse primer 10mM	1
Template DNA 50-100ng/µl	1
	50

Table 2.2B. Lysate (Colony PCR) Rections

Component	Volume (µl)
Pure water (Sigma)	38
Taq Polymerase 5U/µl (Biotools)	1
10x Reaction Buffer (Biotools)	5
dNTPs 10mM each (Biotools)	1
Forward primer 10mM	1
Reverse primer 10mM	1
Lysate	3
	50

Table 2.2C. Taq PCR Thermocycling

Stage	Temperature (^{o}C)	Time	
Initial denaturation	95	5 minutes	
Denaturation	95	30 seconds	30 Cycles
Primer annealing	55-60	30 seconds	
Extension	72	1 minute per kilobase of DNA product	
Extension	72	10 minutes	
Storage	4	Hold	

*Primer annealing temperature is equivalent for all primers in this study.

High fidelity amplification of sugar phosphate transporter genes by proof reading Phusion Polymerase was performed for gene complementation. Table 2.3A lists the composition of high fidelity reactions and Table 2.3B shows the relevant thermocycling protocol.

Table 2.3A. Quantified DNA Phusion PCR Reactions

Component	Volume (µl)
Pure water (Sigma)	32.5
Phusion Polymerase 2U/µl (New England Biolabs)	0.5
5x phusion buffer (New England Biolabs)	10
dNTPs 10mM each (Biotools)	1
Forward primer 10mM	2.5
Reverse primer 10mM	2.5
Template DNA 50-100ng/µl	1
	50

Table 2.3B. Phusion PCR Thermocycling

Stage	Temperature (^{o}C)	Time	
Initial denaturation	98	30 seconds	
Denaturation	98	10 seconds	30 Cycles
Primer annealing	55-60	30 seconds	
Extension	72	30 seconds per kilobase of DNA product	
Extension	72	10 minutes	
Storage	4	Hold	

2.3.4 Gel electrophoresis

DNA products were loaded to a 1% (w/v) agarose TAE (Sigma) gel including a 1.5kb PLUS DNA ladder (Invitrogen). DNA was allowed to migrate at 200V for 25 minutes. Gels were added to a TAE vessel containing small amounts of ethidium bromide for 10-15 minutes to allow DNA staining. DNA was illuminated under ultraviolet light. Specific DNA products were isolated and extracted from the gel or directly from a PCR reaction mixture by using Illustra GFX PCR DNA and gel band purification kit (GE Healthcare).

2.3.5 Sequencing

DNA products were prepared for sequencing in accordance with the Sanger Institute guidelines. Sequencing of DNA fragments was completed by Sanger Sequencing Institute, University of Edinburgh. Sequences were analysed and aligned using ApE Plasmid Editor Software.

2.3.6 *S. aureus* USA300 LAC mutagenesis

Gene deletion mutations were constructed in *S. aureus* USA300 LAC in accordance with an established protocol (Fitzgerald, 2007). Figure 2.1 outlines the protocol via schematics, and uses the *uhpT* gene as an example.

Figure 2.1A illustrates the method used to construct and introduce a plasmid into USA300 LAC suitable for allele replacement of target transporter genes. Sequences flanking the target gene were amplified in-frame by PCR, using primer pairs UhpT1b_EcoRI – UhpT2 and UhpT3 – UhpT4b_BamHI (described in appendix Table A3). Primers UhpT2 and UhpT3 were designed with complementary sequences to facilitate overlapping PCR amplification. The purified PCR products were used as template DNA (in equal concentrations ~100ng) to perform overlapping PCR using UhpT1b_EcoRI and UhpT4b_BamHI as the forward and reverse primers respectively. This generated a mutant allele which was cloned into pTOPO/pCRBlunt (Invitrogen) for high copy replication. The fragment was sequenced using primers M13 Forward and M13 Reverse, described in appendix Table A3. The mutant allele fragment was digested with restriction enzymes EcoRI and BamHI for 3h at 37^{O}C, purified and ligated into shuttle vector pMAD-Cm, to create the construct pMAD-Cm UhpT. Recombinant allele pMAD-Cm constructs are illustrated in appendix Figure A4. The purified construct was transformed into *E. coli* and plated on LB – erythromycin for 24h at 37^{O}C. Positive colonies were selected using colony PCR to identify the mutant allele via UhpT1b_EcoRI-UhpT4b_BamHI amplification. In addition, the fragment was confirmed by sequencing using

UhpT1b_EcoRI and UhpT 4b_BamHI primers. The construct was purified from *E. coli* and transformed into *S. aureus* RN4220 strain via electroporation (Lee 1995). Transformed RN4220 was plated on BHI-erythromycin and incubated at 30^{o}C (the permissive temperature for pMAD replication) for at least 24h. Colonies harbouring the plasmid construct were confirmed as previously described. Purified constructs were transformed into USA300 LAC via electroporation and plated on BHI-chloramphenicol. Plates were incubated for at least 24h at 30^{o}C and constructs were confirmed by PCR and sequencing.

Figure 2.1B outlines the steps implemented to induce homologous recombination of pMAD-Cm UhpT in USA300 LAC. *S. aureus* USA300 LAC containing pMAD-Cm UhpT was cultured in BHI broth + chloramphenicol (30^{o}C, 200rpm). Serial dilutions were plated on BHI – chloramphenicol and incubated at 45^{o}C for 24 - 48h. At this temperature, plasmid replication is non-permissive and the construct is forced to integrate into the chromosome by homologous recombination at the gene locus. Integrants were confirmed by PCR amplification of the mutant allele by UhpT1b_EcoRI and UhpT4b_BamHI primers. Integrants were grown in BHI broth without antibiotic for 24h at 30^{o}C. Serial dilutions were plated onto BHI without antibiotic and incubated at 30^{o}C for 24h. These conditions promote excision of the plasmid. Double cross-over excisants (where the WT *uhpT* gene is extracted with the plasmid DNA and the mutant allele remains integrated) were screened for chloramphenicol sensitivity. Colonies were selected and patched onto BHI – chloramphenicol and BHI without antibiotic and incubated at 30^{o}C for 24h. Sensitive colonies conferred loss of plasmid. Genomic DNA was extracted and the mutant allele was confirmed by PCR using primers UhpT1b_EcoRI - UhpT4b_BamHI and UhpT C1 - UhpT C2b (appendix Table A3).

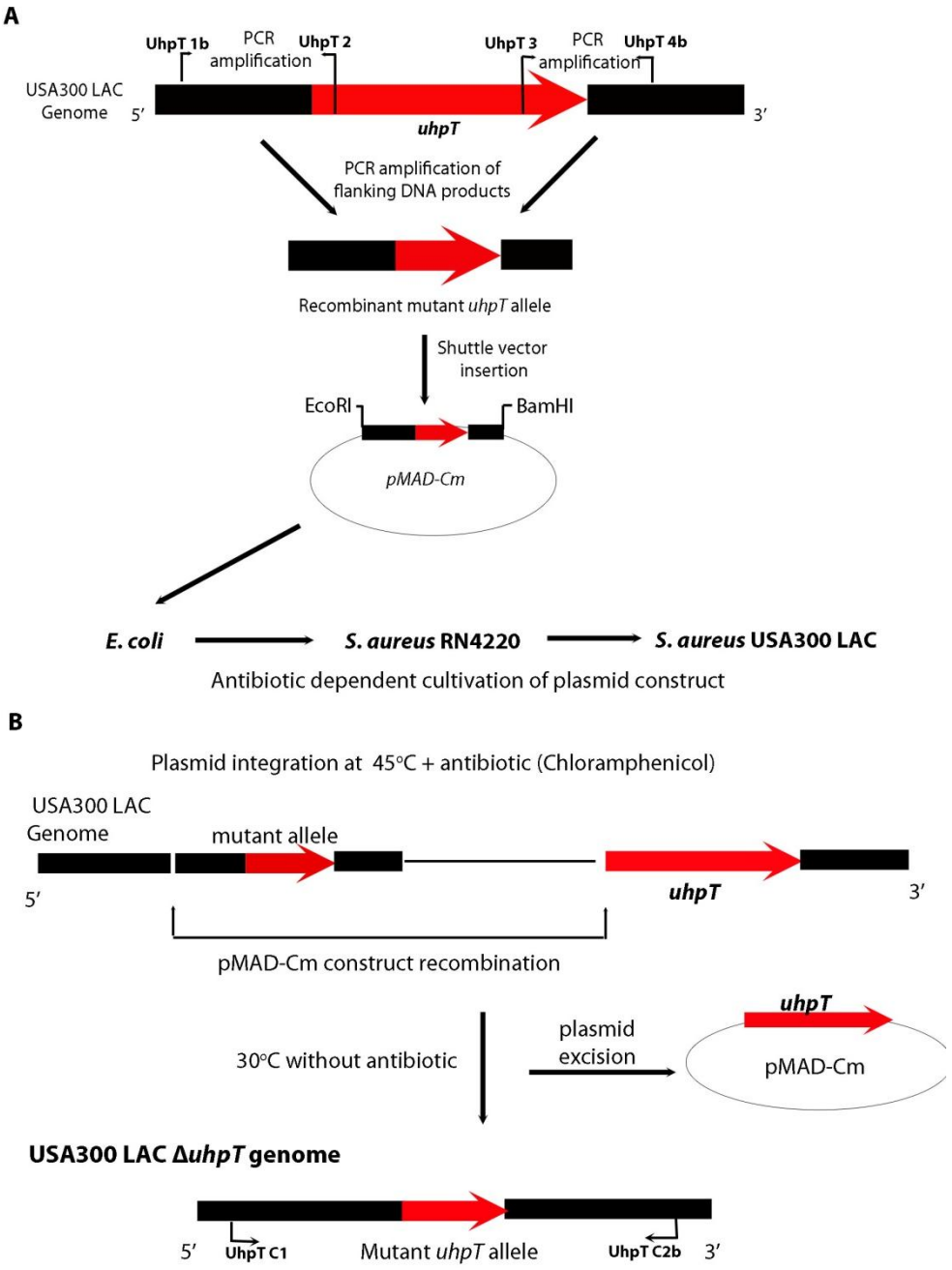

Figure 2.1. Strategy for constructing gene deletion mutants in *S. aureus* USA300 sugar phosphate permeases. A. Construction of the shuttle vector harbouring the truncated transporter allele and passage into USA300 LAC. **B.** Homologous recombination of the mutant transporter allele at the WT genome locus and excision of the shuttle vector to form the single mutant strain.

To construct the double mutation, Δ*uhpT*Δ*glpT,* the same protocol was administered using the single mutant strain Δ*uhpT* as the recipient and pMAD-Cm GlpT as the plasmid construct for homologous recombination. Primer combinations used for corresponding gene mutations are displayed in appendix Table A3. Native plasmids were extracted and profiled on an agarose gel to assess the isogenicity of mutant strains compared to wild type. A wild type USA300 LAC strain was constructed which was cured of the native pUSA03 plasmid. At the final stage of the protocol, antibiotic sensitivity screening, WT *uhpT* revertant colonies were confirmed by PCR, and the loss of pUSA03 was confirmed by plasmid profiling.

2.3.7 Gene complementation of *L. monocytogenes* P14-A Δ*hpt*

Genes were complemented via the listerial integrative vector pPL2 (Lauer *et al.* 2002). This vector provides highly stable, site specific integration into the listerial chromosome (Monk *et al.* 2008) and has been employed in previous studies to successfully demonstrate heterologous gene expression in *Listeria* (Kim *et al.* 2012; Lemon *et al.* 2010).

Vector integrated genes required a constitutive promoter to drive expression. The superoxide dismutase gene promoter of *Listeria*, Psod, was used to demonstrate high intensity, constitutive expression (Kohler *et al.* 2000). Psod was digested from purified pBC(gfp)$_{Psod}$ plasmid using SalI and PstI enzymes and ligated into these pPL2 vector sites directly upstream of permease gene insertion sites. As Psod was found insufficient for generating intense expression, the Psod region was substituted for the PprfA promoter region. The PrfA DNA binding region, known as the PrfA box is located 180-196bp upstream of the *hpt* gene start codon in *L. monocytogenes*. Approximately 200bp of genomic DNA directly upstream of the *hpt* gene was amplified with Phusion polymerase using primers PprfA_KpnI and PprfA_BamHI. This sequence contained the PrfA box and the -10 binding motif, sequences targeted for transcription activation of *hpt* expression. This promoter sequence replaced Psod in the KpnI and

BamHI restriction sites of pPL2. The promoter sequences are presented in appendix Figure A3.

Sugar phosphate transporter gene sequences were amplified by high fidelity Phusion polymerase (New England Biolabs). *L. monocytogenes hpt* was amplified from genomic DNA extracted from *L. monocytogenes* P14. *S. aureus uhpT* and *glpT* genes were amplified from genomic DNA extracted from USA300 LAC. Primer combinations relating to these reactions are described in appendix Table A3. Gene products were cloned into pCRBlunt (Invitrogen) and sequenced using M13 Forward and M13 Reverse primers. Gene sequences were excised from purified pCRBlunt using restriction enzymes BamHI and SpeI, incubated for 3h at 37^{o}C. Genes were ligated into pPL2 constructs in the BamHI – SpeI restriction sites directly downstream of the promoter. Constructs were transformed into *E. coli* which was plated onto LB - chloramphenicol and incubated for 24h at 37^{o}C. Constructs were confirmed by colony PCR using the appropriate gene primers to amplify transporters. The promoter region and gene sequence were sequenced using T3 and pPL2 1R primers (appendix Table A3). Constructs created for complementation are illustrated in appendix Figure A1 and A2.

Purified constructs were electroporated into *L. monocytogenes* P14-A Δ*hpt* using an established transformation protocol (Lauer *et al.* 2002). Transformed *Listeria* were plated onto BHI-chloramphenicol and incubated at 37^{o}C for 24h. Integrants were checked by PCR using PL95 and NC16 primers (appendix Table A3). The *prfA* gene was amplified with MR2 KpnI and MR10 SpeI (appendix Table A3) to confirm *L. monocytogenes*. Appropriate gene primers were used to confirm the presence of transporter genes. Characterisation of complemented strains was performed using *in vitro* growth assays in sugar phosphates.

2.3.8 Bioinformatic analysis

S. aureus gene sequences were located using the NCBI genome database. Homologous protein sequences to *S. aureus* transporters were found using ExPasy Blast protein alignment tool, and searched using default parameters. Relevant data, including protein accession numbers and percentage sequence identity were collated for 10 highly similar sequences. Conserved domains across all homologous proteins were found using NCBI conserved domain search, following the set parameters.

2.4 *In vitro* assays

2.4.1 Bacterial growth

L. monocytogenes and *S. aureus* strains were cultured overnight in BHI. Strains were sub-cultured in BHI (dilution 1:50) until reaching Optical Density 600nm (OD_{600}) 0.6 – 1 (the mid exponential growth phase). 1ml of culture was added to a sterile eppendorf and pelleted via desktop centrifugation (5000rpm, 5 minutes). The bacterial pellet was washed in sterile 1x Phosphate Buffered Saline (PBS), pelleted and re-suspended in 1ml PBS to form the stock inocula.

250µl of stock inocula was added to a separate eppendorf, diluted 1:4 with 1x PBS and vortexed. The OD_{600} of this solution was measured to calibrate the concentration of stock inocula (= OD600 x4). The following calculation was then applied to determine the volume of inocula to add to 1ml of growth media;

$$\text{Volume (µl)} = \frac{1000}{OD_{600} \,/\, 0.02}$$

Growth media was aliquoted into 1ml samples. A fixed starting number of bacteria were added to sample according to the calculated volume. After vortexing, 200 µl of each sample was added in triplicate to a Costar 96 well flat bottom plate. Blanks of growth media were added appropriately. The 96 well plate was loaded into a Fluostar Optima Reader (BMG Labtech).

The OD600 of each well was measured every 30 minutes whilst shaking at 200rpm and incubated at 37^{o}C. Average growth over time was calculated from single experiments in triplicate ± standard deviation from the mean. Replicate experiments were pooled to generate an overall average growth, and the standard error was calculated.

2.4.1.1 Minimal growth media for carbon nutrient growth analysis

A chemically defined minimal growth media was employed to regulate background *in vitro* growth of *S. aureus*. A staphylococcal minimal media has been previously described, named *Hussain-Hastings-White modified* medium (HHWm) (Toledo-arana *et al.* 2005). This media contains glucose as a carbon source, a mixture of amino acids as a source of nitrogen and a variety of vitamins and minerals as trace elements to supplement basal growth. For the purposes of this study the composition of this media was modified to suit the investigation. This study focuses upon the uptake of phosphorylated sugars through OAP transporters. In this family of permeases, the import of organophosphate substrates is coupled to the export of inorganic phosphate and is dependent upon the chemiosmotic gradient for function (Pao *et al.* 1998). It has been previously demonstrated that high external inorganic phosphate had a marked inhibition upon glucose-6-phospate uptake via UhpT due to disruption of the chemiosmotic gradient (Schwöppe *et al.* 2002). The concentration of phosphate buffers in the media composition was reduced as to lessen the disruption of organophosphate substrate import. Glucose was removed as the sole carbohydrate source of this media, in order to analyse individual supplemented substrates. The composition of this formulation, designated HHWm*, is detailed in Table 2.4.

LB broth was used as a minimal media for assessing carbon nutrition of *L. monocytogenes* strains.

Table 2.4. Composition of HHWm* minimal medium.

Compounds	Mass (g/L)	Volume in 1L media (ml)	Final molar conc.	Final conc. (g/L)
Solution A (10x)				
Sodium Phosphate Dibasic	14.2		0.01M	1.42
Potassium Phosphate Monobasic	13.6	100	0.01M	1.36
Ammonium Sulphate	20		0.015M	2.00
Solution B (50x)				
Magnesium Sulphate $7H_2O$	2.5		0.2mM	0.05
Manganese Sulphate monohydrate	0.19	20	22.5uM	0.0038
Ferrous Sulphate Heptahydrate	0.14		10.0uM	0.0028
Solution C (100x)				
Biotin	0.01		0.409uM	0.0001
Nicotinic acid	0.2		16.2uM	0.002
D-Panthothenic acid Ca Salt	0.2	10	8.39uM	0.002
Pyridoxal hydrochloride	0.39		19.45uM	0.0039
Riboflavin	0.2		5.31uM	0.002
Thiamine Hydrochloride	0.2		5.93uM	0.002
Adenine Solution (20x)				
Adenine 1/2 H_2SO_4	0.3	50	81.5uM	0.015
Guanine Solution (20x)				
Guanine HCl	0.375	50	100uM	0.019
Trace Elements Solution (100x)				
Calcium Chloride	0.55		49.5uM	0.0055
Zinc Chloride	0.17		12.5uM	0.0017
Copper Chloride $2H_20$	0.043	10	2.52uM	0.00043
Cobalt Chloride $6H_20$	0.06		2.52uM	0.0006
Sodium Molybdate $2H_20$	0.06		2.48uM	0.0006
RPMI1640 amino acids (50x) (Sigma)		20	Variable	Variable
Glutamine Solution (100x)				
L-Glutamine	29.2	10	2mM	0.292
Calcium Solution (1000x)				
Calcium Chloride	7.77	1	70uM	0.0078
ddH_20 Sterile		730		

2.4.1.2 Carbon nutrient supplementation of minimal media

Sugar substrates were added as carbon based growth sources to minimal media at a concentration of 20mM. Apart from glucose and glycerol solutions, sugar powders were dissolved in ddH_20 and stored at -20^{o}C. The exact nomenclatures of all sugars used in this thesis are stated in Table 2.5. All sugars were purchased from Sigma.

Table 2.5. Carbohydrate compounds used in this study.

Product	Reference
D (+) Glucose solution	G8769
D (-) Fructose	F0127
D (+) Mannose	M2069
Glycerol	G5516
D-Glucose-1-phosphate disodium salt hydrate	G7000
D-Glucose-6-phosphate disodium salt hydrate	G7250
D-Fructose-6-phosphate disodium salt hydrate	F3627
D-Fructose-1,6-bisphosphate trisodium salt hydrate	F6803
racGlycerol-1-phosphate disodium salt hydrate	G2138
Glycerol-2-phosphate disodium salt hydrate	G6501
snGlycerol-3-phosphate bis(cyclohexylammonium) salt	G7886

2.4.2 Mammalian cell cytotoxicity

The integrity of the mammalian cell monolayer, grown in Costar 24 well plates, was tested using the Tox7 Lactic Dehydrogenase Based *In Vitro* Toxicology Assay Kit (Sigma). Cells that become detached from the monolayer are released into suspension. The suspension is collected and subjected to lysis, which releases lactate dehydrogenase (LDH) enzyme. LDH is used to produce an enzymatic reaction *in vitro*, which causes a colorimetric change (measured at OD_{490}). This quantifiably measures the amount of LDH in the suspension. Doubling dilutions of suspended uninfected mammalian cells were subjected to the Tox7 assay as a control to correlate absorbance with cell total. The percentage of the monolayer that became detached due to bacterial cytotoxicity was therefore calculated using the control assay. The assay was performed in accordance with the manufacturers' protocol.

2.4.3 Haemolytic titre

A haemolytic titre was performed using *S. aureus* USA300 LAC strains to assess the potency of haemolytic toxin production as a measure of *agr* activity. Rabbit erythrocytes were isolated from whole blood. Whole blood was centrifuged at 5000rpm for 10minutes at 4^{o}C. The supernatant was removed and erythrocytes were washed three times with an equal volume of 1xPBS (1500xg 10min 4 ^{o}C). Erythrocytes were re-suspended in 1xPBS to 2% (w/v) and stored at 4^{o}C. *S. aureus* strains were cultured overnight in BHI, 1ml centrifuged (6000rpm, 5minutes) and the supernatant retained for titre. Doubling dilutions of bacterial supernatant were prepared with 1xPBS (100µl/well), in a Costar 96 well round bottom plate. Rabbit erythrocytes were added to each well in an equal volume (100µl/well). The plate was incubated at 37^{o}C for 1 hour and stored overnight at 4^{o}C. The plate was briefly centrifuged to pellet intact erythrocytes. A visualisation of pelleted erythrocytes was correlated with increase in dilution of bacterial supernatant. The plate was visualised using a desktop scanner.

2.4.4 Fosfomycin susceptibility testing

The minimum inhibitory concentration (MIC) of fosfomycin was determined for *S. aureus* strains. MICs were verified using Fosfomycin Epsilometer-Test antibiotic strips (Biomerieux), and performed in accordance with the British Society for Antimicrobial Chemotherapy methods for antimicrobial susceptibility testing. A scraping of at least half a dozen fresh bacterial colonies were suspended in saline solution and adjusted to OD_{600} 0.2. 120µl of inocula was coated onto agar plates using a swab. Once the surface was dry, the E-test strip was placed on the bacterial lawn and gently pressed to maximize surface contact. The plate was incubated for 18-24 hours at 37^{o}C. The exponential concentration gradient (µg/ml) of the antibiotic strip diffuses into the agar. The point at which the bacterial lawn ceases to grow can be measured on both sides of the concentration scale imprinted on the strip. The point of bacterial

convergence at the E-test strip represents the minimum inhibitory concentration.

Fosfomycin disodium salt (Sigma) was dissolved in sterile ddH_2O and added to *in vitro* growth assay media (2.4.1).

2.5 Mammalian cell culture

2.5.1 Cells and maintenance

Mammalian cells were grown in 80cm^3 tissue culture flasks, at 37^oC 5% CO_2, until ~80% confluent. All cells were maintained in Delbucco's Modified Eagle's Medium (DMEM, Invitrogen) containing 2mM L-Glutamine and 25mM glucose. Fetal bovine serum (FBS) was added to the culture medium at a concentration specific to cell type. A summary of cells and growth conditions used in this study are presented in Table 2.6.

Table 2.6. Cell lines maintained in this thesis.

Cell type	Origin	Characteristics	Growth medium	Source
HeLa	Human cervical carcinoma	Epithelial	DMEM 10% (v/v) FBS	Our Lab
Caco-2	Human colorectal adenocarcinoma	Epithelial	DMEM 20% (v/v) FBS	Our Lab
A549	Human alveolar adenocarcinoma	Basal epithelial	DMEM 10% (v/v) FBS	Hupp Lab (ECRC)
FTO2B	Rat hepatoma	Hepatocyte	DMEM 10% (v/v) FBS	Our Lab

2.5.2 Carbon source manipulation

The glucose content of the growth medium was altered to manipulate the intracellular nutrient environment in preparation for bacterial infection. The normal physiological blood glucose level (which supplies cells) was created by adding 5mM glucose to DMEM[-glucose] (Invitrogen) containing appropriate concentration of FBS (see Table 2.6). After flask culture cells were trypsinized, they were centrifuged (1000rpm, 3min) in 15ml falcon tubes and re-suspended in the 5mM Glucose DMEM medium. This

suspension was used to seed 24 well plates which were incubated overnight to set up infection experiments at 5mM glucose.

Cells were also starved of extracellular glucose. Firstly cells suspended in 5mM glucose media were seeded to 24 well plates and allowed to attach during incubation for 4-5 hours. This media was replaced by DMEM[-glucose] containing FBS and incubated overnight ready for infection.

2.5.3 Bacterial intracellular proliferation assays

2.5.3.1 *S. aureus* infection

Mammalian cells were trypsinized from 80cm^3 culture flasks, counted using a haemocytometer and seeded into 24 well plates at a concentration of ~150,000 cells per well. Cells were incubated in specific carbon source conditions and allowed to reach confluence overnight. *S. aureus* strains were cultured overnight in BHI broth. On the day of infection, the overnight bacterial cultures were sub-cultured in BHI to OD_{600} 0.4. 1ml of sub-culture was pelleted using a table top centrifuge (8000rpm, 4min), washed in sterile 1xPBS before pelleting and re-suspended in 1ml 1xPBS. The CFU/ml of this inocula suspension was calculated by replicate serial dilution plating. The appropriate volume of inocula required to infect each well of mammalian cells at a specific multiplicity of infection (MOI) was calculated:

$$\text{Volume of inocula per well (µl)} = \frac{\text{(Ratio no.bacteria : no.cells) x 150000}}{\text{CFU/ml inocula}} \text{ X 1000}$$

Media was aspirated from confluent monolayers, washed with sterile 1xPBS, and fresh media containing the bacterial inocula was added. The 24 well plates were centrifuged at 1000rpm for 3 minutes before cells were incubated for 35 minutes (37^{o}C) allowing the bacteria to attach and invade. Media containing bacteria was aspirated from cells and fresh media containing 100 µg/ml gentamicin (Sigma) and 10 µg/ml lysostaphin (Ambi) was directly overlaid. This media ensures killing of extracellular *S. aureus*,

allowing specific monitoring of intracellular bacterial replication. After 30 minutes of incubation, this represented time 0h and the commencement of the time course infection. At appropriate time points, antibiotic media was aspirated, cells were washed twice in 1xPBS and 100µl of 0.1% (v/v) TritonX-100 (Sigma) was applied to the monolayer for 10 minutes whilst the plate was incubated at 37^{o}C. 400µl of 1xPBS was added to the well and using a sterile pipette tip, cells were scraped from the well in a systematic manner. The samples were serially diluted and 100µl of appropriate dilutions were plated on BHI overnight at 37^{o}C. The numbers of colony forming units per ml were calculated for each time point. Time points for each infection were preferentially performed in triplicate. The average CFU/ml was calculated over biological replicates to generate mean values for comparison.

The percentage bacterial invasion is defined as the number of bacteria isolated at time 0h as a percentage of the total number of bacteria that were exposed to the cell monolayer.

$$\% \text{ invasion} = \frac{\text{CFU/ml at t=0h}}{\text{Bacterial MOI}} \times 100$$

The mean generation time is defined as the average time taken for intracellular bacteria to double from time 0h to the last measured time point.

$$\text{Mean generation number} = \frac{(\text{Log mean CFU/ml at t= Yh}) - (\text{Log mean CFU/ml at t=0h})}{\text{Log2}}$$

$$\text{Mean generation time (minutes)} = \frac{\text{Generation number}}{\text{Number of hours}} \times 60 \text{ minutes}$$

Standard error was calculated for all experiments.

2.5.3.2 *L. monocytogenes* infection

L. monocytogenes strains were cultured overnight in BHI broth. Cultures were sub-cultured in 200ml BHI until reaching an OD_{600} of 1. Bacterial culture was transferred to a sterile 500ml centrifugation bottle and pelleted (8000rpm, 10mins, 4^{o}C). The bacterial pellet was washed three times in ice cold 1xPBS before re-suspending the pellet in ice cold 20% (v/v) glycerol / PBS. Inoculum was aliquoted into eppendorfs to store at -80^{o}C. Three aliquots were thawed and pooled for replicate serial dilution plating to calculate an average CFU/ml for the inoculum. Three frozen inoculum aliquots were pooled and vortexed before each infection experiment to minimise variation from the calibrated CFU/ml.

The same general mammalian cell infection procedure was followed as described for *S. aureus*. Inoculum was exposed to cells at an MOI of 1-3, with an invasion time of 20 minutes. Inoculated media was removed, cells washed in 1xPBS and media containing 100µg/ml gentamicin was added. Incubation of antibiotic media for 1 hour constituted time 0h, where 1% (v/v) Triton X-100 was used to break open cells. At 8-10 hours post invasion intracellular bacteria were plated via serial dilution and the CFU/ml was calculated at appropriate dilutions.

For experiments where time 0h and 8h were measured only, the intracellular growth coefficient (IGC) was calculated. This effectively measures the fold change in intracellular bacterial numbers at time 8h relative to the numbers isolated at time 0h. This quantification allows a comparison to the control strain *L. monocytogenes* P14-A.

$$\text{Intracellular Growth Coefficient (IGC)} = \frac{\text{CFU/ml at t=8h} - \text{Mean CFU/ml at t=0h}}{\text{Mean CFU/ml at t=0h}}$$

For each experiment, average CFU/ml was calculated at time 0h which was used to calculate IGC for technical replicates. The IGC values from separate experiments were pooled to calculate a mean IGC ± standard error.

2.5.4 Immunofluorescence microscopy

2.5.4.1 Preparation of coverslips

Sterile round 23mm glass cover slips were added to 24 well plates using sterile tweezers. Mammalian cells were seeded to ~150,000 cells per well and incubated overnight until confluent. *S. aureus* infection protocols were performed as previously described in 2.5.3.1, until removal of antibiotic killing media. Coverslips were transferred to a fresh 24 well plate and washed twice with sterile 1xPBS. 500µl of 4% (w/v) paraformaldehyde was overlaid and incubated for 15minutes at room temperature (RT) to fix cells. Paraformaldehyde was aspirated and coverslips were washed three times with 1xPBS before storage in 1xPBS at 4^{o}C.

2.5.4.2 Antibody staining

PBS was removed from coverslips and cells were immersed in 0.2% (v/v) TritonX-100 for 10 minutes to permeablize the cell membrane. Triton was removed and non-specific epitope blocking was then completed by sterile PBS 3% (w/v) bovine serum albumin (BSA) application for 1 hour at RT. Primary antibodies were diluted as appropriate in PBS 3% BSA. Blocking solution was exchanged for primary antibody suspension and incubated at RT for 1 hour. Primary antibodies were taken off and cells were washed three times in 1xPBS. Secondary antibodies and/or fluorophores were diluted as appropriate in PBS 3% BSA. Secondary antibodies/ fluorophores were incubated for 30 minutes at RT. A comprehensive table of antibodies/fluorophores used including the working dilutions is presented in Table 2.7. Cells were washed three times in 1xPBS. Coverslips were placed face up on Whatman blotting paper for 10-15 minutes to remove excess moisture. Coverslips were cemented cells facing down onto

Superfrost glass slides by mounting medium (Invitrogen) containing dissolved antifade reagent (Invitrogen). Slides were stored at RT on a dark, flat surface until required for microscopy analysis.

Table 2.7. Antibodies and fluorophores employed in immunofluorescence microscopy.

Antibody type	Antibody name	Working dilution	Use	Manufacturer (Reference)
1°	Anti-*Staphylococcus aureus* Rabbit Polyclonal IgG	1:1000	Labelling intracellular *S. aureus*	Abcam (Ab20920)
1°	Anti-58K Golgi Protein Mouse monoclonal IgG	1:1000	Labelling cell Golgi membranes	Abcam (Ab27043)
1°	Anti-Rab7mouse monoclonal IgG	1:700	Labelling cell vacuole marker Rab7 GTPase	Sigma (R8779-200UL)
1°	Anti-LAMP1(H4A3) mouse monoclonal IgG	1:100	Labelling cell vacuole marker LAMP1	Santa Cruz Biotechnology (sc-20011)
2°	AlexaFluor568 Goat anti-Rabbit IgG	1:1000	Detection of anti-*Staphylococcus aureus* IgG	Invitrogen (A-11011)
2°	Alexa Fluor568 Goat anti-Mouse IgG	1:1000	Detection of anti-Rab7 IgG and anti-LAMP1 IgG	Invitrogen (A-11004)
2°	Alexa Fluor 350 Goat anti-Rabbit IgG	1:1000	Detection of anti-*Staphylococcus aureus* IgG when present with other anitbody markers	Invitrogen (A-11046)
	Non-antibody fluorophores incubated with Secondary antibodies			
	Alexa Fluor405-conjugated DAPI	1:100,000	Staining nuclear DNA	Invitrogen
	Alexa Fluor 488-conjugated Phalloidin	1:1000	Staining cell F-actin	Invitrogen (A12379)

2.5.4.3 Microscopy analysis

Coverslip slides prepared for fluorescence microscopy were viewed under a Leica DMI 6000 inverted microscope with 63x objective (oil immersion). Imaging was captured using Leica LAS imaging software and pictures were processed for presentation using Adobe Photoshop.

Duplicate cell coverslip preparations were used to quantify infection. At each time point, 10 random samples (5 from each coverslip) were imaged using the same imaging area size (field). Cells with nuclei within these areas were counted as were the number of cells that contained at least a single bacterium. The numbers of bacterial clusters inside infected cells were also counted. A bacterial 'cluster', for the purposes of this study, was defined as a free standing body of bacteria, ranging from a single bacterium to an infinite number, as long as the bacteria were in contact as part of that cluster. As the sampling areas contained variable numbers of cells, the average values were calculated by summing the raw values and dividing by the sample size.

Co-localisation of fluorescent *S. aureus* clusters and cellular proteins was qualified by visual association. Duplicate cell coverslip preparations were analysed by selecting at least 10 random fields from each time point. The number of bacterial clusters that were positively associated with mammalian cell proteins was expressed as a percentage of the total number of intracellular clusters that were observed in all fields. This calculation determined the % co-localisation and standard error was applied for each time point.

Phase contrast images were captured of cell monolayers within 24 well plates at 20x objective.

2.5.5 Inhibitor treatment of mammalian cells

Golgicide A (Sigma) is a reversible inhibitor of the cis-Golgi GTPase GF1, and designed to disrupt Golgi assembly. Golgicide A was dissolved in dimethyl

sulphoxide (Sigma) at a stock concentration of 10mg/ml and stored at 4^{o}C. During the *S. aureus* infection assay (2.5.3.1) inhibitor was added at a working concentration of 10μg/ml to the antibiotic killing media. Golgicide A remained exposed to cells for the remainder of the infection course.

2.6 Statistical analysis

A student's T-test was performed to determine whether data sets were significantly different.

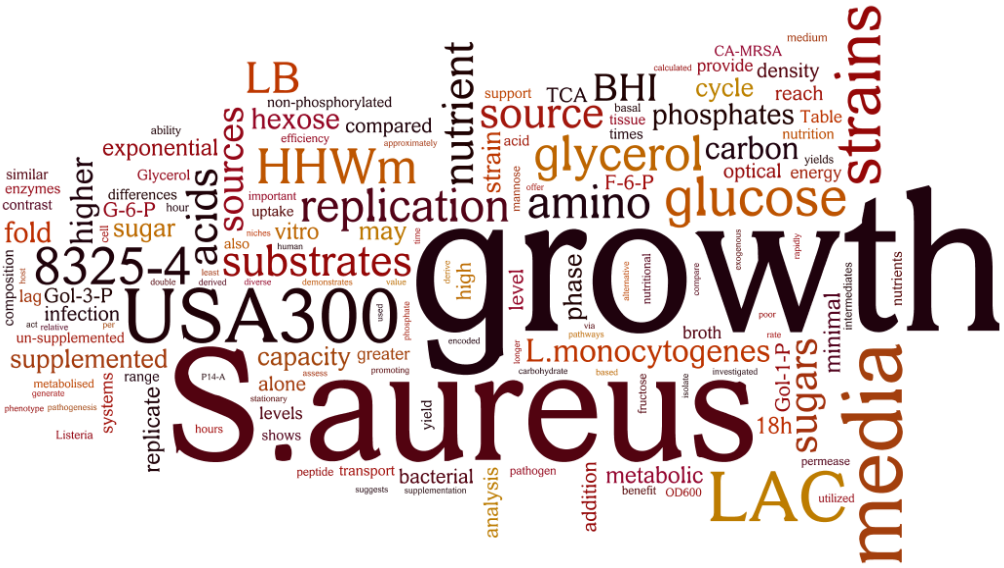

Chapter 3

Carbon based nutrition of *Staphylococcus aureus*

3.1 Introduction

Staphylococcus aureus is a prolific animal and human pathogen. It is estimated that *S. aureus* naturally colonises the nasal passages of 20% of the human population, while 60% are intermittent carriers (Kluytmans 1997). This pathogen is most commonly isolated from skin and soft tissue infections, such as impetigo and foliculitis. Infection can reach the subcutaneous and connective tissue and cause inflammation, known as cellulitis. In addition, infections have been localised to the fatty connective tissue of the breast (mastitis). *S. aureus* is frequently found to be the underlying cause of more serious diseases such as blood sepsis, endocarditis (inner heart tissue infection), pneumonia (lung tissue infection) and osteomyelitis (bone infection) (Nimmo 2012). This organism demonstrates colonisation of multiple, diverse niches for successful replication. The genomic make-up of *S. aureus* incorporates a host of transport systems to capture nutrients from these environments, in addition to redundant metabolic energy pathways (Fuchs *et al.* 2012). The ability of pathogens to exploit nutrients from the host environment is integral to replication and pathogenesis. *S. aureus* is a pathogen that has the metabolic versatility to do this in various niches; however the nutritional determinants that support this ability are poorly understood.

3.2 Objectives

The primary aim was to identify and compare carbon based substrates that promote *in vitro* media based growth of *S. aureus* strains. Individual carbohydrate substrates were investigated which can be metabolised using the glycolytic pathway outlined in Figure 3.1. This strategy integrated phosphorylated sugars which were particularly scrutinized as nutrient sources contributing to replication. *S. aureus* USA300 LAC, a hyper-virulent clinical CA-MRSA isolate, was primarily investigated to probe nutritional determinants of virulence. This isolate was compared to *S. aureus* 8325-4, a well documented laboratory strain, to examine the diversity of nutrition.

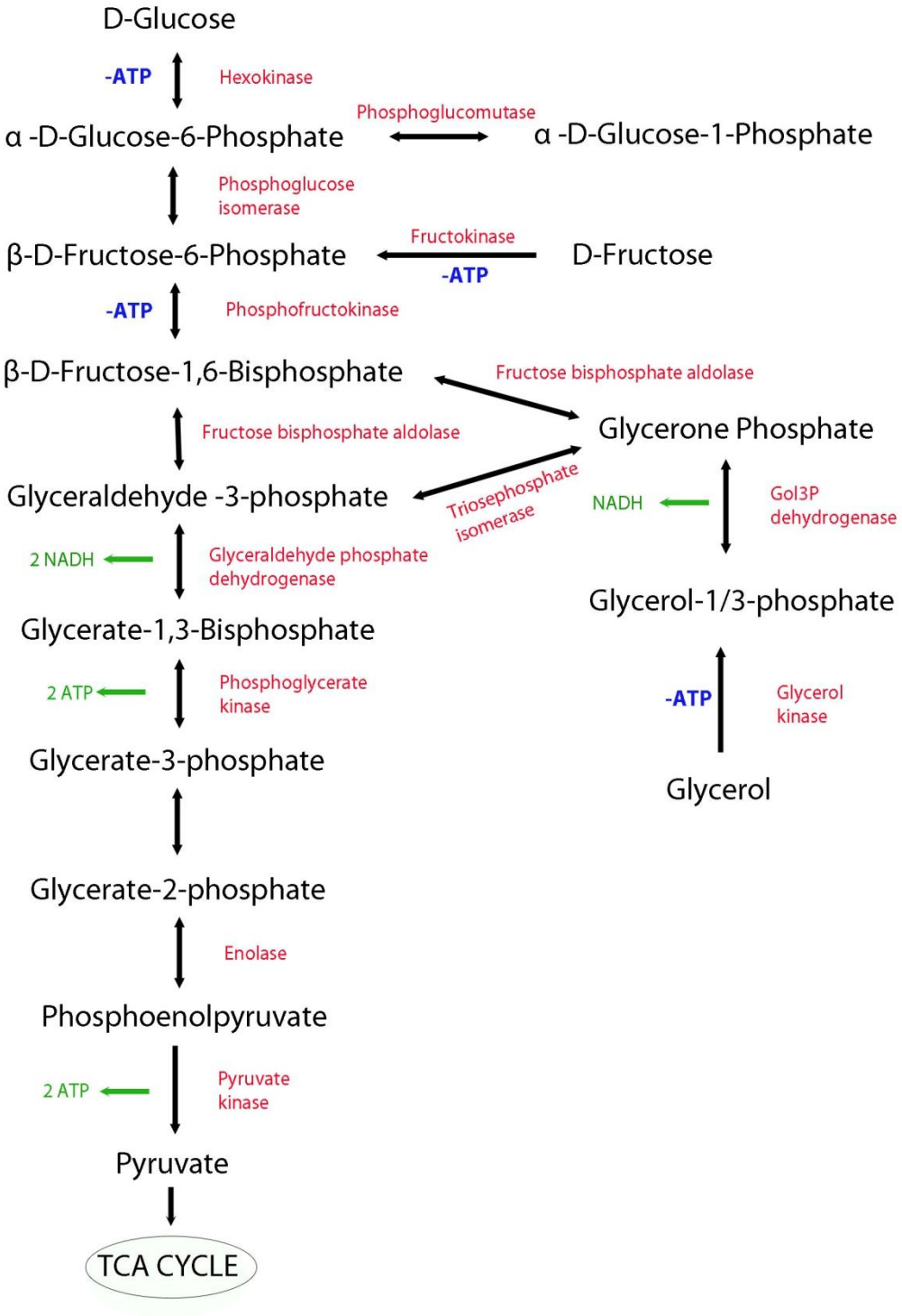

Figure 3.1. Glycolysis energy pathway (adapted from Kegg pathways). Energy dependent steps are highlighted in blue , energy producing steps are highlighted in green and metabolic enzymes catalysing reactions are shown in red.

3.3 Relevant materials and methods

***In vitro* assays (2.4)** Bacterial growth (2.4.1)

Statistical analysis (2.6) Significant difference was calculated between un-supplemented vs supplemented data sets of *in vitro* growth at the final measured point (18h).

3.4 Results

S. aureus strains were characterised *in vitro* using nutrient supplemented media to monitor bacterial growth and assess the capacity for nutrient metabolism. A minimal media was required to support a basal growth of *S. aureus*. In this media, individual carbon sources could be added to compare bacterial growth and assess the value of substrates towards replication.

3.4.1 Multi-nutrient media

Two different complex bacterial broths were used to assess the capacity of *S. aureus* to replicate in multi-nutrient environments. Brain heart infusion (BHI) broth is an extremely nutritious media containing an abundance of proteins, peptones, carbohydrates and lipids. It also includes ~10mM glucose. Luria Bertani (LB) broth is a rich source of peptides and amino acids whilst is relatively poor in sugars compared to BHI. The composition of BHI and LB media can be compared in appendix Tables A4 and A5. *L. monocytogenes* was analysed in parallel to provide a reference strain to compare the growth capacity in BHI and LB.

Figure 3.2 shows the *in vitro* growth of *S. aureus* strains in BHI and LB media, compared to *L. monocytogenes* strain P14-A. Panels A and B show that 8325-4 and USA300 LAC strains can derive rapid, high growth yield from both BHI and LB broth. Notably, *Listeria* can reach an optical density at 600nm (OD_{600nm}) of around 1 in BHI (Figure 3.2C), which was calculated via dilution plating to be ~5 - 7 $x10^{10}$ CFU/ml. At the same optical density, *S. aureus* strains were calculated to reach 2 – 5 $x10^{10}$ CFU/ml in this media. *S. aureus* strains can reach higher bacterial yields than *L. monocytogenes* among the same rich nutrient composition of BHI. In addition, the lag phase of growth in both BHI and LB is at least half the time in *S. aureus* strains compared to P14-A. This indicates that *S. aureus* strains are particularly proficient at utilising the wealth of nutrients offered in BHI and LB.

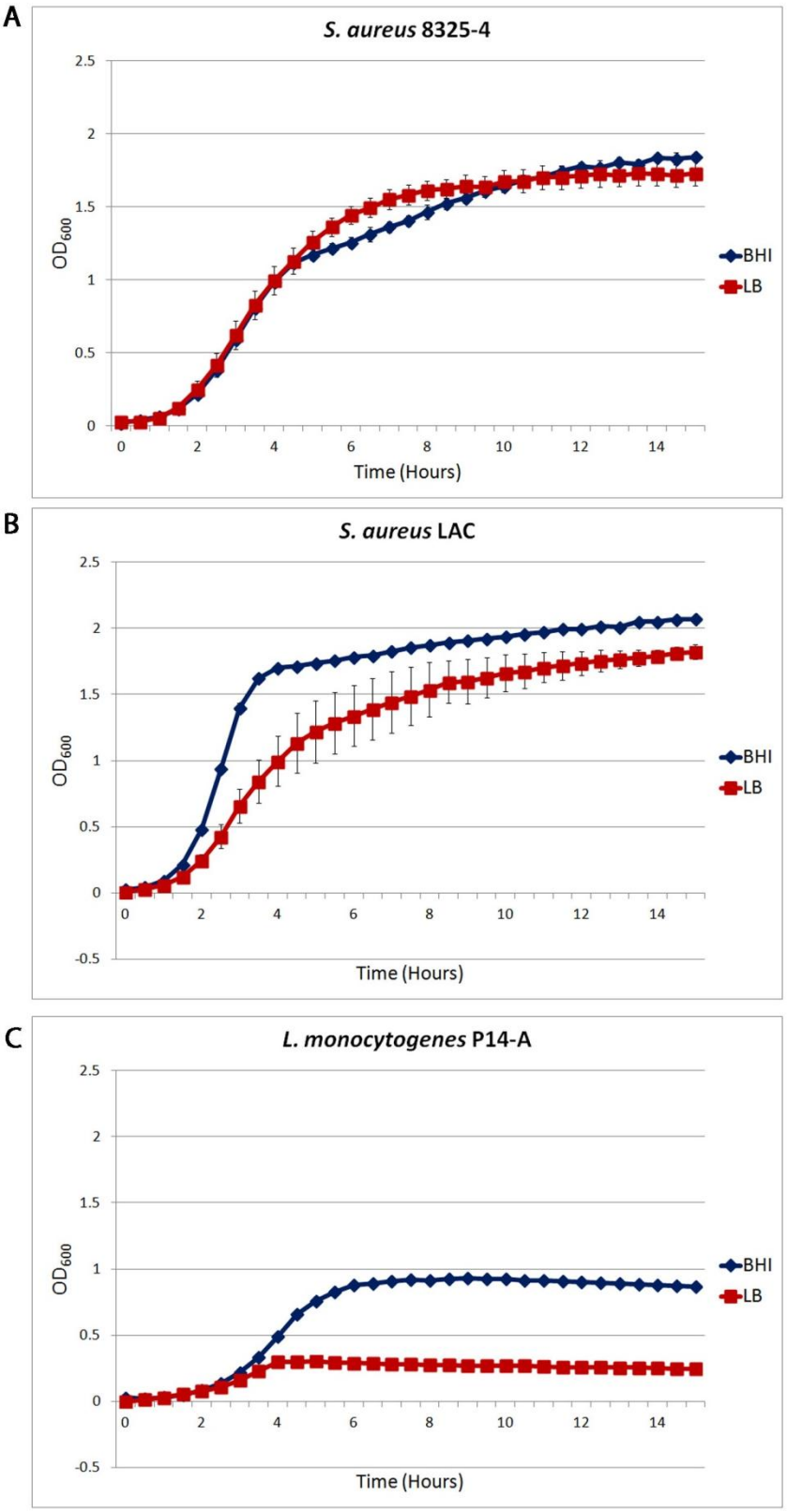

Figure 3.2. Growth of *S. aureus* and *L. monocytogenes* in multi-nutrient broth. *In vitro* growth assays in BHI and LB media. Average growth is formulated from at least 2 separate assays and shows the standard error of the mean.

Figure 3.2C demonstrates LB media cannot support replication of *L. monocytogenes* in the same manner as BHI due to the nutritional dependence of *Listeria* upon carbohydrate sources. LB broth can act as a minimal media to measure growth of *L. monocytogenes* when carbon sources are supplemented. *S. aureus* strains replicate in LB to an optical density of approximately 6 fold higher than P14-A, which nullifies this broth as a minimal medium for monitoring staphylococcal growth.

3.4.2 Chemically defined minimal media

As LB and BHI promote rapid and high capacity growth of *S. aureus*, neither could serve as a basal medium to characterise replication upon addition of specific carbon sources. Chemically defined staphylococcal minimal medium, termed HHWm*, was formulated to fulfil this requirement. The formulation of this media is outlined in 2.4.1.1 and the composition is illustrated in Table 2.4.

Selected non-phosphorylated sugars and phosphorylated 3 carbon (C3) and 6 carbon (C6) carbohydrate intermediates (as highlighted in Figure 3.1) were supplemented individually to HHWm* media. The capacity of *S. aureus* 8325-4 and USA300 LAC to replicate in these conditions are presented in Figure 3.3 and 3.4 respectively.

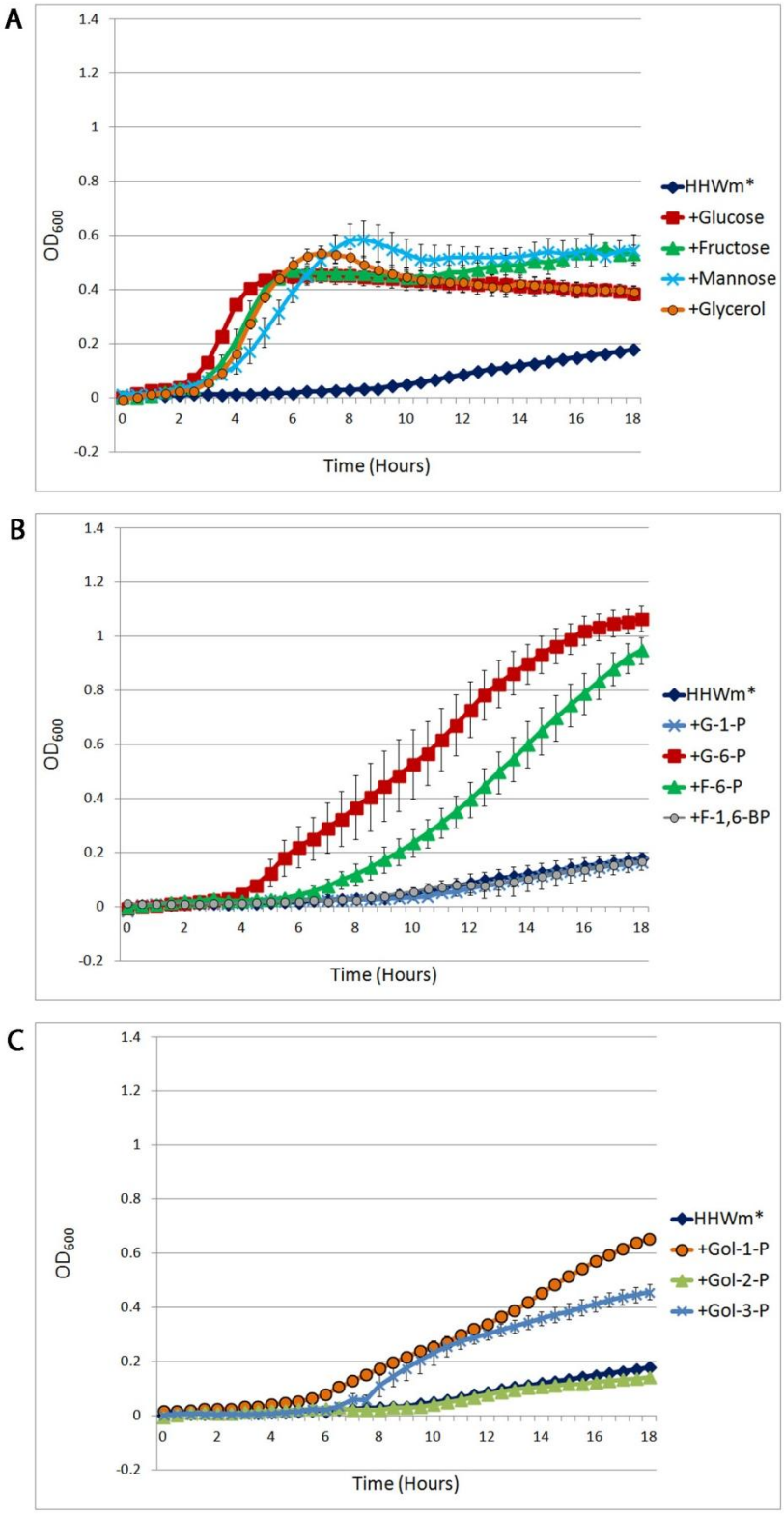

Figure 3.3. Growth of *S. aureus* 8325-4 in chemically defined minimal media. *In vitro* growth assays in HHWm* media supplemented with 20mM sugars. Average growth is from at least 2 separate assays and shows standarderror of the mean.
A. Non-phosphorylated sugars **B.** Phosphorylated C6 sugars
C. Phosphorylated C3 sugars.

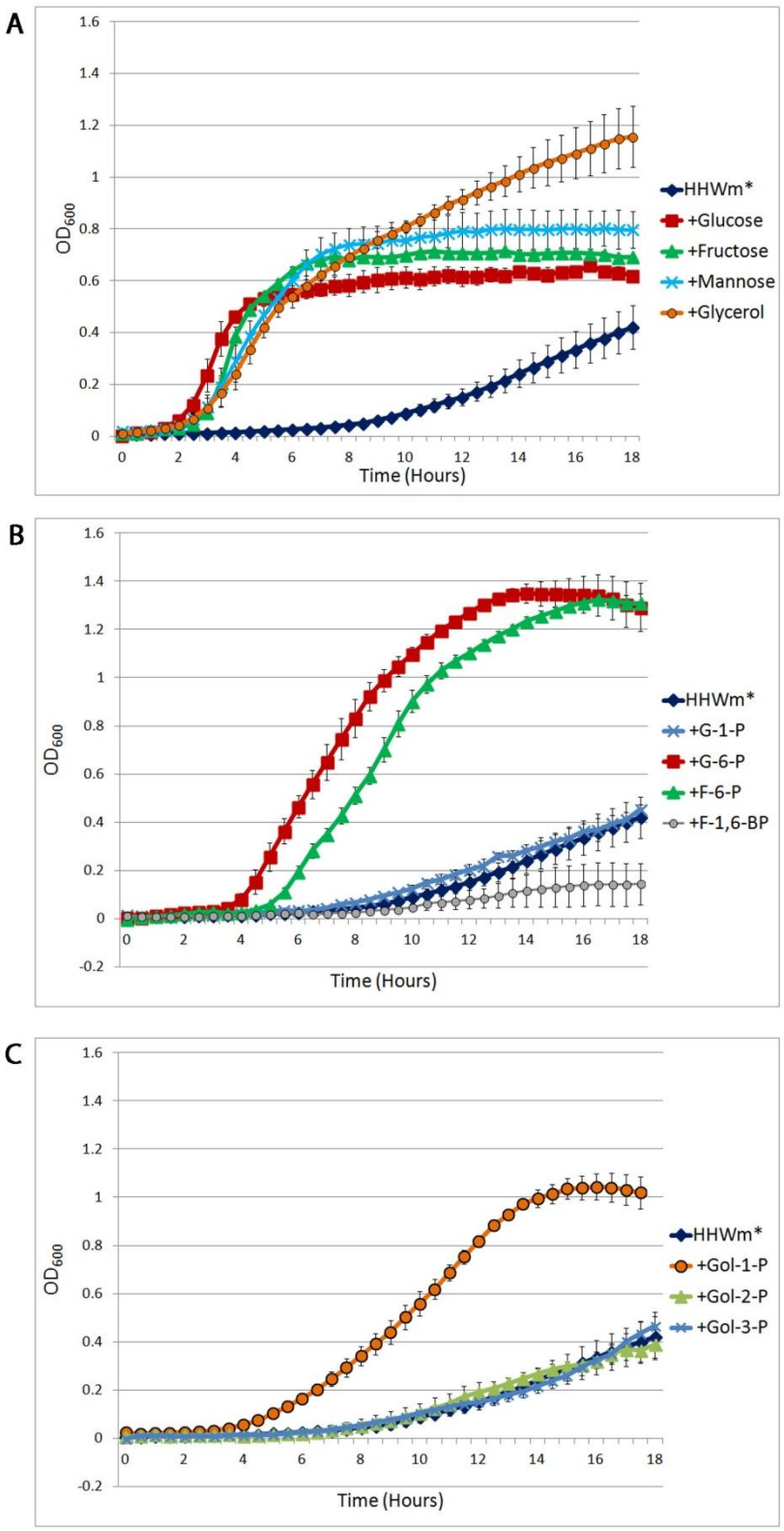

Figure 3.4. Growth of *S. aureus* USA300 LAC in chemically defined minimal media. *In vitro* growth assays in HHWm* media supplemented with 20mM sugars. Average growth is from at least 2 separate assays and shows standard error of the mean.
A. Non-phosphorylated sugars **B.** Phosphorylated C6 sugars
C. Phosphorylated C3 sugars.

3.4.2.1 Non-phosphorylated sugars

Figure 3.3A and 3.4A shows the average growth of *S. aureus* 8325-4 and USA300 LAC in sugar supplemented HHWm* relative to un-supplemented HHWm*. When both strains are supplemented with non-phosphorylated sugars, the lag phase of growth is consistent, lasting 2 hours. Glucose provides the most efficient energy source as both strains enter the exponential growth phase most rapidly and reach stationary phase by 5 hours. PTS dependent sugars fructose and mannose are also utilised rapidly in both strains and support replication to an optical density of 0.1-0.2 higher than glucose. Glycerol serves as an effective supplement of growth in both *S. aureus* strains. In 8325-4, glycerol is metabolised in a similar capacity to glucose whilst in USA300 LAC, this source provides a 2 fold higher level of optical density than glucose. All individual sugar sources benefit growth of 8325-4 by 2-3 fold more than HHWm* alone at 18h. Glucose, fructose and mannose offer USA300 LAC the capability to replicate to 0.5-1 fold more than HHWm* alone at 18h but the levels of optical density reached are at least 0.5 fold greater than 8325-4 growth. Glycerol is the outstanding growth supplement for USA300 LAC, improving replication to 3-fold higher than HHWm* alone and 3-fold higher than the 8325-4 counterpart at 18h. These significant differences in growth by 18h were confirmed via T-test, presented in Table 3.1.

3.4.2.2 Phosphorylated C6 sugars

Figure 3.3B and 3.4 B charts the growth of *S. aureus* strains in HHWm* media supplemented with hexose phosphate sugars. Neither strain can derive a growth benefit beyond the basal minimal medium from glucose-1-phosphate (G-1-P) or fructose-1,6-bisphosphate (F-1,6-BP). By contrast glucose-6-phosphate (G-6-P) and fructose-6-phosphate (F-6-P) are utilised to produce pronounced levels of growth beyond un-supplemented media. In strain 8325-4, the optical density of these hexose phosphates reaches 5 times the level of HHWm* alone by 18h and 1.5 times greater than glucose

and glycerol. Similarly in USA300 LAC, the OD_{600} rises over 2 fold higher than HHWm* alone and replication levels exceed double the value of glucose at 18h. Significant differences are confirmed in Table 3.1. However, the lag phase of growth elicited by hexose phosphates is double the length of glucose, which is consistent in both *S. aureus* strains. The exponential growth of *S. aureus* 8325-4 in HHWm* + glucose was OD_{600} 0.2 per hour. By contrast, exponential growth of hexose phosphates was 2 fold lower than glucose in 8325-4. In USA300 LAC, exponential growth in glucose and hexose phosphates was similar, at OD_{600} 0.2 per hour.

3.4.2.3 Phosphorylated C3 sugars

Figure 3.3C and 3.4C illustrates the value of glycerol monophosphates as growth promoting nutrients of *S. aureus* strains. Glycerol-1-phosphate (Gol-1-P) is utilised by both strains to generate a significant growth benefit by 18h (Table 3.1). In 8325-4, growth is supported to 3 times the level of un-supplemented media and 0.5 fold higher than glucose supplementation. Despite offering a higher yield of growth, glycerol-1-phosphate elicits an exponential growth of approximately OD_{600} 0.05 per hour in 8325-4 , which is 6 times lower than that of glucose. In USA300 LAC, glycerol-1-phosphate is an effective nutrient source, offering a 1.5 fold higher growth yield than un-supplemented media, reaching levels almost as high as hexose phosphates at approximately half the exponential growth rate. Glycerol-2-phosphate (Gol-2-P) and glycerol-3-phosphate (Gol-3-P) are not utilised as sources for replication in USA300 LAC whereas glycerol-3-phosphate can provide a growth advantage twice the basal level in 8325-4. Again, the lag phase of growth in glycerol monophosphates is a least double the length of glucose growth in both strains.

Table 3.1. Results of T-test analysis comparing sugar supplemented growth with non-supplemented growth at 18h.

Supplement	8325-4	USA300 LAC
+ Glucose	0.004	0.042
+ Glycerol	0.014	0.0008
+ Fructose	0.002	0.008
+ Mannose	0.016	0.009
+ G-1-P	0.51	0.71
+ G-6-P	0.001	0.0008
+ F-6-P	0.002	<<0.05
+ F-1,6-BP	0.82	0.09
+ Gol-1-P	0.0029	<<0.05
+ Gol-2-P	0.068	0.77
+ Gol-3-P	0.002	0.68

3.4.2.4 Amino acids

In HHWm* minimal media alone, *S. aureus* strains exhibited poor growth. However, it was noticeable after 10 hours, especially in USA300 LAC, that growth gradually increased. Components of the HHWm* media were proving a source of nutrition for *S. aureus*. *In vitro* grow assays were performed over a longer period of time to determine the extent of growth exhibited by USA300 LAC in HHWm* media without carbohydrates. Figure 3.5 shows that over a 24 hour period, USA300 LAC could reach yields similar to those attained in hexose phosphates and glycerol by growing in this media alone.

The HHWm* media composition incorporates an amino acids solution which supplies all amino acids ranging from 25µM to 1mM in concentration. The proficient growth of USA300LAC in peptide rich-carbohydrate poor LB media suggested that amino acids may provide a nutrient source. Removal of amino acids as part of the HHWm* media composition (HHWm* -αα) completely abolishes any growth of USA300

LAC (Figure 3.5). Although the lag phase is 10 hours (5 times longer than glucose supplemented growth), this demonstrates that small quantities of amino acids (relative to 20mM sugar supplementation) can provide an important nutrient source to support growth of *S. aureus* USA300 LAC.

Taken together, the results show that *S. aureus* USA300 LAC, in particular, can effectively and readily use a diverse range of nutrients to generate a substantial growth yield.

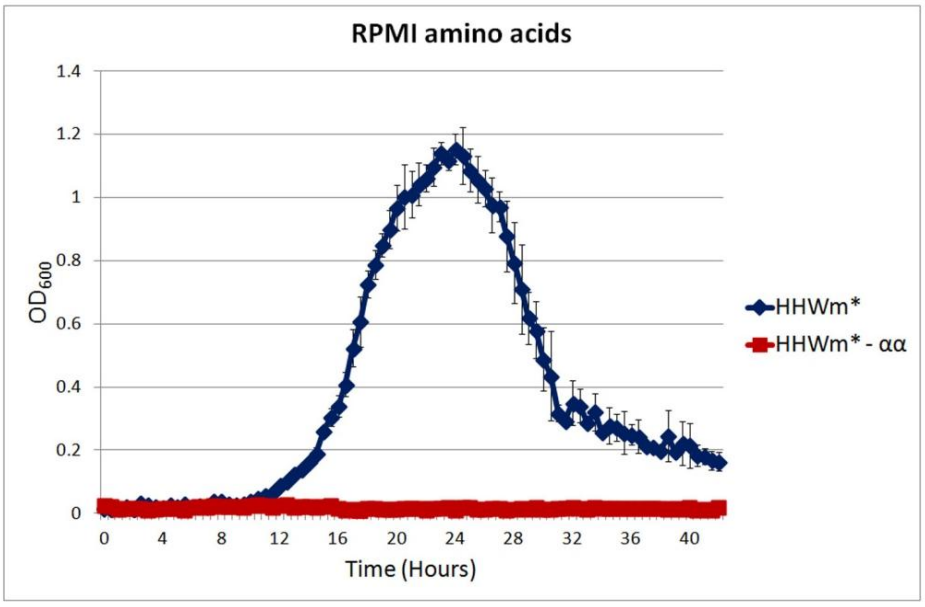

Figure 3.5. Growth of *S. aureus* USA300 LAC in amino acids.
Growth in HHWm* minimal media with and without (-αα) RPMI 1640 amino acids solution. A representative experiment is shown ± SD.

3.5 Discussion

In vitro growth analysis has demonstrated the extent of *S. aureus* replication derived from the utilisation of distinct exogenous substrates.

3.5.1 *S. aureus* is metabolically adept

S. aureus strains encode a putative glycerol uptake facilitator, in addition to independent PTS systems specific to glucose, fructose and mannose, almost certainly owing to the growth phenotype shown in each of these supplementations. Hexose sugars offer a rapidly metabolised source of nutrition for *S. aureus* which boosts replication to an arrested stationary level. Glycerol can also provide a valuable *in vitro* nutrient source to *S. aureus*. Glycerol is a precursor for the synthesis of triacylglycerols and phospholipids inside mammalian cells (Guo 1999) and may be considered an alternative nutrient source for bacterial growth. Discernible up regulation of glycerol uptake and metabolism genes has been observed in *S. aureus* infection of human lung cells (Garzoni *et al.* 2007) which suggests glycerol may be an important nutrient in this cellular environment. *S. aureus* USA300 LAC utilises glycerol to replicate to significantly higher yields than with hexose sugar supplementation. Given this information, this may implicate a role for glycerol scavenging as a means to replicate during invasive CA-MRSA pneumonia infection.

Hexose phosphate substrates glucose-6-phosphate and fructose-6-phosphate were utilised by *S. aureus* to generate the highest measured levels of replication, far exceeding the stationary levels of growth elicited by most non-phosphorylated sugars. Glycerol monophosphate (excluding glycerol-2-phosphate) also stimulated replication to a level greater than that of glucose albeit at a reduced rate. Specific sugar phosphates have the potential to offer a valuable intracellular source of nutrition for *S. aureus*. These substrates have singular capacity, as a carbon nutrient source, to induce high level replication which can directly influence pathogenesis and

virulence of *S. aureus*. It was noted that *S. aureus* strains underwent a 2-fold longer lag phase upon growth in sugar phosphates compared to non-phosphorylated sugars. Speculation can be made that this pause is attributed to the sensory inducible expression mechanism that governs the sugar phosphate transport systems (Winkler 1973; Dietz 1976). Upon identification of external substrate, single genomic expression systems must initiate production of permease proteins which are incorporated to the cell membrane. The time taken to reach the exponential growth phase may represent the accumulation of permeases at the membrane interface.

S. aureus USA300 LAC demonstrated a noticeable growth benefit from amino acids as sole carbon sources. *S. aureus* encode a number of amino acid permeases such as proline permease (*putP),* glutamine permease (*glnP*), arginine antiporter (arcD) and the putative amino acid permease (*pheP*) (Horsburgh *et al.* 2004; Wengender & Miller 1995; Zhu *et al*. 2007; Zhu *et al.* 2009). *S. aureus* encodes all enzymes involved biosynthesis of amino acids (Nuxoll *et al.* 2012), meaning the endogenous metabolic pathways are capable of producing these raw materials from other nutrient sources. Exogenous amino acids are therefore not exclusively taken up by *S. aureus* to fulfil a metabolic deficiency and so they apparently serve as a suitable alternative carbon nutrient source.

3.5.2 *S. aureus* USA300 LAC has greater metabolic proficiency

Clinical, hyper-virulent CA-MRSA strain USA300 LAC revealed a greater capacity for utilising substrates over the laboratory strain 8325-4. In virtually every analysis, USA300 LAC exploited substrates to a notably greater replicative yield than 8325-4. The clinical strain displayed similar rates of exponential growth to 8325-4 upon non-phosphorylated sugars. Noticeably, USA300 LAC derived growth from hexose phosphates as efficiently as glucose and only reduced rate of growth in glycerol monophosphate by 0.5 fold. By contrast, 8325-4 shows marked reduction in growth efficiency upon sugar phosphates relative to glucose growth. S.

aureus USA300 has the ability to replicate extensively from a range of exogenous substrates, with similar efficiency. This analysis suggests why this pathogen has become so dominant in establishing infection in diverse niches.

3.5.3 Intrinsic differences between *S. aureus* and *L. monocytogenes* may account for divergent nutritional gains

The high growth yields of *S. aureus* strains derived from LB media suggest that amino acids are utilised from this broth. By contrast, LB is not a nutritious media for *L. monocytogenes*. This suggests intrinsic differences between *L. monocytogenes* and *S. aureus* in the ability to derive growth from peptide and amino acid sources. *L. monocytogenes* encodes numerous amino acid and peptide transport systems, which are necessary to scavenge important substrates during host cell infection (Fuchs *et al.* 2012). Although *Listeria* are dependent upon exogenous uptake of several amino acids (Eisenreich *et al.* 2010), these substrates cannot act as a growth source (Premaratne *et al.* 1991). This may be attributed to differences in the constitution of the tricarboxylic acid (TCA) cycle. Figure 3.6 shows the metabolic enzymes that are encoded in the genome of *S. aureus* which act to convert substrates of the TCA cycle. Figure 3.6 compares the encoded enzymes of *L. monocytogenes*.

S. aureus has a complete set of TCA enzymes and in addition, a ferrodoxin oxidoreductase enzyme is encoded which serves to shorten the cycle and improve the efficiency. By contrast, *Listeria* species lack three enzymes necessary to convert 2-oxoglutarate to succinate meaning the cycle is bifurcated. TCA cycle function produces NADH, which is used to set up a proton gradient in the bacterial transport chain. Electrons donated by NADH oxidation drives export of H+ protons, which are ultimately coupled to production of ATP by ATP synthase (Alberts *et al.* 2002). In short, the TCA cycle can produce energy for growth as well as biosynthetic intermediates.

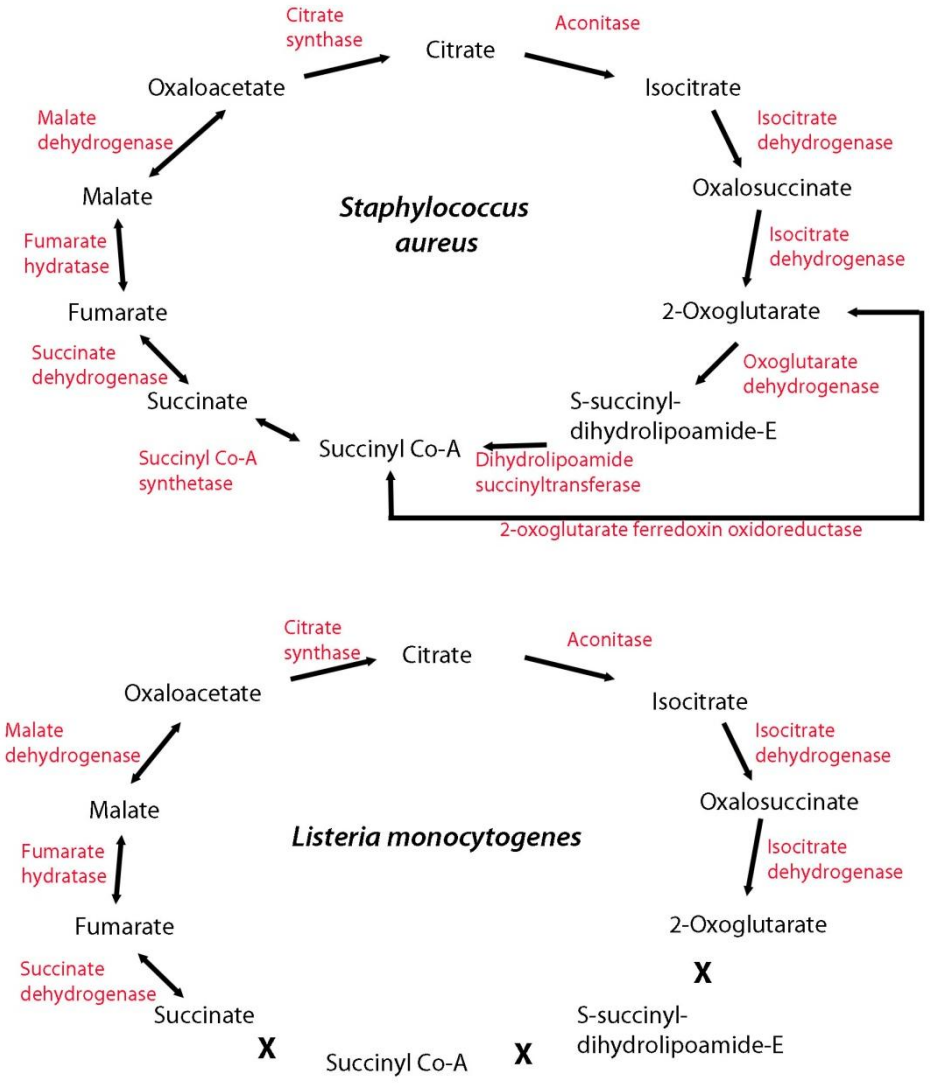

Figure 3.6. Tricarboxylic acid cycles of *S. aureus* and *L. monocytogenes* (adapted from Kegg Pathways). Enzymes catalysing conversion of intermediates are shown in red. Missing corresponding enzymes in *Listeria* are marked with an **X**.

In addition the synthesis of oxaloacetate can potentiate the gluconeogenic energy pathway. Amino acids can be metabolised to one of a number of TCA cycle precursors and intermediates which are incorporated into the energy cycle (according to Kegg Pathways). The TCA cycle may provide an efficient energy mechanism for *S. aureus* to replicate in an environment where amino acids/ peptides become the most primary carbon nutrient source. This may reflect the superior efficiency and high capacity replication of *S. aureus* in LB and indeed BHI media compared to *L. monocytogenes.*

Chapter 4

Construction and characterisation of sugar phosphate transporter mutants in *S. aureus* USA300 LAC

4.1 Introduction

S. aureus strains exploited exogenous hexose phosphates and glycerol monophosphate from minimal media to replicate to bacterial yields significantly higher than those attained through PTS-dependent sugars. Sugar phosphates can be recognised as highly nutritious sources from which *S. aureus* may thrive during invasive infection. In particular, *S. aureus* USA300 LAC growth benefitted greatly from sugar phosphates *in vitro*. Intracellular replication, and subsequent pathogenesis, may be attributed to the exploitation of these substrates. Given the highly destructive, disseminate and invasive nature of USA300, it was essential to investigate the value of sugar phosphate acquisition towards CA-MRSA infection.

4.2 Objectives

The means by which *S. aureus* imports exogenous hexose phosphates and glycerol monophosphate needed to be established by bioinformatic analysis. The *S. aureus* genes encoding putative transporters were subject to mutagenesis in order to disable access to extracellular sugar phosphates. The substrate specificity could then be investigated for each channel. In addition to single mutants, a double deletion mutation was constructed with the intent of abolishing the ability of USA300 LAC to derive *in vitro* growth from G-6-P, F-6-P and Gol-1-P as sole carbon nutrient sources. This strategy was implemented to establish whether redundant mechanisms contributed to sugar phosphate uptake, and to create a strain that was impaired specifically in sugar phosphate uptake for analysis of intracellular replication.

It has been known for decades that the organophosphate antibiotic fosfomycin penetrates susceptible bacteria almost exclusively through UhpT and GlpT transporters (Kahan *et al.* 1974). It is well documented, that *S. aureus* strains are particularly vulnerable to fosfomycin *in vitro* (Alvarez *et al.* 1985; Falagas *et al.* 2010; Popovic *et al.* 2010). Fosfomycin was

therefore investigated in the context of a transporter substrate to determine specificity of fosfomycin uptake in USA300 LAC.

4.3 Relevant materials and methods

Molecular Techniques (2.3); *S. aureus* USA300 LAC mutagenesis (2.3.6), Bioinformatic analysis (2.3.8).

***In vitro* assays (2.4);** Bacterial growth (2.4.1), Haemolytic titre (2.4.3), Fosfomycin susceptibility testing (2.4.4).

Statistical analysis (2.6) Significant difference was calculated between un-supplemented vs supplemented data sets of *in vitro* growth at the final measured points.

4.4 Results

4.4.1 Bioinformatic analysis of putative sugar phosphate permeases

4.4.1.1 Localisation of putative transporter genes in *S. aureus* USA300

The genome of *S. aureus* USA300 has been sequenced (Diep *et al.* 2006) and it contains two chromosomally encoded putative sugar phosphate permease genes, *uhpT* and *glpT*.

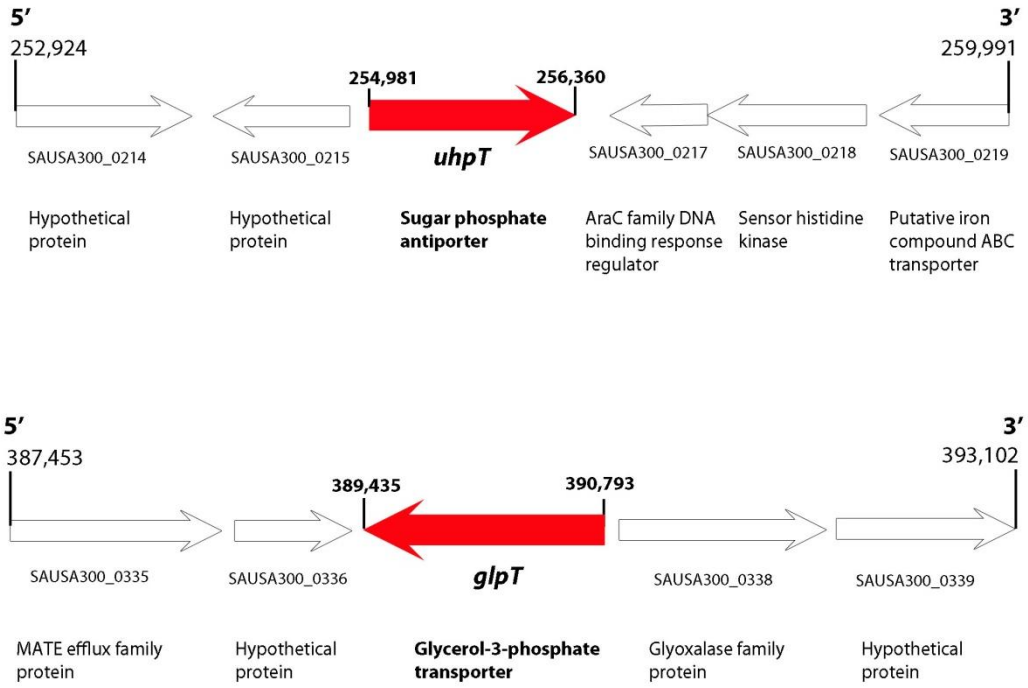

Figure 4.1. *S. aureus* USA300 genome loci of putative sugar phosphate permeases *uhpT* and *glpT*.

Figure 4.1 illustrates the USA300 chromosome locus of both these alleles. The putative hexose phosphate transporter, *uhpT* (annotated sugar phosphate antiporter) is encoded between 254 and 257 kb in the 2.76 million base pair genome of USA300. A designated glycerol-3-phosphate transporter gene, *glpT,* is encoded between 389 and 391 kilobase pairs of

the genome, in the reverse sense. These two homologous proteins are the only putative sugar phosphate transporters present in the *S. aureus* genome. All sequenced *S. aureus* genomes encode identical gene sequences for *uhpT* and *glpT*.

4.4.1.2 Homology of putative sugar phosphate transporters

Protein residue sequence analysis of *S. aureus* UhpT and GlpT was performed using Blast alignment. Amino acid sequences were matched to documented similar sequences, which indicate homology between proteins. Table 4.1 lists a variety of bacterial species encoding proteins which scored highly in sequence identity to *S. aureus* USA300 LAC UhpT. Table 4.2 lists bacterial proteins with high homology referenced to *S. aureus* USA300 LAC GlpT protein sequence.

Table 4.1. Blast alignment analysis showing highly similar proteins using USA300 LAC UhpT as the reference sequence.

Accession	Gene	Designation	Species	% Amino acid sequence identity
Q8CQE4	SE_0164	Hexose phosphate transport protein	*Staphylococcus epidermidis*	96
H2I4B4	*uhpT*	Sugar phosphate antiporter	*Corynebacterium diphtheriae*	76
B2V3Q5	CLH_1068	Hexose phosphate transport protein	*Clostridium botulinum*	65
T2KWZ2	*uhpT*	Hexose phosphate transport protein	*Listeria monocytogenes*	53
H8IC88	*uhpT*	Sugar phosphate antiporter	*Pasteurella multocida*	53
V3M5E4	L386_04434	Hexose phosphate transporter	*Klebisella pneumoniae*	51
V2GQY6	*uhpT*	Sugar phosphate antiporter	*Salmonella enterica*	51
H1R2P0	*uhpT*	Sugar phosphate antiporter	*Vibrio fischeri*	50
C8TZ30	*uhpT*	Hexose phosphate transporter	*Escherichia coli*	48
Q329E9	*uhpT*	Hexose phosphate transport protein	*Shigella dysenteriae*	48

Table 4.2. Blast alignment analysis showing highly similar proteins using USA300 LAC GlpT as the reference sequence.

Accession	Gene	Designation	Species	% Amino acid sequence identity
Q8CN35	SE_2047	Glycerol-3-phosphate transporter	*Staphylococcus epidermidis*	86
N0DBP7	*glpT*	Glycerol-3-phosphate permease	*Bacillus subtilis*	62
J1YHA1	*glpT*	Glycerol-3-phosphate transporter	*Vibrio cholerae*	61
Q1ZMV1	VAS14_08945	Glycerol-3-phosphate transporter	*Photobacterium angustum*	60
A6VE09	*glpT*	Glycerol-3-phosphate transporter	*Pseudomonas aeruginosa*	57
P08194	*glpT*	Glycerol-3-phosphate transporter	*Escherichia coli*	55
P96335	*glpT*	Glycerol-3-phosphate transporter	*Haemophilus influenzae*	50
A7FD94	*glpT*	Glycerol-3-phosphate transporter	*Yersinia pseudotuberculosis*	56
Q8XNV0	*glpT*	Glycerol-3-phosphate transporter	*Clostridium perfringens*	42
A0Q5L4	*glpT*	Glycerol-3-phosphate transporter	*Francisella tularensis*	42

Homologous UhpT and GlpT protein sequences were analysed for conserved domains in order to confirm functional commonalities. Figure 4.2A and 4.2B shows the common structural domains detected for homologous UhpT and GlpT proteins respectively, as compared in Table 4.1 and 4.2. Together the bioinformatics analysis confirms that *S. aureus* USA300 LAC UhpT and GlpT are major facilitator superfamily (MFS) proteins that are highly related to widespread, redundant bacterial MFS transporters with roles in organophosphate transport. These proteins are therefore the key targets for mutagenesis.

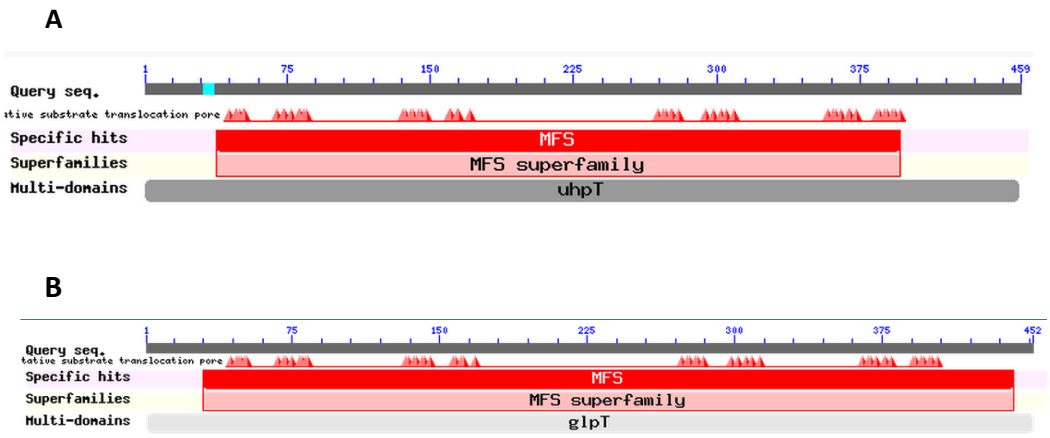

Figure 4.2. Secondary structure analysis of homologous sugar phosphate permeases. Protein sequences depicted in Table 4.1 and 4.2 were analysed for conserved domains using NCBI conserved domain search. Schematics show highly similar sequence regions of homologous proteins and annotates the conserved domains found within the structure. **A.** UhpT analysis **B.** GlpT analysis.

4.4.2 Mutagenesis of putative sugar phosphate permeases

In-frame gene deletion mutations were introduced to *uhpT* and *glpT* alleles encoding the hexose phosphate and glycerol phosphate permease of *S. aureus* USA300 LAC respectively. These mutants, Δ*uhpT* and Δ*glpT,* were constructed by allelic replacement of truncated genes via homologous recombination using pMAD-Cm shuttle vectors. In addition to single mutants, a USA300 LAC strain was created with gene deletions in both transporter alleles, termed Δ*uhpT*Δ*glpT.*

4.4.3 Genotypic characterisation of transporter mutants

Allelic replacement of specific sugar phosphate transporters was confirmed by PCR of mutant genomic DNA and compared to WT gene amplification (Figure 4.3A and B). Native plasmid profiles of all strains were visualised to assess the isogenicity of mutants after undergoing the mutagenesis protocol. Figure 4.3C highlights that the large 27kbp native plasmid of USA300, pUSA03, is only present in the clinical WT strain, with an absent band above 10,000 base pairs for all mutant strains. Further investigation revealed that pUSA03 was lost at the stage of temperature dependent pMAD-Cm excision from the chromosome. Figure 4.3D shows that WT strains containing genome integrated constructs displayed a complete native plasmid profile, while in the single mutant Δ*glpT* strain, pUSA03 is already absent.

Native plasmid pUSA03 was recurrently lost in repeated mutagenesis. Mutant strains were not isogenic to the clinical wild type USA300 LAC background. The cost of replication of pUSA300 may have an impact on the fitness of USA300 LAC and therefore it was important to assess strains in the same genetic background. Allelic replacement of the *glpT* gene yielded a wild type *glpT* revertant strain which was cured of the pUSA03 plasmid, termed $WT^{(-p03)}$. Figure 4.3C shows the native plasmid profile of $WT^{(-p03)}$ with an absent plasmid DNA band above 10,000 bp relative to the clinical WT. A complete set of isogenic strains was established to conduct analysis.

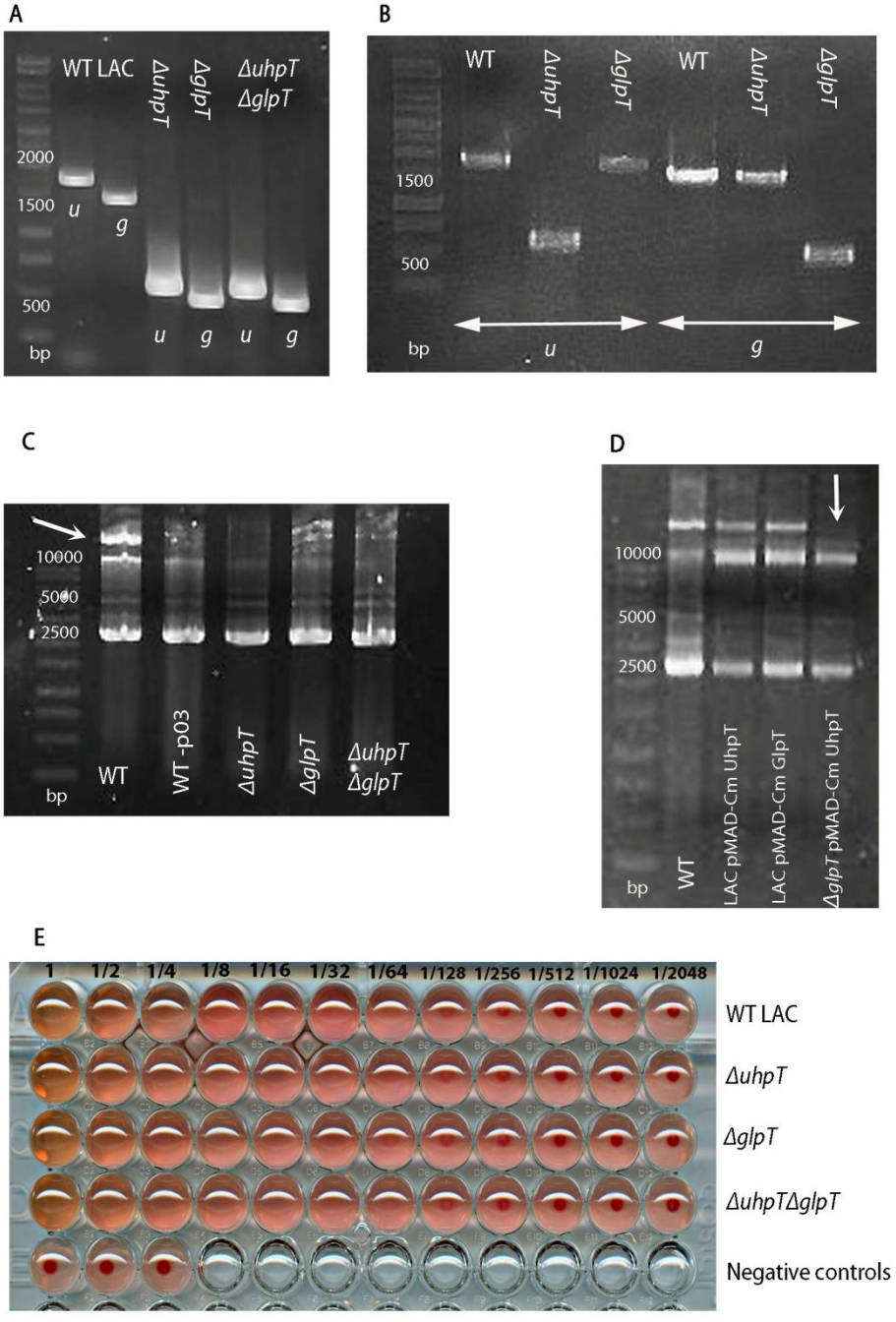

Figure 4.3. Characterisation of *S. aureus* USA300 LAC strains. A. PCR amplification of *uhpT* (u) and *glpT* (g) alleles from genomic DNA using SA UhpTF1_BamHI / R2_SpeI and SA GlpTF1_BamHI/ R2 primers. **B.** PCR amplification of genomic u & g genes showing wild-type sequences. **C.** Native plasmid profiles highlighting absence of pUSA03 in mutant and isogenic WT strains. **D.** Native plasmid profiles of first recombinant strains relative to the WT native plasmid profile. **E.** Hemolysis assay showing doubling dilutions of bacterial supernatant in rabbit erythrocytes.

4.4.4 Phenotypic characterisation of transporter mutants

4.4.4.1 *agr* activity

It is paramount that genetic modification of chromosomal DNA does not cause unspecific mutations in the *agr* system and subsequently affect virulence regulation of USA300 LAC. This system is responsible for controlling haemolytic toxin secretion which causes lysis of erythrocytes. The functionality of *agr* was measured using a haemolytic titre to compare toxin secretion among USA300 LAC strains. Figure 4.3E shows the titration of bacterial supernatant incubated in a fixed amount of rabbit red blood cells. Dark red agglutination of erythrocytes in the centre of the well indicates unaffected, whole red blood cells. In all strains, erythrocytes start to become visible at a dilution of 1/64, indicating that haemolytic toxins are reaching a concentration insufficient to cause full lysis. Toxin production, dependent upon *agr*, causing blood lysis is comparable between all mutants and WT USA300 LAC. This figure confirms that *agr* regulatory activity in mutated strains has not been disturbed by mutant construction and virulence is unaffected.

4.4.4.2 General *in vitro* nutrient growth

Mutant strains were analysed in multi-nutrient media using *in vitro* growth assays in order to verify that the general metabolic capacity was unaffected. Figure 4.4A and B show replication of isogenic strains in BHI and LB media respectively. Rapid and high yield growth of all mutant strains is virtually identical to WT USA300 LAC up to 18h ($p = << 0.05$). *In vitro* growth of mutants was also examined in glucose supplemented HHWm* media to ensure that metabolism of non-phosphorylated sugar remained stable. Figure 4.4C illustrates that mutant strains metabolise glucose with the same efficiency as WT USA300 LAC.

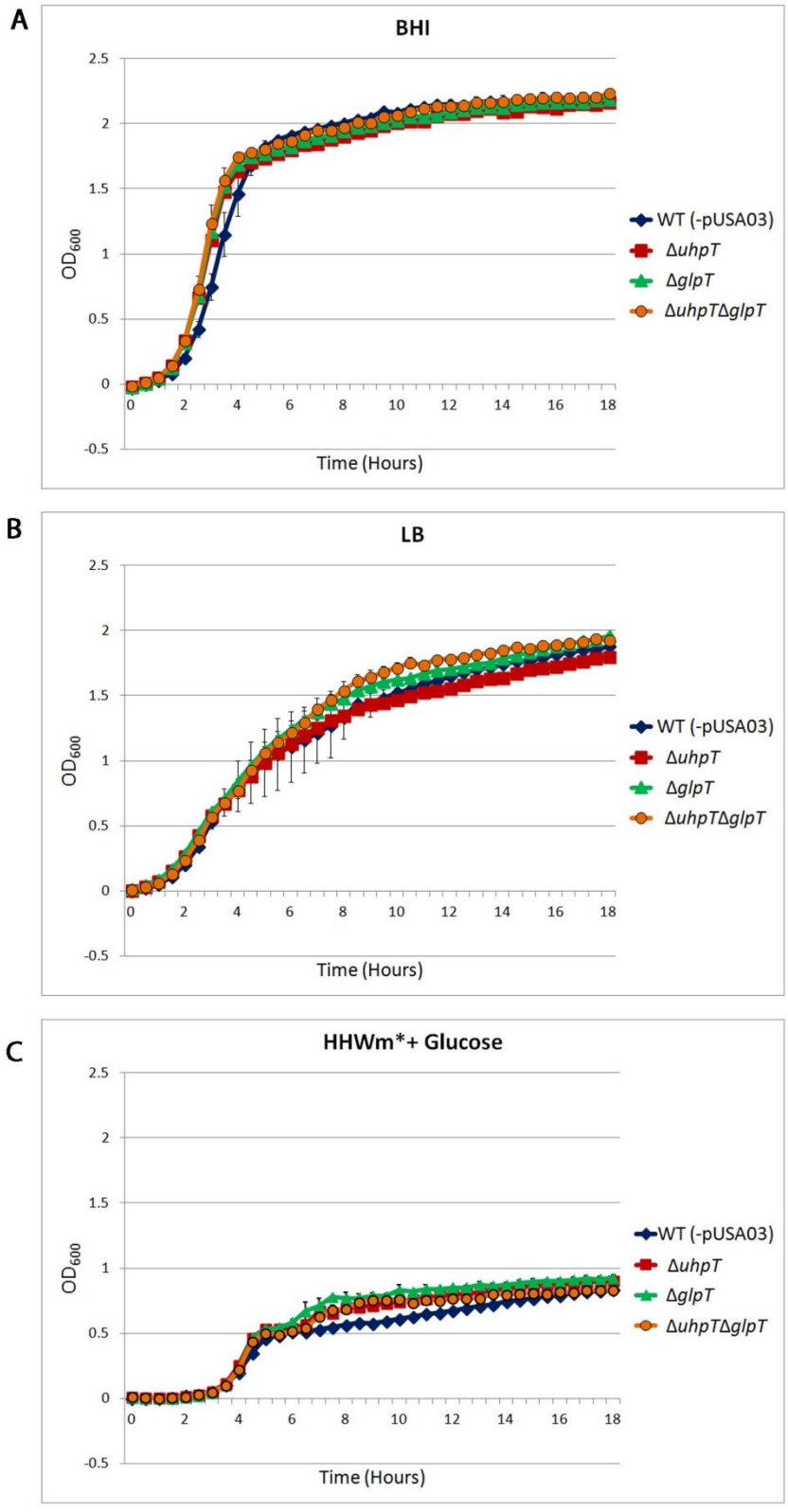

Figure 4.4. *In vitro* growth analysis of isogenic *S. aureus* USA300 LAC strains. **A.** BHI multi-nutrient media **B.** LB multi-nutrient media. **C.** Chemically defined minimal media supplemented with 20mM glucose. Charts show a representative assay ± standard deviation.

4.4.4.3 Substrate specific *in vitro* growth

S. aureus USA300 LAC mutant strains were monitored in HHWm* chemically defined minimal media supplemented with single sugar phosphate substrates that promote WT growth. Figure 4.5 charts the replication of mutant strains in G-6-P, F-6-P and Gol-1-P, comparing the level reached by WT USA300 LAC in the same conditions. The mutant Δ*uhpT* strain does not have the ability to grow in G-6-P or F-6-P beyond basal level (p= <0.05). By 16h, there is a 5.5 – 6 fold reduction in growth yield compared to WT replication in these hexose phosphate sugars. The Δ*glpT* mutant retains the capacity for growth upon hexose phosphates, reaching a similar yield to the WT, with the same efficiency (OD_{600} 0.2 per hour). Hexose phosphates therefore are transported exclusively through the UhpT transporter in *S. aureus* USA300 LAC.

Both Δ*uhpT* and Δ*glpT* single mutant strains maintain the ability to grow upon Gol-1-P to a level significantly higher than the un-supplemented medium at 24h (p= 0.001, p= 0.007). WT USA300 LAC utilised Gol-1-P to reach OD_{600} 1.1 by 16h with an efficiency of OD_{600} 0.1 per hour. By contrast Δ*uhpT* replicated to 4.5 times lower yield by the same time with a marked reduced efficiency. Single mutant Δ*glpT* utilised Gol-1-P to half the yield and half the efficiency of the WT. Glycerol monophosphate is exploited with greater efficiency through the UhpT channel as opposed to the GlpT channel, although simultaneous expression is required to have a synergistic effect upon growth.

Deletion of both sugar phosphate transporters, Δ*uhpT*Δ*glpT*, ensures that *S. aureus* USA300 LAC is totally unable to utilise any sugar phosphate substrates and concludes that no other transport systems exist in this strain which can exploit sugar phosphates.

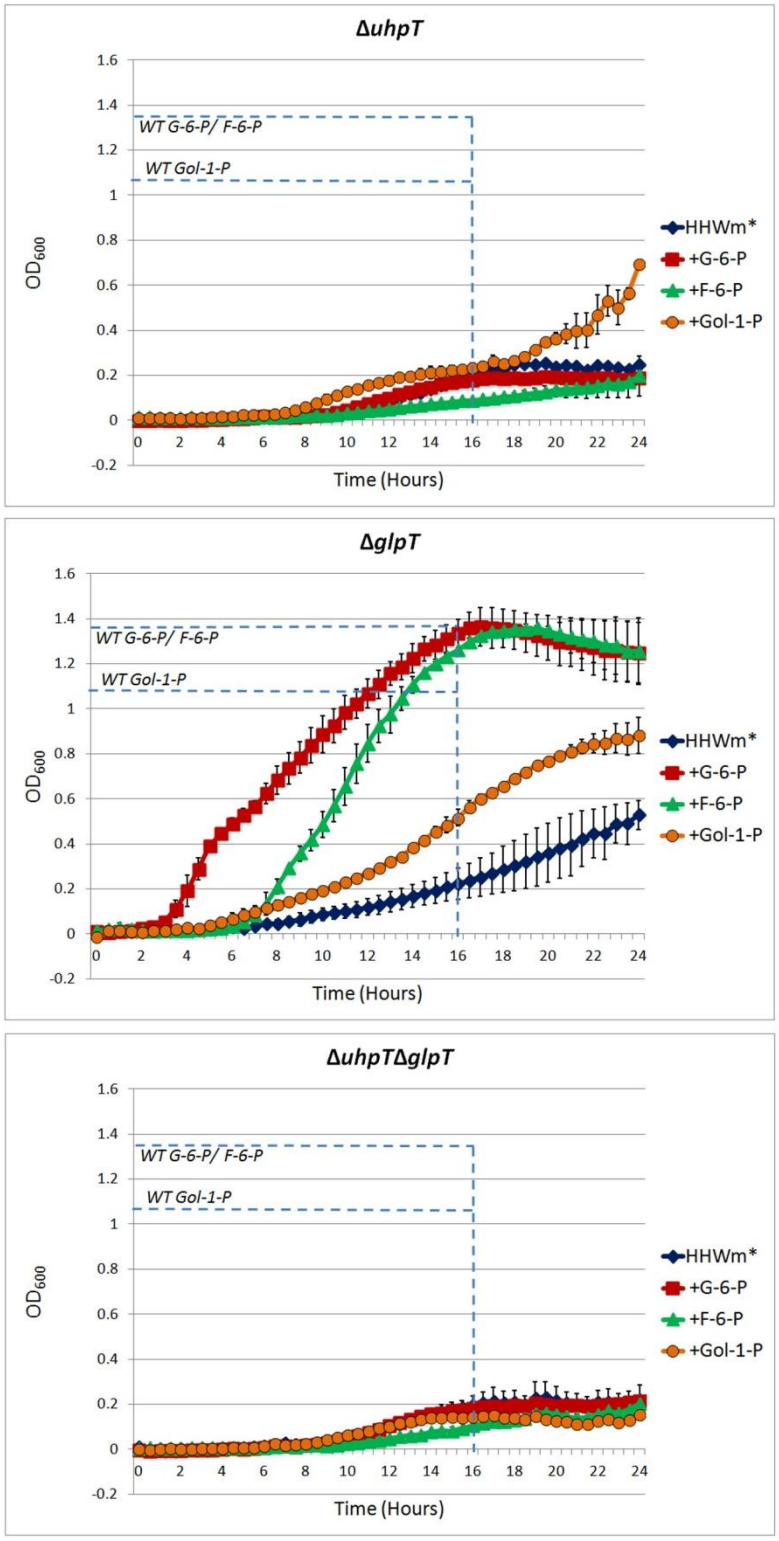

Figure 4.5. *In vitro* growth of *S. aureus* USA300 LAC mutants in sugar phosphates. Average growth in sugar phosphates supplemented HHWm* medium (20mM). Dashed lines represent the WT growth level reached by 16 hours (entry into stationary phase) in appropriately labelled substrates. Average growth is formulated from at least 2 separate assays and include the standard error of the mean.

4.4.4.4 Fosfomycin specificity

S. aureus USA300 LAC mutants were initially analysed via *in vitro* growth assays, performed in LB medium supplemented with fosfomycin solution. Un-supplemented LB media stimulates rapid, high level replication by USA300 LAC strains, providing a platform to study effects of fosfomycin inhibition. Figure 4.6 shows the inhibitory effect of fosfomycin upon isogenic *S. aureus* USA300 LAC strains relative to the collective average growth in un-supplemented LB media. The WT strain, able to express both UhpT and GlpT, is totally inhibited by fosfomycin. Single transporter mutants are severely inhibited in growth until 15h where there is evidence of replication by resistant bacteria. When both UhpT and GlpT are deleted, fosfomycin does not have an effect upon the exponential growth, nor the bacterial yield reached. This evidence indicates that *S. aureus* USA300 LAC primarily uptakes fosfomycin through UhpT and GlpT transporters.

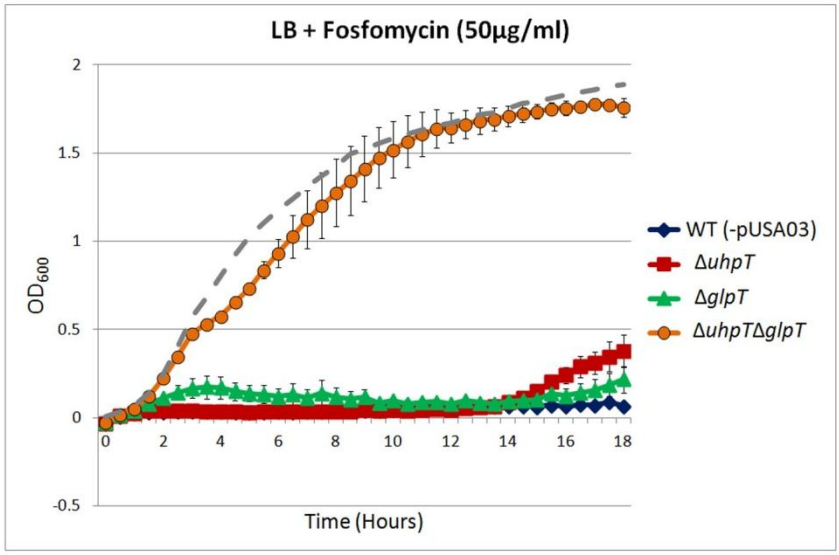

Figure 4.6. *In vitro* growth of isogenic *S. aureus* USA300 LAC strains in LB supplemented with fosfomycin. Average growth was calculated from 2 separate assays and shows standard error of the mean. Collated average growth of all strains in un-supplemented LB is represented by a grey dashed line.

Fosfomycin susceptibility of S. aureus USA300 LAC strains was quantified using an Epsilometer test (E-test). A strip infused with increasing concentrations of fosfomycin was placed on an LB nutrient agar plate containing a lawn of *S. aureus* USA300 LAC. Figure 4.7 displays the inhibitory action of fosfomycin upon mutant and WT strains. The zone of inhibition exhibited by fosfomycin action can be observed until the bacterial lawn converges with the strip. This indicates the minimum inhibitory concentration (MIC). According to Figure 4.7, the MIC for each strain is presented in Table 4.3.

Table 4.3. Minimum inhibitory fosfomycin concentration for *S. aureus* USA300 LAC strains.

Strain	Fosfomycin MIC (µg/ml)
WT	3
Δ*uhpT*	3
Δ*glpT*	5
Δ*uhpT*Δ*glpT*	≥1024

The E-test confirms that *S. aureus* USA300 LAC UhpT and GlpT transporters can uptake fosfomycin at similar capacity. Removal of a single permease does not significantly affect fosfomycin susceptibility, although it increases the frequency of resistant colonies growing within the zone of inhibition. Removal of both functional transporters results in resistance to fosfomycin.

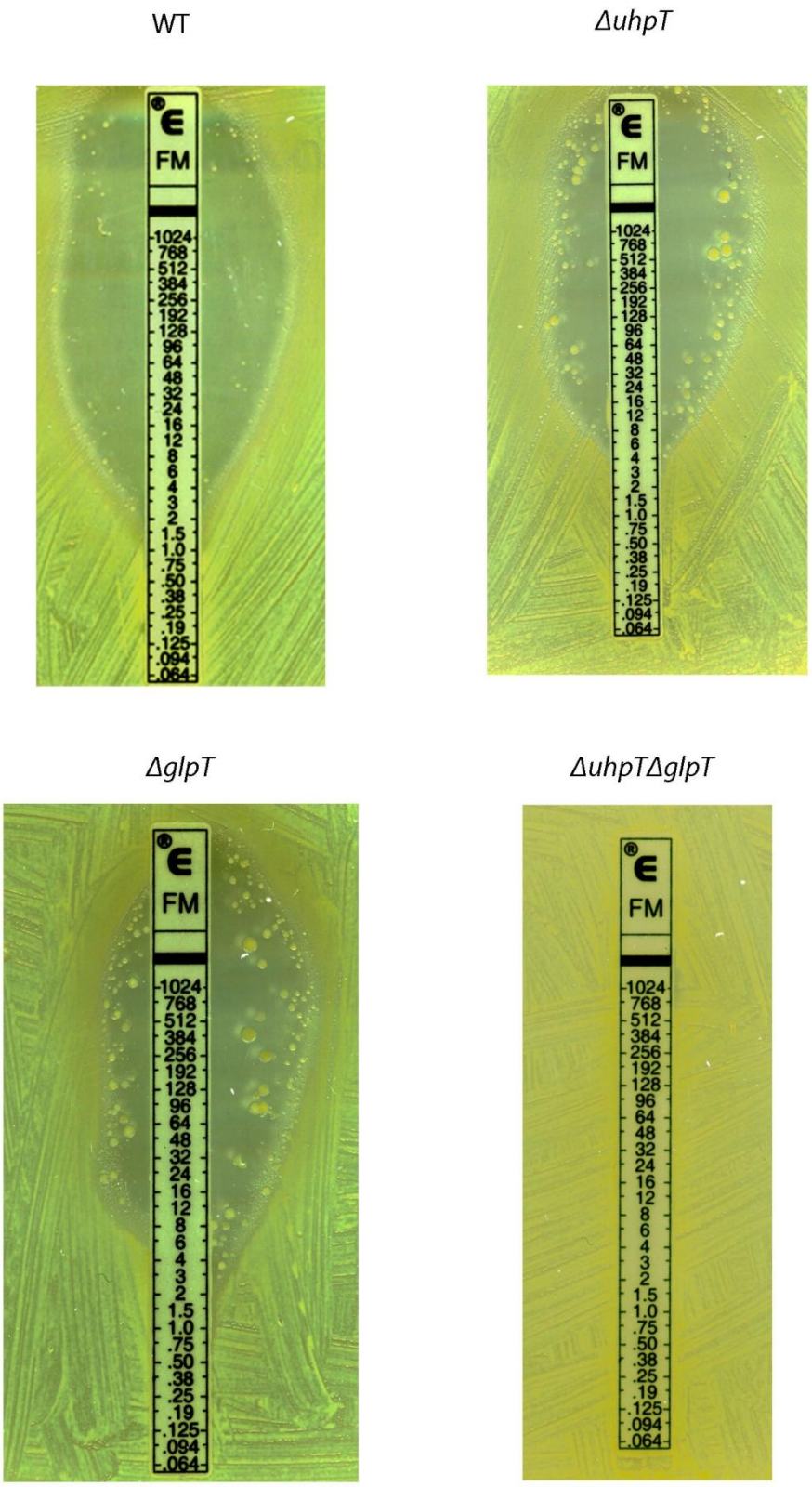

Figure 4.7. Fosfomycin E-Tests performed on LB agar featuring *S. aureus* USA300 LAC strains. Images show the extent of growth inhibition by a fosfomycin concentration gradient.

4.5 Discussion

Through bioinformatic analysis and mutagenesis research, the status of UhpT and GlpT as sugar phosphate transporters was confirmed for *S. aureus* USA300 LAC.

4.5.1 Specificity determination

A single deletion mutation in the hexose phosphate transporter gene of USA300 LAC, Δ*uhpT,* eliminated *in vitro* growth in hexose phosphate sugars G-6-P and F-6-P. The exclusive uptake of hexose phosphates by UhpT is consistent with mutagenesis studies in other species, such as *L. monocytogenes, E. coli*, *S. enterica, S. flexineri* and (Chico-calero *et al.* 2002; Goetz & Goebel 2010; Runyen-Janecky & Payne 2002). Only one study uncovers a novel, redundant and unknown mechanism for uptake of glucose-6-phosphate in the absence of UhpT which occurs in a strain of enteroinvasive *E. coli* (Goetz & Goebel 2010). In *E. coli*, other hexose phosphates have been identified as specific substrates for UhpT, such as 2-deoxyglucose-6-phosphate, fructose-1-phosphate, glucose-1-phosphate and mannose-6-phosphate (Dietz 1976). The latter two substrates have also been confirmed as growth substrates channelled through the listerial Hpt (Chico-Calero *et al.* 2002; Ripio *et al.* 1997).

Construction of a glycerol-3-phosphate transporter mutant, Δ*glpT*, did not abolish growth of *S. aureus* USA300 LAC in glycerol monophosphate. Only when the double deletion mutation was created, Δ*uhpT*Δ*glpT,* did replication cease upon Gol-1-P. This indicates that the hexose phosphate permease does not stringently transport hexose phosphates into the bacterial cell. Indeed, a study identified glycerol-3-phosphate and glyceraldehyde-3-phosphate as substrates transported through the homologous *E. coli* UhpT channel (Guth *et al.* 1980). It has been demonstrated that the UhpT permease of *E. coli* has the capacity to transport a more structurally diverse range of organophosphates, such as

pentose phosphates, heptose phosphates and amino hexose phosphates (Dietz 1976). Similarly, substrate analysis of the *Salmonella* UhpT permease showed that D-arabinose-5-phosphate and D-sedoheptulose-6-phosphate were transported with similar affinity to glucose-6-phosphate (Eidels *et al.* 1974). The selection of 3, 5, 6 and 7 carbon cyclic and linear substrates that are imported via the hexose phosphate permease represents a non-stringent capacity for organophosphate substrates. This may denote a proficient and energy conserving strategy of nutrient acquisition by which many resources can be encompassed using a single channel. Perhaps this may increase the value of the UhpT channel in nutrient scavenging during infection.

Glycerol monophosphate was the only verified organophosphate nutrient imported by USA300 LAC GlpT in the *in vitro* conditions of this study. The only known verified substrates specific for the putative GlpT permease are glycerol monophosphate, fosfomycin and arsenate (Law *et al.* 2009; Elvin *et al.* 1985). Several specific side chain residues in the lumen of the GlpT channel require interaction with glycerol and inorganic phosphate (Pi) moieties of glycerol monophosphate (and residues interacting with the Pi moiety of fosfomycin) in order for the permease to operate (Law *et al.* 2009). This may account for the stringent specificity relative to UhpT.

A *S. aureus* USA300 LAC strain with deletion mutations in both the UhpT and GlpT transporter genes was completely unable to grow in sugar phosphate substrates as sole carbon sources *in vitro*. This confirms that no redundant mechanisms exist in the USA300 LAC genome which allows import of sugar phosphates. The Δ*uhpT*Δ*glpT* strain was unimpaired in capability to grow on other important non-organophosphate nutrients such as amino acids and PTS dependent sugar. This strain can be employed to directly investigate the role of sugar phosphate acquisition in intracellular replication of USA300 LAC.

The organophosphate antibiotic fosfomycin was able to penetrate USA300 LAC, causing inhibition of growth, through UhpT and GlpT permeases to an equal capacity. Deletion mutation of both transporters coincided with complete resistance to the antibiotic, demonstrating that there is no other high capacity import mechanism for fosfomycin.

4.5.2 Emergence of fosfomycin resistant colonies

Upon deletion of a single permease gene, the frequency of fosfomycin resistant colonies increased. Like the majority of antibiotics in use, fosfomycin action is subject to bacterial resistance mechanisms (Popovic *et al.* 2010). *S. aureus* USA300 strains contain a chromosomally encoded fosfomycin resistance protein, FosB (Tenover *et al.* 2006). FosB is an intracellular metallo-enzyme which catalyses the opening of the epoxide ring of fosfomycin, thereby changing its structure and eliminating its function (Wright 2005). FosB expression is one possible mechanism by which resistant USA300 colonies can develop. Alternative strategies of fosfomycin resistance have been verified among other bacteria. A single amino acid mutation in the active site of the fosfomycin target, UDP-GlcNAc enolpyruvyl transferase (MurA) conferred resistance in *E. coli* isolates (Kim *et al.* 1996). A recent study found that the most common traits of resistant clinical *E. coli* isolates were mutations to the UhpT and GlpT protein sequences. In some isolates the entire *uhpT* gene was lost, and frequently the GlpT protein was severely truncated (Takahata *et al.* 2010). Similarly, the single fosfomycin resistance mechanism found in *P. aeruginosa* was mutation to the GlpT transporter, the only sugar phosphate permease found in this species, which conferred a lack of uptake of glycerol-3-phosphate and fosfomycin (Castañeda-García *et al.* 2009). The connotations of these studies are that bacterial sugar phosphate permeases can be dispensable in order to promote fitness under fosfomycin pressure. This raises questions regarding importance of sugar phosphate uptake as a mechanism to promote intracellular replication.

Chapter 5

Heterologous expression of *S. aureus* sugar phosphate permeases

5.1 Introduction

A narrow range of organophosphate substrates was confirmed to be imported by *S. aureus* USA300 LAC through UhpT and GlpT channels. The unexamined expression system of *S. aureus* UhpT and GlpT, together with the complex metabolic background of this species, complicates the direct study of sugar phosphate metabolism. *L. monocytogenes* has a metabolic background that relies upon carbohydrates for growth (Eisenreich *et al.* 2010). In particular, the uptake of sugar phosphates, via the listerial hexose phosphate transporter, has a demonstrable advantage both intracellularly (*ex vivo*) and *in vivo* (Chico-calero *et al.* 2002). In the genetic background of *L. monocytogenes*, sugar phosphates are a valuable carbon nutrient source and as expression of Hpt is inducible by the endogenous virulence regulator PrfA, substrate specificity is not discriminated by extracellular sensory induction of expression by organophosphates. *L. monocytogenes* therefore offers a background in which *S. aureus* UhpT and GlpT can be expressed to explicitly analyse substrate specificity and functionality.

5.2 Objectives

L. monocytogenes strain P14-A Δ*hpt* was used as a recipient strain for complementation of *S. aureus* permease genes. In this background staphylococcal permeases were compared to listerial Hpt in an expanded range of transported organophosphates and their capacity for growth on these sugar phosphate nutrients. Replication of *S. aureus* permease complemented strains was monitored during cell infection to determine whether transporters performed a similar intracellular function to listerial Hpt. Complementation analysis was performed in order to consolidate the functionality of *S. aureus* UhpT and GlpT relative to the established homologous *L. monocytogenes* Hpt permease.

5.3 Relevant materials and methods

Molecular techniques (2.3) Gene complementation of *L. monocytogenes* P14-A Δ*hpt* (2.3.7)

***In vitro* assays (2.4)** Bacterial growth (2.4.1)

Mammalian cell culture (2.5) *L. monocytogenes* infection (2.5.3.2)

Statistical analysis (2.6) Significant difference was calculated between;
i) Un-supplemented vs supplemented data sets of *in vitro* growth at the final measured point (18h).

ii) Intracellular growth coefficient data sets at 8h intracellular infection.

5.4 Results

5.4.1 Complementation of *L. monocytogenes* P14-A Δ*hpt*

L. monocytogenes P14-A is a *prfA* mutant, conferring constitutive activation of PrfA regulator which induces continual expression of *hpt*. P14-A therefore has the ability to grow *in vitro* upon sugar phosphates as single carbon nutrient sources. For this reason P14-A was used in order to compare replication of permease complemented strains with a background strain expressing WT listerial *hpt*. Complementation of *L. monocytogenes* P14-A Δ*hpt* was performed using a stable, integrative listerial plasmid, pPL2, which incorporated an appropriate constitutive promoter for permease gene expression. The construction methods are outlined in 2.3.8.

5.4.2 Substrate specific *in vitro* growth of P14-A strains

In vitro growth assays were performed in LB medium, which produced a basal level of replication, to which sugar phosphate carbon sources were added individually.

5.4.2.1 P14-A and P14-A Δ*hpt*

L. monocytogenes P14-A and Δ*hpt* were analysed to establish the parameters for listerial growth in sugar phosphates. Figure 5.1A shows the capability of P14-A to grow in a range of C6 and C3 phosphorylated sugars. G-6-P and F-6-P were utilised equally efficiently (OD_{600} 0.2 per hour) to reach the same level, 5.5 fold higher than the un-supplemented growth level ($p=<<0.05$). G-1-P was utilised to 3 fold higher yield than basal level ($p=<<0.05$). G-1-P was exploited as efficiently as other hexose phosphates but growth is arrested at 60% of their stationary level. Glycerol-1-phosphate was metabolised to reach double the level of LB alone ($p=<<0.05$) while Gol-3-P was utilised to reach double the basal level by 14h with very poor efficiency. Gol-2-P does not contribute to replication above the background level ($p=0.85$) and therefore was excluded from

further analyses. Figure 5.1B illustrates the capacity of *hpt* deficient *L. monocytogenes* P14-A for replication in the same range of sugar phosphates as Figure 5.1A. This strain cannot exploit any sugar phosphate substrates from supplemented media, as growth is non-significantly different from un-supplemented LB ($p = >0.05$). The conditions provide explicit evidence that listerial Hpt is responsible for exclusive uptake of exogenous C6 and C3 phosphorylated sugars. These parameters form a solid base for studying heterologous expression of UhpT and GlpT.

A

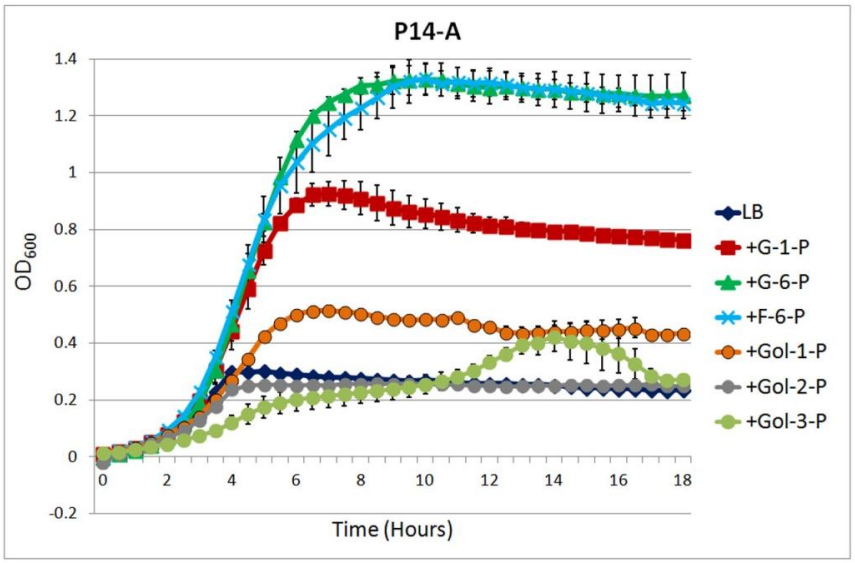

B

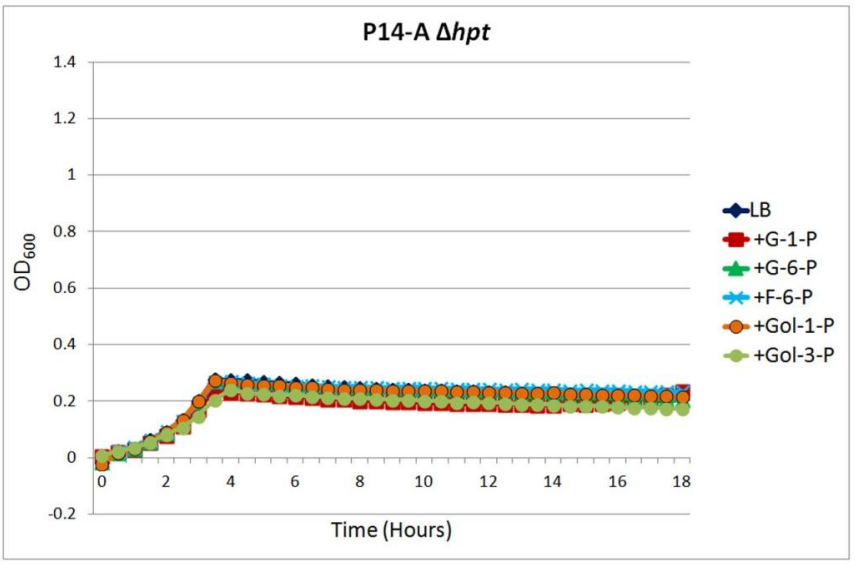

Figure 5.1. *In vitro* growth of *L.monocytogenes* strains in sugar phosphates. A. P14-A **B.** Δ*hpt*. Average growth in sugar phosphates supplemented LB media is calculated from at least 2 separate assays and shows standard error of the mean.

5.4.2.2 pPL2$_{(Psod)}$ complemented strains

Sugar phosphate permease genes were firstly expressed in *L. monocytogenes* P14-A Δ*hpt* under the control of listerial superoxide dismutase promoter (Psod). In addition to *S. aureus uhpT* and *glpT*, P14-A Δ*hpt* was complemented with the listerial *hpt* gene to serve as a positive control for sugar phosphate uptake.

Complemented strains were analysed for *in vitro* growth capacity in core sugar phosphates using LB as minimal medium. Figure 5.2A shows replication of Δ*hpt* expressing listerial *hpt* upon individual sugar phosphates. This strain is able to use G-6-P and F-6-P to replicate to OD_{600} 0.9 – 1 by 18h, which is to 80% of the level reached by P14-A. However, the efficiency of exponential growth in these substrates was half the rate of P14-A (OD_{600} 0.1 per hour). Replication of pPL2$_{(Psod)}$*hpt* using G-1-P follows a similar projection to other hexose phosphates. Importantly, P14-A utilised hexose phosphates to attain stationary phase growth by 6-8h (Figure 5.1A). By contrast pPL2$_{(Psod)}$*hpt* utilised the same hexose phosphates with poor efficiency and by 18h growth was still in exponential phase. Figure 5.2A demonstrates the Δ*hpt* strain expressing listerial *hpt* was incapable of replicating upon Gol-1-P or Gol-3-P (p=>0.05) which is in contrast to the background parameters established for P14-A (Figure 5.1A).

Figure 5.2B shows the replication of Δ*hpt* expressing staphylococcal u*hpT* using the same substrate range. The projection of growth using hexose phosphate sugars follows a similar pattern to pPL2$_{(Psod)}$*hpt.* Notably, complementation of Δ*hpt* with staphylococcal UhpT allows exploitation of G-1-P for replication. Strain pPL2$_{(Psod)}$*uhpT* was unable to use Gol-1-P or Gol-3-P to replicate beyond the minimal level (p=>0.05). This trait was shared by the Δ*hpt* strain expressing staphylococcal *glpT* as shown in Figure 5.2C.

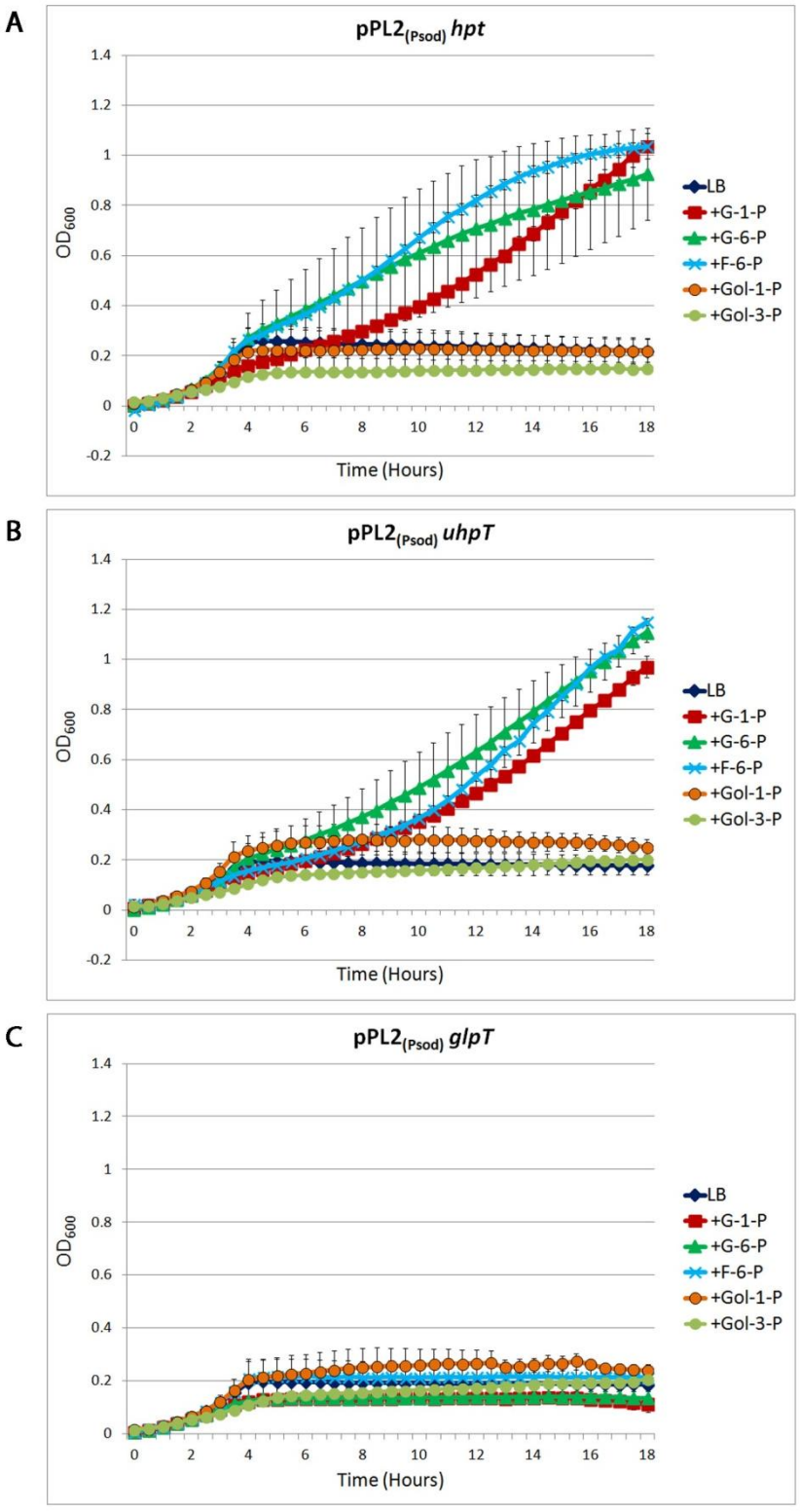

Figure 5.2. *In vitro* growth of pPL2$_{(Psod)}$ complemented *L. monocytogenes* P14-A Δ*hpt* strains in sugar phosphates. Average growth in sugar phosphate supplemented LB media is calculated from at least 2 separate assays and shows standard error of the mean. **A.** + *hpt* (*L. monocytogenes*). **B.** + *uhpT* (*S. aureus*) **C.** + *glpT* (*S. aureus*)

Taken together, the data concludes that while the complementation of *L. monocytogenes* Δ*hpt* with sugar phosphate permeases was successful, the expression of transporters from the Psod promoter was not strong enough to provide sugar phosphate uptake equivalent to P14-A.

5.4.2.3 pPL2$_{(PprfA)}$ complemented strains

The listerial *sod* promoter was substituted for the listerial *hpt* gene PrfA binding promoter region (PprfA) in an effort to influence increased expression of permeases. Complemented genes were placed under the control of constitutively expressed PrfA regulator, which represented the closest technique to replicate listerial *hpt* expression in control strain P14-A. *L. monocytogenes* P14-A Δ*hpt* strain was complemented with an empty expression vector, designated pPL2$_{(PprfA)}$ to serve as a negative control.

In vitro replication of complemented strains was monitored in LB supplemented with sugar phosphates. Figure 5.3A depicts pPL2$_{(PprfA)}$ growth in hexose phosphates and Gol-1-P. Replication did not significantly differ from basal level in any substrate (p=>0.05), indicating that this strain behaves in the same manner as background strain P14-A Δ*hpt.* Figure 5.3B shows growth of Δ*hpt* expressing listerial *hpt* in the same range of substrates. This strain replicates upon G-1-P and F-6-P to exponential growth efficiency similar to P14-A (Figure 5.1A). Growth upon G-6-P was marginally less efficient than G-1-P and F-6-P. By 18h, the growth yield reached in G-6-P and F-6-P was 3 fold greater than basal level (p=<<0.05) but 60-70% of the level reached by P14-A in the same substrates. G-1-P was utilised by pPL2$_{(PprfA)}$*hpt* to the same capacity as P14-A.Gol-1-P was utilised to double the basal level and is comparable to P14-A growth.

Figure 5.3C depicts replication of Δ*hpt* expressing staphylococcal *uhpT*. G-6-P and F-6-P were utilised with the same efficiency as P14-A, and reached the same stationary phase level of growth. G-1-P was used with equal efficiency as F-6-P and uptake through UhpT allowed for higher stationary

phase level of growth than P14-A. Gol-1-P was utilised by pPL2$_{(PprfA)}$*uhpT* to the same capacity of growth as P14-A.

Figure 5.4D depicts growth of Δ*hpt* expressing staphylococcal *glpT*. As predicted, this strain was unable to derive growth from hexose phosphate sugars (G-6-P data not completed) with growth projections not surpassing basal level (p=>0.05). Gol-1-P was utilised to reach twice the basal level by 18h (p=<0.05) and was comparable to the growth projection displayed by P14-A.

Figure 5.3E compares growth of complemented strains upon LB supplemented with glycerol-3-phosphate. The basal level of growth upon LB was lower than normal in this analysis and so replication upon Gol-3-P was presented separately to appreciate the significant difference. Strains expressing hexose phosphate permeases used Gol-3-P to reach a level 0.5 fold greater than negative control strain by 18h (p=<0.05). The Δ*hpt* strain expressing staphylococcal *glpT* was able to replicate upon Gol-3-P to 1.5 fold greater than basal level at 18h (p=<0.05).

Under the control of the PprfA promoter, permeases are expressed to promote replication of complemented Δ*hpt* strains upon sugar phosphates to growth efficiencies and stationary phase levels comparable to the positive background strain P14-A. This expression system could therefore be used to directly compare complemented strains expressing permeases and P14-A during intracellular infection.

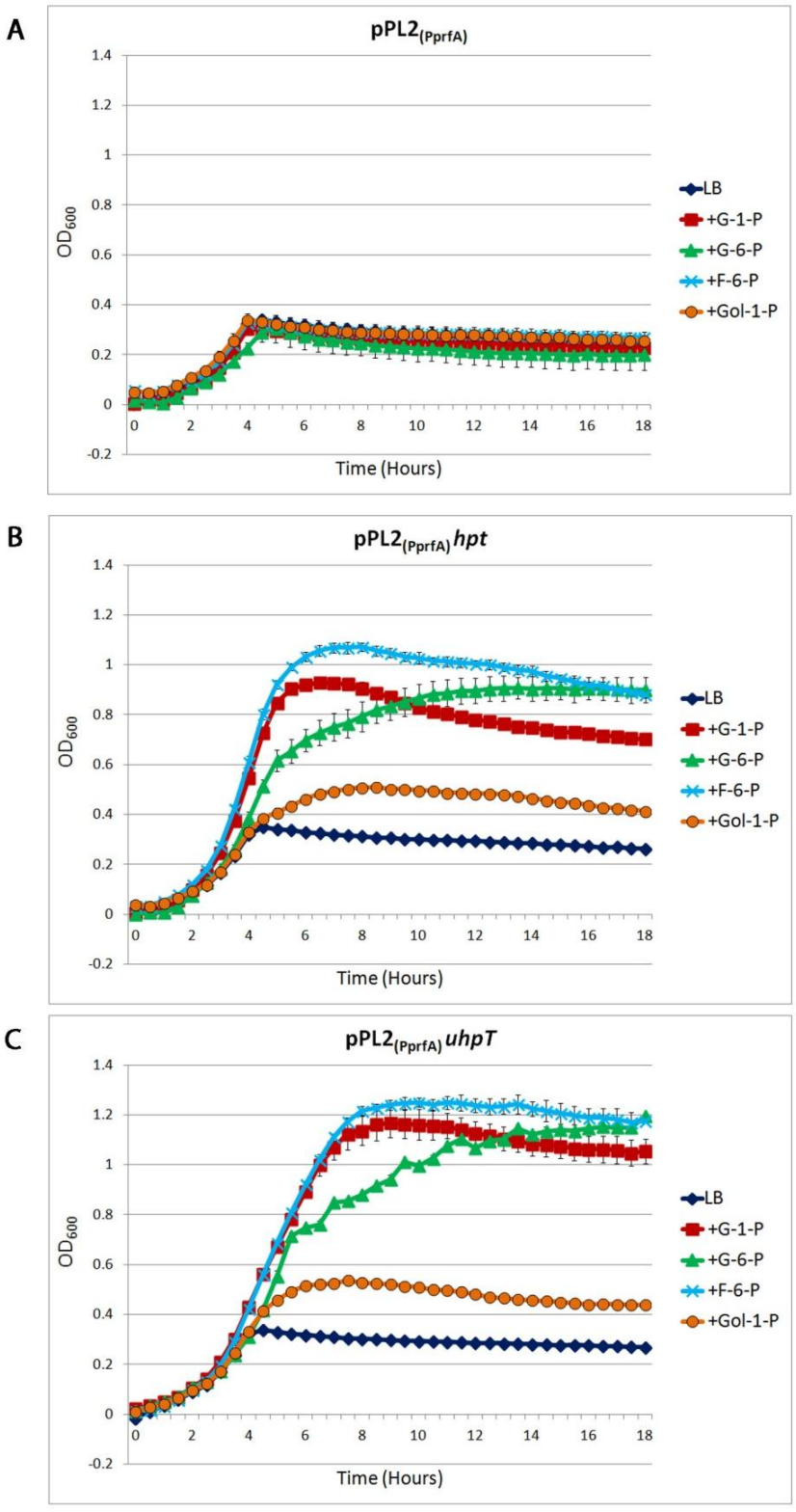

Figure 5.3. *In vitro* growth of pPL2 $_{(PprfA)}$ complemented *L.monocytogenes* P14-A Δ*hpt* strains in sugar phosphates. Average growth in sugar phosphate supplemented LB media is calculated from 2 separate assays and shows standard error of the mean. **A.** + Empty vector **B.** + *hpt* (*L. monocytogenes*). **C.** + *uhpT* (*S. aureus*)

D

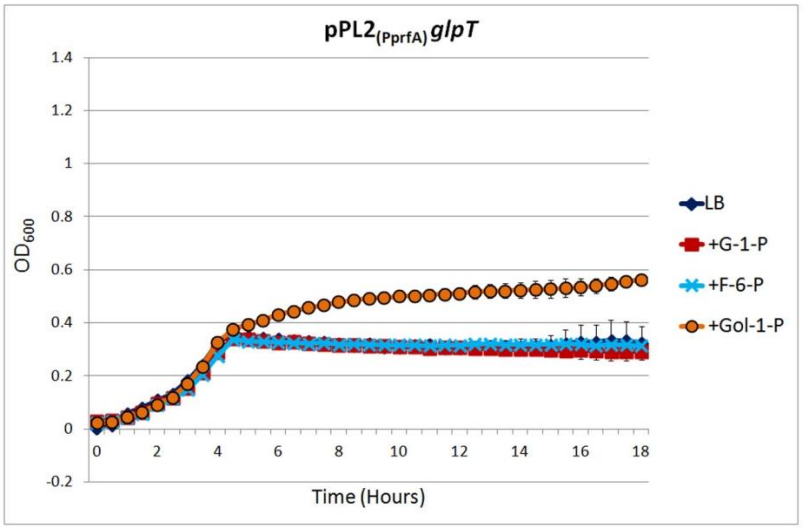

E

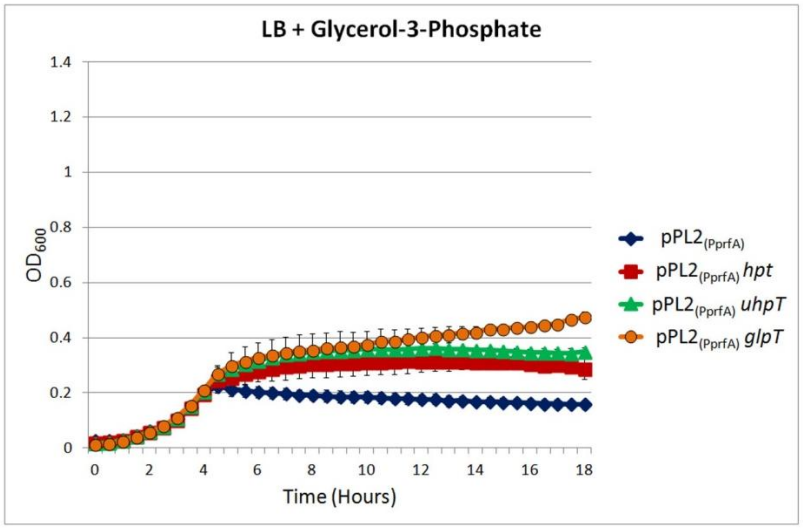

Figure 5.3 Continued. **D.** + *glpT* (*S. aureus*) **E.** Average growth ± SE of all $pPL2_{(PprfA)}$ complemented strains in LB supplemented with glycerol-3-phosphate.

5.4.2.4 Fosfomycin susceptibility of pPL2$_{(PprfA)}$ complemented strains

Strains were analysed by *in vitro* growth in fosfomycin to confirm the uptake of this antibiotic through *S. aureus* sugar phosphate transporters. Figure 5.4A shows the consistent, high capacity replication of background strains (P14-A, Δ*hpt*), negative control (pPL2$_{(PprfA)}$) and permease complemented strains in BHI medium. By comparison, Figure 5.4B shows replication of the same strains in BHI supplemented with fosfomycin. The projection of replication for Δ*hpt* and pPL2$_{(PprfA)}$ remained consistent in fosfomycin, conferring resistance, as these strains do not express a sugar phosphate permease. P14-A, which expresses listerial Hpt, was completely inhibited by fosfomycin until 11h, which proves that Hpt is responsible for fosfomycin uptake. Beyond 11h, replication of resistant P14-A becomes noticeable. Complemented strains expressing *hpt* and *uhpT* were totally inhibited by fosfomycin for 6h until replication of resistant bacteria occurs to the same capacity. Finally, pPL2$_{(PprfA)}$ *glpT* was completely inhibited until 10h, where replication of resistant bacteria occurred to more than 2 fold lower level than resistant growth of pPL2$_{(PprfA)}$ *hpt* and pPL2$_{(PprfA)}$ *uhpT.* These results confirm that fosfomycin enters bacteria through *S. aureus* UhpT and GlpT transporters.

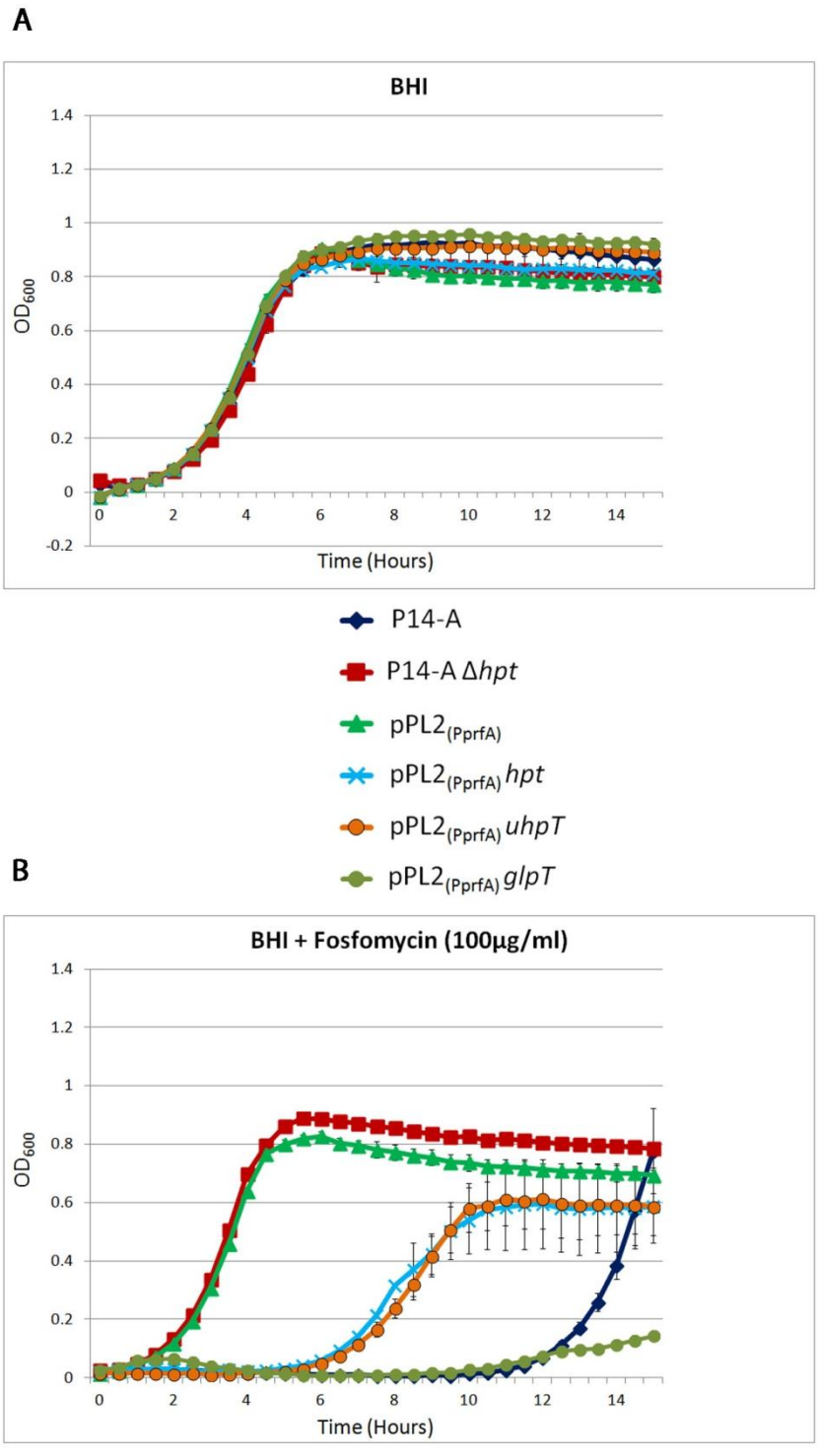

Figure 5.4. *In vitro* growth of *L.monocytogenes* strains in the presence of fosfomycin. Average growth ± SD shows a representative assay. **A.** Growth in BHI media alone **B.** Growth in BHI supplemented with 100 µg/ml fosfomycin.

5.4.3 Intracellular replication of pPL2$_{(PprfA)}$ complemented strains

Intracellular proliferation assays were performed using *L. monocytogenes* P14-A strains in order to measure the impact of *S. aureus* permeases in host cell replication relative to the listerial Hpt. Fixed numbers of cells, incubated in 5mM glucose, were infected with an equal number of bacteria. *Listeria* strains were allowed to replicate for 8h, at which point the intracellular numbers were counted. The intracellular growth coefficient (IGC) was calculated which compares the fold change in intracellular numbers from time 0h to time 8h. Figure 5.5A and B charts the average IGC of complemented strains against background strains in cell infections and divulges the significance of values VS P14-A (Figure 5.5C).

Figure 5.5A compares intracellular replication of *L. monocytogenes* strains in HeLa cells. The IGC of P14-A, expressing *hpt*, was more than double that of P14-A Δ*hpt* which highlights the value of sugar phosphate uptake during infection. The negative control strain, pPL2$_{(PprfA)}$ had an IGC that was not significantly different from P14-A Δ*hpt.* Complemented strains expressing *hpt* ,*uhpT* and *glpT* reached IGCs which were statistically non-significant from P14-A. Figure 5.5B displays IGC values for the same strains in Caco-2 cells, recreating infection of the human intestinal epithelium, the primary entry site for *L. monocytogenes*. This model consolidates results in HeLa, with all strains expressing permeases showing a non-significantly different IGC value to P14-A.

The results demonstrate that expression of related sugar phosphate transporters restores the ability of P14-A Δ*hpt* to replicate to the Hpt+ P14-A background level.

A

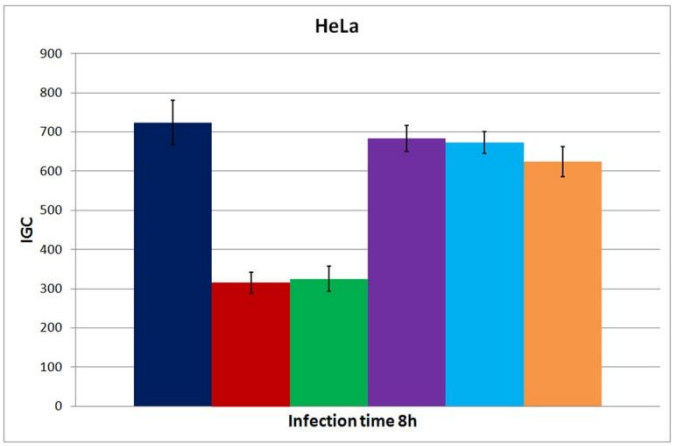

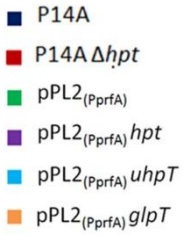

B

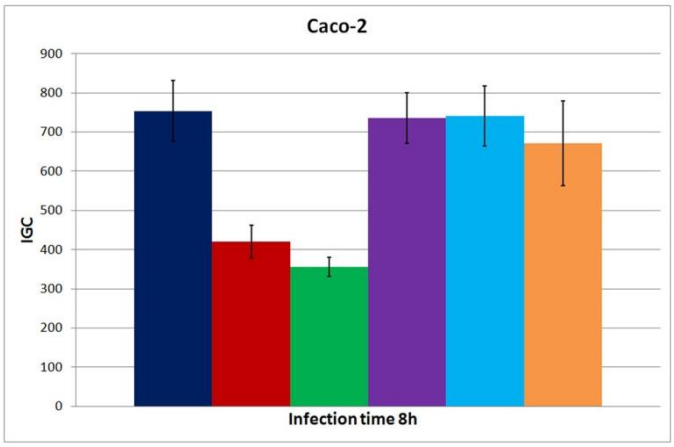

C

Cell type	P values of T-test between strain VS P14-A				
	P14-A Δ*hpt*	pPL2$_{(PprfA)}$	pPL2$_{(PprfA)}$ *hpt*	pPL2$_{(PprfA)}$ *uhpT*	pPL2$_{(PprfA)}$ *glpT*
HeLa	<0.01	<0.01	0.54	0.42	0.15
Caco-2	<0.01	<0.01	0.86	0.90	0.55

Figure 5.5. Proliferation of *L. monocytogenes* strains in mammalian cells. Intracellular proliferation assays show the intracellular growth coefficient (IGC) of *Listeria* strains at 8h post invasion of bacteria. **A.** Average IGC of strains in HeLa cells is calculated from 3 separate assays and shows standard error of the mean. **B.** Average IGC of strains in Caco-2 cells is calculated from 2 separate assays and shows standard error of the mean. **C.** Results of T-test analysis comparing IGC of each strain to P14-A.

5.5 Discussion

An expression system was developed which allowed constitutive expression of homologous sugar phosphate permeases in *hpt* deficient *L. monocytogenes*. This gene complementation allowed a more extensive characterisation of organophosphates that pass through *S. aureus* UhpT and GlpT as well as comparing the functionality of staphylococcal permeases to listerial Hpt in a bacterial system where sugar phosphate uptake is valuable.

5.5.1 Further substrate specificity determination

The substrate specificity of *S. aureus* UhpT and GlpT channels is summarised in Figure 5.6.

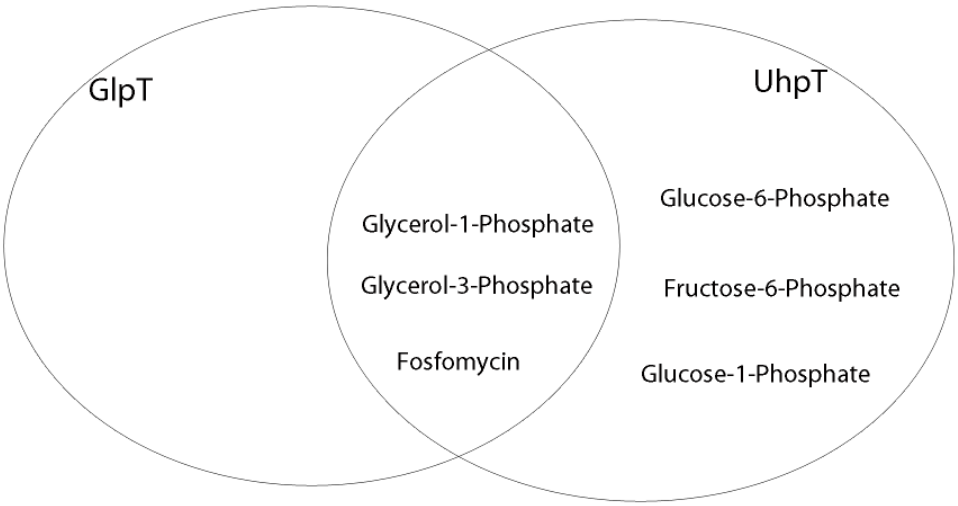

Figure 5.6. Organophosphates that traverse the UhpT and GlpT channels of *S. aureus*.

The glycerol phosphate transporter has a more explicit function in transporting C3 phosphorylated sugars to the bacterial cell. *In vitro* growth analysis using Gol-1-P and Gol-3-P suggested that UhpT can uptake the same C3 phosphorylated sugars with very similar capacity to GlpT. *In vitro*

growth using fosfomycin confirmed that both channels facilitated uptake of the antibiotic to cause inhibition of *L. monocytogenes*. This demonstrates an overlap in the function of these homologous transporters. It was noted that Δ*hpt* complemented with staphylococcal *uhpT* produced a resistant growth phenotype in broth supplemented with fosfomycin. By contrast, Δ*hpt* expressing *glpT* displayed an unremarkable resistance growth phenotype. This may suggest a higher capacity of fosfomycin transport through the staphylococcal GlpT permease which increases the antibiotic pressure and reduces the frequency of resistance. In Chapter 4, the MIC of fosfomycin was greater for Δ*glpT* as compared to Δ*uhpT*, which may substantiate this theory. The GlpT channel contains specific side chain residues which are important in interacting with the fosfomycin structure (Law *et al.* 2009). This may contribute to an increased affinity for this substrate.

By constitutively expressing staphylococcal permeases in *L. monocytogenes*, it was revealed that G-1-P is transported via UhpT and Gol-3-P is facilitated via UhpT and GlpT. These substrates did not stimulate *in vitro* growth in *S. aureus* USA300 LAC which raises questions about the expression of transporters in the *S. aureus* background. S*. aureus* strains encode a putative phosphoglucomutase enzyme, responsible for interconversion of glucose-1-phosphate and glucose-6-phosphate. This enzymatic reaction is required to supply glucose-1-phosphate for the biosynthesis of glycolipids to form the Gram positive lipoteichoic acid cell wall structure (Gründling & Schneewind 2007; Richter *et al.* 2013). In addition, glucose-1-phosphate can be catalysed to glucose-6-phosphate, which can enter bacterial energy producing pathways present in *S. aureus*. It would seem unlikely that the lack of *S. aureus* USA300 LAC growth in glucose-1-phosphate is due to an inability to metabolise the substrate. Glycerol-3-phosphate is formed naturally by phosphorylation of incoming glycerol in the USA300 cell. There is no other metabolic enzyme encoded in *S. aureus* which diverts this immediate step. Glycerol must therefore be

immediately converted to glycerol-3-phosphate before this is metabolised for energy. The high capacity growth derived from extracellular glycerol, seen in Chapter 3, must directly be passed to the glycerol-3-phosphate pathway, before energy can be metabolised. Expression of *glpT* would, in theory, allow uptake of the immediate glycerol metabolite (glycerol-3-phosphate) and allow growth of *S. aureus* USA300 LAC. As this is not the case, perhaps this introduces the issue of substrate specific induced transporter expression.

5.5.2 Functionality of homologous sugar phosphate permeases

In the established metabolic context of *L. monocytogenes*, staphylococcal permeases had an explicit gap to fill as metabolic virulence factors that directly benefit replication. *In vitro* analysis of growth upon selected sugar phosphates revealed that *S. aureus* UhpT and *L. monocytogenes* Hpt operate at a similar capacity for the same substrates. Uptake of Gol-1-P and Gol-3-P, which allowed replication, was remarkably similar between Δ*hpt* strains complemented with hexose phosphate permeases. Replication of Δ*hpt* expressing *uhpT*, due to uptake of G-6-P and F-6-P, reached higher levels of stationary growth than Δ*hpt* expressing *hpt*, suggesting that staphylococcal UhpT has an even greater capacity for hexose phosphates. Both of these strains displayed similar growth projections in the presence of fosfomycin, which suggests an equal capacity for antibiotic transport.

Intracellular replication analysis demonstrated that Δ*hpt* strains complemented with *S. aureus* UhpT and GlpT restored replication to levels consistent with P14-A. In addition, the intracellular growth advantage gained by expression of staphylococcal permeases was statistically indistinguishable to a strain expressing listerial Hpt. All homologous proteins serve to acquire intracellular nutrients which increase growth of *L. monocytogenes* and provide the same function during cell infection. Staphylococcal permeases therefore have provable intracellular functions

which act to restore virulence to *L. monocytogenes* Δ*hpt* by facilitating the import of nutrients for replication.

Expression of *glpT* in P14-A Δ*hpt* exposed a significant value for glycerol phosphates as exclusive intracellular growth sources. Glycerol metabolism is commonly implicated in bacterial nutrition during invasive cell infection. *L. monocytogenes* in particular is a pathogen in which glycerol metabolism has been strongly linked to virulence. Transcription profiling of *L. monocytogenes* in macrophage and epithelial infection has revealed up regulation of the glycerol uptake and metabolism genes (Chatterjee *et al.* 2006; Joseph *et al.* 2006). Glycerol-3-phosphate dehydrogenase, responsible for converting glycerol-1/3-phosphate to glycerine phosphate, is strongly up regulated in these studies. Perhaps, glycerol monophosphate, acquired through the Hpt permease, may provide an important contribution to *L. monocytogenes* metabolism during infection. Indeed, deletion of glycerol metabolism enzymes contributes to significantly impaired cellular replication of *L. monocytogenes* (Joseph *et al.* 2008).

Chapter 6

The role of sugar phosphate transporters in *S. aureus* USA300 LAC infection

6.1 Introduction

Research investigating the impact of listerial Hpt deficiency upon intracellular replication has established that sugar phosphates are accessible in the intracellular compartment by invasive bacteria (Chico-calero *et al.* 2002). Substrate specificity of putative UhpT and GlpT transporters of *S. aureus* has been confirmed and compared to the listerial Hpt homolog. It was demonstrated that staphylococcal permeases scavenge sugar phosphates from the intracellular compartment allowing *L. monocytogenes* to replicate effectively. This provides evidence for the functional role of UhpT and GlpT towards intracellular bacterial nutrition. The impact of this function was investigated in the metabolic background of *S. aureus* USA300 LAC.

Induction of sugar phosphate permeases has been previously reported during *S. aureus* epithelial cell infection. A clinical isolate, *S. aureus* 6850, was monitored during infection of human lung adrenocarcinoma cells (A549) (Garzoni *et al.* 2007). Expression of *uhpT* was up-regulated over 4 fold greater by 2h intracellularly, compared to extracellular media, and this increase was maintained up to 6h infection. Expression of *glpT* was also up-regulated and maintained intracellularly to a similar magnitude as *uhpT*. Infection of human blood with *S. aureus* USA300 revealed the expression of *uhpT* was 45 fold higher relative to *in vitro* tryptic soy broth culture (Malachowa *et al.* 2011). Significant up-regulation of UhpT and GlpT permeases during *S. aureus* human cell infection implicates these carbohydrate uptake systems as factors that enhance replication. As investigated in this study, hexose phosphates and glycerol phosphates influence significantly higher *in vitro* replication than any other single nutrient source. *S. aureus* USA300 LAC UhpT and GlpT therefore exist as potential determinants of virulence which act to drive staphylococcal replication inside the cell compartment.

6.2 Objectives

A mutant strain of USA300 LAC was created, Δ*uhpT*Δ*glpT*, which is totally unable to use sugar phosphates as exogenous carbon growth sources. This strain was analysed against WT USA300 LAC in the ability to replicate inside mammalian cells to uncover a direct role for sugar phosphate acquisition in infection.

To perform a reproducible and accurate analysis, a model of mammalian cell infection by *S. aureus* USA300 LAC was standardised and characterised in HeLa cells. This model was applied to epithelial cell lines relevant to studying the impact of replication due to UhpT and GlpT. Human lung adrenocarcinoma cells (A549) were selected due to the clinical relevance of USA300 associated pneumonia (Hidron *et al*. 2009) and the evidence showing significant *uhpT* and *glpT* expression during *S. aureus* A549 infection (Garzoni *et al.* 2007). Rat hepatocytes (FTO2B) were selected due to their specialised metabolic functions. Hepatocytes are specialised for glucose homeostasis and are able to rapidly uptake large amounts of surplus exogenous glucose (Sherwin 1980). Glucose must be converted to glucose-6-phosphate in order for glycogenesis to occur in hepatocytes (Cadefau *et al.* 1997). In the absence of glucose, glucose-6-phosphate can be equally replenished by gluconeogenesis of non-carbohydrate sources in FTO2B cells (Gomis *et al*. 2003) Furthermore, hepatocytes are specialised for lipid and cholesterol biosynthesis (Yang *et al.* 2001) which may offer alternative sources of bacterial nutrition. In this environment, the importance of sugar phosphates, among a diverse range of growth intermediates, was examined in *S. aureus* USA300 LAC replication.

The intracellular fate of *S. aureus* USA300 LAC was characterised in order to investigate the accessibility to the cell cytosol, which contains sugar phosphates. The intracellular fate of *L. monocytogenes* determines the impact of the Hpt permease. Upon invasion of host cells, *L. monocytogenes* rapidly escapes the bacterial endosome to the cytosol (Dussurget *et al.*

2004) where sugar phosphates can be scavenged freely. The intracellular localisation after *S. aureus* invasion of epithelial cells is variable among strains and cell types (Fraunholz & Sinha 2012). Studies have reported that USA300 localises to specific autophagosome vacuoles during infection of HeLa cells and osteocytes (Mauthe *et al.* 2012; Schnaith *et al.* 2007). This would introduce a barrier between *S. aureus* USA300 LAC and cytosolic sugar phosphates, meaning these substrates may not be readily accessible, in contrast to *L. monocytogenes*. It was therefore important to confirm the cellular localisation of *S. aureus* USA300 LAC throughout the course of epithelial cell infection.

In order to visualise the localisation of *S. aureus* LAC, Rab7 GTPase was selected as a vacuole marker. Rab GTPases are initially soluble proteins that localise to the cytosolic face of intracellular membranes (Seto *et al.* 2011). They are integral to the regulation of vesicle formation, motility and fusion (Stenmark & Olkkonen 2001). In particular, Rab7 is involved in the maturation of late endosomes, and typically localises with these membranes (Santillo 1997). Rab7 is routinely recruited to *S. aureus* containing endophagosomes in epithelial cells (Schnaith *et al.* 2007*)* and macrophages (Seto *et al.* 2011). In addition, Rab7 is found to associate with the autophagosome membrane and plays an important role in normal progression of mammalian cell autophagy (Gutierrez *et al.* 2004).

6.3 Relevant materials and methods

***In vitro* assays (2.4)** Mammalian cell cytotoxicity (2.4.2)

Mammalian cell culture (2.5) *S. aureus* infection (2.5.3.1); *L. monocytogenes* infection (2.5.3.2); Immunofluorescence microscopy (2.5.4)

Statistical analysis (2.6)

6.4 Results

6.4.1 Standardisation and characterisation of *S. aureus* USA300 LAC intracellular infection

In order to examine the role of *S. aureus* USA300 LAC sugar phosphate permeases, a reliable mammalian cell infection model needed to be established. Intracellular proliferation assays are used to monitor the replication of bacteria specifically inside the intracellular compartment. Using this technique, bacterial strains with mutants in metabolic genes can be compared to the wild type in the capacity for replication, uncovering determinants of virulence.

Mammalian cells were added to 24 well plates and allowed to attach and grow until the well monolayer reached confluence. The number of cells per well was calibrated which would form the platform for repeatable bacterial infection. *S. aureus* USA300 LAC was exposed to the monolayer in numbers relative to the number of mammalian cells per well, known as the multiplicity of infection (MOI). After a period of incubation which allows bacteria to invade cells, any extracellular bacteria are killed by appropriate antibiotics. From this point, intracellular numbers of bacteria can be determined at recurrent time points by lysis of mammalian cells and nutrient agar plating of lysate. Parameters needed to be standardised for reproducible *S. aureus* USA300 LAC infection.

6.4.1.1 Bacterial invasion

Bacterial invasion of mammalian cells needed to be consistent in order to comparably measure replication. Invasion was compared between bacterial inocula that was either prepared in advance and stored at -80^{o}C, or cultured on the day of infection and prepared freshly. Inoculums were applied to confluent cell monolayers and allowed to invade for various times after addition. After a period of extracellular bacterial inhibition, the intracellular bacteria were plated to determine the percentage of total

bacteria added that have invaded the monolayer (the % invasion). It was found that frozen inocula produced huge inconsistency in invasion numbers which were irreproducible (data not shown). Inocula prepared from *S. aureus* USA300 LAC freshly cultured to early exponential phase of growth demonstrated much greater stability of percentage invasion.

Next, the invasion time was assessed, meaning the time that the cell monolayer would be exposed to the inocula before addition of antibiotic to kill the extracellular bacteria. Figure 6.1A shows the number of colony forming units per ml (CFU/ml) isolated from HeLa cells infected with *S. aureus* USA300 LAC after increasing invasion times. Invasion times ranging from 15 – 45 minutes was analysed before addition of antibiotic media. Inocula applied for 45 minutes lead to a 4 fold increase in bacterial numbers compared to 35 minutes. Incubation for periods less than 35 minutes exhibited low invasion rates of less than 0.5%. As a result, bacterial inoculum was applied for 35 minutes, as this allowed suitable numbers of *S. aureus* USA300 LAC to invade. In addition the number was low enough to study the increase in replication more effectively. The corresponding invasion percentages for these assays are shown in Figure 6.1B.

The next variable investigated was the minimum time required to kill extracellular bacteria. This needed to be adjusted to minimise replication of intracellular bacteria in the time frame before CFU/ml is measured at time 0h. Antibiotic media was applied for 30 minutes and 60 minutes and plated to determine the numbers of viable extracellular *S. aureus* USA300 LAC. This revealed no difference in the CFU/ml, which were both negligible. Antibiotic media was therefore added for 30 minutes.

The average percentage invasion of *S. aureus* USA300 LAC in HeLa cells could be investigated using these established parameters. Figure 6.2 compares the average percentage invasion of HeLa cells by WT USA300 LAC at MOI 10 and MOI 1. At MOI 10, tenfold more bacteria are exposed to the cell monolayer than MOI 1 which leads to 2 fold reduction in the

percentage invasion. Therefore the percentage of invasion is lower relative to the higher total inocula CFU/ml. These results show that *S. aureus* USA300 LAC has marked ability to invade human epithelial cells, which indicates that this pathogen is adapted for invasive pathogenesis.

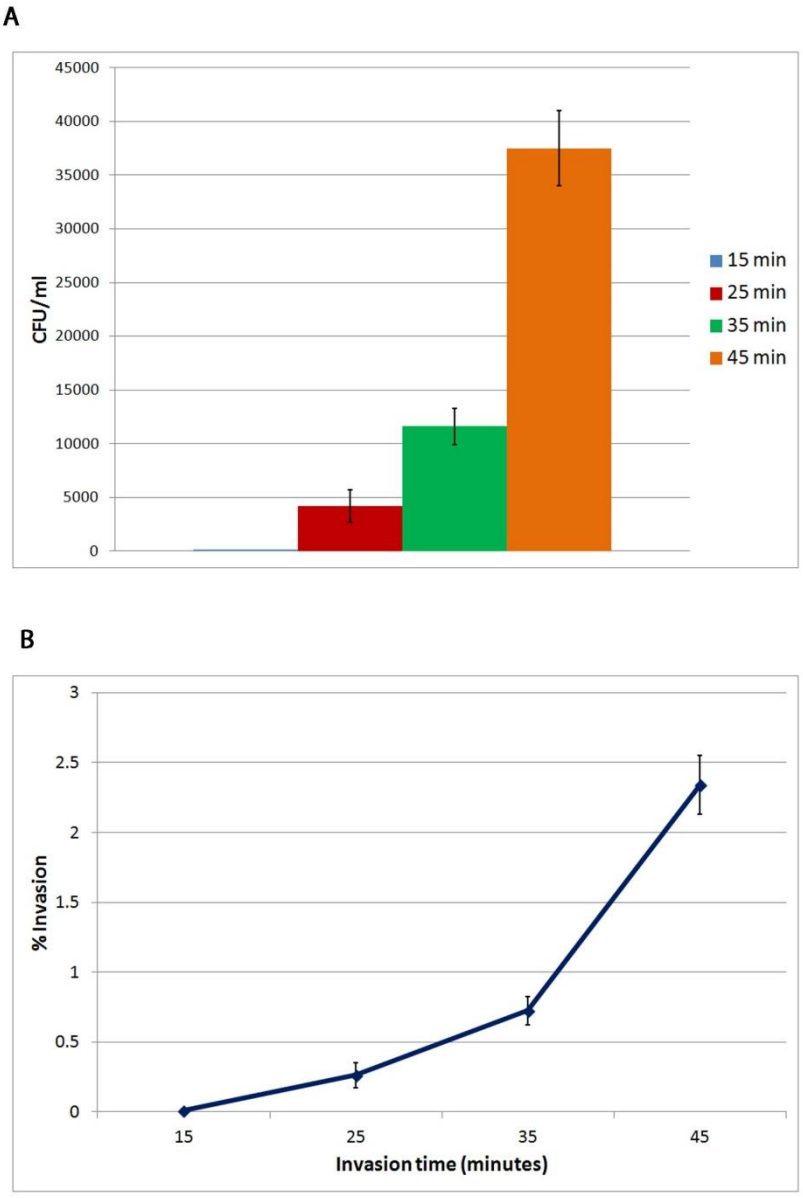

Figure 6.1. Invasion of *S. aureus* USA300 LAC in HeLa cells at MOI 10. **A.** Numbers of intracellular bacteria isolated from the HeLa cell monolayer after incubation at increasing time periods. **B.** The average percentage invasion at each incubation period. Values show a representative experiment ± standard error of the mean.

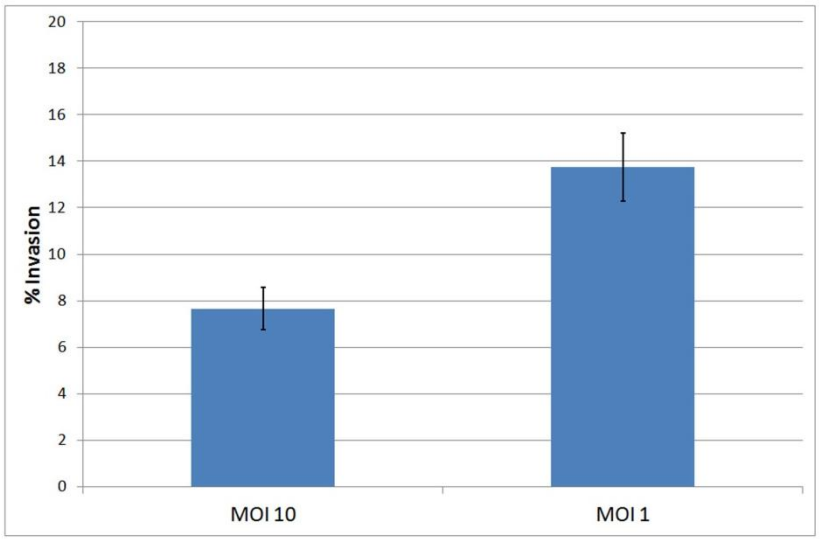

Figure 6.2. Average percentage invasion of *S. aureus* USA300 LAC in HeLa cells. Average invasion is calculated from at least 3 separate assays and shows standard error of the mean.

6.4.1.2 Bacterial induced cytotoxicity

During infection assays, it is critical that the integrity of the cell monolayer remains undisturbed, allowing for more accurate discrimination of intracellular replicating bacteria. The integrity of mammalian cells was monitored during infection of *S. aureus* USA300 LAC strains at MOI 10 and MOI 1 in the invasion conditions established. Figure 6.3 shows cell cytotoxicity assays to determine the percentage destruction of the cell monolayer in 24 well plates during infection. Cell media was collected from each well at successive time points. Any cells that were present in this media, due to detachment from the monolayer, can be lysed which releases lactate dehydrogenase enzyme (LDH). The activity of this enzyme can be quantitatively measured using the Sigma Tox7 kit. This is a direct measure of cell cytotoxicity caused by bacterial infection.

Figure 6.3A shows the standard curve of LDH activity according to the number of HeLa cells involved in the assay. HeLa cells were counted and

doubling dilutions were made, allowing different proportions of HeLa cells to be lysed and measure the LDH activity. The assay has been transposed onto a colour chart for easy distinction of the severity of detachment expressed as percentage cell cytotoxicity. Figure 6.3B shows the depiction of mammalian cell monolayer integrity during infection using this colour co-ordination. At MOI 10, the wild type USA300 LAC strain causes severe cytotoxicity of HeLa cells by 6 hours. Around 50% of the cell monolayer is destroyed at this time of infection. By contrast infections at MOI 1 do not cause any cell cytotoxicity. This evidence can be substantiated by viewing phase contrast microscopy slides of the monolayer during infection at MOI 10 and MOI 1 (Figure 6.4). The evidence indicates that HeLa cell infection at MOI 10 can only be reliably measured until 4 hours. After this time, infection of *S. aureus* USA300 LAC becomes cytotoxic and the integrity of the monolayer decreases, meaning intracellular replication cannot be directly measured.

An *agr* deficient USA300 LAC strain, Δ*agr,* was introduced as a comparative avirulent control for establishing the factors involved in intracellular replication. Infection of HeLa cells with Δ*agr* at MOI 10 revealed a lack of cytotoxicity by 6h, which is in contrast to the virulent WT (Figure 6.3B). The cytotoxicity of WT USA300 LAC and Δ*agr* was monitored inside A549 cells. At MOI 10, the integrity of the monolayer was undisturbed by infection, up to 8 hours post invasion, therefore intracellular replication could be reliably measured up to MOI 10 (Figure 6.3).

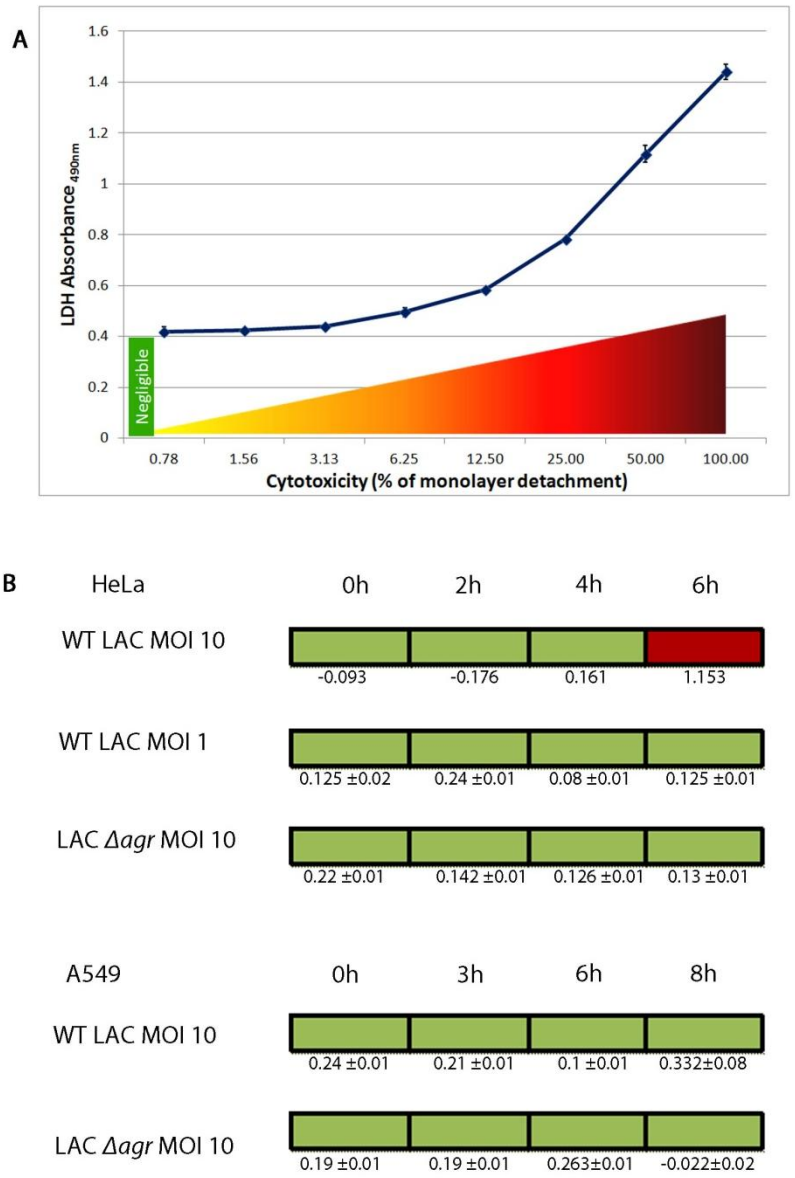

Figure 6.3. LDH based cytotoxicity monitoring of infected mammalian cells. **A.** Standard curve showing LDH assay absorbance at 490nm of HeLa cell samples (100% is equal to a confluent monolayer of cells cultured in a 24 well plate ~150,000) The colour gradient represents the severity of cell detachment (cytotoxicity) according to the 490nm reading. Green represents values under Abs_{490} 0.4 , a virtually unaffected confluent monolayer. **B.** Schematics representing the monolayer integrity in *S. aureus* infections, according to the gradient scheme in A. Mean LDH assay absorbance values ± standard deviation from 2 assays are shown for each timepoint.

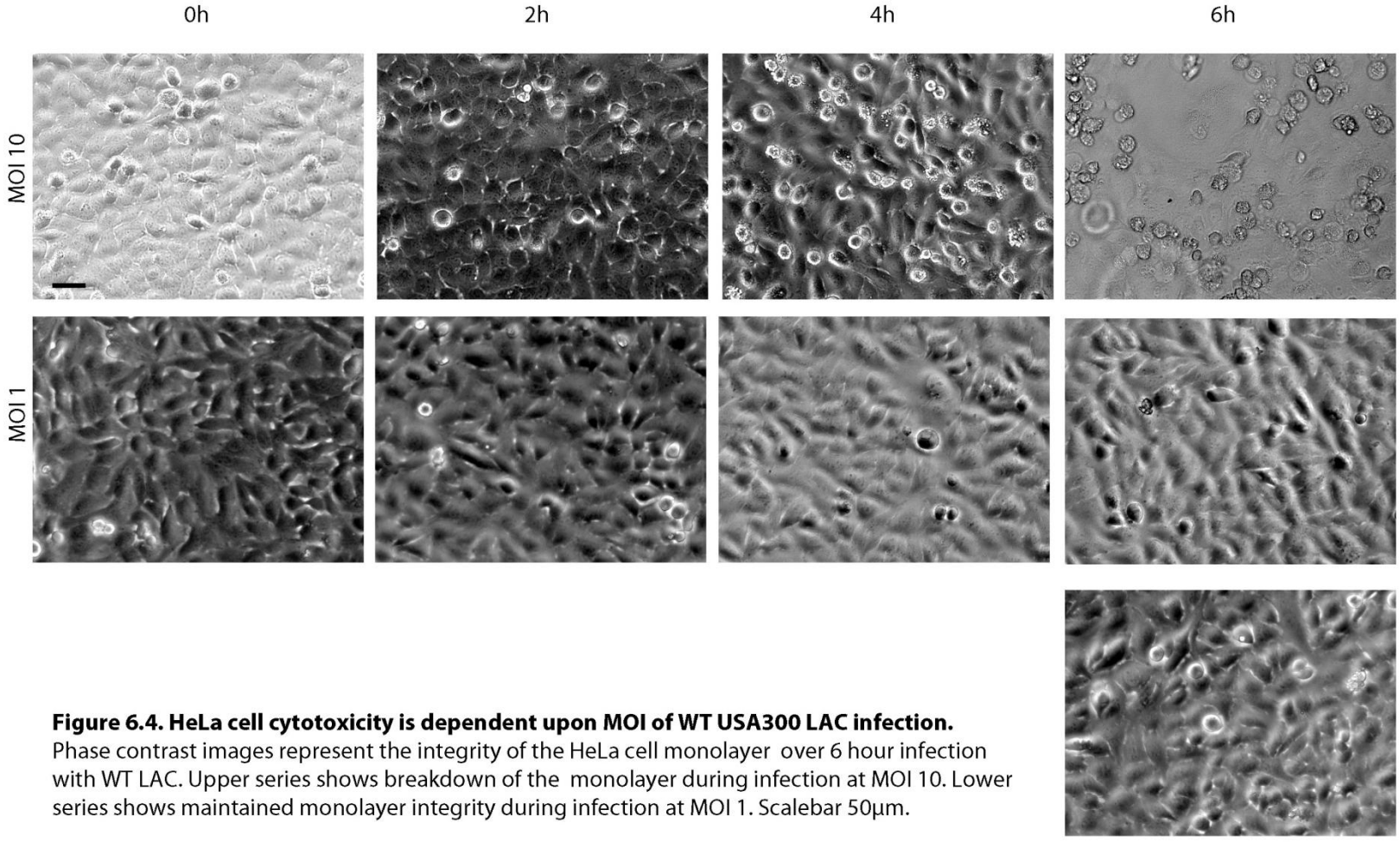

Figure 6.4. HeLa cell cytotoxicity is dependent upon MOI of WT USA300 LAC infection.
Phase contrast images represent the integrity of the HeLa cell monolayer over 6 hour infection with WT LAC. Upper series shows breakdown of the monolayer during infection at MOI 10. Lower series shows maintained monolayer integrity during infection at MOI 1. Scalebar 50µm.

6.4.1.3 Intracellular replication

Intracellular infection assays were completed in HeLa cells cultured at physiological blood glucose concentration (5mM) using the parameters established. Wild type USA300 LAC was infected at an MOI of 10 and 1 to compare the replicative ability.

For each time point post bacterial invasion, intracellular numbers of *S. aureus* USA300 LAC WT were counted and an overall average CFU/ml was established. The averaged results for infections performed at MOI 10 and MOI 1 are presented in Figure 6.5A and 6.5B respectively. At time 0h, approximately 5.5 fold more bacteria invade the HeLa monolayer when exposed at MOI 10 compared to MOI 1.Figure 6.5A shows the significant increase in bacterial numbers between 2h and 4h of infection. By 4 hours, bacterial numbers proliferated to almost 10 fold higher than the average CFU/ml isolated at 2 hours and 36 times greater than CFU/ml at 0h. This major boost in proliferation yields intracellular numbers that are on the threshold of HeLa monolayer destruction. By contrast Figure 6.5B shows that *S. aureus* USA300 LAC infected at an MOI of 1 experience around an 8 fold increase in numbers by 3 hours post invasion. Replication appears to be arrested for the remainder of the infection course. The replicative ability of *S. aureus* USA300 LAC is dependent upon the number of bacteria that are initially exposed to the cell monolayer.

A

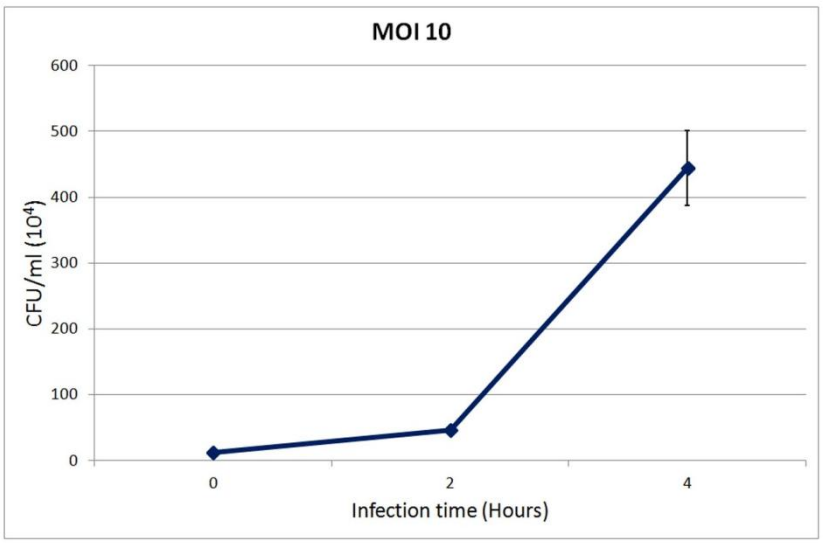

B

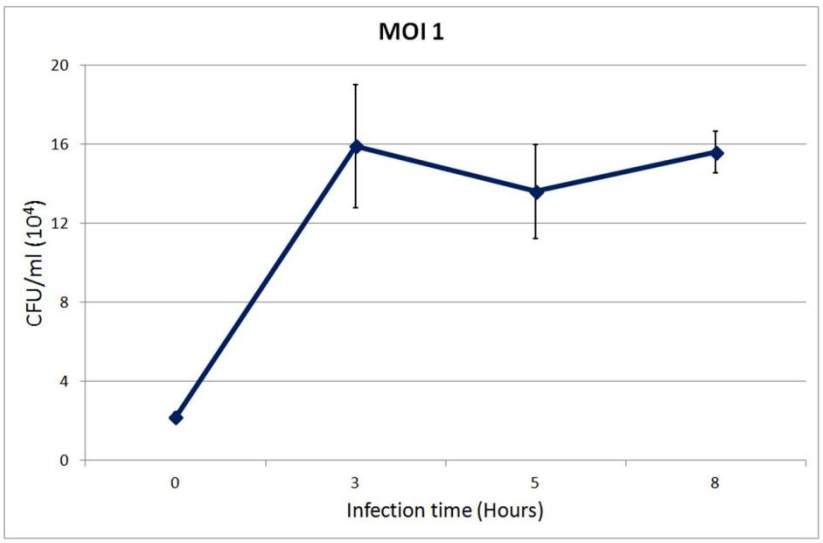

Figure 6.5. Intracellular replication of *S. aureus* USA300 LAC in HeLa cells A. Average CFU/ml isolated from cells infected at MOI 10 . **B.** Average CFU/ml isolated from cells infected at MOI 1. Average values are calculated from at least 3 separate assays and show standard error of the mean.

6.4.1.4 Infection characterisation by immunofluorescence microscopy

Intracellular replication of *S. aureus* USA300 LAC within the HeLa monolayer was further characterised by immunofluorescence microscopy. Cells monolayers, infected at MOI 10 and 1, were visualised to quantify the percentage infection of the monolayer, and observe differences that underpin the gulf in replication dynamics seen in Figure 6.5.

Intracellular *S. aureus* USA300 LAC was stained at infection time points with anti-*Staphylococcus aureus* Rabbit IgG antibody. Cell nuclei were stained using DAPI and phalloidin conjugated to Alexa fluor 488 was used to visualise cellular F-actin.

Figure 6.6 displays representative immunofluorescence images throughout the infection time course at MOI 10. Upon infection it is noticeable that there are several freestanding bacterial clusters inside each cell at time 0h. As infection advances, USA300 clusters converge at a perinuclear location. By 4 hours post invasion, staphylococci are amassed in a perinuclear replication complex in the majority of infected cells. Figure 6.7A quantifies the percentage of infected cells at MOI 10 while Figure 6.7B quantifies the number of freestanding bacterial clusters inside each infected cell at MOI 10. Over 80%± 5.95% of cells in the assay monolayer were infected with at least one *S. aureus* USA300 LAC bacterium. Figure 6.7A shows throughout the course of infection, the number of infected cells at 4h does not significantly differ from numbers at 0h ($p= 0.84$). At time 0h, the average number of bacterial clusters stood at 3.74 ± 0.5 clusters per cell (Figure 6.7B). By 4 hours post invasion, this number significantly dropped to 2.79 ± 0.17 clusters ($p= 0.02$), which is consistent with the visual merging of clusters into one integrated body of bacteria.

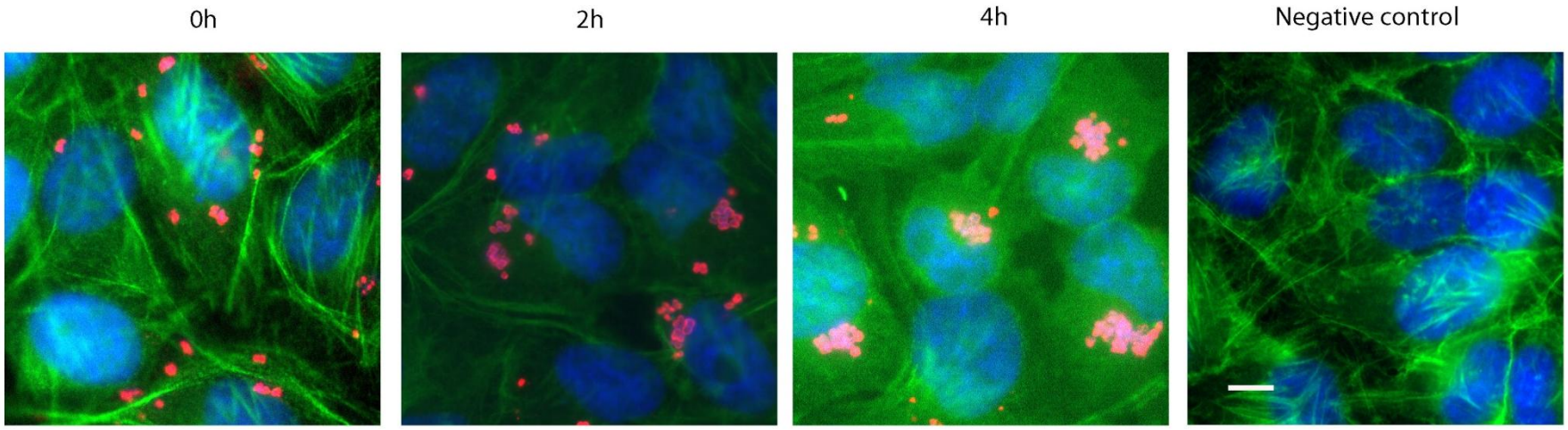

Figure 6.6. *S. aureus* USA300 LAC infection of HeLa cells at MOI 10. Time course infection up to 4 hours post invasion of bacteria. Merged images show fluorescence of *S. aureus* stained with anti-*Staphylococcus aureus* polyclonal IgG/ Alexa Fluor 568-conjugated anti-Rabbit IgG (**Red**), F-actin visualised with Alexa Fluor 488-conjugated phalloidin (**Green**) and DNA visualised with Alexa Fluor 305-conjugated DAPI (**Blue**). Scalebar10µm.

A

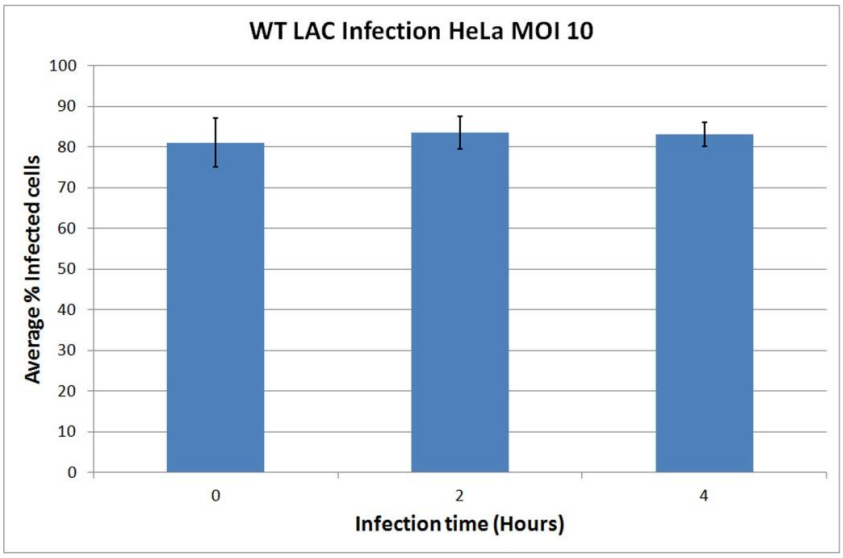

B

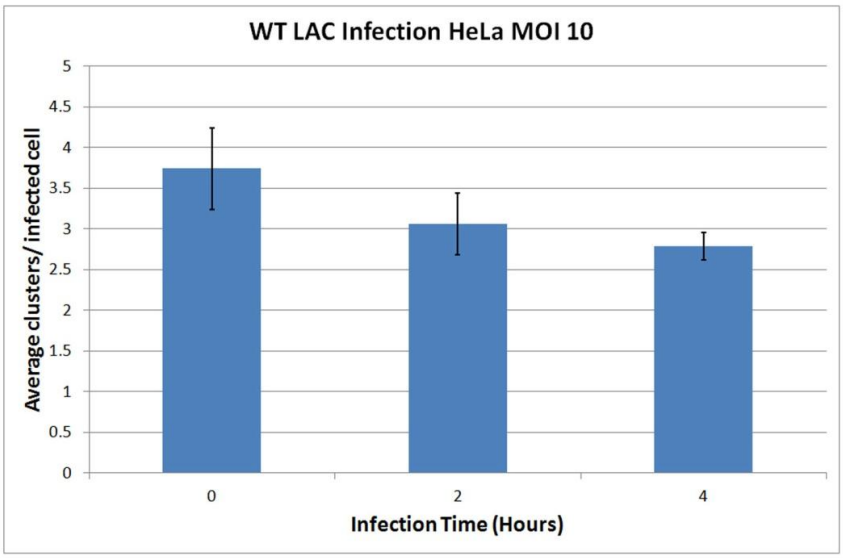

Figure 6.7. Quantification of HeLa cell infection at MOI 10. A. Average percentage of infected cells ± standard error. **B.** Average bacterial clusters per infected cell ± standard error. Values are taken from 10 fields per time point with 15.5 ± 1.3 cells per field.

HeLa cell monolayers infected with *S. aureus* USA300 LAC at MOI 1 were also quantified. Figure 6.8 shows immunofluorescence images of an infection time course spanning 24h at MOI 1. At time 0h, the number of intracellular clusters is sparse compared to MOI 10. However, by 5 and 8 hours post infection, substantial perinuclear bacterial expansions are present. This provides evidence that single staphylococci are able to replicate to greater loads inside single mammalian epithelial cells. Figure 6.9A shows the percentage of infected cells at corresponding time points. The average percentage of infected HeLa cells at MOI 1 is much lower, at 27.9% ± 4.27%. This percentage does not significantly differ up to 8 hours (Figure 6.9A) ($p = 0.88$). At 24 hours, the cell monolayer is confluent, and only 5.58% ± 1.45% of cells remain infected by *S. aureus* USA300 LAC (substantiated by Figure 6.8). Figure 6.9B quantifies the number of bacterial clusters per infected cell. On average, at time 0h each infected cell is inhabited by 1 bacterial cluster. By 5 and 8 hours, this figure had doubled, corresponding with the more expansive proliferation seen in Figure 6.8. By 24 hours, this figure drops to 1 bacterial body per infected cell again.

In addition, the infection of A549 cells by *S. aureus* USA300 LAC at MOI 10 was also quantified. At 0h, 64% ± 5% of the cell monolayer was infected. By 6h post invasion, 66% ± 2.5% of cells contained *S. aureus*, which is statistically non-significant to time 0h ($p = 0.74$). Taken together, the epithelial cell infection results suggest that USA300 does not spread from cell to cell, in contrast to *L. monocytogenes* infection.

This confirmed important differences between infection at MOI 10 and 1 which accounts for variation in replication. At MOI 10 exposure, 2.8 times more cells become invaded by over 3 times more bacterial clusters than at MOI 1 exposure. The co-ordinated replication of several bacterial clusters per cell is more effective than a single bacterium per cell.

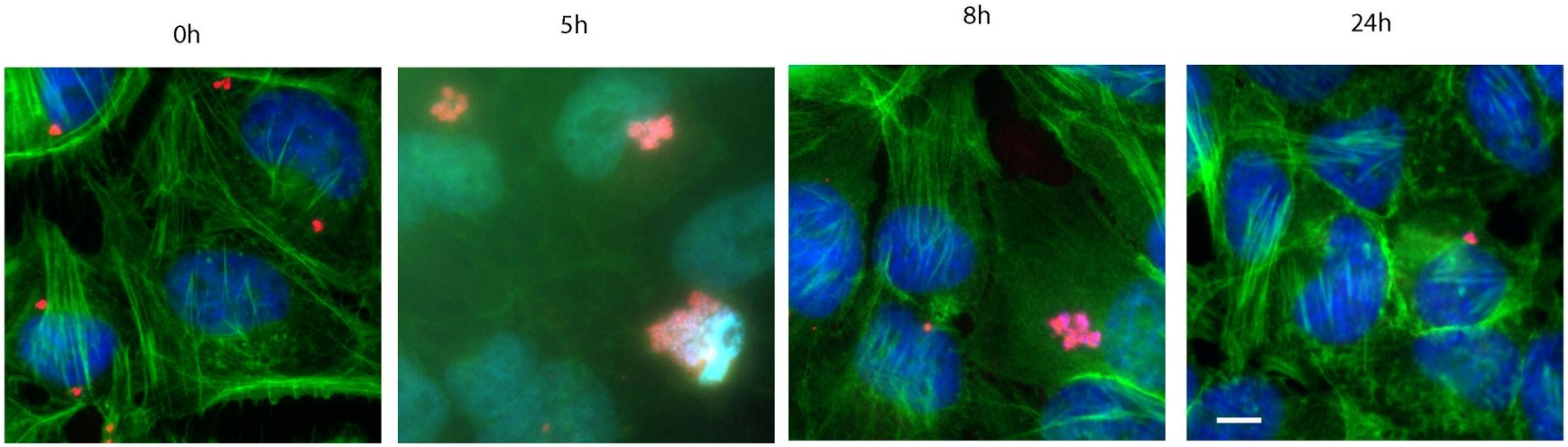

Figure 6.8. *S. aureus* USA300 LAC infection of HeLa cells at MOI 1. Time course infection up to 24 hours post invasion of bacteria. Merged images show fluorescence of *S. aureus* stained with anti-*Staphylococcus aureus* polyclonal IgG/ Alexa Fluor 568-conjugated anti-Rabbit IgG (**Red**), F-actin visualised with Alexa Fluor 488-conjugated phalloidin (**Green**) and DNA visualised with Alexa Fluor 305-conjugated DAPI (**Blue**). Scalebar 10µm.

A

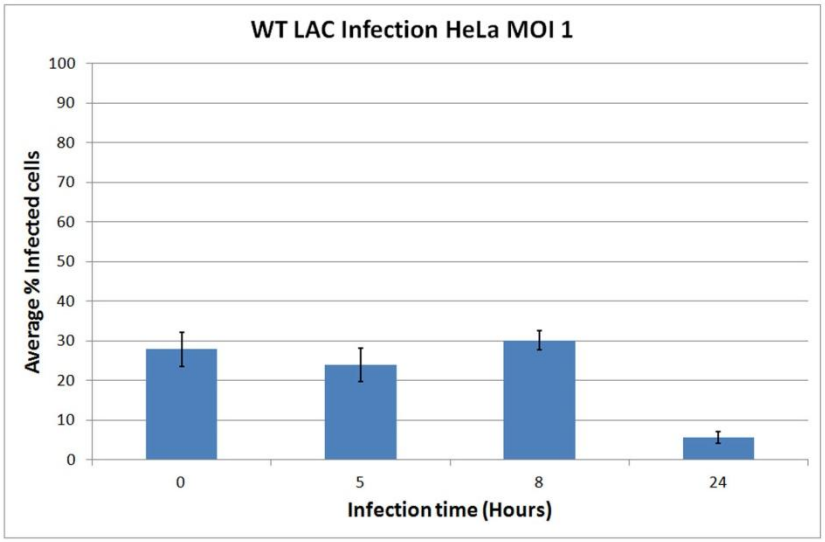

B

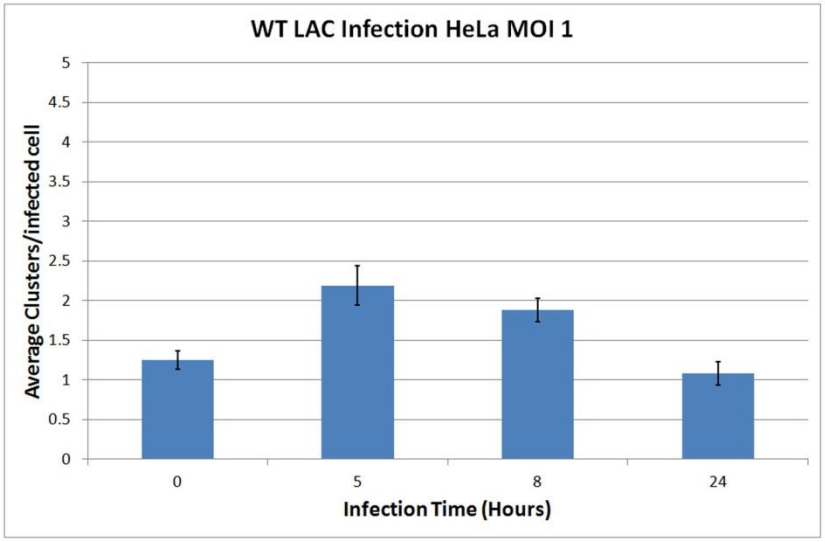

Figure 6.9. Quantification of HeLa cell infection at MOI 1. A. Average percentage of infected cells ± standard error. **B.** Average bacterial clusters per infected cell ± standard error. Values are taken from 10 fields per time point with 17.25 ± 1.5 cells per field.

6.4.2 Intracellular replication of *S. aureus* USA300 LAC deficient in sugar phosphate uptake

Double mutant strain, Δ*uhpT*Δ*glpT* was analysed relative to WT USA300 LAC to determine whether uptake of sugar phosphates contributed to intracellular replication. Relevant mammalian cell lines were cultured in specific conditions and infected to monitor intracellular proliferation.

6.4.2.1 HeLa cell infection

The metabolism of HeLa cells was manipulated by exposing the cell monolayer to distinct glucose concentrations in the culture medium, 25mM, 5mM and 0mM. As a positive control, *L. monocytogenes* P14-A and P14-A Δ*hpt* were used to infect HeLa cells exposed to these glucose concentrations, which elegantly demonstrates conditions in which Hpt becomes an advantage to replication.

Figure 6.10A plots the average CFU/ml of *Listeria* strains proliferating inside HeLa cells grown in 25mM glucose. P14-A and P14-A Δ*hpt* had the same capacity for replication in these conditions substantiated by a similar mean generation time, the average time taken for the population to double (Figure 6.10D). Figure 6.10B compares replication when the exogenous glucose concentration is reduced to 5mM, the physiological blood glucose concentration. By 10h post invasion, P14-A Δ*hpt* reached a CFU/ml 2.76 fold lower than P14-A with a significantly increased mean generation time (Figure 6.10D). In epithelial cells cultured in 5mM glucose, sugar phosphates become a significant nutrient source which impacts replication. When HeLa cells were cultured in the absence of glucose, replication of *L. monocytogenes* was highly impaired (Figure 6.10C). In these cell conditions, expression of *hpt* is not advantageous to growth and the mean generation time of P14-A increased by 2.8 fold compared to growth in glucose exposed cells. These distinctive infection profiles are indicative of the nutrient requirements of *L. monocytogenes*. These results provide a comparative reference for interpreting *S. aureus* metabolism during infection.

A

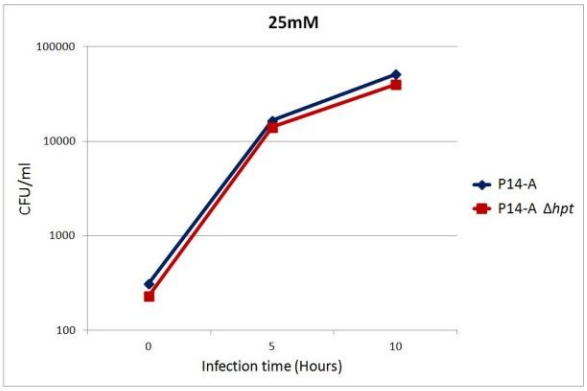

B

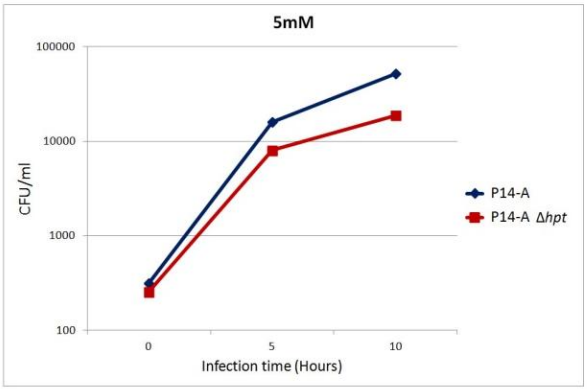

C

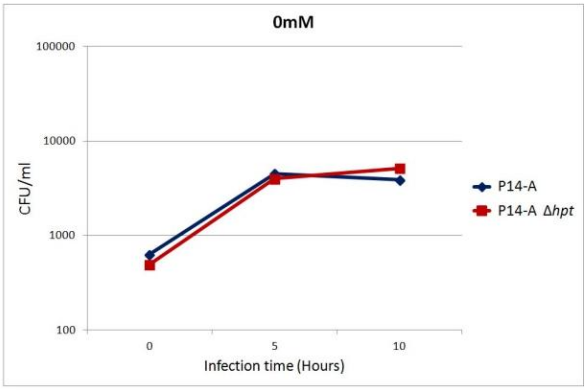

D

	Mean generation time (minutes)	
Cell media	P14-A	P14-A Δ*hpt*
25mM Glucose	81.7 ± 3.75	80.625 ± 3.6
5mM Glucose	81.35 ± 4.165	96.5 ± 0.772
0mM Glucose	228.6 ± 8	178.8 ± 2.4

Figure 6.10. Replication of *Listeria monocytogenes* P14-A strains in HeLa cells. Intracellular proliferation assays compare the average CFU/ml of P14-A and P14-A Δ*hpt* at times of infection. Charts show a representative assay to depict the common replication profile and include standard error. **A.** Cells cultured in 25mM glucose **B.** Cells cultured in 5mM glucose **C.** Cells cultured without glucose **D.** Average doubling times ± standard error of bacteria by 10 hours during infection in cells cultured in varying glucose conditions.

HeLa monolayers were infected by *S. aureus* USA300 LAC strains at an MOI of 1 and CFU/ml was determined up to 5h post invasion. The replication of *agr* deficient strain, Δ*agr*, was monitored alongside WT and Δ*uhpT*Δ*glpT* as an avirulent control for infection.

Figure 6.11A shows replication of WT and Δ*uhpT*Δ*glpT* in cells exposed to 25mM glucose. By 5h, WT and Δ*uhpT*Δ*glpT* replicated to 164 fold and 187 fold greater CFU/ml than 0h respectively, and the final CFU/ml were statistically non-significant (p=0.73). The mean generation times of both strains were similar; around 40 minutes per generation (Figure 6.11D). Figure 6.11B compares the replication of WT and Δ*uhpT*Δ*glpT* in HeLa (5mM glucose). There was no significant difference between the CFU/ml reached at 5h (p=0.75) and similar rates of doubling were observed over these infection times (Figure 6.11D). In these conditions, the WT and Δ*uhpT*Δ*glpT* strains reached a bacterial yield of approximately half the CFU/ml to replication in HeLa (25mM glucose). Finally, in HeLa (0mM glucose) there was no significant difference in CFU/ml between WT and Δ*uhpT*Δ*glpT* at 5h (p=0.60). Interestingly, the mean generation times of both strains in 0mM conditions was comparable to 25mM conditions, showing that glucose starvation does not affect replication proficiency (Figure 6.11D). In 0mM conditions, WT and Δ*uhpT*Δ*glpT* numbers increased 130 and 200 fold respectively over 5h in comparison to 60 and 70 fold in 5mM conditions. In contrast to *L. monocytogenes*, this shows *S. aureus* USA300 LAC actually benefits from glucose starvation in HeLa cells.

Compared with the WT, replication of avirulent Δ*agr* was heavily impaired in HeLa cultured in 5mM and 0mM glucose conditions (Figure 6.11B – C). Despite invading to a similar CFU/ml, Δ*agr* reached 16 and 14 fold lower CFU/ml than WT by 5h infection in 5mM and 0mM conditions respectively. The mean doubling time of Δ*agr* was significantly longer than WT, with 2.4 times greater in cells cultured at 5mM glucose (Figure 6.11D).

A

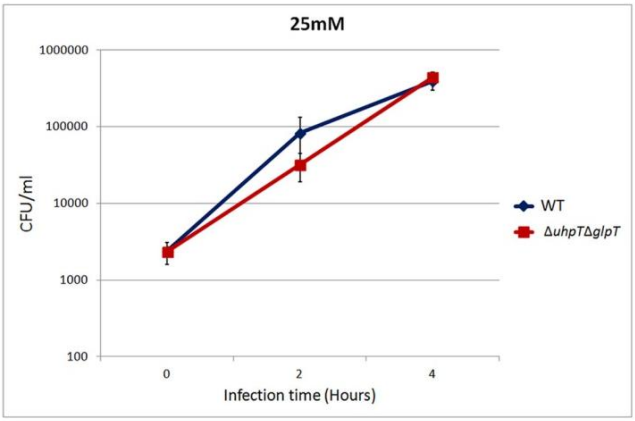

B

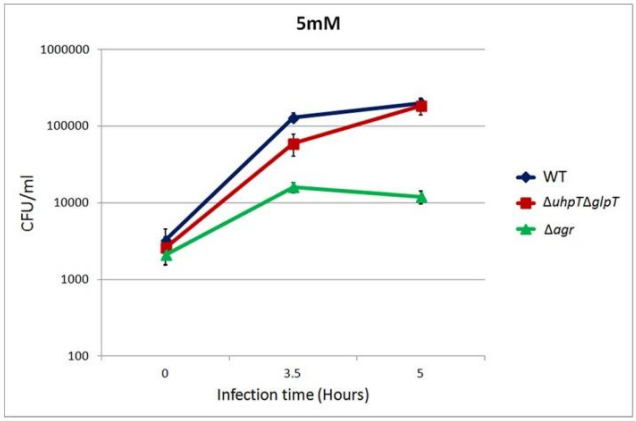

C

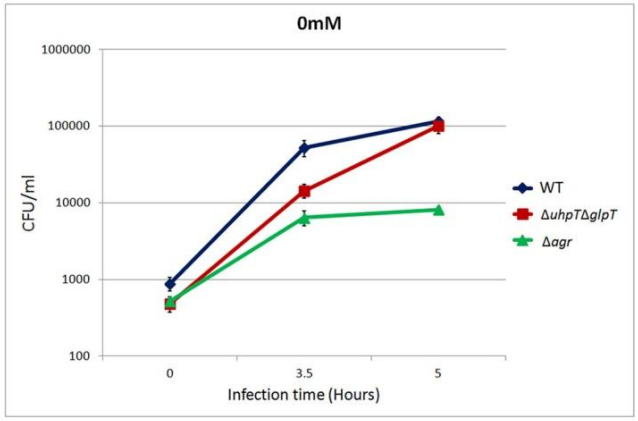

D

	Mean generation time (minutes)		
Cell media	WT	Δ*uhpT*Δ*glpT*	Δ*agr*
25mM Glucose	40.8 ± 9.9	39.77 ± 6.5	-
5mM Glucose	50.16 ± 7.8	48.8 ± 11.15	120.4 ± 22.25
0mM Glucose	42.79 ± 6	38.9 ± 7.7	75.25 ± 6.25

Figure 6.11. Replication of *S. aureus* USA300 LAC strains in HeLa cells. Intracellular proliferation assays compare the average CFU/ml of WT, Δ*uhpTΔglpT* and Δ*agr* up to 5 hours during infection. Charts show averaged values from 2 separate assays and show standard error of the mean. **A.** Cells cultured in 25mM glucose **B.** Cells cultured in 5mM glucose **C.** Cells cultured without glucose **D.** Average doubling times ± standard error of bacteria by 5 hours during infection in cells cultured in varying glucose conditions.

6.4.2.2 A549 cell infection

Figure 6.12 illustrates replication of *S. aureus* USA300 LAC strains in human alveolar adenocarcinoma cells. Cell infections in 25mM glucose medium were not performed as these conditions displace sugar phosphates as a potential growth source. Figure 6.12A compares replication of WT and Δ*uhpT*Δ*glpT* in 5mM glucose conditions. The mutant strain was able to reach 31 fold higher CFU/ml by 5h, by comparison to WT which reached 17 fold higher. The average doubling times of these strains did not significantly differ in these cell conditions (Figure 6.12C). Figure 6.12B displays replication of the same strains in 0mM cell conditions. WT USA300 LAC was able to replicate over 5h to reach a 57 fold greater CFU/ml, while Δ*uhpT*Δ*glpT* proliferated to 40 fold higher CFU/ml in the same time. The mean generation times between these strains were not significantly different, and were not increased compared to rates in 5mM glucose cell conditions (Figure 6.12C).

Figure 6.12A and B display the impaired growth of Δ*agr* in cells cultured in 5mM and 0mM glucose conditions. This strain replicated with a 3.3 fold and 7.7 fold increase in numbers over 5h in 5mM and 0mM glucose conditions respectively, which represented a significantly reduced rate of replication compared to WT and Δ*uhpT*Δ*glpT* (Figure 6.12C).

A

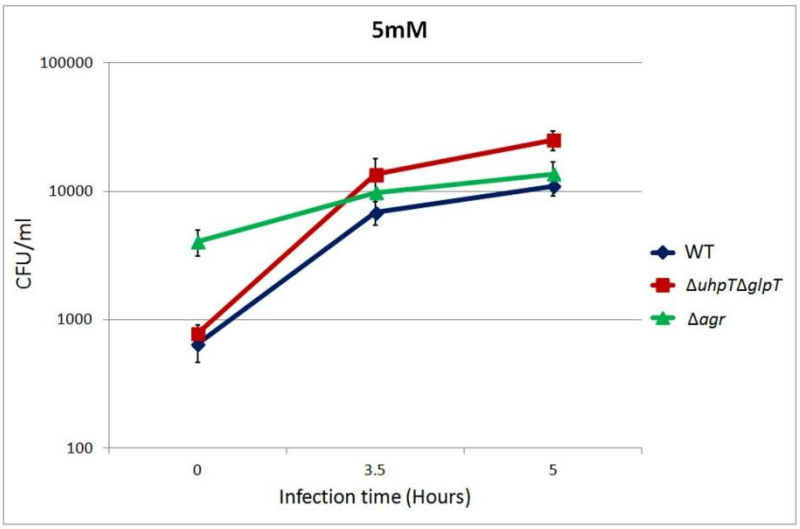

B

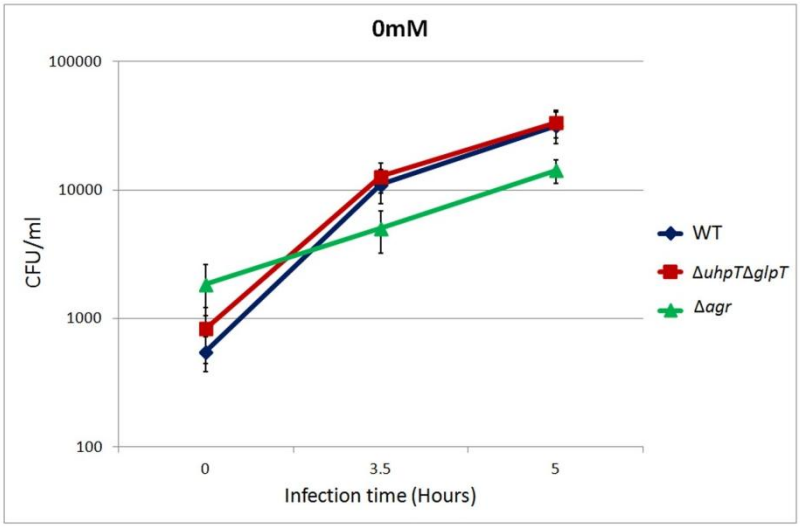

C

	Mean generation time (minutes)		
Cell media	WT	Δ*uhpT*Δ*glpT*	Δ*agr*
5mM Glucose	75.6 ± 12.6	59.8 ± 9.98	276 ± 67
0mM Glucose	51.3 ± 14.4	56.47 ± 13.7	101.46 ± 20.7

Figure 6.12. Replication of *S. aureus* USA300 LAC strains in A549 cells. Intracellular proliferation assays compare the average CFU/ml of WT, Δ*uhpTΔglpT* and Δ*agr* up to 5 hours during infection. Charts show averaged values from 2 separate assays and show standard error of the mean. **A.** Cells cultured in 5mM glucose **B.** Cells cultured without glucose **C.** Average doubling times ± standard error of bacteria by 5 hours during infection in cells cultured in varying glucose conditions.

6.4.2.3 FTO2B cell infection

S. aureus USA300 LAC strains were monitored inside rat hepatocytes. Replication of WT in 5mM and 0mM conditions was mirrored by Δ*uhpT*Δ*glpT* (Figure 6.13A and B). Figure 6.13A depicts in 5mM conditions, both strains replicated over 5h to reach a CFU/ml 24 times greater than time 0h, with virtually identical average doubling times (Figure 6.13C). Figure 6.13B shows that Δ*uhpT*Δ*glpT* replicated over 5h to 30 fold greater CFU/ml in 0mM conditions, compared to WT which proliferated to 24 times greater CFU/ml. The final CFU/ml for WT and Δ*uhpT*Δ*glpT* did not significantly differ in either cell conditions ($p = >0.05$). The average doubling times did not significantly differ between WT and Δ*uhpT*Δ*glpT* among cell conditions (Figure 6.13C).

The replication of Δ*agr* yielded a 2.6 fold and 6.3 fold reduction in final CFU/ml compared to WT in 5mM and 0mM glucose conditions respectively (Figure 6.13A and B). Impaired intracellular growth in 5mM and 0mM conditions was verified by doubling times of 1.5 and 2.6 fold longer than WT (Figure 6.13C).

6.4.2.4 Summary of infection

When mammalian cells were cultured in 5mM glucose, this provided conditions in which sugar phosphates become a valuable nutrient source for bacterial growth. The ability of Δ*uhpT*Δ*glpT* to replicate in these cell conditions was completely unimpaired relative to WT USA300 LAC. Both the magnitude of bacterial growth yield and the average doubling times did not significantly differ between WT and Δ*uhpT*Δ*glpT* in three epithelial cell lines. When WT and Δ*uhpT*Δ*glpT* USA300 LAC strains were infected into glucose starved cells, the magnitude of replication was routinely greater than in cells cultured in 5mM glucose. Finally, the ability of avirulent Δ*agr* to replicate was severely impaired in all cell types and conditions compared to WT USA300 LAC.

A

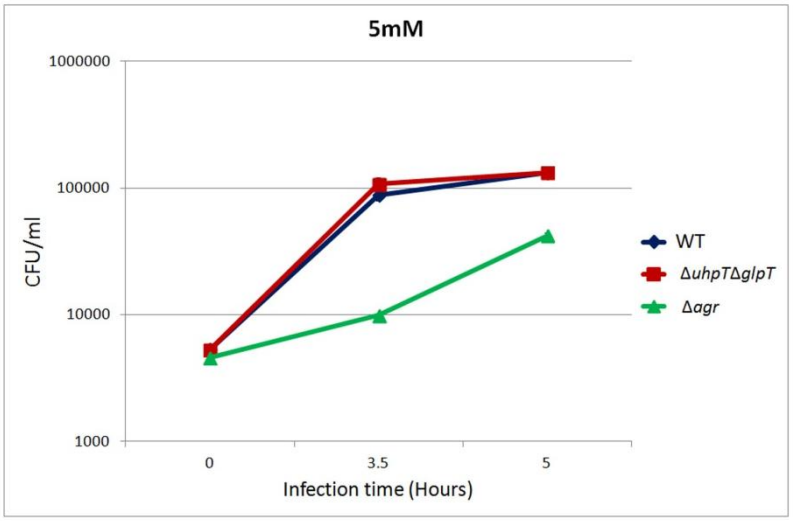

B

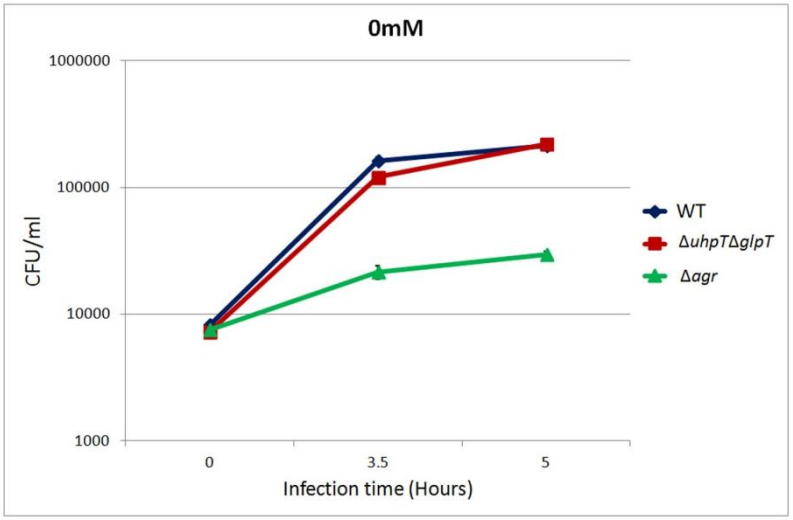

C

	Mean generation time (minutes)		
Cell media	WT	*ΔuhpTΔglpT*	*Δagr*
5mM Glucose	64.96 ± 1.2	64.5 ± 3.2	96 ± 4.7
0mM Glucose	64.5 ± 0.3	61.01 ± 2.6	172 ± 12.2

Figure 6.13. Replication of *S. aureus* USA300 LAC strains in FTO2B cells. Intracellular proliferation assays compare the average CFU/ml of WT,Δ*uhpT*-Δ*glpT*.and Δ*agr* up to 5 hours during infection. Charts show a representative assay including standard error of the mean. **A.** Cells cultured in 5mM glucose **B.** Cells cultured without glucose **C.** Average doubling times ± standard error of bacteria by 5 hours during infection in cells cultured in glucose conditions.

6.4.3 *S. aureus* USA300 LAC replication correlates with vacuole inclusion

The intracellular localisation of *S. aureus* USA300 LAC was investigated to ascertain the compartment occupied during infection. As sugar phosphate permease deficiency does not affect replication, it was important to determine the accessibility to sugar phosphates as nutrient sources. The cellular GTPase Rab7 was selected as a vacuole marker to probe the localisation of WT *S. aureus* USA300 LAC within HeLa and A549 epithelial cell infection.

Figure 6.14 and 6.15 shows immunofluorescence microscopy imaging of Rab7 and *S. aureus* USA300 LAC during infection of HeLa cells and A549 cells, respectively at an MOI of 10. According to this infection assay, bacterial invasion events occur within the hour after first exposing inocula to cells. At this point, time 0 hours, the majority of bacterial clusters were clearly co-localised with Rab7 proteins. The merged image shows areas of distinct co-localisation are pink, produced by blue/red mixing. Greyscale single channels allow for distinct, explicit contrast, and show the most concentrated areas of *S. aureus* and Rab7. The aggregation of Rab7 at staphylococcal clusters, confirms co-localisation. Throughout infection this association is prominent in both cell types. At later time points, large expanses of aggregated bacteria can be seen with defined, sharp red Rab7 boundaries enclosing blue staphylococcal bodies (Figure 6.14, 6h and Figure 6.15, 3h).

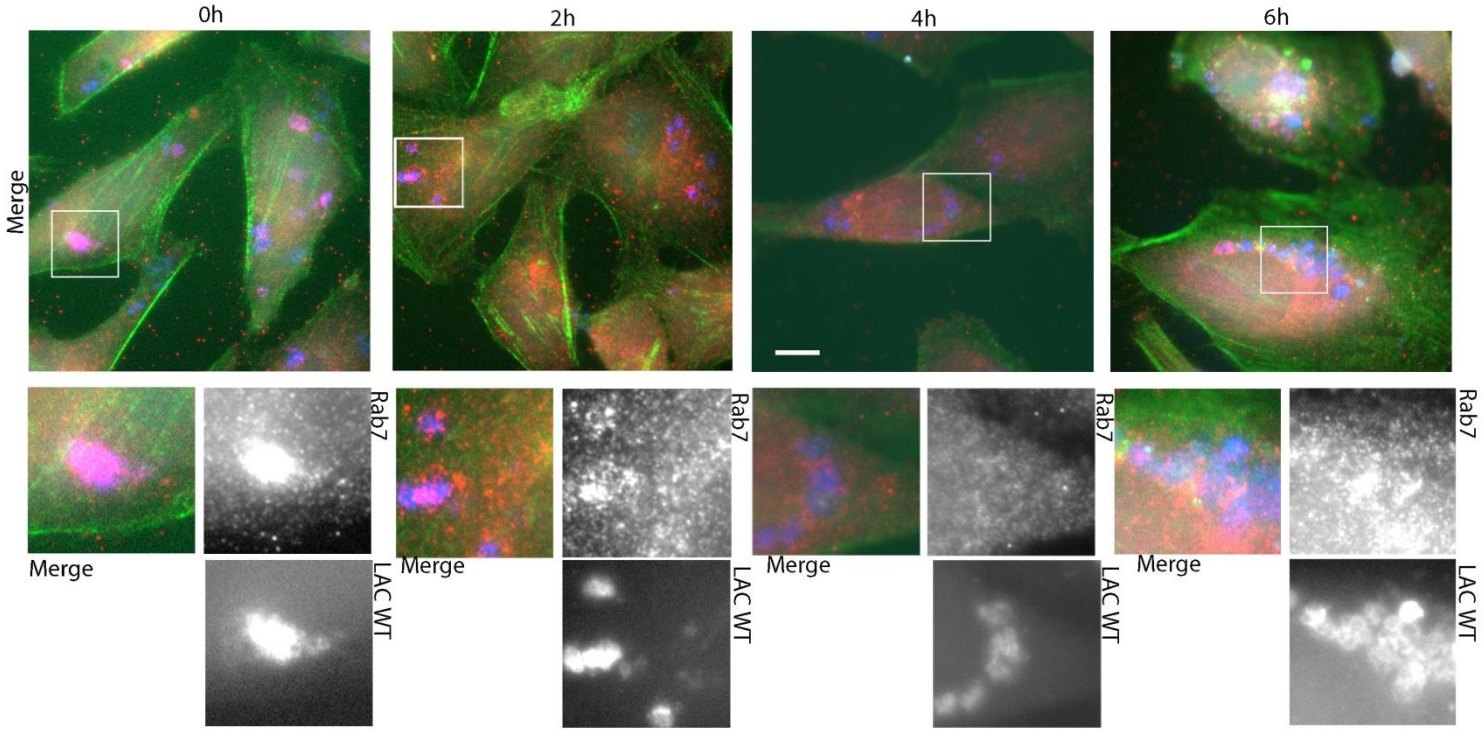

Figure 6.14. Co-localisation of *S. aureus* WT LAC with Rab7 in HeLa infection (MOI 10).
Time course infection to 6 hours post invasion of bacteria. Merged images show fluorescence of *S. aureus* stained with anti-*Staphylococcus aureus* polyclonal IgG/ Alexa Fluor 350-conjugated anti-Rabbit IgG (**Blue**), Rab7 visualised with anti-Rab7 monoclonal IgG/ Alexa Fluor 568-conjugated anti-Mouse IgG (**Red**) and F-actin highlighted using Alexa Fluor 488-conjugated phalloidin (**Green**). Individual channels are shown in **greyscale** for greater contrast.
Scalebar 10µm.

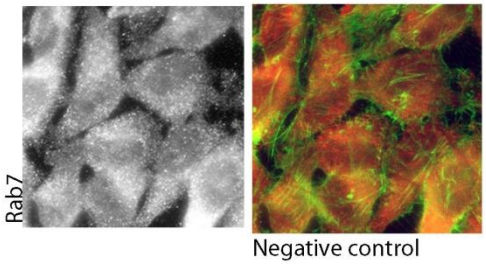

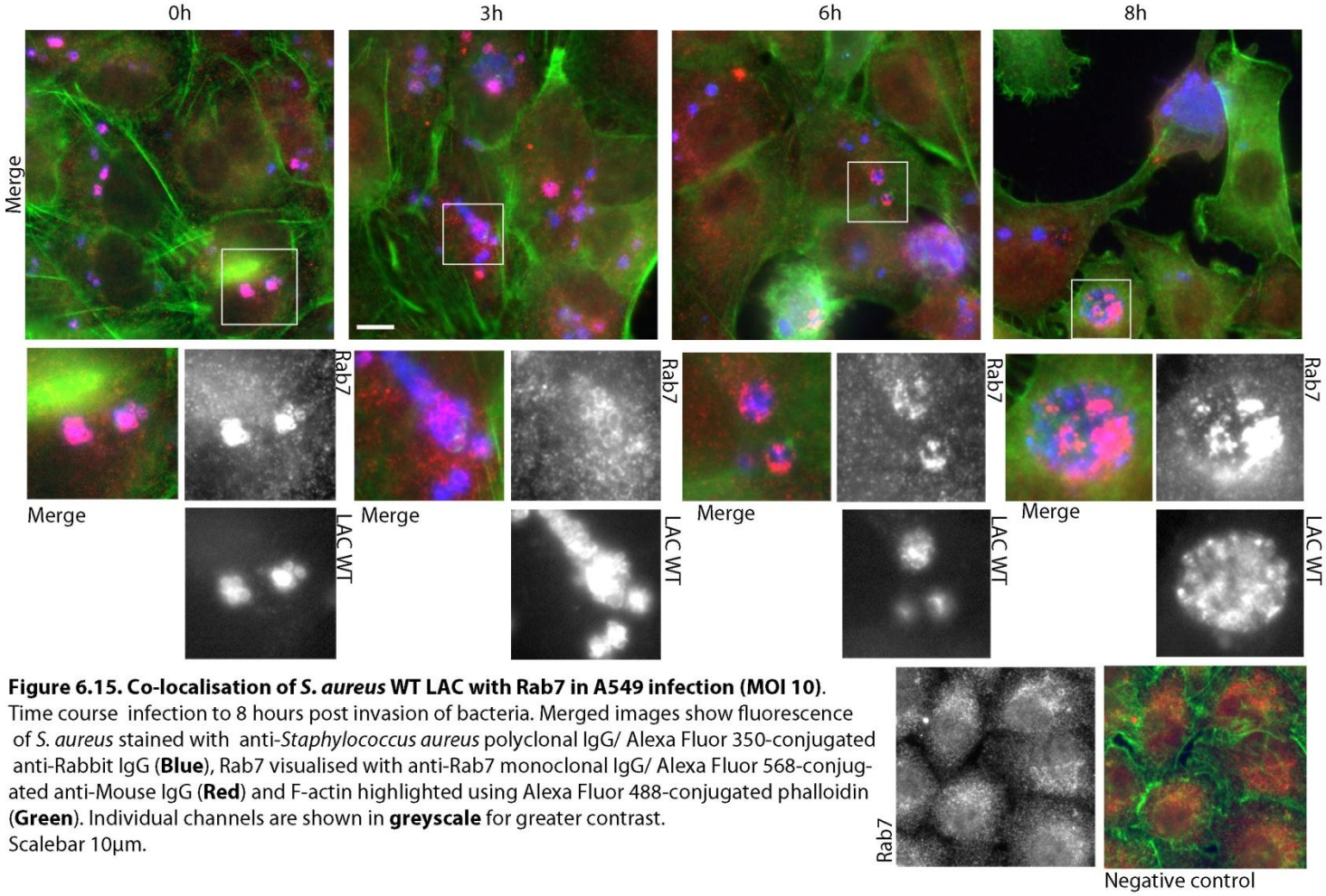

Figure 6.15. Co-localisation of *S. aureus* WT LAC with Rab7 in A549 infection (MOI 10).
Time course infection to 8 hours post invasion of bacteria. Merged images show fluorescence of *S. aureus* stained with anti-*Staphylococcus aureus* polyclonal IgG/ Alexa Fluor 350-conjugated anti-Rabbit IgG (**Blue**), Rab7 visualised with anti-Rab7 monoclonal IgG/ Alexa Fluor 568-conjugated anti-Mouse IgG (**Red**) and F-actin highlighted using Alexa Fluor 488-conjugated phalloidin (**Green**). Individual channels are shown in **greyscale** for greater contrast.
Scalebar 10µm.

The number of intracellular USA300 clusters positively co-localised with Rab7 was quantified in infected cells an expressed as a percentage. Figure 6.16A and 6.16B show that over 70% co-localisation was observed at 0h in both HeLa and A549 cells. By 2-3 hours into the infection, Rab7 association is maximal, peaking above 80%. This association remained consistent to 4 hours in HeLa cell infection (the final measureable time point before cell monolayer destruction) and to 6 hours in A549 cell infection.

When HeLa cells were infected at an MOI of 10, bacterial numbers were found to increase sharply between 2 and 4h (Figure 6.5A). Figure 6.16A confirms that proliferation in HeLa is principally intravacuolar. In order to confirm the same connection in A549 cells, intracellular replication assays were performed, infecting USA300 at MOI 10. Figure 6.17 shows the average CFU/ml of WT USA300 LAC inside A549 cells up to 6 hours post bacterial invasion. This confirmed that at MOI 10, the highest increase in proliferation occured between 4 and 6 hours, as the bacterial load escalates 5 fold. By 6 hours, almost 70% of USA300 clusters were co-localised with Rab7 (Figure 6.16B).

Crucially, the timing of greatest bacterial generation is consistent with vacuole inclusion. Immunofluorescence microscopy has verified that throughout the entire period of monitored intracellular bacterial replication, *S. aureus* USA300 LAC is principally residing within Rab7 associated vacuoles.

A

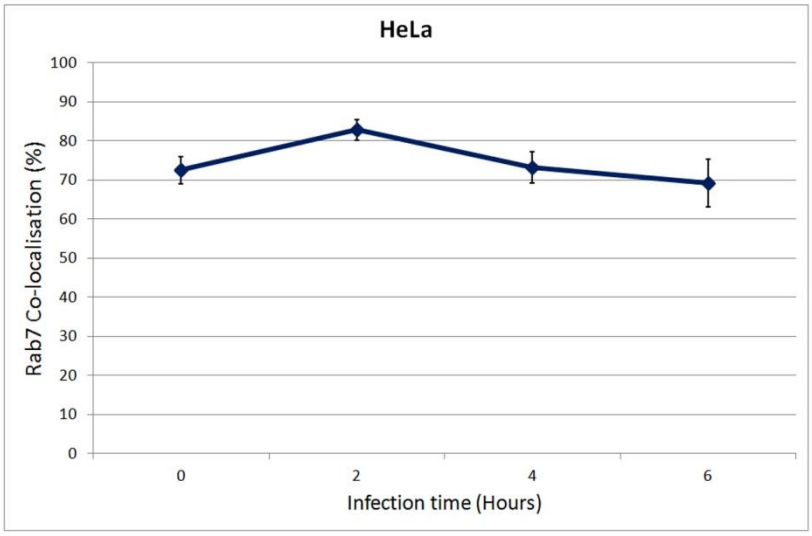

B

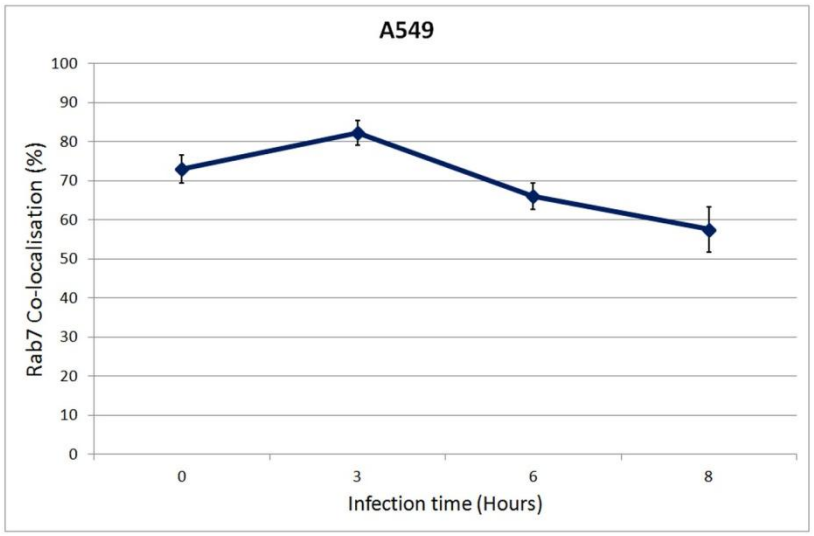

Figure 6.16. Co-localisation of intracellular Rab7 GTPase and *S. aureus* USA300 LAC. The average percentage of total bacterial clusters positively co-localised with Rab7 during intracellular infection of mammalian epithelial cells. The % at each time point is calculated from at least 10 fields with on average 24.7±1.6 cells per field and shows standard error of the mean. **A.** HeLa cell infection. **B.** A549 cell infection.

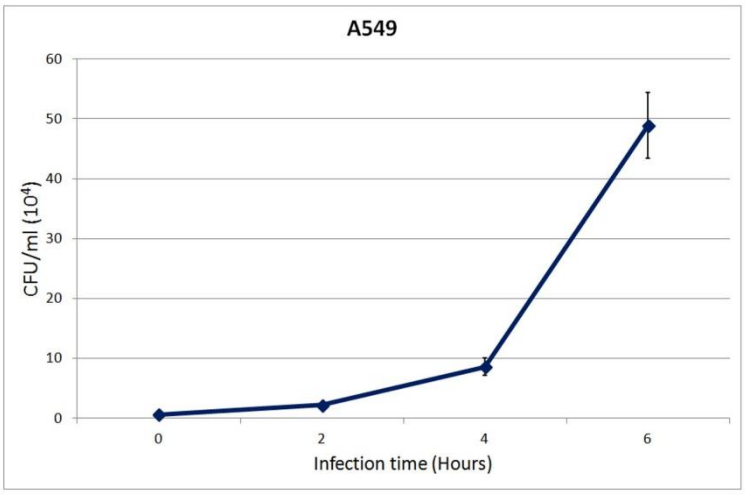

Figure 6.17. Replication of *S. aureus* USA300 LAC in A549 cells at MOI 10. Intracellular proliferation assay shows the average CFU/ml of WT USA300 LAC in A549 cells cultured in 5mM glucose. Average values are calculated from 2 separate assays and show standard error of the mean.

6.5 Discussion

A robust intracellular model of *S. aureus* USA300 LAC epithelial cell infection was standardised which quantified replication. This research disclosed features of CA-MRSA invasive infection. The magnitude of intracellular replication varies depending upon the number of bacteria initially exposed to the monolayer. A significantly higher percentage of cells were subject to invasion by over 3 fold more bacteria per cell at an MOI of 10 compared to an MOI of 1. In addition, this loading of cells with *S. aureus* contributed to a prolific increase in numbers which caused cytotoxicity, affecting half of the HeLa cell monolayer. By contrast, monolayers infected with *S. aureus* at an MOI of 1 were found to harbour on average 1 bacterial cluster per cell which replicated without damaging the integrity of the epithelial monolayer. The levels of infected cells remained stable throughout all USA300 LAC infection, suggesting that cell-to-cell spread is not a feature of pathogenesis. The bacterial load invading cells therefore commands pathogenesis. It is plausible that this feature can be attributed to the *agr* quorum sensing system, which may be synergistically up-regulated in multiple *S. aureus* sharing the same infected cells (Novick & Geisinger 2008). As this system is responsible for up-regulation of various cytotoxic proteins that destroy tissue for dissemination (Gordon & Lowy 2008), this explains why Δ*agr* was non-cytotoxic to the epithelial monolayer compared to the destructive WT strain. Regulation by *agr* was also discovered to be essential towards effective intracellular replication. This finding is in agreement with a previous study that demonstrated *S. aureus* RN6390 replicates during bovine mammary cell infection, whereas an *agr* mutant derivative cannot (Wesson *et al.* 1998). In addition, a recent study also identifies three independent *agr* deficient strains of *S. aureus* that lack the capability to replicate efficiently inside HeLa cells (Schnaith *et al.* 2007). The replication deficiency of *S. aureus* USA300 LAC Δ*agr* was further explored in Chapter 7.

6.5.1 Contextual role of sugar phosphate transporters

Epithelial cell infection assays were performed to monitor replication of *S. aureus* USA300 LAC strains in cellular conditions which promote *L. monocytogenes* growth specifically due to expression of sugar phosphate permeases. *S. aureus* USA300 LAC unable to express functional sugar phosphate permeases, Δ*uhpT*Δ*glpT*, was totally unaffected in growth capability compared to WT. In this model of infection, sugar phosphates are non-essential substrates towards intracellular replication of USA300, despite demonstrating they promote extensive *in vitro* replication. In the *S. aureus* background, sugar phosphate transporters UhpT and GlpT are dispensable to invasive pathogenesis. It was previously demonstrated in this study that complementation of *L. monocytogenes* P14-A Δ*hpt* with homologous staphylococcal permeases restored intracellular replication to background level P14-A expressing listerial *hpt*. In the genetic background of *L. monocytogenes*, sugar phosphate uptake is an important function involved in invasive pathogenesis. By contrast *S. aureus* is able to employ other nutrient uptake mechanisms which promote WT level replication in the absence of sugar phosphate uptake. This distinction represents a contextual role for sugar phosphate permeases in which their significance is dependent upon the metabolic demands of the bacteria able to express them.

Research in this thesis has contributed an additional bacterial species which possesses sugar phosphate permeases that have no palpable role in bacterial intracellular replication. Enteroinvasive *Salmonella* Typhimurium is an isolate that replicates largely within *Salmonella* containing vacuoles (SCVs) inside host cells (Knodler & Steele-Mortimer 2003). A study noted no difference in the intracellular doubling time in Caco-2 cells when the *uhpT* permease was deleted (Götz & Goebel 2010). In addition, an enteroinvasive *E. coli* species, which escapes the endosome and replicates inside the cytosol was unhindered in growth without the UhpT transport system. Another study, using *Shigella flexineri*, demonstrated no marked

difference in Henle cell plaque formation between the wild type and the Δ*uhpT* strains (Runyen-Janecky & Payne 2002). Together with the infection results described in this chapter, the unessential role of UhpT has been reported for bacteria residing in two distinct cellular locations. *E. coli* and *S. flexineri* have unrestricted access to sugar phosphates in the cytosol. *S.* Typhimurium and *S. aureus* USA300 LAC are confined within a membrane bound vacuole, which impedes free uptake of cytosolic intermediates. Sugar phosphates have proven to be an excellent source of *in vitro* nutrition for every one of these species, and moreover significant up regulation of their homologous *uhpT* genes during cell infection is reported (Lucchini *et al.* 2005; Hautefort *et al.* 2008; Garzoni *et al*. 2007). In these cases, hexose phosphate transport is commonly implicated in host cell pathogenesis but is not effectual.

6.5.2 Metabolic redundancy

Redundancy of bacterial nutrient uptake systems and metabolic pathways may offer adaptability to the cellular environment. A recent study monitored Caco-2 cell infection of invasive *E. coli* and *S.* Typhimurium (Götz *et al.* 2010). Successive mutants for each strain were created in metabolic transport genes. A single mutant of the UhpT permease, a double mutant removing the major glucose PTS uptake system (*ptsG*) and a mannose PTS uptake system (*manXYZ*) and finally a strain incorporating all three mutations were constructed. Intracellular replication assays showed that the mean generation time of each mutant strain was comparable to the respective wild type. This work also demonstrated that radiolabelled glucose is preferentially taken up by both wild type strains when it is available intracellularly. Similarly, a double mutant involving the two primary PTS uptake systems for glucose and mannose was analysed in *L. monocytogenes* (Stoll & Goebel 2010) . In epithelial cells and mouse macrophages grown in 10mM glucose, this strain was unaffected in growth despite exhibited severe impairment in glucose and mannose *in vitro*. In a *Salmonella* strain, the glucokinase enzyme was deleted in a strain already

containing a Δ*ptsG*Δ*manXYZ* genotype. Only this additional mutation, which severed the glycolysis pathway at the initiating step, was able to significantly attenuate replication of *Salmonella* in macrophages (Bowden *et al.* 2009).

The evolution and conservation of multiple, diverse bacterial transport systems is testament to the inherent function to parasitise host cells for growth (Pao *et al.* 1998; Lewis *et al.* 2012). Mutations in carbohydrate transport systems largely do not affect virulence in distinctly compartmentalised invasive bacteria (Götz *et al.* 2010; Stoll & Goebel 2010; Bowden *et al.* 2009). The likelihood is that redundant uptake mechanisms and metabolic pathways can fill the gap presented by mutational analysis. Indeed, the genetic background of *S. aureus* provides extensive redundancy of transport systems and metabolic pathways to ensure replication in a broad range of nutrients (Fuchs *et al.* 2012), which was confirmed in this study. Apparently non-essential systems, such as sugar phosphate permeases, should therefore not be labelled impractical or non-contributory as they may provide a positive function when expressed, that may be masked during mutagenesis studies.

6.5.3 Alternative intracellular nutrient sources for replication

Replication of *S. aureus* USA300 LAC was compared in cells supplied with exogenous glucose and cells starved of any sugar supply. It was consistently reported that *S. aureus* replicated with a greater magnitude within sugar starved cells than in cells with a physiological supply of glucose. These observations indicate that *S. aureus* USA300 can replicate with greater effectiveness in cellular starvation, in the absence of cellular glucose metabolism. Increased replication without glucose metabolites may suggest that alternative nutrition is driving pathogenesis.

Using immunofluorescence to visualise infection, it was ascertained that the large majority of *S. aureus* USA300 LAC clusters were co-localised with Rab7 GTPase vacuole marker for a duration of pronounced replication.

Recent publications also verified *S. aureus* USA300 vacuole inclusion during epithelial cell infection and confirmed that the vast majority of clusters were co-localised with autophagosome membrane markers (Schnaith *et al.* 2007; Mauthe *et al.* 2012). Autophagosome formation is the initiating step of the mammalian cell autophagy process. Autophagy is the cellular recycling mechanism for catabolising and degrading excess or injured organelles (Yoshimori 2004). Normally, during steady state homeostasis, autophagy operates at a basal level. Autophagy is strongly induced during cellular stress and starvation as a response to meet energy demands. For example, during amino acid starvation, large protein complexes can be targeted for degradation to produce raw materials for synthesis of fresh macromolecules (Yoshimori 2004). Figure 6.18 outlines the autophagy process in mammalian cells.

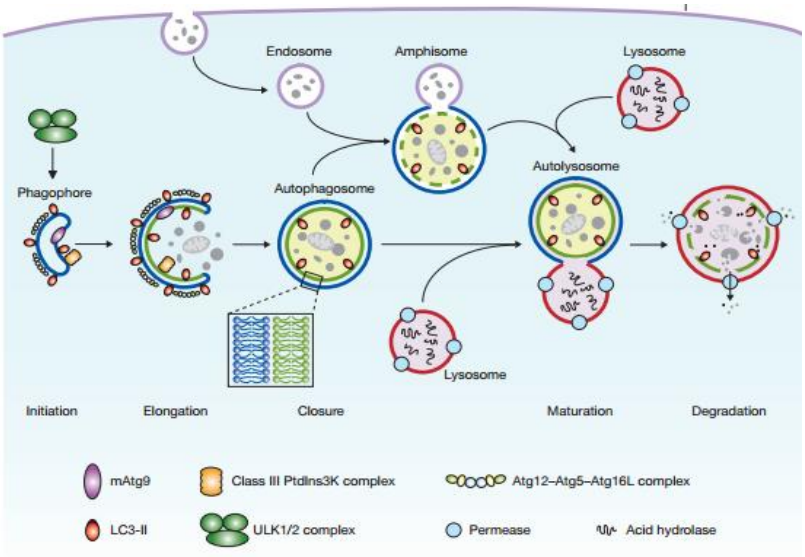

Figure 6.18. Mammalian cell autophagy process. The schematic depicts the formation of the autophagosome, showing proteins that typically localise to this membrane interface, and fusion of cell vesicles to eventually form an autolysosome. (Taken from Yang and Kilonsky 2010).

During macroautophagy, autophagy related proteins such as LC3 and Atg18 are recruited to organise the formation of a double membrane vesicle called a phagophore (Yang & Klionsky 2010). This phagophore expands and closes, capturing cytoplasmic components, and forming the double membrane autophagosome. Endosomes can fuse with the autophagosome to deliver contents into the lumen of the double membrane enclosure. Maturation occurs by lysosomal fusion, forming an autolysosome. The entire autophagosome structure and all of its contents are degraded by the injection of lysosomal acid hydrolases (Yang & Klionsky 2010).

It has been demonstrated that *S. aureus* USA300 induces autophagosome envelopment upon infection and prevents autolysosome maturation to replicate within the autophagosomal compartment (Schnaith *et al.* 2007; Mauthe *et al.* 2012). Maintainance of Rab7 at the staphylococcal vacuole interface, as confirmed in this chapter, may advocate maturation of the autopahgosomal membrane (Gutierrez *et al.* 2004). This can be substantiated by immunofluorescence microcopy vacuole detection using autophagosomal membrane markers. The induction of the autophagy pathway by *S. aureus* infection signifies a specific vacuolar niche in which replication occurs. The very nature of autophagy involves sequestering proteinous cytosolic components for digestion during cell stress, such as glucose starvation. Autophagy would deliver a source of peptides and amino acids to the staphylococcal inclusion, which have been confirmed as nutritious sources for replication. In addition, envelopment of the cytosol by the autophagy phagophore can enclose any cytosolic substrates that are present, including glucose and glucose derived compounds if provided to cells. Induction of the autophagic process could potentially provide a micro-environment of nutrients, into which *S. aureus* USA300 LAC is deposited.

A feature shared by bacterial species in which Hpt related transporters have been found dispensible in infection is the possession of a complete tricarboxylic acid cycle. *S. aureus*, *S.* Typhimurium*, E. coli* and *S. flexineri*

all have the ability to derive substantial growth from amino acids as a sole nutrient source (Erlandson & Mackey 1958; Dawes 1952; Gutnick *et al.* 1969) which may be attributed to TCA cycle metabolism. By contrast, *L. monocytogenes* has a broken TCA cycle and cannot replicate using amino acids exclusively (Joseph & Goebel 2007). These intrinsic metabolic differences may account for impaired replication in the *L. monocytogenes* Δ*hpt* mutant, as amino acids/peptides cannot offer a replaceable, effective nutrient source in this species. The opposite may be true for those species with complete TCA cycles, such as *S. aureus*, with proteinous sources contributing a marked benefit to intracellular growth.

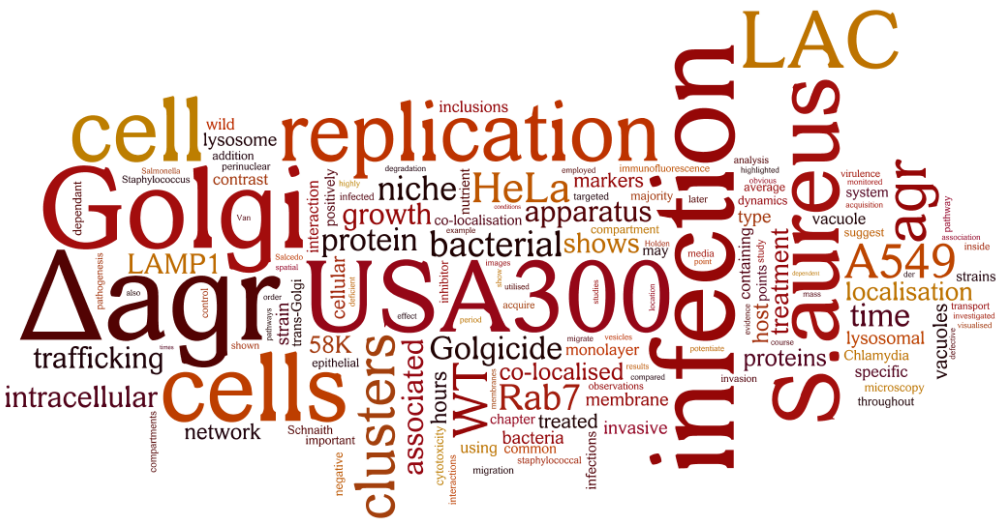

Chapter 7

Host cell interactions that potentiate replication of *S. aureus* USA300 LAC

7.1 Introduction

In chapter 6, an epithelial cell infection model was established for *S. aureus* USA300 LAC, discovering that extensive replication correlated with majority vacuole enclosure. Intravacuolar pathogens are highly adapted to ensure survival and replication from within this niche (Kumar & Valdivia 2009; Saka & Valdivia 2010; Knodler & Steele-Mortimer 2003; Isberg *et al.* 2009). Vacuole modification and interaction with host cell signalling proteins is fundamental to the success of established vacuole based bacteria (Gruenberg & Van der Goot 2006). These mechanisms are essential in ensuring replication niches are established, and therefore can be the prerequisite for nutrient acquisition supporting growth (Heuer *et al.* 2009; Kyei *et al.* 2006; Salcedo & Holden 2003).

Research in this study indicates that WT *Staphylococcus aureus* containing vacuoles can competently establish a replication niche within the cell. By contrast, it was noted that a *S. aureus* USA300 strain with a defective *agr* regulatory system showed markedly impaired intracellular replication compared to the WT. As a functional *agr* system is apparently integral to intracellular replication, research was directed towards understanding the mechanisms and interactions that set apart WT *S. aureus* USA300 LAC and Δ*agr*.

7.2 Objectives

In order to compare the capability of Δ*agr* with WT USA300 LAC for replication upon nutrient sources, *in vitro* growth analysis was performed using Δ*agr.* This was done in order to identify any metabolic defects, caused by *agr* deficiency, which may highlight nutritional differences that account for intracellular growth impairment.

Recent publications have identified that Δ*agr* mutants of other *S. aureus* strains do not follow the same vacuole inclusion dynamics as WT. In contrast to wild type strains , which typically acquire autophagosomal

membrane markers and proliferate, Δ*agr* derivatives are found to remain closely associated with lysosomal associated membrane proteins (LAMPs) and fail to replicate (Schnaith *et al.* 2007; Jarry *et al.* 2008). This suggests that *agr* defective *S. aureus* containing phagosomes are subjected to lysosomal fusion and targeted for acid hydrolysis and proteolytic degradation (Ciechanover 2005; Levine & Kroemer 2008). To determine the cellular localisation of the *S. aureus* USA300 LAC Δ*agr* compartment, immunofluorescence microscopy was used to investigate endocytic pathway marker associations.

Visualisation of *S. aureus* USA300 LAC epithelial cell infection by immunofluorescence microscopy showed the routine convergence of separate staphylococcal clusters at a common perinuclear location. At this site, bacteria were seen to expand in a uniform mass which suggests that interaction of staphylococcal clusters at this cellular location is important in promoting replication. Most invasive vacuole based pathogens migrate to a perinuclear region of the cell (Gruenberg & Van der Goot 2006). *Salmonella* Typhimurium and *Chlamydia trachomatis* are invasive intravacuolar species which hijack host cell trafficking pathways to manoeuvre to the perinuclear replicative niche (McGhie *et al.* 2009; Méresse *et al.* 1999; Sinai & Joiner 1997; Yasir *et al.* 2011). In both cases, bacterial inclusions become closely associated with markers of the Golgi apparatus (Salcedo & Holden 2003; Heuer *et al.* 2009). This association has proven to be integral to both nutrient acquisition and capability for replication of these species. *Salmonella* recruits cell trafficking protein Rab7 to the SCV, an interaction that is maintained for migration to the replication niche (Méresse et al. 1999; Harrison *et al.* 2004). *S. aureus* USA300 clusters remained largely associated with Rab7 until the aggregation of bacteria at the perinuclear region. Immunofluorescence microscopy was therefore employed to investigate associations between the Golgi apparatus and *S. aureus* USA300 LAC strains, with a view to uncovering the cellular niche which promotes replication.

7.3 Relevant materials and methods

In vitro **assays (2.4)** Bacterial growth (2.4.1); Mammalian cell cytotoxicity (2.4.2)

Mammalian cell culture (2.5) *S. aureus* infection (2.5.3.1); Immunofluorescence microscopy (2.5.4); Inhibitor treatment of mammalian cells (2.5.5)

Statistical analysis (2.6)

7.4 Results

7.4.1 *In vitro* growth of *S. aureus* USA300 LAC Δ*agr*

In vitro growth analysis was undertaken, assessing the ability of the Δ*agr* strain to multiply in a variety of growth conditions and individual substrates. This would determine the metabolic capacity compared to WT USA300 LAC.

Figure 7.1A and B shows *in vitro* growth analysis of Δ*agr* in nutrient rich BHI and LB broth relative to WT. In these media, nutrients were utilised by Δ*agr* to generate rapid, high yield replication that is not significantly different to the WT by stationary phase (p=>>0.05). Figure 7.1C demonstrates the growth of Δ*agr* in minimal media supplemented with glucose, fructose-6-phosphate and glycerol-1-phosphate indicating that growth was unimpaired in non-phosphorylated, C6 phosphorylated and C3 phosphorylated nutrient sources relative to WT USA300 LAC. Figure 7.1D compares growth of WT LAC and Δ*agr* in minimal media using RPMI amino acids as a sole nutrient source. Substantiating growth in LB, this shows that Δ*agr* can derive high level growth from amino acids alone. These results demonstrate that the *agr* mutation confers no obvious defects in carbon nutrient acquisition or metabolism.

Impaired replication could therefore potentially be the effect of defective vacuole maturation. In this situation, Δ*agr* may be unable to affect the escape from the degradation pathway or fail to localise at a bacterially targeted cell location for replication.

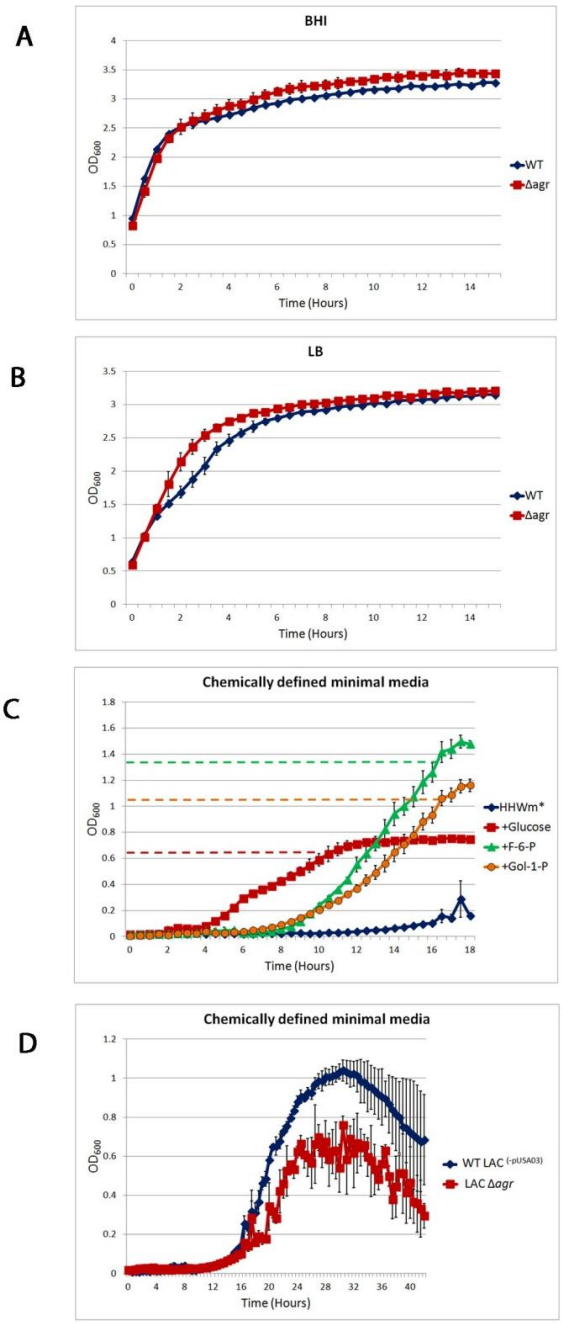

Figure 7.1. *In vitro* growth of *S. aureus* LAC Δ*agr*. A. Comparison of wild type LAC with Δ*agr* in rich BHI growth media. **B.** Comparsion of wild type LAC with Δ*agr* in amino acid rich LB media. **C.** Growth of Δ*agr* in minimal media HHWm* supplemented with 20mM sugar substrates. Coloured lines represent the level of growth elicited by WT LAC in the same substrates. **D.** Growth of Δ*agr* in amino acid containing minimal media HHWm* compared to WT LAC. Growth assays were performed in triplicate and show standard deviation.

7.4.2 Cellular localisation of *S. aureus* USA300 LAC Δ*agr*

7.4.2.1 Rab7 co-localisation

Co-localisation of Rab7 was investigated to compare the nature of the Δ*agr* containing vacuole to the WT. Epithelial cell infections were performed with Δ*agr* and the antibody markers and conditions for detecting Rab7 and *S. aureus* were utilised as described in Chapter 6.

Figure 7.2 shows the infection time course of HeLa cells by *S. aureus* USA300 LAC Δ*agr.* Representative images show that throughout the infection, the large majority of staphylococcal inclusions were not co-localised with Rab7. However, Δ*agr* clusters were not totally independent of Rab7 association. At 4h, an example is highlighted to convey that few clusters of Δ*agr* can be positively co-localised with Rab7. Greyscale images depict clearly, there were few visible concentrations of Rab7 protein in the same cell space as *S. aureus* USA300 LAC Δ*agr* clusters.

Figure 7.3 demonstrates the same experiment in A549 cells, modelling USA300 human lung cell infection. Again, throughout infection, the majority of intracellular inclusions could not be positively co-localised with Rab7. At 3h post invasion, an example of definite Rab7 co-localisation is shown to substantiate that lack of marker acquisition by Δ*agr* was not absolute during infection.

The quantification of *S. aureus* USA300 LAC Δ*agr* infection in HeLa and A549 cells is shown in Figure 7.4. On average, fewer than 20% of bacterial clusters were positively co-localised with Rab7 at time 0h. By contrast, greater than 70% of wild type USA300 clusters could be positively identified at the same time ($p=<<0.05$). In HeLa cells, the number of Rab7 co-localised clusters diminished to 4% by 8h (Figure 7.4A) while this figure fell to 10% by 6h in A549 cells (Figure 7.4B). The majority of Δ*agr* inclusions were not occupying the same niche as WT USA300 during epithelial cell infection.

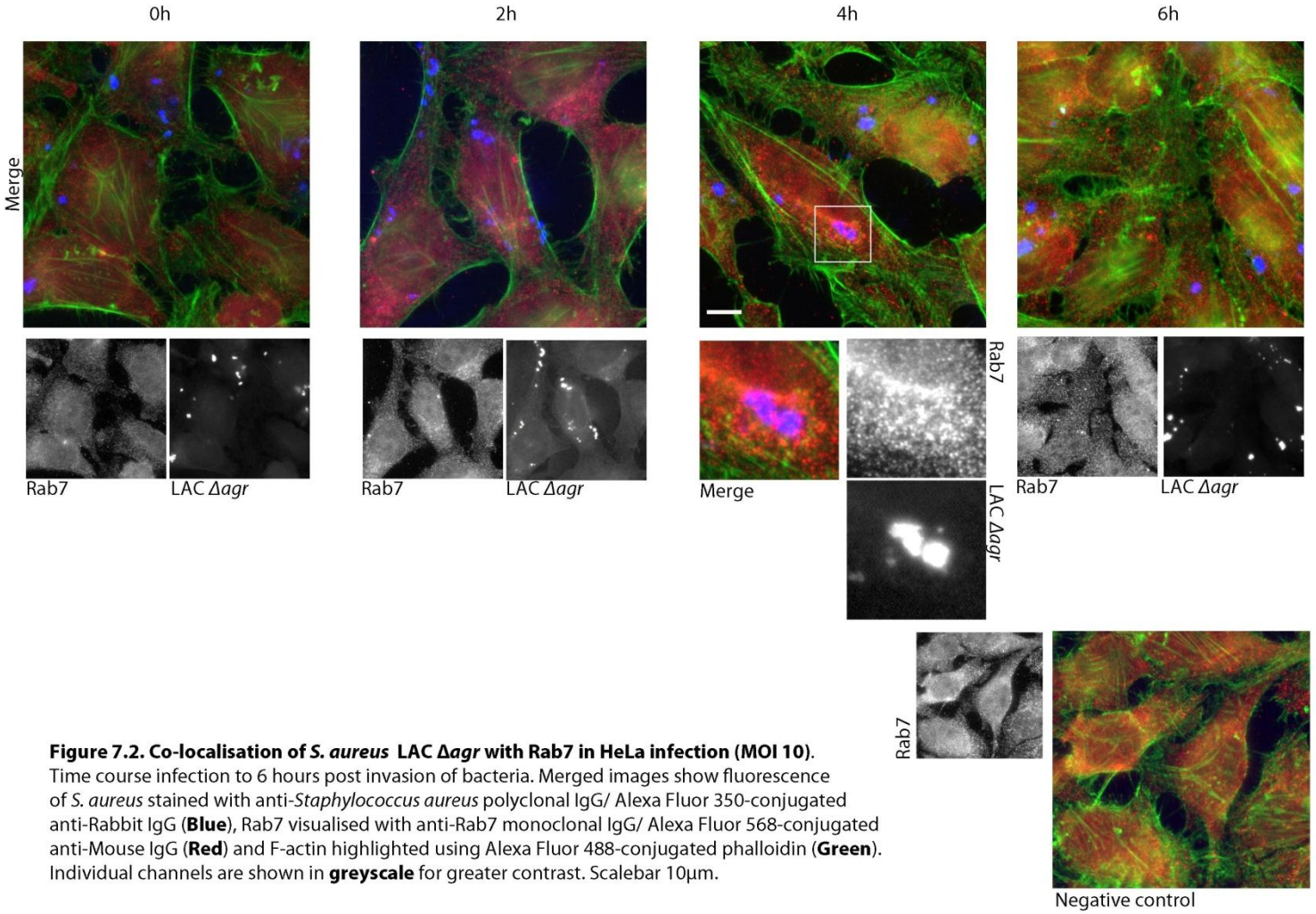

Figure 7.2. Co-localisation of *S. aureus* LAC Δ*agr* with Rab7 in HeLa infection (MOI 10). Time course infection to 6 hours post invasion of bacteria. Merged images show fluorescence of *S. aureus* stained with anti-*Staphylococcus aureus* polyclonal IgG/ Alexa Fluor 350-conjugated anti-Rabbit IgG (**Blue**), Rab7 visualised with anti-Rab7 monoclonal IgG/ Alexa Fluor 568-conjugated anti-Mouse IgG (**Red**) and F-actin highlighted using Alexa Fluor 488-conjugated phalloidin (**Green**). Individual channels are shown in **greyscale** for greater contrast. Scalebar 10μm.

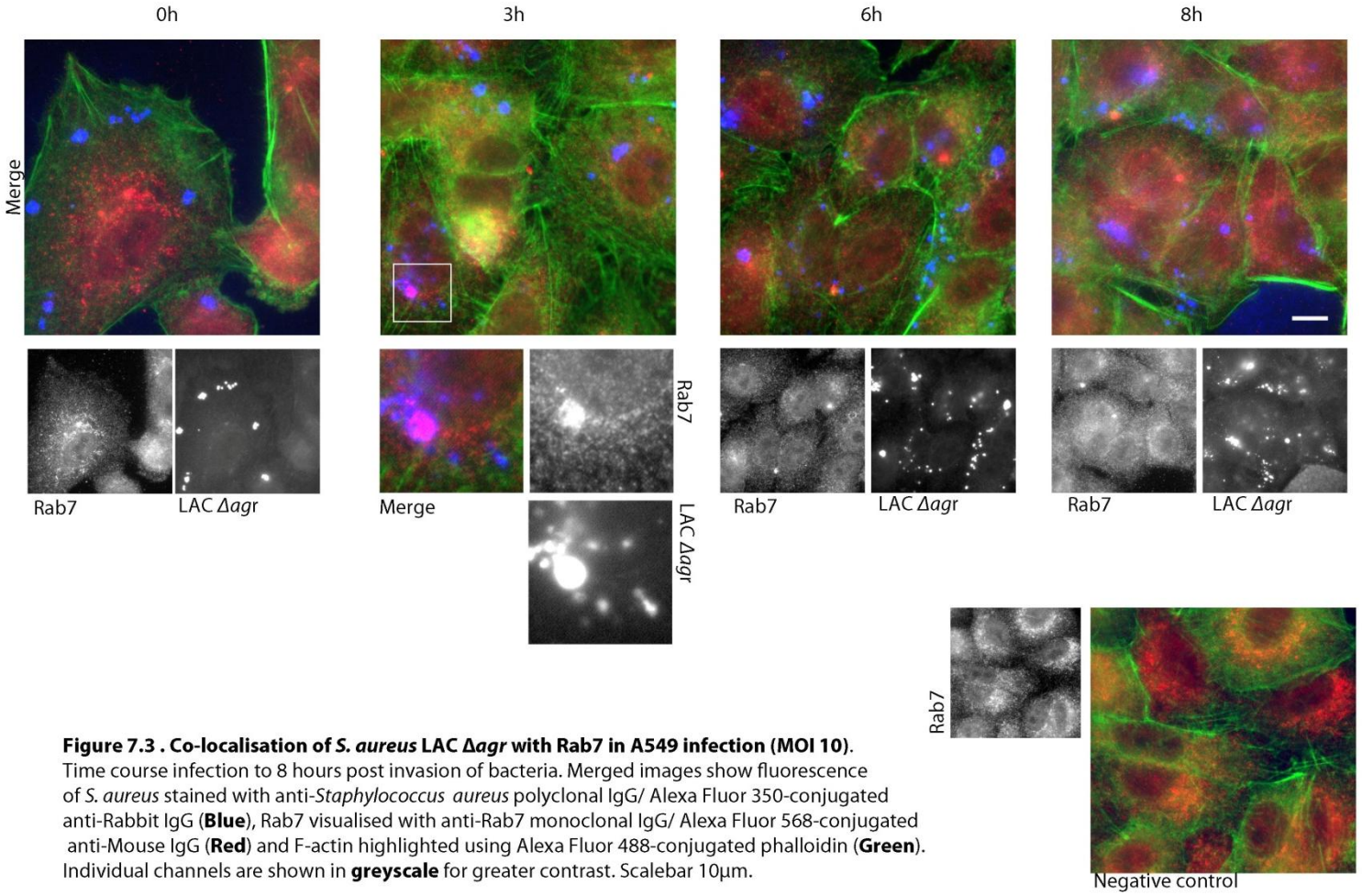

Figure 7.3 . Co-localisation of *S. aureus* LAC Δ*agr* with Rab7 in A549 infection (MOI 10).
Time course infection to 8 hours post invasion of bacteria. Merged images show fluorescence of *S. aureus* stained with anti-*Staphylococcus aureus* polyclonal IgG/ Alexa Fluor 350-conjugated anti-Rabbit IgG (**Blue**), Rab7 visualised with anti-Rab7 monoclonal IgG/ Alexa Fluor 568-conjugated anti-Mouse IgG (**Red**) and F-actin highlighted using Alexa Fluor 488-conjugated phalloidin (**Green**). Individual channels are shown in **greyscale** for greater contrast. Scalebar 10μm.

A

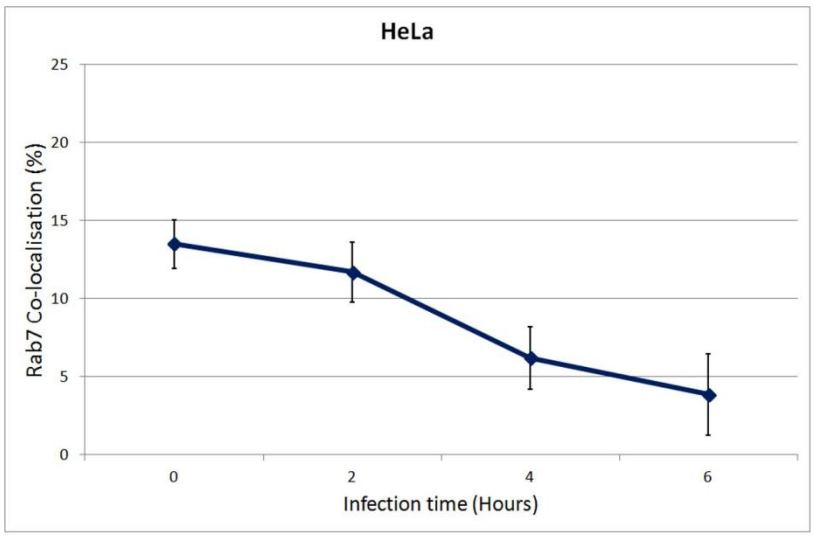

B

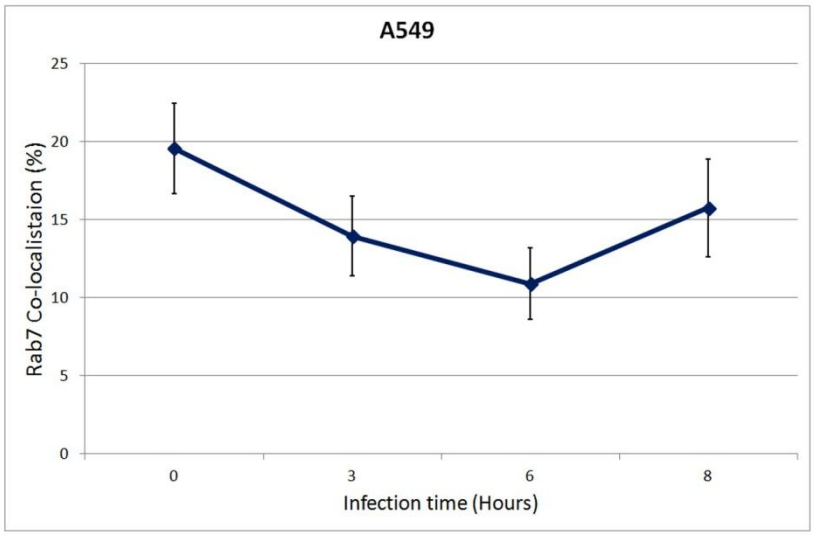

Figure 7.4. Co-localisation of intracellular Rab7 GTPase and *S. aureus* LAC Δ*agr*. The average percentage of total bacterial clusters positively co-localised with Rab7 during intracellular infection of mammalian epithelial cells. The % at each time point is calculated from at least 10 fields with on average 24.7±1.6 cells per field and shows standard error of the mean. **A.** HeLa cell infection. **B.** A549 cell infection.

7.4.2.2 LAMP1 co-localisation

Lysosomal associated membrane protein 1 (LAMP1) was targeted to mark cell lysosome localisation during Δ*agr* infection. The presence of LAMP proteins 1 and 2 make up around 50% of all lysosomal membrane proteins and are thought to contribute to the protection and preservation of the membrane from acid hydrolysis action (Eskelinen 2006). These proteins are recruited specifically to lysosome membranes.

Figure 7.5 and 7.6 depict infection of HeLa and A549 cells by *S. aureus* USA300 LAC Δ*agr* highlighting lysosomes via LAMP1 detection. At earlier times during infection, co-localisation of Δ*agr* with LAMP1 was not common. At time 0h the spatial distribution of lysosomes was in contrast to Δ*agr* localisation. With each successive time point of infection, there was greater association of LAMP1 and Δ*agr.* Expanded images at later times show clearly that LAMP1 protein encloses bacterial clusters, with an evident red border around the blue bacterial inclusion. White arrows highlight the higher number of clusters co-localised with LAMP1 at later time points.

Figure 7.7 charts the percentage of cellular Δ*agr* clusters co-localised with LAMP1 during infections. As illustrated in the immunofluorescence microscopy figures, co-localisation was on average much lower at earlier time points. However, progression of infection leads to greater numbers of bacterial clusters that were associated with LAMP1. In HeLa, 80% of Δ*agr* inclusions were co-localised with LAMP1 by 4h (Figure 7.7A). Similarly, on average 70% of clusters were enveloped by LAMP1 by 8h in A549 infection (Figure 7.7B). The majority of intracellular *S. aureus* USA300 LAC Δ*agr* compartments acquire LAMP1 markers by 4 hours in HeLa infection and by 6 hours in A549 infection.

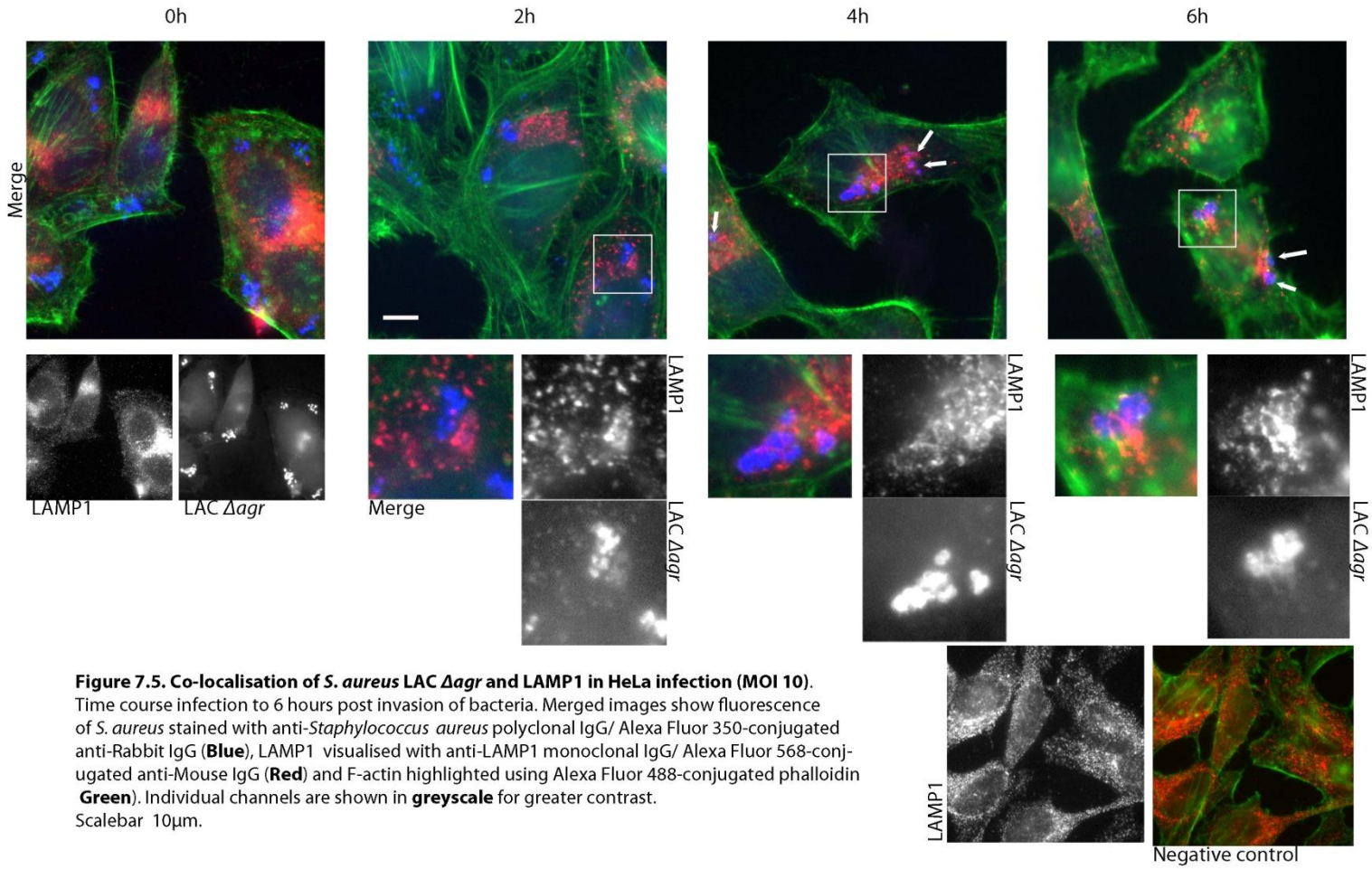

Figure 7.5. Co-localisation of *S. aureus* LAC *Δagr* and LAMP1 in HeLa infection (MOI 10).
Time course infection to 6 hours post invasion of bacteria. Merged images show fluorescence of *S. aureus* stained with anti-*Staphylococcus aureus* polyclonal IgG/ Alexa Fluor 350-conjugated anti-Rabbit IgG (**Blue**), LAMP1 visualised with anti-LAMP1 monoclonal IgG/ Alexa Fluor 568-conjugated anti-Mouse IgG (**Red**) and F-actin highlighted using Alexa Fluor 488-conjugated phalloidin (**Green**). Individual channels are shown in **greyscale** for greater contrast.
Scalebar 10µm.

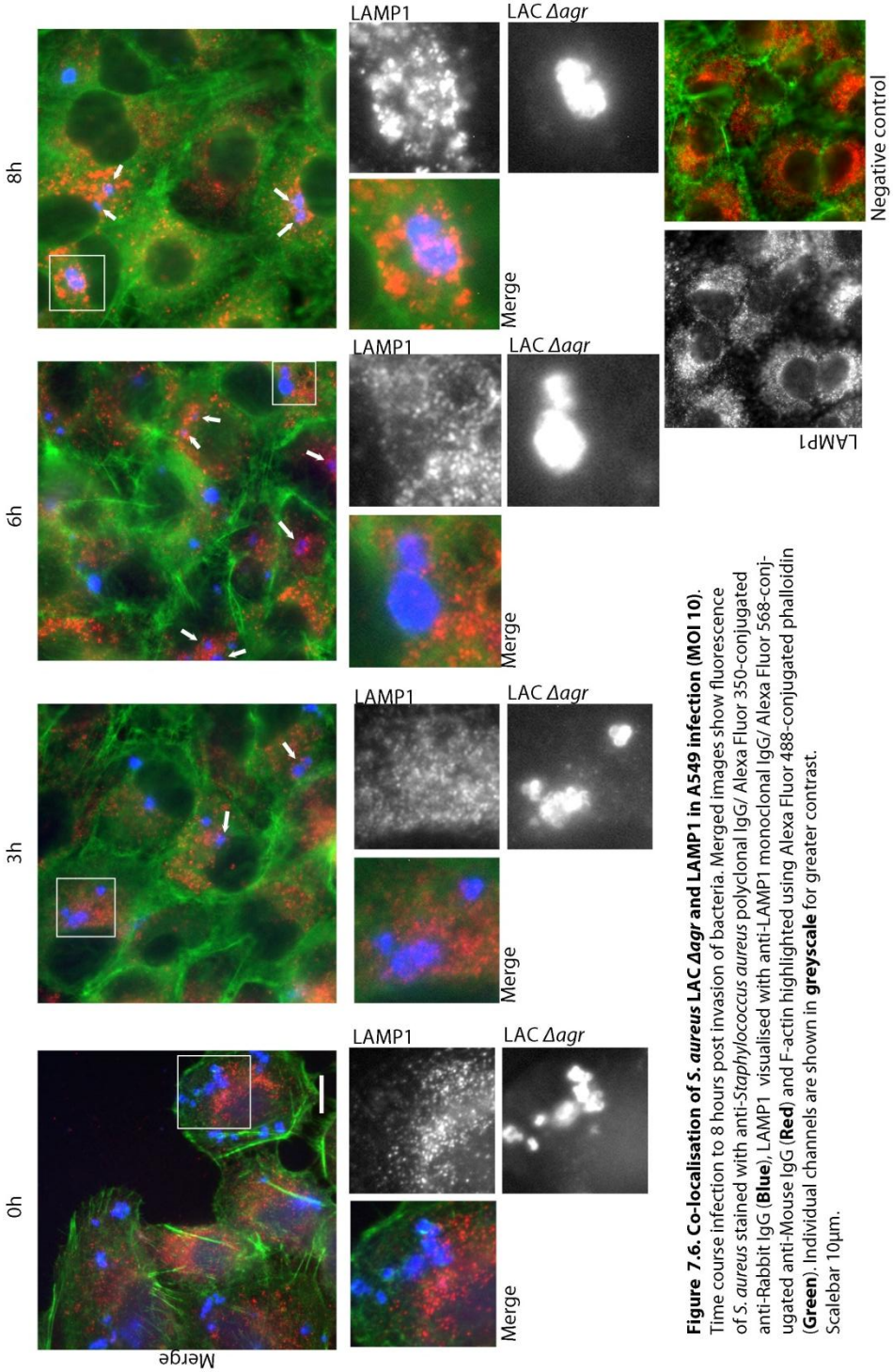

Figure 7.6. Co-localisation of *S. aureus* LAC *Δagr* and LAMP1 in A549 infection (MOI 10). Time course infection to 8 hours post invasion of bacteria. Merged images show fluorescence of *S. aureus* stained with anti-*Staphylococcus aureus* polyclonal IgG/ Alexa Fluor 350-conjugated anti-Rabbit IgG (**Blue**), LAMP1 visualised with anti-LAMP1 monoclonal IgG/ Alexa Fluor 568-conjugated anti-Mouse IgG (**Red**) and F-actin highlighted using Alexa Fluor 488-conjugated phalloidin (**Green**). Individual channels are shown in **greyscale** for greater contrast. Scalebar 10µm.

A

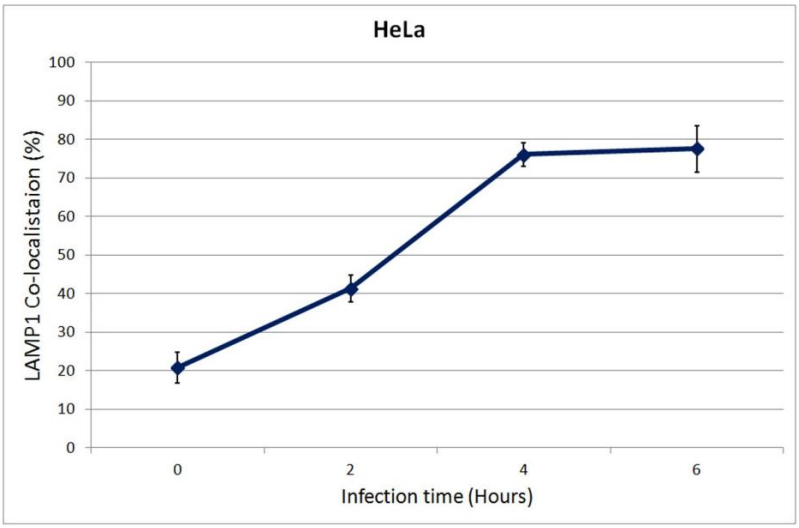

B

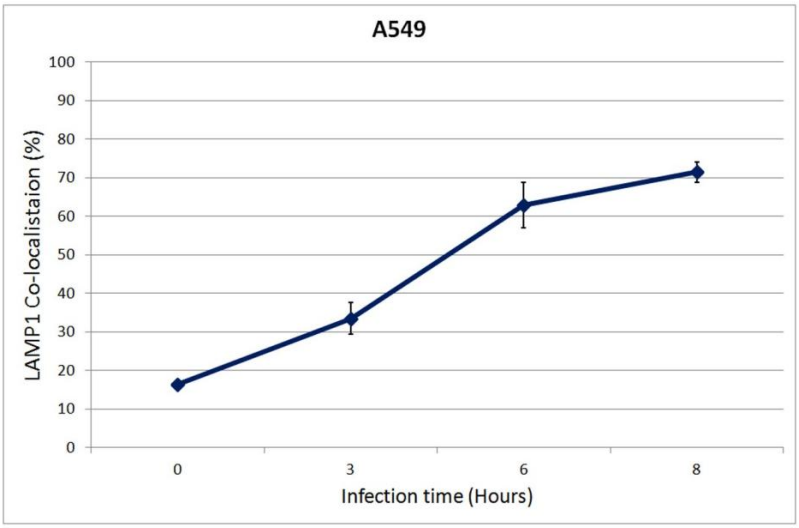

Figure 7.7. Co-localisation of intracellular LAMP1 and *S. aureus* LAC Δ*agr*. The average percentage of total bacterial clusters positively co-localised with LAMP1 during intracellular infection of mammalian epithelial cells. The % at each time point is calculated from at least 10 fields with on average 24.7±1.6 cells per field and shows standard error of the mean. **A.** HeLa cell infection. **B.** A549 cell infection.

Together these results suggest that WT USA300 LAC arrests the Rab7 positive compartment which promotes replication, while Δ*agr* cannot prevent phagolysosomal fusion which leads to inhibition of replication and degradation. However, further experiments are needed to quantify lysosome association of WT USA300 LAC and Δ*agr* in order to affirm this distinction.

7.4.3 Association of *S. aureus* USA300 LAC with the Golgi apparatus

7.4.3.1 WT USA300 LAC inclusions acquire Golgi markers

In order to visualise a co-localisation of *S. aureus* clusters and Golgi apparatus, immunofluorescence microscopy was employed to highlight these specific bodies during infection of epithelial cells. Epithelial Golgi membranes were visualised using the trans-Golgi associated marker, 58K protein. *S. aureus* were labelled using anti-*Staphylococcus aureus* Rabbit IgG. Cellular F-actin was visualised using Phalloidin to define the cell boundaries.

Figure 7.8 and 7.9 depict representative images of *S. aureus* USA300 LAC infection of HeLa cells and A549 cells. The negative control shows clearly, the compact and orderly nature of the Golgi body in uninfected cells. Immediately after bacterial entry, at 0h, bacteria were spatially dispersed throughout cells and are not regularly localised at the perinuclear region. By 2 hours post invasion, bacterial clusters had migrated to periphery of the Golgi apparatus. As early as 2 hours into infection, expansive staphylococcal masses were co-localised with 58K. As highlighted in expanded sections, 58K markers are no longer compact and ordered in the periphery of the nucleus. The Golgi apparatus appeared to encompass the entire bacterial mass, which was characterised by a dispersal of 58K markers. Many examples are highlighted by white arrows and expanded sections in Figure 7.8 and 7.9 that this was a regular event occurring throughout invasive infection. The boundary of bacterial expanse and 58K dispersal was strikingly similar and consistent among cells. In addition, cells

that bare this bacterial load which is co-localised with 58K, are commonly rounded and shrivelled (Figure 7.8 2h). This may suggest cells become apoptotic in this situation which would correlate with the increasing cytotoxicity of the HeLa cell monolayer at later time points of infection. By contrast, infected cells can be seen, in which bacteria did not co-localise at the Golgi apparatus, for example in Figure 7.8 at 6h. These cells do not carry a significant bacterial load, and do not appear to be abnormal which suggests they are not subject to cell death.

These results demonstrate that *S. aureus* USA300 clusters use cell trafficking pathways to migrate to the Golgi network. The expansion of Golgi membranes to encompass the replicating *S. aureus* mass implicates the Golgi network as the replication niche for *Staphylococcus* containing vacuoles.

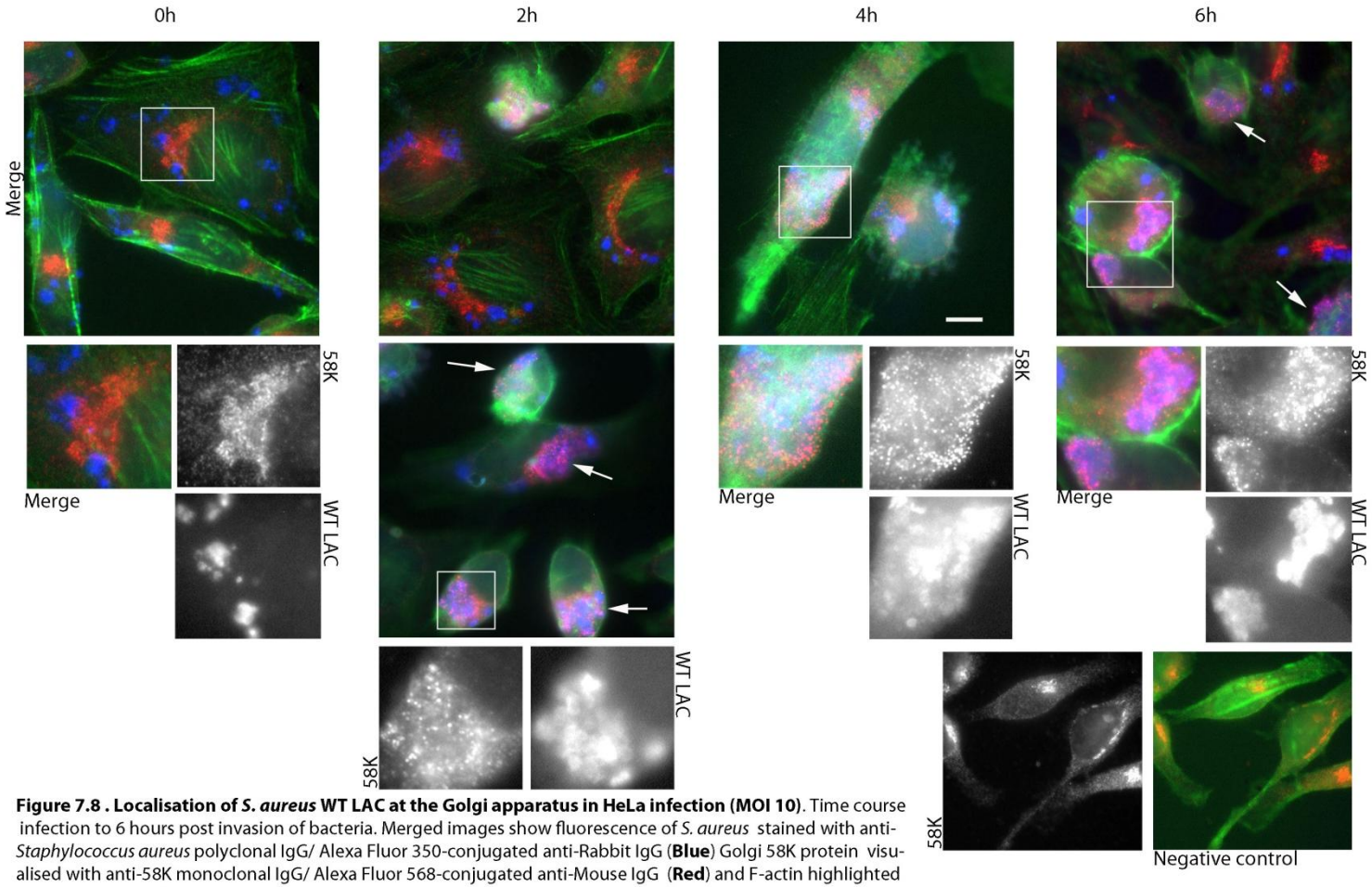

Figure 7.8 . Localisation of *S. aureus* WT LAC at the Golgi apparatus in HeLa infection (MOI 10). Time course infection to 6 hours post invasion of bacteria. Merged images show fluorescence of *S. aureus* stained with anti-*Staphylococcus aureus* polyclonal IgG/ Alexa Fluor 350-conjugated anti-Rabbit IgG (**Blue**) Golgi 58K protein visualised with anti-58K monoclonal IgG/ Alexa Fluor 568-conjugated anti-Mouse IgG (**Red**) and F-actin highlighted using Alexa Fluor 488-conjugated phalloidin (**Green**). Individual channels are shown in **greyscale** for greater contrast. Scalebar 10µm.

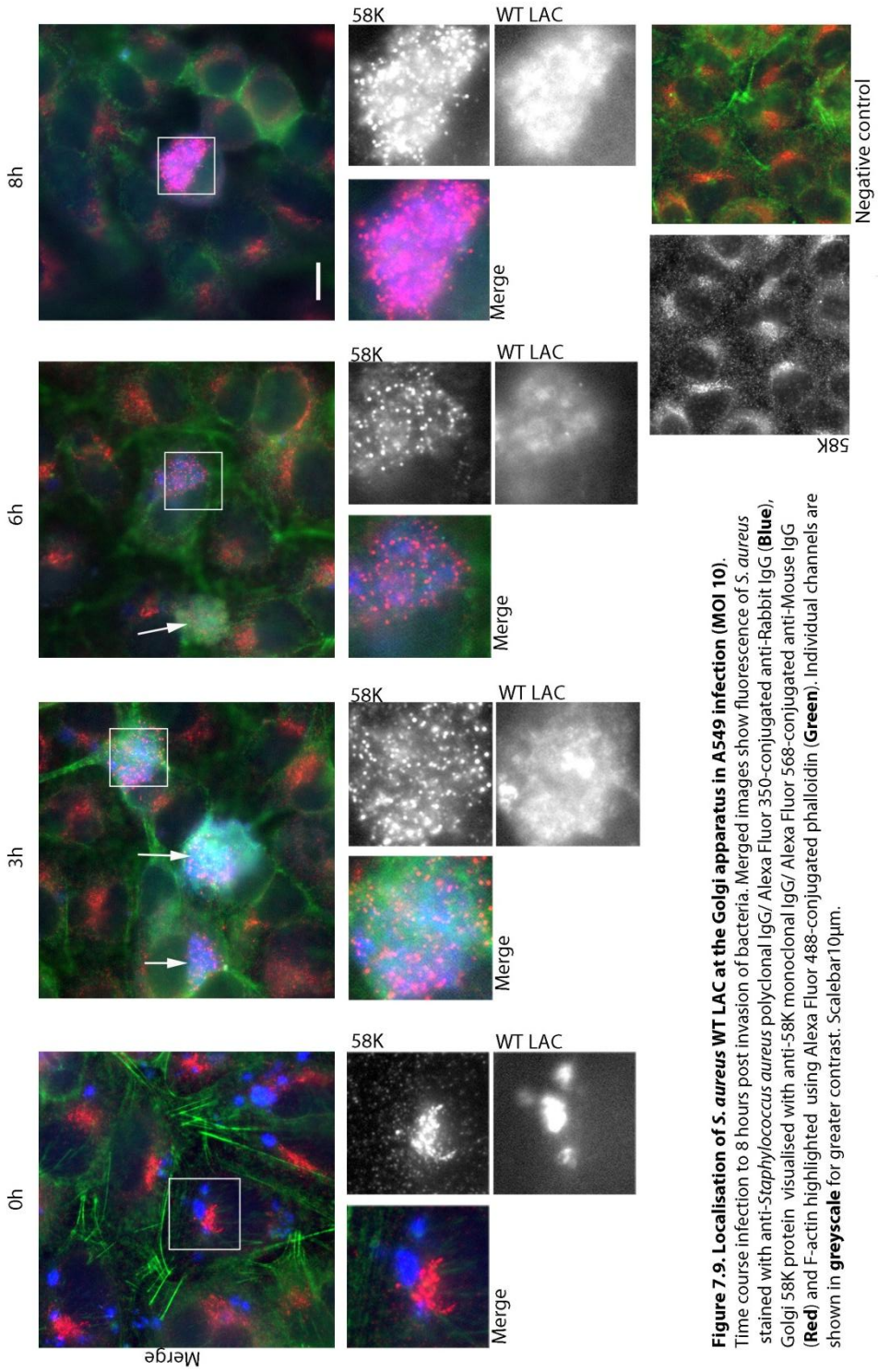

Figure 7.9. Localisation of *S. aureus* WT LAC at the Golgi apparatus in A549 infection (MOI 10).
Time course infection to 8 hours post invasion of bacteria. Merged images show fluorescence of *S. aureus* stained with anti-*Staphylococcus aureus* polyclonal IgG/ Alexa Fluor 350-conjugated anti-Rabbit IgG (**Blue**), Golgi 58K protein visualised with anti-58K monoclonal IgG/ Alexa Fluor 568-conjugated anti-Mouse IgG (**Red**) and F-actin highlighted using Alexa Fluor 488-conjugated phalloidin (**Green**). Individual channels are shown in **greyscale** for greater contrast. Scalebar10µm.

7.4.3.2 Δ*agr* clusters fail to acquire Golgi markers

S. aureus USA300 LAC Δ*agr* containing vacuoles do not conform to wild type cell dynamics which relates to a severe impairment in replication. It was investigated whether Δ*agr* clusters migrated and localised at the Golgi, as a cellular niche.

Immunofluorescence microscopy was employed to image Golgi membrane structure during infection of HeLa cells and A549 cells by Δ*agr*. Figure 7.10 and 7.11 shows representative imaging of the infection of HeLa and A549 cells, respectively, by Δ*agr.* As infection progresses, there was very little evidence to suggest that Δ*agr* vacuoles localise to a common cell vicinity. In addition, by later time points of infection, there were virtually no clusters of Δ*agr* that co-localised with Golgi 58K protein. All infected cell Golgi remained as compact and ordered as seen in negative controls. Throughout the chapter figures have been presented which reproduce Δ*agr* infection. In each case, Δ*agr* clusters fail to regularly migrate to a common location. This provides corroborating evidence that the cellular spatial distribution of *S. aureus* USA300 LAC Δ*agr* infection differs from that of wild type infection.

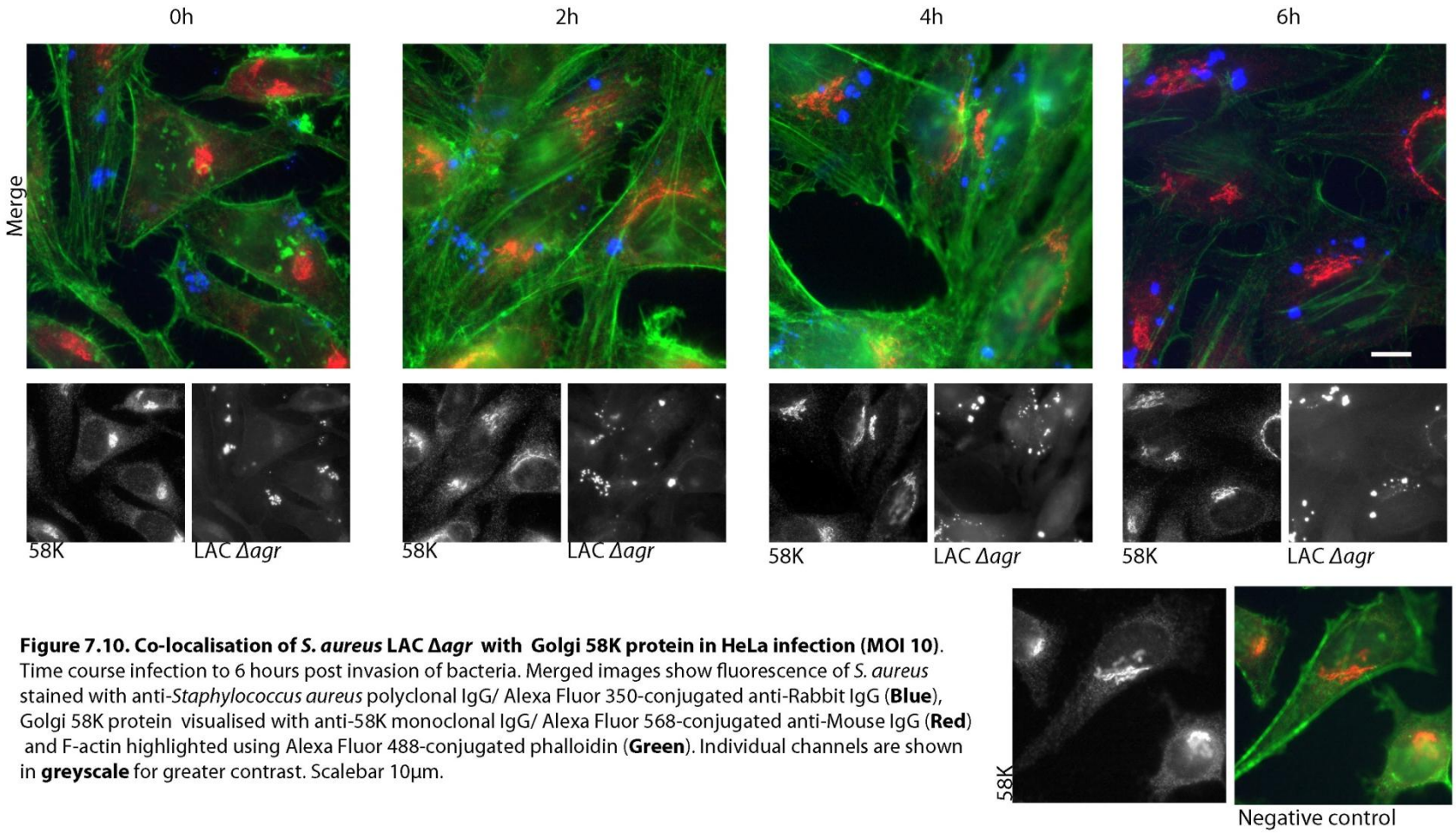

Figure 7.10. Co-localisation of *S. aureus* LAC Δ*agr* with Golgi 58K protein in HeLa infection (MOI 10). Time course infection to 6 hours post invasion of bacteria. Merged images show fluorescence of *S. aureus* stained with anti-*Staphylococcus aureus* polyclonal IgG/ Alexa Fluor 350-conjugated anti-Rabbit IgG (**Blue**), Golgi 58K protein visualised with anti-58K monoclonal IgG/ Alexa Fluor 568-conjugated anti-Mouse IgG (**Red**) and F-actin highlighted using Alexa Fluor 488-conjugated phalloidin (**Green**). Individual channels are shown in **greyscale** for greater contrast. Scalebar 10μm.

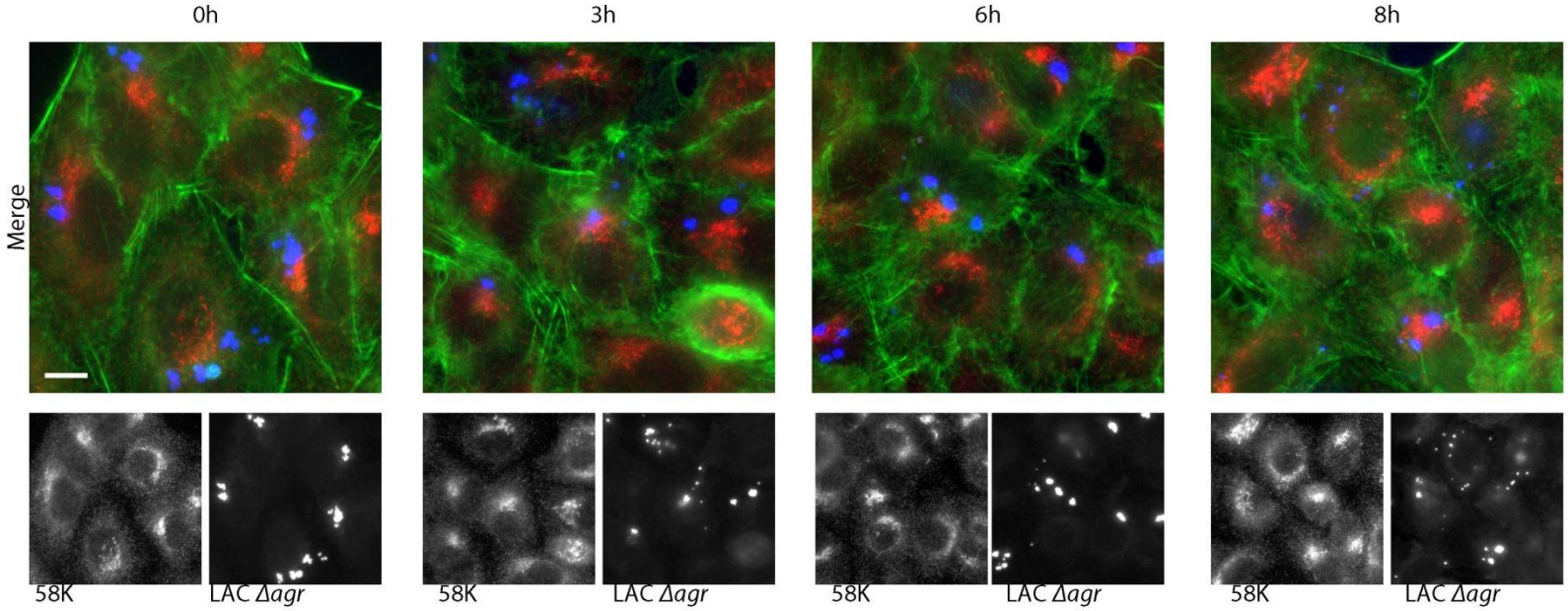

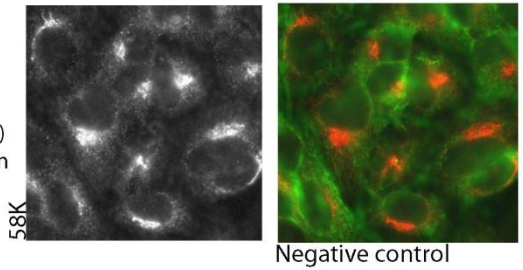

Figure 7.11 . Co-localisation of *S. aureus* LAC *Δagr* lwith Golgi 58K protein in A549 infection (MOI 10). Time course infection to 8 hours post invasion of bacteria. Merged images show fluorescence of *S. aureus* stained with anti-*Staphylococcus aureus* polyclonal IgG/ Alexa Fluor 350-conjugated anti-Rabbit IgG (**Blue**), Golgi 58K protein visualised with anti-58K monoclonal IgG/ Alexa Fluor 568-conjugated anti-Mouse IgG (**Red**) and F-actin highlighted using Alexa Fluor 488-conjugated phalloidin (**Green**). Individualchannels are shown in **greyscale** for greater contrast. Scalebar 10μm.

7.4.4 Golgi disruption to inhibit replication of *S. aureus* USA300 LAC

Wild type USA300 migrates to the Golgi which appears to be a niche for substantial replication. By contrast, Δ*agr* is unable to do so and instead most likely transits to the lysosome. The use of host cell trafficking to travel to and interact with the Golgi, is a critical mechanism in invasive USA300 pathogenesis. Without the regulation of *agr*, virulence factors are non-applicable and the process is not initiated. Ultimately, host cell interactions, mediated through *agr* effectors, is key to proliferation.

As the Golgi apparatus is evidently the terminal replication niche of USA300, an effort was made to disrupt the interaction and inhibit replication. This has been demonstrated with *Salmonella*, as disassembly of the Golgi apparatus by a chemical inhibitor strongly reduced bacterial growth (Salcedo & Holden 2003). A Golgi inhibitor was utilised to disrupt the make-up of the Golgi apparatus during infection. Golgicide A is a highly specific, reversible inhibitor of the cis-Golgi associated protein GBF1. Inhibition of this interaction results in disassociation of Golgi membrane coat proteins and subsequently, the disassembly of the entire Golgi and trans-Golgi structure (Sáenz *et al.* 2009). Golgicide A has been reported to demonstrate effective fragmentation of Golgi vesicles in HeLa cells (Van der Linden *et al.* 2010).

The effectiveness of Golgicide A was tested upon HeLa and A549 cells. Golgicide A treatment was monitored over 2 hours. Immunofluorescence microscopy was used to view Golgi membranes during treatment. Golgi 58K protein was utilised once again for antibody detection of the Golgi apparatus.

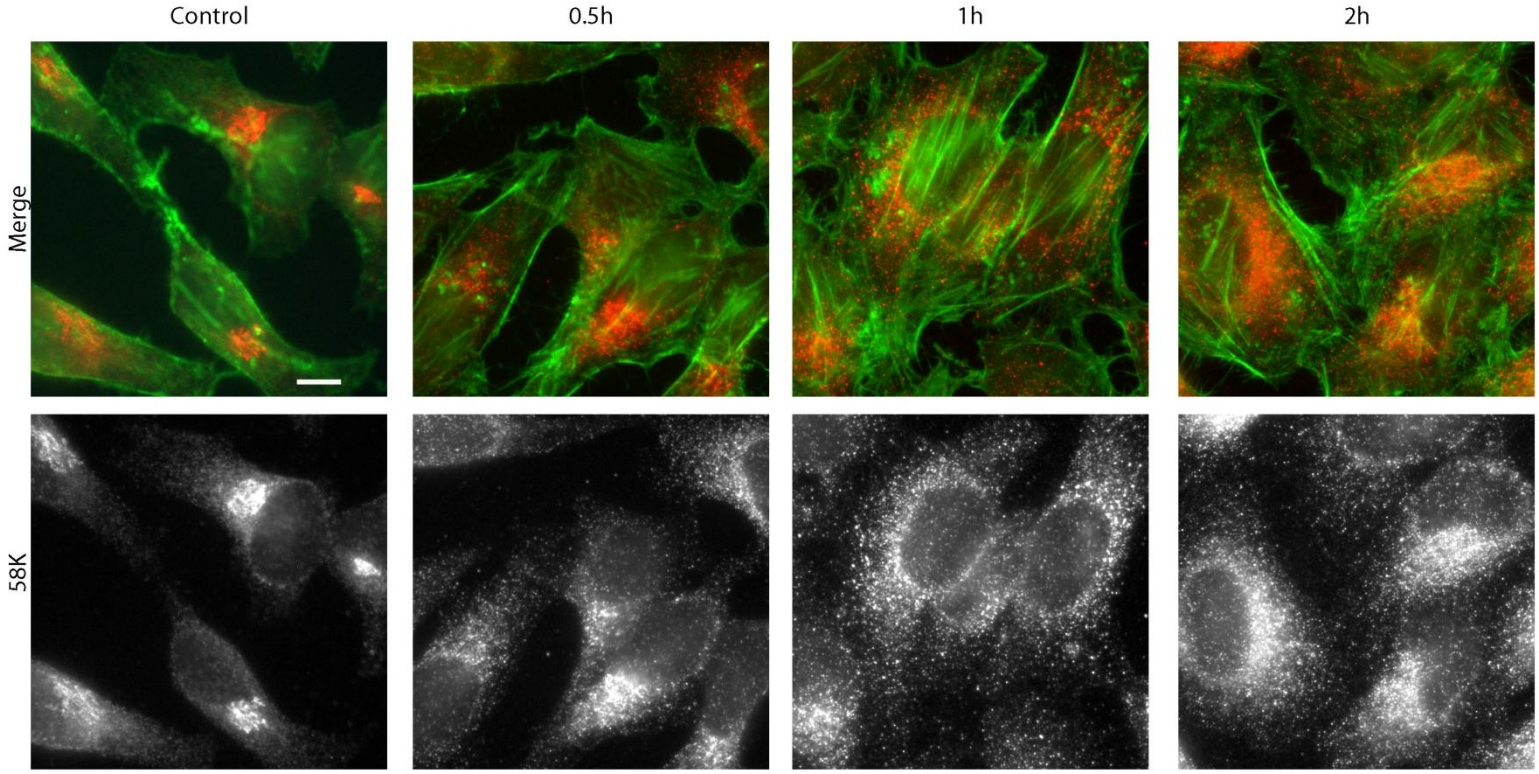

Figure 7.12. Treatment of HeLa cells with Golgicide A (10µg/ml). Golgi apparatus disruption at time points post application of inhibitor. Golgi 58K protein is visible via anti-58K monoclonal IgG/ Alexa Fluor 568-conjugated anti-Mouse IgG (**Red/ Greyscale**) F-actin is stained by Alexa Fluor 488-conjugated phalloidin (**Green**). Scalebar 10µm.

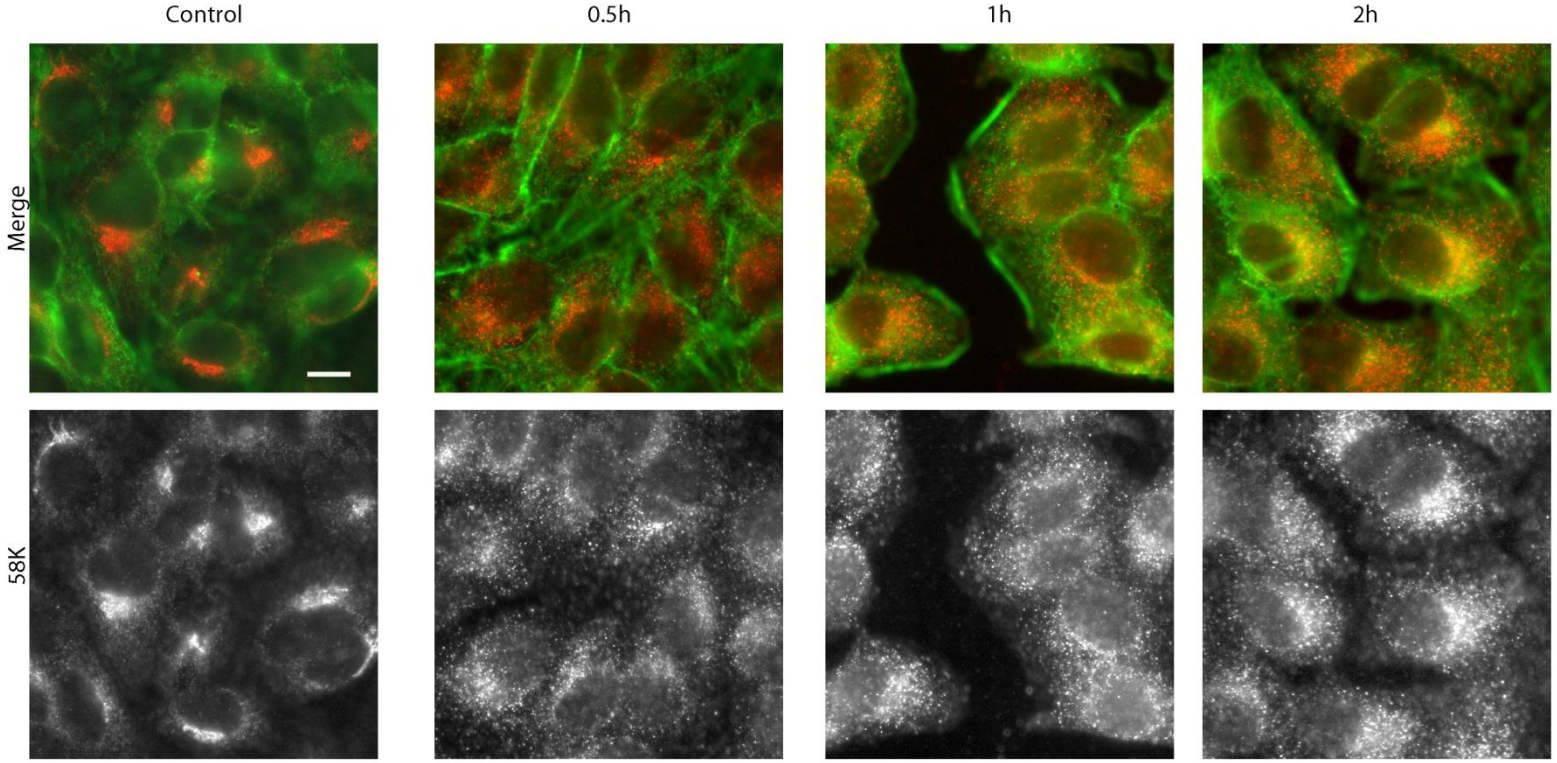

Figure 7.13. Treatment of A549 cells with Golgicide A (10µg/ml). Golgi apparatus disruption at time points post application of inhibitor. Golgi 58K protein is visible via anti-58K monoclonal IgG/ Alexa Fluor 568-conjugated anti-Mouse IgG (**Red/ Greyscale**) F-actin is stained by Alexa Fluor 488-conjugated phalloidin (**Green**). Scalebar10µm.

Figure 7.12 and Figure 7.13 show treatment of HeLa and A549 cells respectively, with Golgicide A over the course of 2 hours. Negative controls were put in place to show the assembled and compressed nature of untreated Golgi apparatus. Inhibitor treatments in both cell types lead to scattering and disassembly of Golgi into the cytosol over the 2 hour time period. The cell Golgi looked to be disrupted, which may interfere with the natural localisation of WT USA300 vesicles.

Intracellular infections were performed alongside treatment of Golgicide A. Bacterial inoculum was added and allowed to invade untreated cells for the allotted incubation time. This was in an effort to ensure that entry rates of bacteria was unaffected by Golgicide A treatment. Inhibitor was added to the antibiotic media, which was applied to cells directly after the invasion period and was left for the remainder of the assay. From this point, the intracellular replication of bacteria was monitored. While the main objective was to observe any negative effects upon WT *S. aureus* USA300 LAC replication, Δ*agr* was monitored in parallel as a control, as this strain typically did not associate with the Golgi.

Infections of WT and Δ*agr* in GCA treated HeLa cells revealed a major discrepancy. Figure 7.14 shows phase contrast imaging of the HeLa cell monolayer during treatment with Golgicide A. The integrity of uninfected, treated cells remained resolute throughout the time points monitored during infection. In contrast, the monolayer of treated cells infected with Δ*agr* was subject to extensive destruction by 6 hours of infection. This reproducible detachment did not occur during Δ*agr* infection of untreated cells. These observations were substantiated using an LDH cytotoxicity assay. Culture media was analysed at various time points during infection to quantify the breakdown of the HeLa monolayer. Figure 7.15 shows a colour schematic of LDH cytotoxocity assays which correlate with monolayer detachment. *S. aureus* USA300 LAC Δ*agr* infection caused substantial cell monolayer destruction by 6h into infection (~25%).

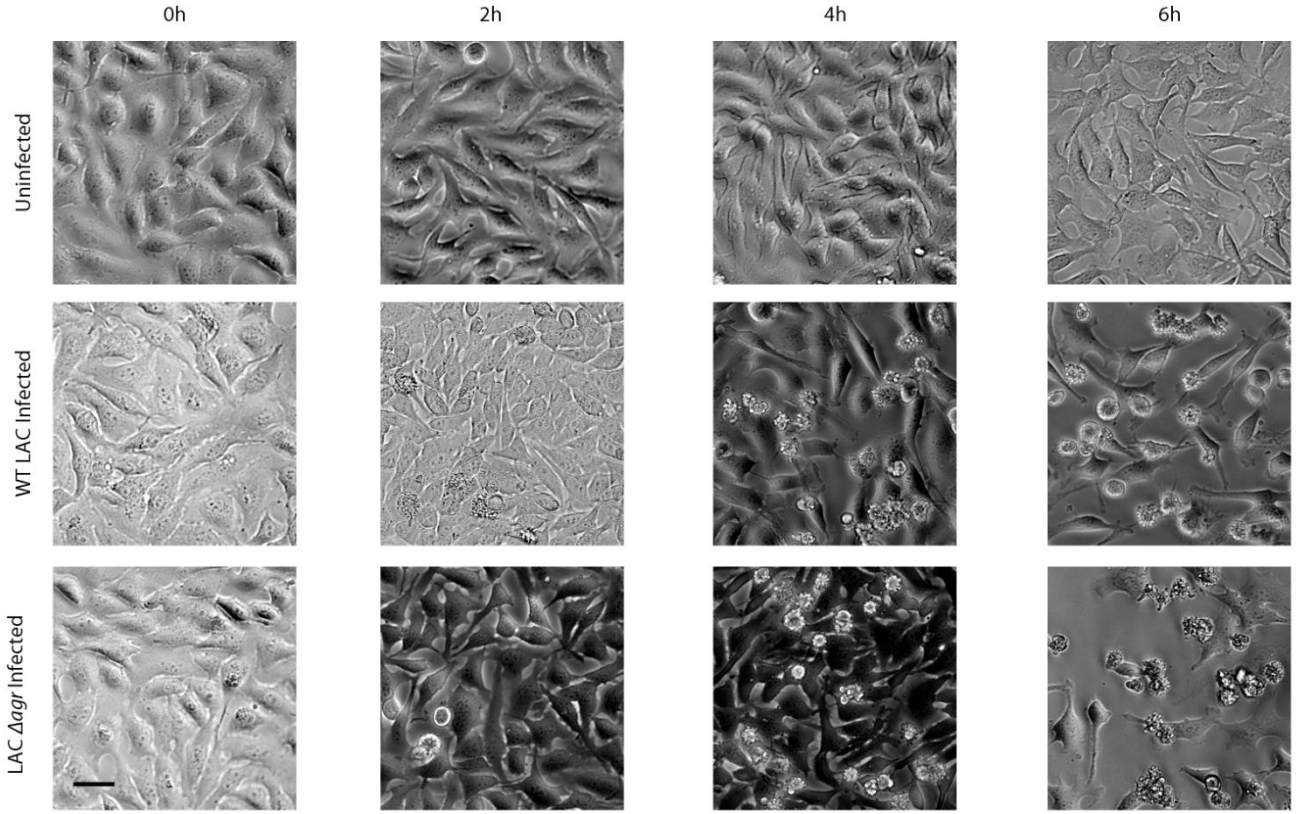

Figure 7.14 . Effect of Golgicide A (10µg/ml) treatment upon HeLa cells. Phase contrast images represent the fate of the HeLa cell monolayer whilst incubated in the presence of Golgi inhibitor. Middle series shows Wild type LAC infection (MOI 10) and bottom series shows *agr* deficient LAC infection (MOI 10) up to 6h post bacterial invasion. Scalebar 40µm.

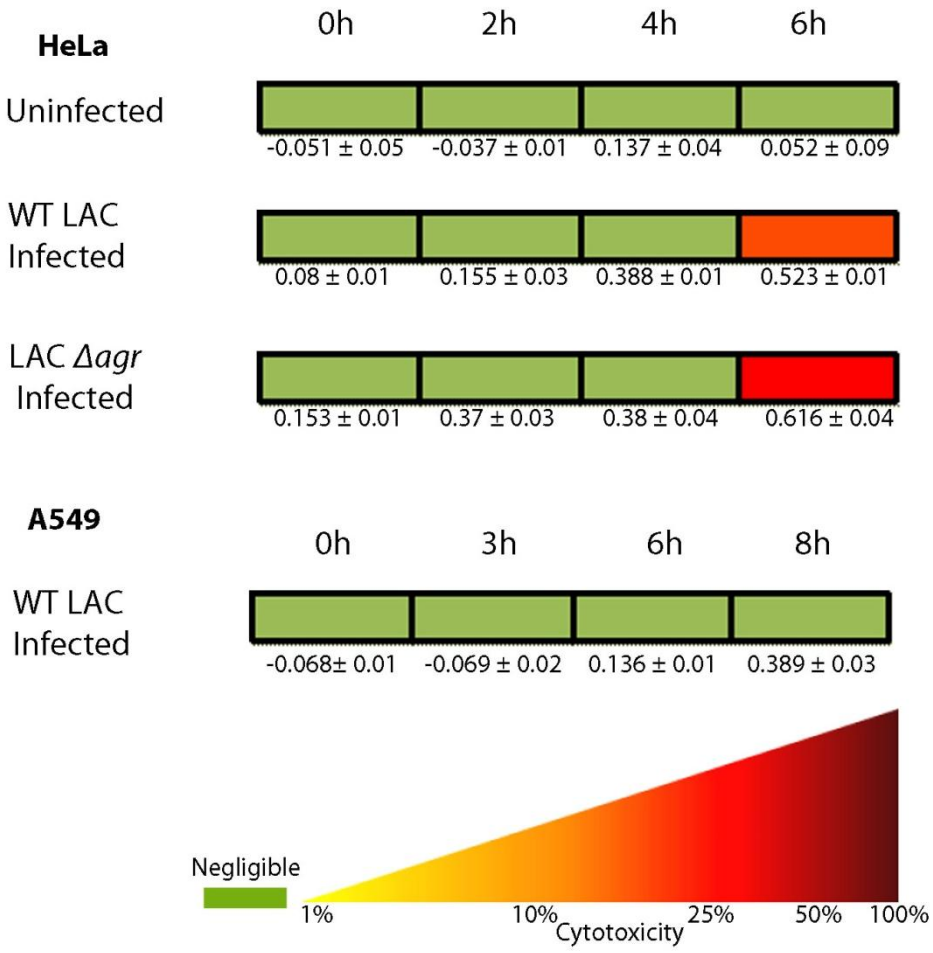

Figure 7.15. Cytotoxicity of Golgicide A treated (10µg/ml) mammalian cells. Colour boxes represent a measure of HeLa monolayer integrity at times post bacterial invasion. Green is representative of a confluent monolayer.The yellow to crimson gradient co-ordinates the percentage of the confluent monolayer that has detached. Mean LDH absorbance $_{490nm}$ ± standard deviation (LDH cytotoxicity assay) is also shown for each timepoint. *S. aureus* USA300 LAC infections are at MOI 10.

As Δ*agr* is normally non-cytotoxic up to this time point at MOI 10, this raised concerns about the viability of investigating intracellular replication of USA300 LAC strains in Golgicide A treated HeLa cells.

Figure 7.15 also models cytotoxicity testing of WT USA300 infection in Golgicide A treated A549 cells at MOI 10. LDH cytotoxicity analysis shows that the cell monolayer remained largely unaffected over the infection period. This shows that infection of Golgicide A treated A549 cells did not potentiate monolayer destruction. Infections of inhibitor treated A549 cells were therefore considered for intracellular replication analysis.

Figure 7.16 shows the average CFU/ml of *S. aureus* USA300 LAC strains during intracellular proliferation assays in A549 cells. Figure 7.15B compares the intracellular replication of Δ*agr* in cells with and without treatment of Golgicide A. Replication was comparable in both cellular conditions and therefore served as a negative control for intracellular growth without Golgi affiliation. Figure 7.16A shows the average bacterial numbers of WT USA300 in A549 cells. Replication in A549 cells was not affected by inhibition of Golgi assembly by Golgicide A. The mean generation times of LAC WT and Δ*agr* in A549 cells with and without Golgicide A treatment are shown in Figure 7.16C. Golgi disruption did not have a negative effect upon the average doubling time of either strain.

Immunofluorescence microscopy was used to authenticate replication of *S. aureus* USA300 LAC in inhibitor treated A549 cells. Figure 7.17 images the infection of WT and Δ*agr* using 58K labelling to visualise the Golgi. Throughout infections, dispersal of the Golgi was observed. During WT infection, by 6 hours there were numerous examples of large expansive staphylococcal masses, highlighted by white arrows. Greyscale contrasting of 58K and *S. aureus* at 6 hours shows that for the most part, there is still an apparent co-localisation of Golgi 58K and USA300 WT. Infection of Δ*agr* shows no obvious difference in spatial localisation during A549 cell treatment.

A

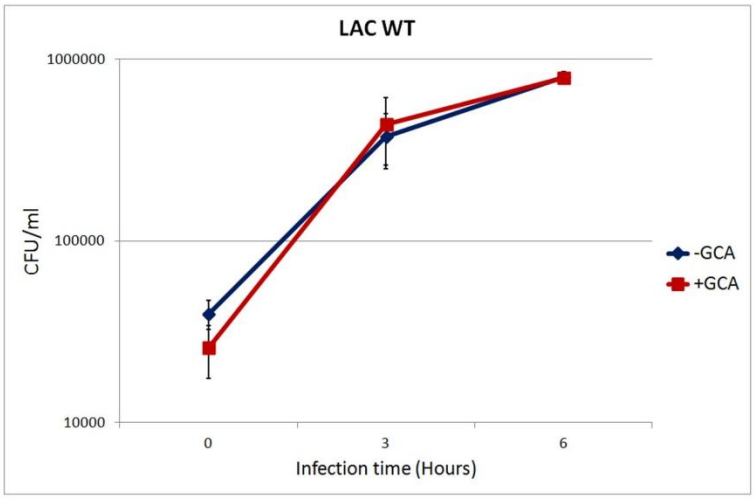

B

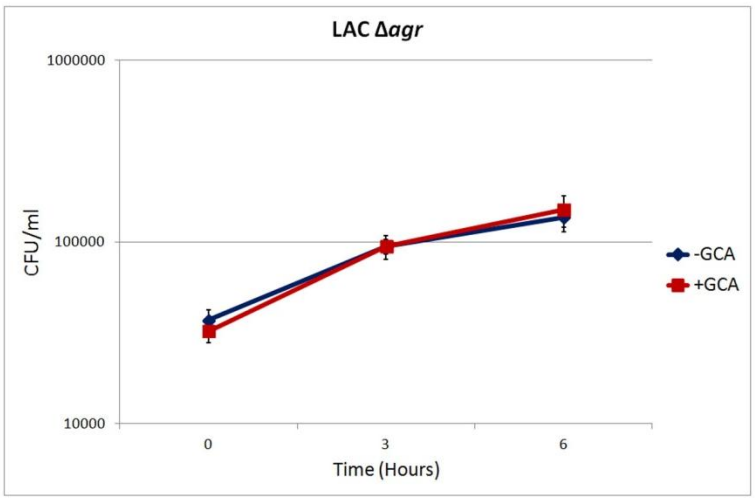

C

	Mean generation time (minutes)	
Cell treatment	WT	*Δagr*
-GCA	83.22 ± 6.2	204.4 ± 35
+GCA	73.21 ± 1.3	162.7 ± 31.7

Figure 7.16. Replication of *S. aureus* LAC strains in Golgicide A treated and untreated A549 cells. Average CFU/ml of **A.** *S. aureus* WT USA300 LAC and **B.**Δ*agr* during infection of A549 cells. Infections compare untreated cells **(-GCA)** and Golgicide A (10µg/ml) treated cells **(+GCA)**. **C.** Mean generation times ± standard error of *S. aureus* strains in GCA treated and untreated A549 cells. Averages values are calculated from at least 2 separate assays and show standard error of the mean.

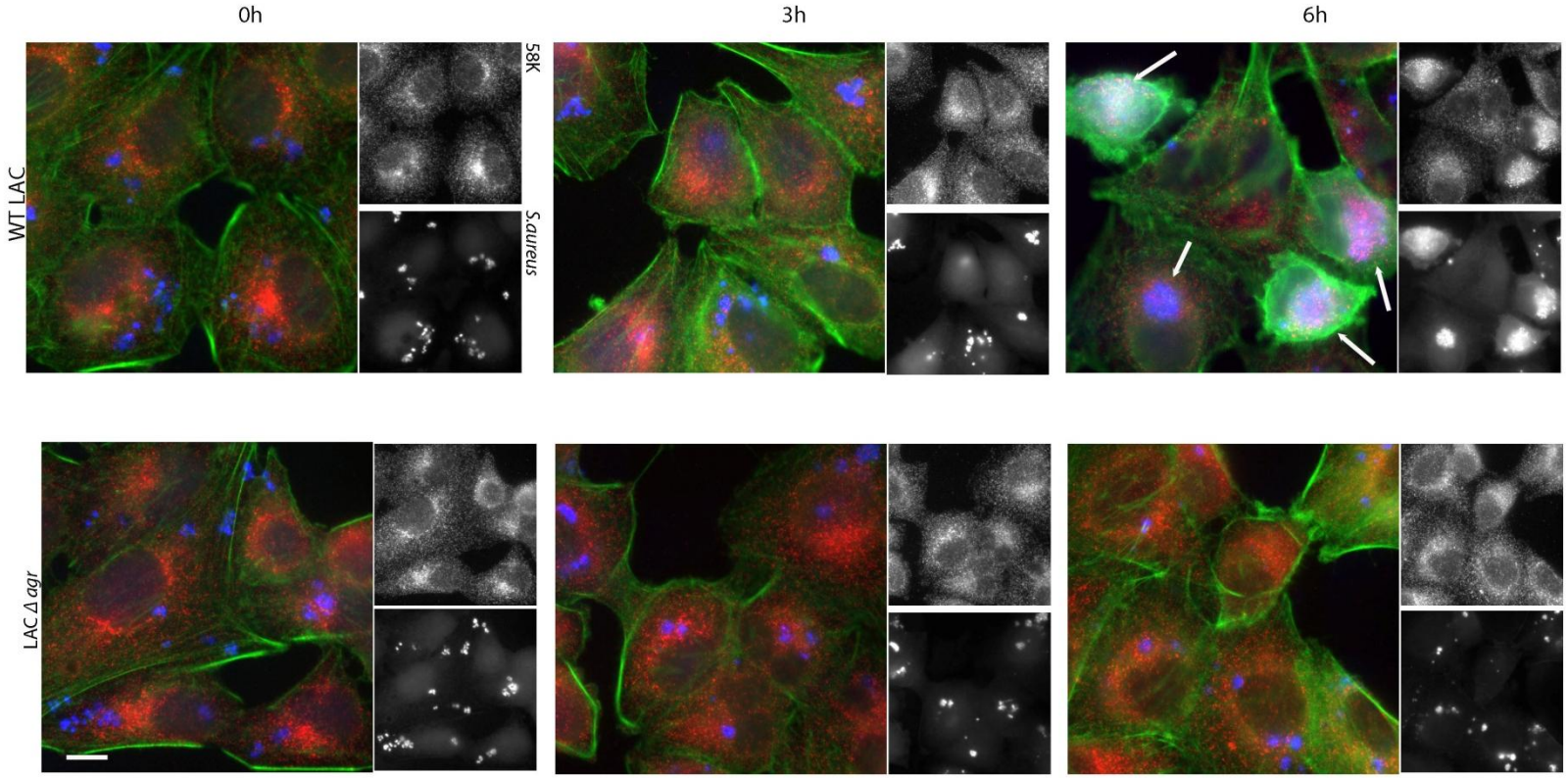

Figure 7.17. Infection of *S. aureus* LAC strains (MOI 10) in Golgicide A treated A549 cells. Time course infection up to 6 hours post bacterial invasion. A549 cells were incubated in 10µg/ml Golgicide A after 35mins of bacterial invasion. The top series shows infection of wild type LAC in comparison to infection of LAC *Δagr* in the bottom series. Merged images show fluorescence of *S. aureus* stained with anti-*Staphylococcus aureus* polyclonal IgG/ Alexa Fluor 350-conjugated anti-Rabbit IgG (**Blue**), Golgi 58K protein visualised with anti-58K monoclonal IgG/ Alexa Fluor 568-conjugated anti-Mouse IgG (**Red**) and F-actin highlighted using Alexa Fluor 488-conjugated phalloidin (**Green**). Individual channels are shown in **greyscale** for greater contrast. Scalebar 10µm.

7.5 Discussion

The intracellular associations elucidated in this study, which are involved in replication and pathogenesis of *S. aureus* USA300 LAC, are summarised in Figure 7.18.

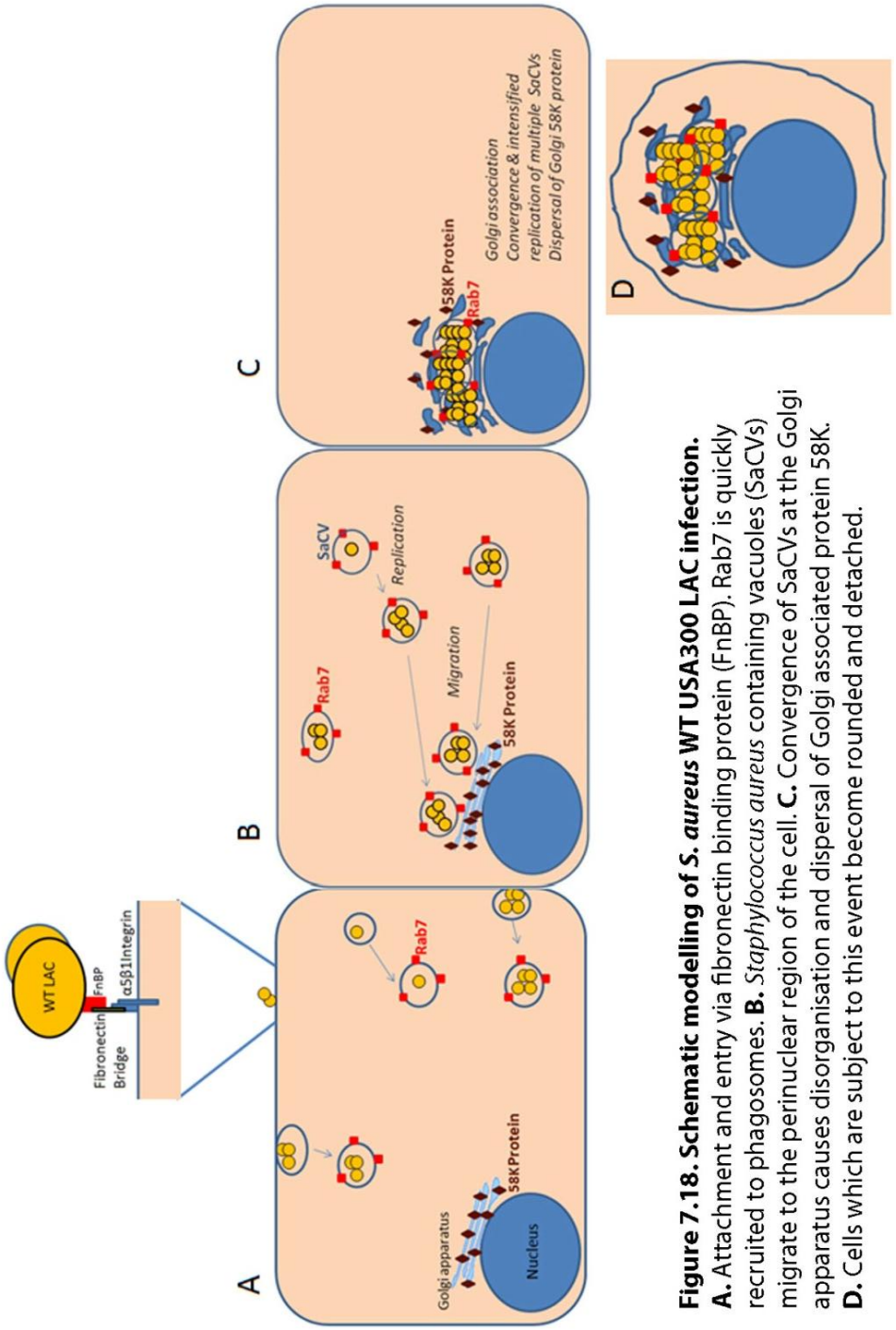

Figure 7.18. Schematic modelling of *S. aureus* WT USA300 LAC infection. **A.** Attachment and entry via fibronectin binding protein (FnBP). Rab7 is quickly recruited to phagosomes. **B.** *Staphylococcus aureus* containing vacuoles (SaCVs) migrate to the perinuclear region of the cell. **C.** Convergence of SaCVs at the Golgi apparatus causes disorganisation and dispersal of Golgi associated protein 58K. **D.** Cells which are subject to this event become rounded and detached.

The host cell dynamics of *agr* deficient USA300 LAC are summarised in Figure 7.19.

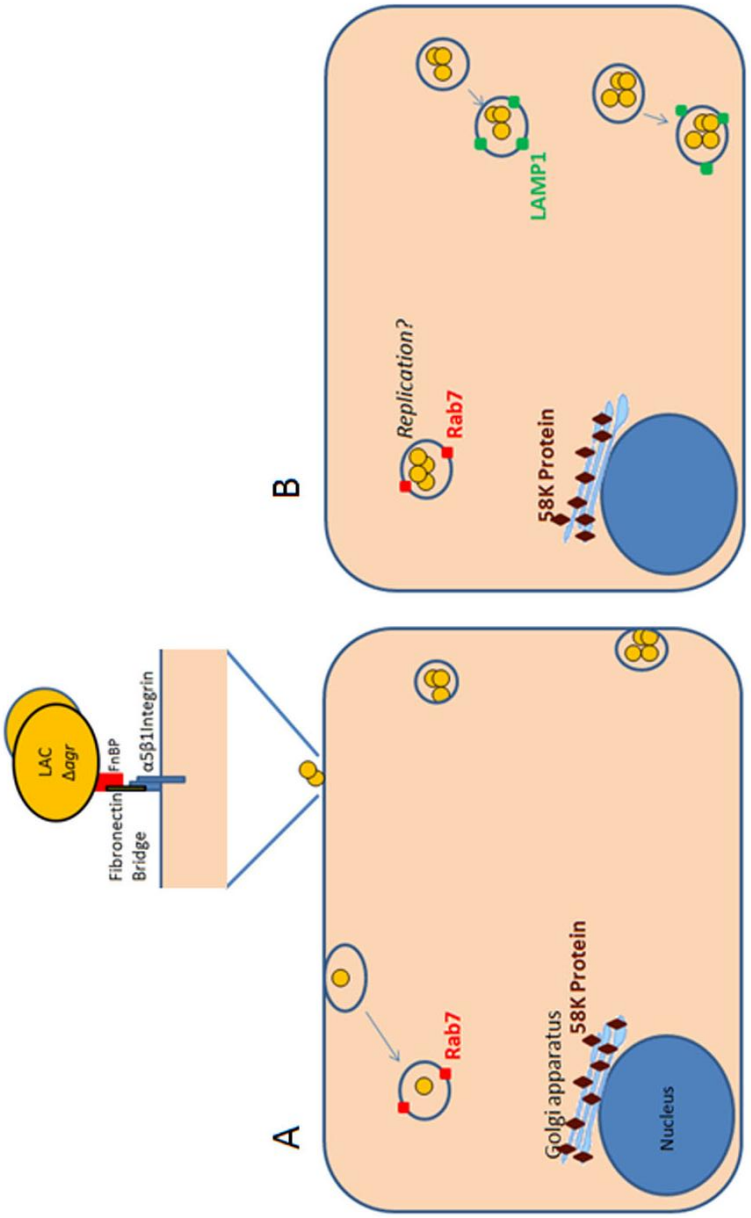

Figure 7.19. Schematic modelling of *S. aureus* USA300 LAC *Δagr* infection. **A.** Attachment and entry via fibronectin binding protein. Rab7 is not commonly recruited to phagosomes. **B.** As infection progresses *Δagr* SaCVs co-localise with LAMP1. *Δagr* SaCVs do not habitually migrate to the Golgi apparatus or interfere with Golgi 58K assembly. Small increases in intracelular numbers may be attributed to low percentage SaCV-Rab7 associated clusters.

7.5.1 *agr*-dependent interactions promoting migration to the Golgi for replication

Invasive infection of a USA300 LAC strain lacking the *agr* regulatory system displayed different dynamics to the wild type. This strain does not commonly localise to Rab7 associated inclusions and does not migrate to the Golgi apparatus. Instead, Δ*agr* becomes increasingly co-localised with lysosomal membrane protein LAMP1 as the infection progresses. According to existing literature, co-localisation with lysosomal membrane associated proteins is a common observation among *S. aureus* Δ*agr* infections (Schnaith *et al.* 2007; Jarry *et al.* 2008). These publications strongly suggest that Δ*agr* becomes sequestered inside the lysosomal compartment, the antimicrobial degradation niche.

S. aureus USA300 LAC Δ*agr* is not noticeably impaired in important carbon based nutrient sources compared to the wild type. The differences in cellular localisation can therefore be significant and linked to the inability of Δ*agr* to divert the lysosomal degradation pathway and transport to the Golgi replication niche. Effector proteins which are expressed under the control of *agr* can be crucial in manipulating host cell trafficking to ensure co-ordinated migration and proximity of invasive USA300 clusters. It has been demonstrated that single phagosomal *S. aureus* bacterium can auto regulate the *agr* quorum sensing system to induce expression of virulence factors (Carnes *et al.* 2009). Perhaps upon cell invasion, cellular effectors are expressed and secreted due to autoactivation of *agr,* and this modulates trafficking of the phagosome to the Golgi. Convergence of multiple USA300 clusters into the uniform mass seen at the Golgi would potentiate proximal *agr* quorum sensing. This would increase cytolytic toxin expression and secretion which would provide an escape mechanism, most probably explaining the cell cytotoxicity observed at later time points of infection. Recent publications have proposed that USA300 subverts the autophagy pathway to avoid seclusion in the lysosomal compartment (Schnaith *et al.* 2007; Mauthe *et al*. 2012). This not only ensures survival,

but also replication inside this specific vacuolar niche. Induction of autophagy by rapamycin treatment has shown to increase the number of autophagosome specific USA300 vacuoles and in turn, significantly increase bacterial multiplication. A study reported that *agr* deficient *S. aureus* localises at the lysosomal vacuole and did not exhibit intracellular growth. Rapamycin treatment of cells infected with *agr* deficient strains promotes localisation of these bacteria to WT autophagosomes and induces replication and even restores cytotoxicity (Schnaith *et al.* 2007). This evidence further promotes the notion that *agr* effector(s) control cell trafficking to induce specific vacuole inclusion which ultimately leads to replication.

Various studies have investigated the virulence of USA300 mediated by the *agr* system (Li *et al.* 2010; Montgomery *et al.* 2008; Montgomery *et al.* 2010).In general, the high concentrations of secreted toxins and proteases, that are under the control of *agr*, are thought to be the central factors that make USA300 pathogenesis so destructive. Necrotising pneumonia is a particular infection caused by USA300 that has been consistently linked to *agr* dependent pore forming toxins (Wardenburg *et al.* 2007). Observations in human lung carcinoma cells, presented in this chapter, suggest that *agr* dependent host cell interactions are the underlying cause of necrotising pneumonia, and subsequent *agr* dependent toxin secretion is the effect.

The *agr* dependent phagosome migration seems to be necessary to access nutrient sources providing energy for replication. As the Golgi network is evidently the niche for replication, nutrients may be provided by vesicle trafficking pathways. *Chlamydia* exploits the host Golgi vesicle trafficking network to deliver specific nutrients into the bacterial inclusion. Sphingolipids, cholesterol and lipid droplets are directed to *Chlamydia* to provide the sustenance needed for intravacuolar replication (Saka & Valdivia 2010). A recent study in *Chlamydia* has reported a fragmentation of the HeLa cell Golgi network into mini stacks during infection. Disassembly of the Golgi network by knock down of Golgi associated

proteins actually potentiated *Chlamydia* replication. Prevention of Golgi breakdown reduced the availability of lipid vesicle and severely inhibited the growth of *Chlamydia (*Heuer *et al.* 2009). In addition, *Legionella pneumophila* diverts and fuses with ER-Golgi trafficking vesicles to acquire proteinous materials for nutrition (Robinson & Roy 2006).

The interaction of USA300 at the Golgi network can be a crucial event in pathogenesis. In an attempt to validate this notion the Golgi apparatus was disrupted using Golgicide A. In A549 cells, the treatment was ineffectual upon bacterial localisation and replication. Further studies need to be implemented in demonstrating the importance of this interaction. Perhaps, similarly to *Chlamydia*, the apparent fragmentation of the Golgi by USA300 may be bacterially induced in order to potentiate replication.

The *agr* system of USA300 has a pivotal role in regulating host cell molecular interactions. Pathogenesis of invasive infections can be dependent upon *agr* mediated maturation and transport of *Staphylococcus aureus* containing vacuoles. This implies that important infections such as necrotizing pneumonia can be targeted at the molecular level. In *Salmonella* Typhimurium, targeting of the bacterial vacuole to the Golgi network has been narrowed down to a single protein, encoded by *sseG*. Removal of this protein eliminates interaction with the Golgi complex, inhibits replication and impedes pathogenesis (Salcedo & Holden 2003). *S. aureus* does not encode a homolog of this protein.

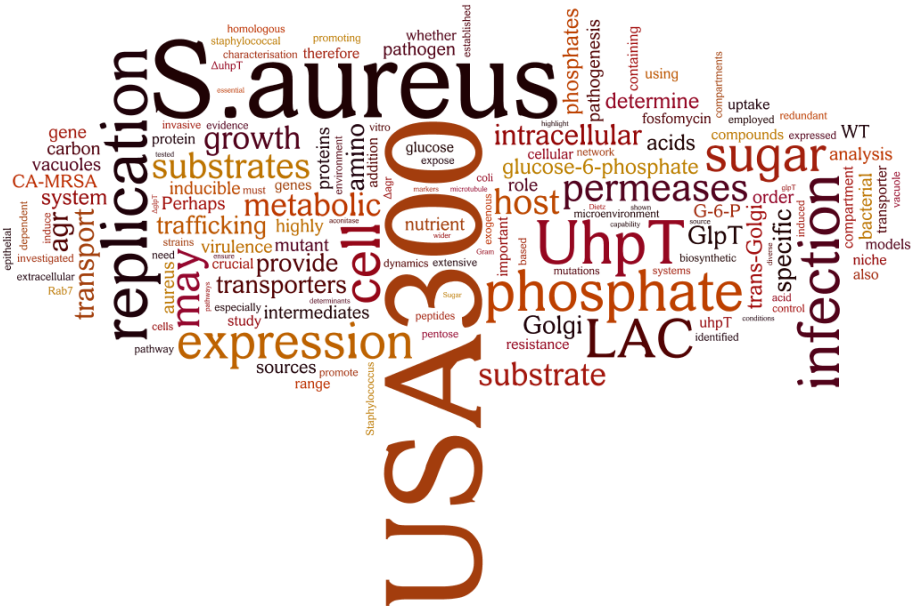

Chapter 8

Conclusions & future work

8.1 Conclusions

S. aureus USA300 is a sophisticated pathogen with an enhanced ability to extract and metabolise diverse carbon compounds from the surrounding environment to benefit fitness. This advanced metabolic capacity may reflect the versatility of this pathogen to colonise many host niches and adapt to the variable microenvironments to inflict destructive infection. Sugar phosphate transporters, UhpT and GlpT, operated with overlapping function, readily ingesting sugar phosphates to support tremendous replication of USA300 *in vitro*. These transporters functioned in *L. monocytogenes* to exploit substrates from the intracellular compartment and promote replication, demonstrating a purposeful role in pathogenesis. However, in USA300 the purpose of UhpT and Glpt was not explicit, as they were dispensible to intracellular replication. Further to this, USA300 could parasitize carbohydrate starved mammalian cells with even greater efficiency than glucose metabolising cells, highlighting the persistence of this pathogen in disparate conditions. It is highly plausible that multiple redundant transport systems exist to compensate for metabolic fluxes in host niches, and maintain growth in the absence of specific permeases, such as UhpT and GlpT. The interconnecting metabolic pathways encoded by *S. aureus* offer malleable, biosynthetic routes by which essential intermediates can be replenished using changeable exogenous nutrients. Ultimately, this can ensure that USA300 proliferates to increase the effect of proximal quorum sensing and promote co-ordinated virulence.

Further examination of USA300 infection determined that replication was confined within *Staphylococcus aureus* containing vacuoles and was closely linked to Golgi apparatus association. In the absence of the *agr* system, USA300 vacuoles did not co-ordinately migrate to the Golgi which was connected with impairment of replication. In order for vacuole based replication to occur, USA300 must affect the host cell phagosome membrane and hijack host cell proteins to manufacture a favourable

intracellular environment. A crucial aspect of this process may be mediated by *agr*. As *agr* deficient USA300 had no obvious metabolic impairment, *agr* mediated host cell modifications may be critical in introducing the pathogen to a microenvironment containing growth promoting nutrients. It is therefore important that host cell vacuole manipulation and bacterial metabolism are jointly considered to expose the source of USA300 pathogenesis. This research may lay the foundation for innovative approaches in CA-MRSA prevention, especially in more serious invasive forms of infection.

8.2 Future work

8.2.1 Growth substrate characterisation

A narrow selection of sugar phosphate compounds were confirmed in this thesis as substrates of *S. aureus* USA300 LAC UhpT and GlpT transporters. A diverse range of organophosphates have been identified which traverse bacterial membranes through homologous hexose phosphate permeases. These intermediates include fructose-1-phosphate, mannose-6-phosphate, galactose-6-phosphate, glucosamine-6-phosphate, glyceraldehyde-3-phosphate, pentose phosphates and heptose phosphates (Dietz 1976; Chico-calero *et al.* 2002; Schwöppe *et al.* 2002; Gluth *et al.* 1980; Eidels *et al.* 1974). In the context of homology, it is important to determine whether the *S. aureus* UhpT protein exhibits the same substrate flexibility. Conducting a more extensive substrate characterisation will also determine the value of phosphorylated intermediates in staphylococcal replication, especially if encompassed by the single UhpT transporter.

A limitation of investigating the substrate specificity of many bacterial organophosphate transporters is the issue of inducible expression. The homologous UhpT transporter of *E. coli* is only inducibly expressed upon highly specific substrate interaction. The only known extracellular inducers of this system are glucose-6-phosphate and 2-deoxyglucose-6-phosphate

(Dietz 1976). In order for transported substrates to be identified, the system needs to first be induced by glucose-6-phosphate. Similarly, glycerol monophosphate is the only extracellular nutrient which can induce expression of GlpT in *E. coli* (Lemieux *et al.* 2004). Although demonstrated to be inducible, the expression systems of putative sugar phosphate permeases of *S. aureus* have not been elucidated. It is probable that these homologous transporters require substrate specific induction of expression, which is necessary to determine transported substrates. Alternative approaches could therefore be taken in order to characterise uptake of substrates through the inducible sugar phosphate transporters of *S. aureus*. Expression analysis can be performed *in vitro* in order to confirm exogenous compounds which induce the expression of *S. aureus uhpT* and *glpT.* This may provide evidence that accounts for lack of USA300 LAC replication in glucose-1-phosphate and glycerol-3-phosphate, for example. A study investigated the substrate specificity of the *E. coli* UhpT permease by using ^{14}C glucose-6-phosphate to induce the UhpT system and monitor the rate of uptake of G-6-P (Schwöppe *et al.* 2002). The uptake of ^{14}C G-6-P was monitored after substrate competitors were added to determine if they displaced G-6-P and were imported through the UhpT channel. As glucose-6-phosphate induces expression of *uhpT* in *S. aureus* (Winkler 1973), this technique could provide subsidiary analysis on substrates that may traverse the channel.

Further investigation of substrates promoting replication of *S. aureus* USA300 LAC is required. The most comprehensive and high-throughput approach involves conducting a phenotype microarray characterisation. This technique would test countless metabolic intermediates, in a minimal growth media, to expose a wider range of substrates that singularly stimulate growth. The metabolic compounds range from extensive carbon sources to nitrogen, phosphorus and sulphur sources. A plethora of peptides can also be scrutinised. A recent study presents phenotype microarray analysis of *S. aureus* strain COL, an early MRSA isolate (Eiff *et al.*

2006). This work cites alternative carbon based substrates as growth stimulants such as fatty acids, nucleosides, nucleotides and urea. Perhaps similar phenotypes can be attributed to USA300 and uncover a wider range of intermediates which can be scavenged from the intracellular compartment to enhance replication. Diverse mechanisms of nutrient acquisition can then be targeted by mutagenesis to further explore nutritional determinants of CA-MRSA pathogenesis.

8.2.2 Fosfomycin resistance

During *in vitro* fosfomycin susceptibility testing, *S. aureus* USA300 LAC exhibited resistance to highly inhibitory concentrations. Isolate WT, Δ*uhpT* and Δ*glpT* colonies which grow within the zone of fosfomycin inhibition can be selected to investigate resistance mechanisms. The ability of these isolates to replicate upon sugar phosphates can be analysed to indicate whether genetic mutations have conferred structural changes to UhpT and GlpT which affect transport. Sugar phosphate permease genes can be sequenced, in addition to *murA* gene (encoding the target protein of fosfomycin), to build an extensive library of possible mutations which influence fosfomycin resistance in *S. aureus* USA300.

8.2.3 Further analysis of sugar phosphate permeases in *S. aureus* USA300 LAC infection

It was established that sugar phosphate permeases are not required for promoting WT *S. aureus* USA300 LAC intracellular replication in the epithelial models tested in this thesis. However, expression of *uhpT* and *glpT* needs to be monitored over the course of infection to determine whether these genes are induced intracellularly. Confirmation of up-regulation would implicate staphylococcal permeases as supplementary nutrient uptake proteins which may contribute to growth when they are functional.

The role of *S. aureus* USA300 LAC permeases should be robustly investigated *in vivo*. In animal models of infection, bacteria can be subjected to changing microenvironments, rather than metabolically controlled *ex vivo* cancer cell monolayers. Ultimately, this would provide realistic and comprehensive data to conclude the importance of UhpT and GlpT as nutritional determinants of CA-MRSA infection. In particular, human blood may provide a microenvironment that uncovers a role for UhpT. A recent study reported that *S. aureus* USA300 *uhpT* expression was up-regulated by 45 fold upon infection of human blood (Malachowa *et al.* 2011). The hexose phosphate transporter was the most highly induced of any other metabolic gene in USA300, which suggests that sugar phosphates are valuable to growth in this niche. Human erythrocytes must combat oxidative stress using only the pentose phosphate pathway, which is initiated exclusively by converting glucose-6-phosphate to gluconate-6-phosphate (Capellini & Fiorelli 2008). Erythrocytes must ensure a constant supply of G-6-P to promote the pentose phosphate pathway and avoid lytic damage. Erythrocytes therefore may provide a valuable supply of sugar phosphate which necessitates metabolic adaptation by *S. aureus* and hence intense induction of UhpT expression. Models of *S. aureus* USA300 bacteremia have been well established in mice and in rabbits (Diep *et al.* 2008; Wang *et al.* 2007). It is crucial that these models are tested using at least the Δ*uhpT* mutant created in this study. This could unvail a significant role for UhpT in CA-MRSA bacteremia and possibly highlight a scenario in which this transport system is a virulence determinant.

Listerial *hpt* expression is inducible by PrfA activation, which is intensely up-regulated during cell infection (De las Heras *et al.* 2011). This control system eliminates exogenous G-6-P as the inducer of expression and guarantees rapid deployment of Hpt transporter upon infection. By contrast, the UhpT transporters in *S. flexineri*, *S. enterica*, *E. coli* and *S. aureus* are only inducibly expressed by the extracellular presence of specific substrates e.g. glucose-6-phosphate (Island *et al.* 1992; Runyen-

Janecky & Payne 2002; Winkler 1973). In addition it has been established that sugar phosphate permeases of Gram negative bacteria are subject to catabolite repression, especially by glucose (Elashvili *et al.* 1998; Verhamme *et al.* 2002; Merkel *et al.* 1995). *S. aureus* permeases are under regulation by carbon catabolite control protein A, the Gram positive metabolic effector activated by glucose metabolism (Seidl *et al.* 2009). The expression status of sensory inducible sugar phosphate permeases during the changing microenvironment of the cell compartment is therefore ambiguous, and depends upon the cellular nutrient conditions. This introduces further complexity into the issue of sugar phosphate involvement during pathogenesis of *S. aureus*. A strategy can be implemented in which expression of sugar phosphate permeases are placed in the same context as *L. monocytogenes*. *S. aureus* USA300 LAC Δ*uhpT* and Δ*glpT* can be complemented with their respective wild type genes under the control of a consitutive gene promoter. In this background, UhpT and GlpT can be definitely expressed in the glucose incorporated models of infection. The capability for specific substrate acquisition in the same cellular environment would be constant. Perhaps this may potentiate bacterial replication, increase virulence and expose whether sugar phosphates can be accessible from the vacuolar niche of *S. aureus* USA300.

8.2.4 Investigation of amino acids / peptides as nutrient sources for intracellular *S. aureus* USA300 LAC

Amino acids/ peptides were postulated to be potential sources of intracellular nutrition for *S. aureus* USA300 which are metabolised to drive vacuole based replication. Interference with amino acid transport and/or amino acid biosynthetic enzymes has shown to have a negative impact upon the intravacuolar replication of several invasive bacterial species (Wieland *et al. 2005;* Foulongne *et al.* 2000; Klose & Mekalanos 1997). As *S. aureus* USA300 may exhibit similar intravacuolar dependence, the impact of amino acids should be investigated. Clinical *S. aureus* strains have been

constructed with insertion mutations in the chromosomal aconitase gene, the enzyme of the TCA cycle that converts citrate to isocitrate (Sadykov *et al.* 2010). These mutant strains have a broken TCA cycle and have been characterised with an incapability to replicate upon amino acids as a sole carbon source for growth. This mutation can be constructed in *S. aureus* USA300 LAC to investigate replication during infection without the capability to metabolise amino acids as growth sources. Prospective replication attenuation of an aconitase mutant can direct attention towards individual amino acid transport systems and/or anapleurotic pathways which are crucial to infection. Perhaps single virulence factors could then be identified to characterise pathogenesis of USA300.

8.2.5 Trafficking of *S. aureus* USA300 to the host cell Golgi

Despite showing strong evidence for WT *S. aureus* USA300 LAC Golgi association in two independent epithelial cell lines, redundant intracellular markers need to be visualised to provide robust evidence of infection dynamics. Giantin and GM130 are commonly used as immunofluorescence markers to visualise the cis-Golgi while TGN46 can also be used to highlight the trans-Golgi (Salcedo & Holden 2003).

The fact that *S. aureus* USA300 LAC is rapidly co-localised with Rab7 upon cell entry indicates that this pathogen is integrated into the phagocytic pathway (Santillo 1997). Migration of *Staphylococcus aureus* containing vacuoles (associated with Rab7) to the Golgi apparatus signifies that cellular trafficking is employed to establish a common replication niche. Retrograde transport from the endosomal compartments to the trans-Golgi network is an important trafficking process in mammalian cells (Johannes & Popoff 2008). Receptor proteins, enzymes and lipids are directed to the trans-Golgi by specific transport proteins for recycling through the biosynthetic and secretory compartments (Johannes & Popoff 2008). Rab9 is typically recruited to late endosomes that require transport of mannose-6-phosphate receptors to the trans-Golgi and motility is

microtubule dependent (Barbero *et al.* 2002). Perhaps immunolabelling of *Staphylococcus aureus* containing vacuoles with Rab9 may support the co-option of retrograde trafficking proteins to allow migration to the trans-Golgi network. A highly specific and potent inhibitor of Rab7 has been described which can be applied to block the maturation of the staphylococcal phagosome (Agola *et al.* 2012). In addition, inhibitors of microtubule dependent motility of endosomal vesicles, such as nocozadole and dynamitin have shown to significantly reduce trafficking to the trans-Golgi network (Itin *et al.* 1999). These strategies could be employed to disrupt trafficking of USA300 vacuoles and potentially correlate Golgi migration to replication. The importance of host cell trafficking could be elucidated as a major factor in the virulence of invasive USA300 lung infection.

8.2.6 *agr*-dependent host cell interactions

Further observations need to be confirmed for definite localisation of *S. aureus* USA300 LAC Δ*agr* to the phagolysosome compartment. For example, antibody labelling of LAMP2 can offer a redundant lysosome localised protein for co-localisation studies. In addition, increased acidification of lysosomal compartments can be mapped by chemical dyes such as LysoTracker, which can determine the localisation of Δ*agr* in an unfavourable niche (Jarry *et al.* 2008). Of course, these investigations need to be compared to WT USA300 LAC in order to differentiate the cell dynamics. Complementation of the *agr* mutant is also essential in demonstrating restoration of wild type host cell dynamics to prove that the observations reported are not non-specific artefacts of *agr* mutant construction.

Transcriptome analysis can be employed to compare the global gene expression of WT and Δ*agr* USA300 LAC strains during epithelial cell infection modelled in this thesis. Discovery of significantly up regulated, *agr* dependent genes can provide a starting point for targeting potential

effectors that play a role in subversion of cellular trafficking and Golgi transit. Perhaps a novel therapeutic target can be uncovered to fight important and aggressive infections caused by CA-MRSA.


Microbiology
Journal
Staphylococcus
aureus
Bacteriology
monocytogenes
Cell
Nature
Immunity
Infection
Escherichia
Clinical
Listeria
virulence
Molecular
methicillin-resistant
Salmonella
coli
Infectious
Biology
Diseases
intracellular
infection
Reviews
host
Goebel
Antimicrobial
community-associated
protein
expression
metabolism
Society
Vázquez-Boland
Otto
PrfA
JA
PNAS
transport
USA300
gene
cells
resistance
fosfomycin
acid
Environmental
Eisenreich
Myocobacterium
pathogenesis
required
synthesis
cell
Applied
macrophages
growth
glucose
system
pathogen
America
Transport
Cheung
human
maturation
Chlamydia
Bacterial
determinants
Current
Shigella
tuberculosis
Legionella
Somerville
Medicine
function
Bayles
Chemistry
Research
DeLeo
PLoS
Role
Golgi
SR
RH
MJ
FR
JR
MG
CM
Suppl
genes
Joseph
Carben
internalization
New
pneumonia
Biological
Chambers
leukocidin
Novick
Braughton
epithelial
Fuchs
Hinton
GA
official
Cellular
International
mechanisms
Science
publication
survival
Annual
community-acquired
typhimurium
global
Agents
RJ
HF
TM
JM
new
DJ
GTPase
Characterization
MZ
BA
Identification
Daum
Lew
MD
bacterial
pathogens
PloS
JC
EA
AR
one
Review
SJ
van
Intracellular
MS
PD
DW
Somerville
Role
PLoS
fosfomycin
MJ
cells
RH
Golgi
SR
FR
JR
MG
Joseph
Eisenreich
Environmental
Carben
Myocobacterium
USA300
internalization
New
pneumonia
gene
Shigella
tuberculosis
Legionella
phagosome
intracellular
Infectious
Biology
Diseases

References

Agola, J O, Hong L, Surviladze Z, Ursu O, Waller A, Strouse J, Simpson DS, Schroeder CE, Oprea TI, Golden JE, Aube J, Buranda T, Sklar LA, and Wandinger-Ness A. 2012. "A Competitive Nucleotide Binding Inhibitor: *In Vitro* Characterization of Rab7 GTPase Inhibition." *ACS chemical biology* 7: 1095–1108.

Alberts B, Johnson A, Lewis J, Raff M, Roberts K and Walter P. 2002. "Electron transport chains and their proton pumps." In *Molecular biology of the cell 4th edition*, Garland Science, New York.

Alix E, Mukherjee S, and Roy CR. 2011. "Subversion of membrane transport pathways by vacuolar pathogens." *The Journal of Cell Biology* 195(6): 943–52.

Alteri CJ, Smith SN, and Mobley HLT. 2009. "Fitness of *Escherichia coli* during urinary tract infection requires gluconeogenesis and the TCA cycle." *PLoS pathogens* 5(5): e1000448.

Alvarez S, Jones M, and Berk SL. 1985. "*In vitro* activity of fosfomycin, alone and in combination, against methicillin-resistant *Staphylococcus aureus*." *Antimicrobial Agents and Chemotherapy* 28(5): 689–90.

Appelberg R. 2006. "Macrophage nutriprive antimicrobial mechanisms." *Journal of Leukocyte Biology* 79(June): 1117–1128.

Arnaud M, Chastanet A, and Debarbouille M. 2004. "New Vector for Efficient Allelic Replacement in Naturally Nontransformable, Low-GC-Content Gram-Positive Bacteria †." *Applied and Environmental Microbiology* 70(11): 6887–6891.

Barbero P, Bittova L, and Pfeffer SR. 2002. "Visualization of Rab9-mediated vesicle transport from endosomes to the trans-Golgi in living cells." *The Journal of Cell Biology* 156(3): 511–8.

Bayles KW, Wesson CA, Liou LE, Fox LK, Bohach GA, and Trumble WR. 1998. "Intracellular *Staphylococcus aureus* escapes the endosome and induces apoptosis in epithelial cells." *Infection and Immunity* 66(1): 336–42.

Becker D, Selbach M, Rollenhagen C, Ballmaier M, Meyer TF, Mann M, and Bumann D. 2006. "Robust *Salmonella* metabolism limits possibilities for new antimicrobials." *Nature* 440(7082): 303–7.

van den Beld MJC and Reubsaet FAG. 2012. "Differentiation between *Shigella*, enteroinvasive *Escherichia coli* (EIEC) and noninvasive *Escherichia coli*." *European Journal of Clinical Microbiology & Infectious Diseases : official publication of the European Society of Clinical Microbiology* 31(6): 899–904.

Benson MA, Lilo S, Wasserman GA, Thoendel M, Smith A, Horswill AR, Fraser J, Novick RP, Shopsin B, and Torres VJ. 2011. "*Staphylococcus aureus* regulates the expression and production of the staphylococcal superantigen-like secreted proteins in a Rot-dependent manner." *Molecular Microbiology* 81(3): 659–75.

Bishai W. 2000. "Lipid lunch for persistent pathogen." *Nature* 406(6797): 683–5.

Bowden SD, Ramachandran VK, Knudsen GM, Hinton JC, and Thompson A. 2010. "An incomplete TCA cycle increases survival of *Salmonella* Typhimurium during infection of resting and activated murine macrophages." *PloS one* 5(11): e13871.

Bowden SD, Rowley G, Hinton JCD and Thompson A. 2009. "Glucose and glycolysis are required for the successful infection of macrophages and mice by *Salmonella enterica* serovar typhimurium." *Infection and Immunity* 77(7): 3117–26.

Bubeck Wardenburg J, Bae T, Otto M, DeLeo FR, and Schneewind O. 2007. "Poring over pores: alpha-hemolysin and Panton-Valentine leukocidin in *Staphylococcus aureus* pneumonia." *Nature Medicine* 13(12): 1405–6.

Cadefau J, Bollen M and Stalmans W. 1997. "Glucose-induced glycogenesis in the liver involves the glucose-6-phosphate-dependent dephosphorylation of glycogen synthase." *Journal of Biochemistry* 750: 745–750.

Capmany A, Leiva N and Damiani MT. 2011. "Golgi-associated Rab14, a new regulator for *Chlamydia trachomatis* infection outcome." *Communicative and Integrative Biology* 4(5): 590–593.

Cappelini MD and Fiorelli G. 2008. "Glucose-6-phosphate dehydrogenase deficiency." *The Lancet* 371: 64–74.

Carnes C, Lopez M, Donegan NP, Cheung A, Gresham H, Timmins GS and Brinker JC. 2009. "Confinement-induced quorum sensing of individual *Staphylococcus aureus* bacteria." *Nature Chemical Biology* 6(1): 41–45.

Castañeda-García A, Rodríguez-Rojas A, Guelfo JR, and Blázquez J. 2009. "The glycerol-3-phosphate permease GlpT is the only fosfomycin transporter in *Pseudomonas aeruginosa*." *Journal of Bacteriology* 191(22): 6968–74.

Chadwick SG, Prasad A, Lamar Smith W, Mordechai E, Adelson ME and Gygax SE. 2013. "Detection of Epidemic USA300 Community-Associated Methicillin-Resistant *Staphylococcus aureus* Strains by Use of a Single Allele-Specific PCR Assay Targeting a Novel Polymorphism of *Staphylococcus aureus* pbp3." *Journal of Clinical Microbiology* 51(8): 2541–50.

Chang D, Smalley DJ, Tucker DL, Leatham MP, Norris WE, Stevenson SJ, Anderson AB, Grissom JE, Laux DC, Cohen PS and Conway T. 2004. "Carbon nutrition of *Escherichia coli* in the mouse intestine." *PNAS* 101(19): 7427–7432.

Chatterjee SS, Hossain H, Otten S, Kuenne C, Kuchmina K, Machata S, Domann E, Chakraborty T and Hain T. 2006. "Intracellular gene expression profile of *Listeria monocytogenes*." *Infection and Immunity* 74(2): 1323–1338.

Cheung GYC, Wang R, Khan BA, Sturdevant DE and Otto M. 2011. "Role of the accessory gene regulator *agr* in community-associated methicillin-resistant *Staphylococcus aureus* pathogenesis." *Infection and Immunity* 79(5): 1927–35.

Chico-Calero I, Suárez M, González-Zorn B, Scortti M, Slaghuis J, Goebel W and Vázquez-Boland JA. 2002. "Hpt, a bacterial homolog of the microsomal glucose- 6-

phosphate translocase, mediates rapid intracellular proliferation in *Listeria*." *PNAS* 99(1): 431–6.

Ciechanover A. 2005. "Proteolysis: from the lysosome to ubiquitin and the proteasome." *Nature Reviews. Molecular Cell Biology* 6(1): 79–87.

Cossart P and Sansonetti PJ. 2004. "Bacterial invasion: the paradigms of enteroinvasive pathogens." *Science* 304: 242–8.

Jaiyanth D, Maamar H, Deb C, Sirakova TD, and Kolattukudy PE. 2011. "*Mycobacterium tuberculosis* uses host triacylglycerol to accumulate lipid droplets and acquires a dormancy-like phenotype in lipid-loaded macrophages." *PLoS Pathogens* 7(6): e1002093.

David MZ, and Daum RS. 2010. "Community-associated methicillin-resistant *Staphylococcus aureus:* epidemiology and clinical consequences of an emerging epidemic." *Clinical Microbiology Reviews* 23(3): 616–87.

Dawes EA. 1952. "Observations on the growth of *Escherichia coli* in media containing amino acids as the sole source of nitrogen." *Journal of Bacteriology* 63: 647–660.

DeLeo FR, and Chambers HF. 2009. "Re-emergence of antibiotic-resistant *Staphylococcus aureus* in the genomics era." *Journal of Clinical Investigation* 119(9): 2464–2474.

Deshayes C, Bielecka MK, Cain R J, Scortti M, de las Heras A, Pietras Z, Luisi BF, Núñez Miguel R and Vázquez-Boland J A. (2012), Allosteric mutants show that PrfA activation is dispensable for vacuole escape but required for efficient spread and *Listeria* survival *in vivo*. *Molecular Microbiology* 85: 461–477. doi: 10.1111/ j.1365-2958.2012.08121.x

Diep BA, Gill SR, Chang RF, Phan THV, Chen JH, Davidson MG, Lin F, Lin J, Carleton HA, Mongodin EF, Sensabaugh GF and Perdreau-Remington F. 2006. "Complete genome sequence of USA300, an epidemic clone of community-acquired meticillin-resistant *Staphylococcus aureus*." *The Lancet* 367: 731–739.

Diep BA, Palazzolo-Ballance AM, Tattevin P, Basuino L, Braughton KR, Whitney AR, Chen L, Kreiswirth BN, Otto M, DeLeo FR and Chambers HF. 2008. "Contribution of Panton-Valentine leukocidin in community-associated methicillin-resistant *Staphylococcus aureus* pathogenesis." *PloS one* 3(9): e3198.

Dietz GW. 1976. "The Hexose Phosphate Transport System of *Escherichia Coli*."In *Advances in Enzymology and Related Areas of Molecular Biology Vol 44*, , p. 237–259.

Dukic VM, Lauderdale DS, Wilder J, Daum RS, and David MZ. 2013. "Epidemics of community-associated methicillin-resistant *Staphylococcus aureus* in the United States: a meta-analysis." *PloS one* 8(1): e52722.

Dussurget O, Pizarro-Cerda , and Cossart P. 2004. “Molecular determinants of *Listeria monocytogenes* virulence.” *Annual Review of Microbiology* 58: 587–610.

Dziewanowska K, Patti JM, Deobald CF, Bayles KW, Trumble WR, and Bohach GA. 1999. “Fibronectin binding protein and host cell tyrosine kinase are required for internalization of *Staphylococcus aureus* by epithelial cells.” *Infection and Immunity* 67: 4673–4678.

Eidels L, Rick PD, Norma P and Osborn MJ. 1974. “Transport of D-Arabinose-5-Phosphate and D-Sedoheptulose-7-Phosphate by the Hexose Phosphate Transport System of *Salmonella* typhimurium.” *Journal of Bacteriology* 119(1): 138–143.

von Eiff C, Mcnamara P, Becker K, Lei X, Ziman M, Bochner BR, Peters G, Proctor RA and Bates D. 2006. “Phenotype Microarray Profiling of *Staphylococcus aureus* menD and hemB Mutants with the Small-Colony-Variant Phenotype.” *Journal of Bacteriology* 188(2): 687–93.

Eisenreich W, Dandekar T, Heesemann J and Goebel W. 2010. “Carbon metabolism of intracellular bacterial pathogens and possible links to virulence.” *Nature Reviews. Microbiology* 8(6): 401–12.

Elashvili I, Defrank JJ and Culotta VC. 1998. “*phnE* and *glpT* genes enhance utilization of organophosphates in *Escherichia coli* K-12.” *Applied and Environmental Microbiology* 64(7): 2601–8.

Elvin CM, Hardy CM and Rosenberg H. 1985. “Pi Exchange Mediated by the GIpT-Dependent sn-Glycerol-3-Phosphate Transport System in *Escherichia coli*.” *Journal of Bacteriology* 161(3): 1054–1058.

Erlandson AL and Mackey WH. 1958. “Nutrition of *Shigella*: growth of *Shigella flexneri* in a simple chemically defined medium.” *Journal of Bacteriology* 75(3): 253–7.

Eskelinen E. 2006. “Roles of LAMP-1 and LAMP-2 in lysosome biogenesis and autophagy.” *Molecular Aspects of Medicine* 27(5-6): 495–502.

Eylert E, Schär J, Mertins S, Stoll R, Bacher A, Goebel W, and Eisenreich W. 2008. “Carbon metabolism of *Listeria monocytogenes* growing inside macrophages.” *Molecular Microbiology* 69(4): 1008–1017.

Falagas ME, Giannopoulou KP, Kokolakis GN, and Rafailidis PI. 2008. “Fosfomycin: use beyond urinary tract and gastrointestinal infections.” *Clinical Infectious Diseases : an official publication of the Infectious Diseases Society of America* 46(7): 1069–77.

Falagas ME, Maraki S, Karageorgopoulos DE, Kastoris AC, Kapaskelis A and Samonis G. 2010. “Antimicrobial susceptibility of Gram-positive non-urinary isolates to fosfomycin.” *International Journal of Antimicrobial Agents* 35(5): 497–499.

Farber JM and Peterkin PI. 1991. "*Listeria monocytogenes*, a food-borne pathogen." *Microbiological Reviews* 55(3): 476–511.

Fitzgerald JR. 2007. "Targeted Gene Disruption for the Analysis of Virulence of *Staphylococcus aureus* 1." In *Methods of Molecular Biology Volume 391*, p. 103–112.

Flannagan R, Cosio R and Grinstein S. 2009. "Antimicrobial mechanisms of phagocytes and bacterial evasion strategies." *Nature Reviews Microbiology* 7(5): 355–367.

Foulongne V, Bourg G, Cazevieille C, Michaux-Charachon S, and O'Callaghan D. 2000. "Identification of *Brucella suis* genes affecting intracellular survival in an in vitro human macrophage infection model by signature-tagged transposon mutagenesis." *Infection and Immunity* 68(3): 1297–1303.

Fraunholz M and Sinha B. 2012. "Intracellular *Staphylococcus aureus*: live-in and let die." *Frontiers in Cellular and Infection Microbiology* 2(April): 43.

Fuchs TM, Eisenreich W, Heesemann J and Goebel W. 2012. "Metabolic adaptation of human pathogenic and related nonpathogenic bacteria to extra- and intracellular habitats." *FEMS Microbiology Reviews* 36(2): 435–62.

Fuchs TM, Eisenreich W, Kern T, and Dandekar T. 2012. "Toward a systemic understanding of *Listeria monocytogenes* metabolism during infection." *Frontiers in Microbiology* 3(February): 1–12.

Garzoni C,Francois P, Huyghe A, Couzinet S, Tapparel C, Charbonnier Y, Renzoni A, Lucchini S, Lew DP, Vaudaux P, Kelley WL and Schrenzel J. 2007. "A global view of *Staphylococcus aureus* whole genome expression upon internalization in human epithelial cells." *BMC genomics* 8(171).

Garzoni C, and Kelley WL. 2009. "*Staphylococcus aureus*: new evidence for intracellular persistence." *Trends in Microbiology* 17(2): 59–65.

Gentschev I, Sokolovic Z, Mollenkopf HJ, Hess J and Kaufmann SH. 1995. "*Salmonella* strain secreting active listeriolysin changes its intracellular localization." *Infection and Immunity* 63(10): 4202–4205.

Glaser P, Frangeul L, Buchrieser C, Rusniok C, Amend A, Baquero F, Berche P, Bloeker H, Brandt P, Chakraborty T, Charbit A, Chetouani F, Couve E, de Daruvar A, Dehoux P, Domann E, Dominguez-Bernal G, Duchard E, Durant L, Dussurget O, Entian KD, Fsihi H, Garcia-del Portillo F, Garrido P, Gautier L, Goebel W, Gomez-Lopez N, Hain T, Hauf J, Jackson D, Jones LM, Kaerst U, Kreft J, Kuhn M, Kunst F, Kurapkat G, Madueno E, Maitournam A, Vicente JM, Ng E, Nedjari H, Nordsiek G, Novella S, de Pablos B, Perez-Diaz JC, Purcell R, Remmel B, Rose M, Schlueter T, Simoes N, Tierrez A, Vazquez-Boland JA, Voss H, Wehland J and Cossart P. 2001. "Comparative genomics of *Listeria* species." *Science (New York, N.Y.)* 294(5543): 849–52.

Goetz M, Bubert A, Wang G, Chico-Calero I, Vazquez-Boland JA, Beck M, Slaghuis J, Szalay AA, and Goebel W. 2001. “Microinjection and growth of bacteria in the cytosol of mammalian host cells.” *PNAS* 98(21): 12221–6.

Gomis RR, Favre C, García-Rocha M, Fernández-Novell JM, Ferrer JC and Guinovart JJ. 2003. “Glucose 6-phosphate produced by gluconeogenesis and by glucokinase is equally effective in activating hepatic glycogen synthase.” *The Journal of Biological Chemistry* 278(11): 9740–6.

Gordon RJ and Lowy FD. 2008. “Pathogenesis of methicillin-resistant *Staphylococcus aureus* infection.” *Clinical Infectious Diseases : an official publication of the Infectious Diseases Society of America* 46 Suppl 5(Suppl 5): S350–9.

Götz A, Eylert E, Eisenreich W and Goebel W. 2010. “Carbon metabolism of enterobacterial human pathogens growing in epithelial colorectal adenocarcinoma (Caco-2) cells.” *PloS one* 5(5): e10586.

Götz A and Goebel W. 2010. “Glucose and glucose 6-phosphate as carbon sources in extra- and intracellular growth of enteroinvasive *Escherichia coli* and *Salmonella enterica*.” *Microbiology* 156(Pt 4): 1176–87.

Gould IM, David MZ, Esposito S, Garau J, Lina G, Mazzei T and Peters G. 2012. “New insights into meticillin-resistant *Staphylococcus aureus* (MRSA) pathogenesis, treatment and resistance.” *International Journal of Antimicrobial Agents* 39(2): 96–104.

Gruenberg J and van der Goot FG. 2006. “Mechanisms of pathogen entry through the endosomal compartments.” *Nature Reviews. Molecular Cell Biology* 7(7): 495–504.

Gründling A and Schneewind O. 2007. “Genes required for glycolipid synthesis and lipoteichoic acid anchoring in *Staphylococcus aureus*.” *Journal of Bacteriology* 189(6): 2521–30.

Guo Z and Jensen MD. 1999. “Blood Glycerol Is an Important Precursor for Intramuscular Triacylglycerol Synthesis.” *Journal of Biological Chemistry* 274(34): 23702–23706.

Guth A, Engel R, and Tropp BE. 1980. “Uptake of glycerol 3-phosphate and some of its analogs by the hexose phosphate transport system of *Escherichia coli*.” *Journal of Bacteriology* 143(1): 538–539.

Gutierrez MG, Munafó DB, Berón W and Colombo MI. 2004. “Rab7 is required for the normal progression of the autophagic pathway in mammalian cells.” *Journal of Cell Science* 117(Pt 13): 2687–97.

Gutnick, D, Calvo JM, Klopotowski T and Ames BN. 1969. “Compounds which serve as the sole source of carbon or nitrogen for *Salmonella typhimurium* LT-2.” *Journal of Bacteriology* 100(1): 215–9.

Harrison RE, Brumell JH, Khandani A, Bucci C, Scott CC, Jiang X, Finlay B and Grinsten S. 2004. "*Salmonella* impairs RILP recruitment to Rab7 during maturation of invasion vacuoles." *Molecular Biology of the Cell* 15(July): 3146–3154.

Hautefort I, Thompson A, Eriksson-Yberg S, Parker ML, Lucchini S, Danino V, Bongaerts RJM, Ahmad N, Rhen M and Hinton JDC. 2008. "During infection of epithelial cells *Salmonella enterica* serovar Typhimurium undergoes a time-dependent transcriptional adaptation that results in simultaneous expression of three type 3 secretion systems." *Cellular Microbiology* 10(4): 958–984.

Heller KB, Lin ECC and Wilson TH. 1980. "Substrate Specificity and Transport Properties of the Glycerol Facilitator of *Escherichia coli*." *Journal of Bacteriology* 144(1): 274–278.

Hess DJ, Henry-Stanley MJ, Erickson EA and Wells CL. 2003. "Intracellular survival of *Staphylococcus aureus* within cultured enterocytes." *Journal of Surgical Research* 114(1): 42–49.

Heuer D, Lipinski AR, Machuy N, Karlas A, Wehrens A, Siedler F, Brinkmann V and Meyer TF. 2009. "*Chlamydia* causes fragmentation of the Golgi compartment to ensure reproduction." *Nature* 457(7230): 731–5.

Hidron AI, Low CE, Honig EG and Blumberg HM. 2009. "Emergence of community-acquired meticillin-resistant *Staphylococcus aureus* strain USA300 as a cause of necrotising community-onset pneumonia." *The Lancet Infectious Diseases* 9(6): 384–92.

Hornef MW, Wick MJ, Rhen M and Normark S. 2002. "Bacterial strategies for overcoming host innate and adaptive immune responses." *Nature Immunology* 3(11): 1033–1040.

Horsburgh MJ, Aish JL, White IJ, Shaw L, Lithgow JK, Foster SJ, and England S. 2002. "SigmaB Modulates Virulence Determinant Expression and Stress Resistance : Characterization of a Functional *rsbU* Strain Derived from *Staphylococcus aureus* 8325-4." *Journal of Bacteriology* 184(19): 5457–5467.

Horsburgh MJ, Wiltshire MD, Crossley H, Ingham E and Foster SJ. 2004. "PheP , a Putative Amino Acid Permease of *Staphylococcus aureus* , Contributes to Survival *In Vivo* and during Starvation." *Infection and Immunity* 72(5): 3073–3076.

Isberg RR, O'Connor TJ and Heidtman M. 2009. "The *Legionella pneumophila* replication vacuole: making a cosy niche inside host cells." *Nature Reviews. Microbiology* 7(1): 13–24.

Island MD, Wei BY, and Kadner RJ. 1992. "Structure and function of the *uhp* genes for the sugar phosphate transport system in *Escherichia coli* and *Salmonella typhimurium*." *Journal of Bacteriology* 174(9): 2754–62.

Itin C, Ulitzur N, Mu B and Pfeffer SR. 1999. "Mapmodulin, Cytoplasmic Dyenin, and Microtubules Enhance the Transport of Mannose 6-Phosphate Receptors

from Endosomes to the Trans-Golgi Network." *Molecular Biology of the Cell* 10(July): 2191–2197.

Jarry TM, and Cheung AL. 2006. "*Staphylococcus aureus* escapes more efficiently from the phagosome of a cystic fibrosis bronchial epithelial cell line than from its normal counterpart." *Infection and Immunity* 74(5): 2568–2577.

Jarry TM, Memmi G and Cheung AL. 2008. "The expression of alpha-haemolysin is required for *Staphylococcus aureus* phagosomal escape after internalization in CFT-1 cells." *Cellular Microbiology* 10(9): 1801–14.

Johannes L and Popoff V. 2008. "Tracing the retrograde route in protein trafficking." *Cell* 135(7): 1175–87.

Joseph B and Goebel W. 2007. "Life of *Listeria monocytogenes* in the host cells' cytosol." *Microbes and Infection / Institut Pasteur* 9(10): 1188–95.

Joseph B, Mertins S, Stoll R, Scha J, Umesha KR, Luo Q, Mu S and Goebel W. 2008. "Glycerol Metabolism and PrfA Activity in *Listeria monocytogenes*." *Journal of Bacteriology* 190(15): 5412–5430.

Joseph B, Przybilla K, Stühler C, Slaghuis J, Fuchs TM, Goebel W, Stu C, and Schauer K. 2006. "Identification of *Listeria monocytogenes* Genes Contributing to Intracellular Replication by Expression Profiling and Mutant Screening." *Journal of Bacteriology* 188(2): 556–568.

Junutula JR, De Mazie AM, Peden AA, Ervin KE, Advani RJ, Van Dijk SM, Klumperman J and Scheller RH. 2004. "Rab14 Is Involved in Membrane Trafficking between the Golgi Complex and Endosomes." *Molecular Biology of the Cell* 15(May): 2218–2229.

Kahan FM, Kahan JS, Cassidy PJ and Kropp H. 1974. "The mechanism of action of fosfomycin (phosphonomycin)." *Annals of the New York Academy of Sciences* 235: 364–386.

Kim DH, Lees WJ, Kempsell KE, Lane WS, Duncan K and Walsh CT. 1996. "Characterization of a Cys115 to Asp substitution in the *Escherichia coli* cell wall biosynthetic enzyme UDP-GlcNAc enolpyruvyl transferase (MurA) that confers resistance to inactivation by the antibiotic fosfomycin." *Biochemistry* 35(15): 4923–8.

Kim J, Dutta V, Elhanafi D, Lee S, Osborne JA and Kathariou S. 2012. "A novel restriction-modification system is responsible for temperature-dependent phage resistance in *Listeria monocytogenes* ECII." *Applied and Environmental Microbiology* 78(6): 1995–2004.

Klein E, Smith D, and Laxminarayan R. 2007. "Hospitalizations and Deaths Caused by Methicillin-Resistant *Staphylococcus aureus*." *Emerging Infectious Diseases* 13(12): 1999–2005.

Klose KE, and Mekalanos JJ. 1997. “Simultaneous prevention of glutamine synthesis and high-affinity transport attenuates *Salmonella typhimurium* virulence.” *Infection and Immunity* 65(2): 587–596.

Kluytman JAN, van Belkum A, and Verbrugh H. 1997. “Nasal carriage of *Staphylococcus aureus* : epidemiology , underlying mechanisms , and associated risks.” *Clinical Microbiology Reviews* 10(3): 505–520.

Knodler LA and Steele-Mortimer O. 2003. “Taking Possession: Biogenesis of the *Salmonella*-Containing Vacuole.” *Traffic* 4: 587–599.

Kobayashi SD, Malachowa N, Whitney AR, Braughton KR, Gardner DJ, Long D, Bubeck Wardenburg J, Schneewind O, Otto M, and DeLeo FR. 2011. “Comparative analysis of USA300 virulence determinants in a rabbit model of skin and soft tissue infection.” *The Journal of Infectious Diseases* 204(6): 937–41.

Köhler R, Bubert A, Goebel W, Steinert M, Hacker J and Bubert B. 2000. “Expression and use of the green fluorescent protein as a reporter system in *Legionella pneumophila*.” *Molecular & General Genetics : MGG* 262(6): 1060–9.

Kreiswirth BN, Löfdahl S, Betley MJ, O’Reilly M, Schlievert PM, Bergdoll MS, and Novick RP. 1983. “The toxic shock syndrome exotoxin structural gene is not detectably transmitted by a prophage.” *Nature* 305: 709 – 712.

Kumar Y, Cocchiaro J and Valdivia RH. 2006. “The obligate intracellular pathogen *Chlamydia trachomatis* targets host lipid droplets.” *Current Biology* 16(16): 1646–51.

Kumar Y and Valdivia RH. 2009. “Leading a sheltered life: intracellular pathogens and maintenance of vacuolar compartments.” *Cell Host & Microbe* 5(6): 593–601.

Kyei GB, Vergne I, Chua J, Roberts E, Harris J, Junutula JR, and Deretic V. 2006. “Rab14 is critical for maintenance of *Mycobacterium tuberculosis* phagosome maturation arrest.” *The EMBO Journal* 25(22): 5250–9.

Labandeira-Rey M, Couzon F, Boisset S, Brown EL, Bes M, Benito Y, Barbu EM, Vazquez V, Höök M, Etienne J, Vandenesch F, and Gabriela Bowden M. 2007. “*Staphylococcus aureus* Panton-Valentine leukocidin causes necrotizing pneumonia.” *Science* 315(5815): 1130–3.

Laguna RK, Creasey EA, Li Z,Valtz N and Isberg RR. 2006. “A *Legionella pneumophila*-translocated substrate that is required for growth within macrophages and protection from host cell death.” *Proceedings of the National Academy of Sciences of the United States of America* 103(49): 18745–50.

De las Heras A, Cain RJ, Bielecka MK and Vázquez-Boland JA. 2011. “Regulation of *Listeria* virulence: PrfA master and commander.” *Current Opinion in Microbiology* 14(2): 118–27.

Lauer P, Chow MYN, Loessner MJ, Portnoy DA and Calendar R. 2002. "Construction, characterization, and use of two *Listeria monocytogenes* site-specific phage integration vectors." *Journal of Bacteriology* 184(15): 4177–4186.

Law CJ, Enkavi G, Wang D and Tajkhorshid E. 2009. "Structural basis of substrate selectivity in the glycerol-3-phosphate: phosphate antiporter GlpT." *Biophysical Journal* 97(5): 1346–53.

Law CJ, Maloney PC and Wang D. 2008. "Ins and outs of major facilitator superfamily antiporters." *Annual Review of Microbiology* 62: 289–305.

Lee, JC. 1995. "Electrotransformation of Staphylococci." *Methods in Molecular Biology (Clifton, N.J.)* 47: 209–16.

Lehman D, Tseng CW, Eells S, Miller LG, Fan X, Beenhouwer DO and Liu GY. 2010. "*Staphylococcus aureus* Panton-Valentine leukocidin targets muscle tissues in a child with myositis and necrotizing fasciitis." *Clinical Infectious Diseases : an official publication of the Infectious Diseases Society of America* 50(1): 69–72.

Lemieux MJ, Huang Y and Wang D. 2005. "Crystal structure and mechanism of GlpT ,the glycerol-3-phosphate transporter from *E .coli*." *Journal of Electron Microscopy* 54 (Supplement 1): 43–46.

Lemieux MJ, Huang Y, and Wang D. 2004. "Glycerol-3-phosphate transporter of *Escherichia coli*: structure, function and regulation." *Research in Microbiology* 155(8): 623–9.

Lemon KP, Freitag NE and Kolter R. 2010. "The virulence regulator PrfA promotes biofilm formation by *Listeria monocytogenes*." *Journal of Bacteriology* 192(15): 3969–76.

Levine B and Kroemer G. 2008. "Autophagy in the Pathogenesis of Disease." *Cell* 132(1): 27–42.

Lewis VG, Ween MP and McDevitt CA. 2012. "The role of ATP-binding cassette transporters in bacterial pathogenicity." *Protoplasma* 249(4): 919–42.

Li M, Cheung GYC, Hu J, Wang D, Joo H, FeLeo FR and Otto M. 2010. "Comparative analysis of virulence and toxin expression of global community-associated methicillin-resistant *Staphylococcus aureus* strains." *Journal of Infectious Diseases* 202(12): 1866–76.

van der Linden L, van der Schaar HM, Lanke KHW, Neyts J and van Kuppeveld FJM. 2010. "Differential effects of the putative GBF1 inhibitors Golgicide A and AG1478 on enterovirus replication." *Journal of Virology* 84(15): 7535–42.

Lloyd AD and Kadner RJ. 1990. "Topology of the *Escherichia coli* uhpT Sugar-Phosphate Transporter Analyzed by Using TnphoA Fusions." *Journal of Bacteriology* 172(4): 1688–1693.

Lowe S L, Wong SH, and Hong W. 1996. “The mammalian ARF-like protein 1 (Arl1) is associated with the Golgi complex.” *Journal of Cell Science* 109 209–20.

Lucchini S, Liu H, Jin Q, Hinton JCD, and Yu J. 2005. “Transcriptional Adaptation of *Shigella flexneri* during Infection of Macrophages and Epithelial Cells : Insights into the Strategies of a Cytosolic Bacterial Pathogen.” *Infection and Immunity* 73(1): 88–102.

Luzio PJ, Pryor PR and Bright NA. 2007. “Lysosomes: fusion and function.” *Nature Reviews. Molecular Cell Biology* 8(8): 622–32.

Malachowa N, Whitney AR, Kobayashi SD, Sturdevant DE, Kennedy AD, Braughton KR, Shabb DW, Diep BA, Chambers HF, Otto M and DeLeo FR. 2011. “Global changes in *Staphylococcus aureus* gene expression in human blood.” *PloS one* 6(4): e18617.

Mauthe M, Yu W, Krut O, Krönke M, Götz F, Robenek H and Proikas-Cezanne T. 2012. “WIPI-1 Positive Autophagosome-Like Vesicles Entrap Pathogenic *Staphylococcus aureus* for Lysosomal Degradation.” *International Journal of Cell Biology* 2012(3): 179207.

McGhie EJ, Brawn LC, Hume PJ, Humphreys D and Koronakis V. 2009. “*Salmonella* takes control: effector-driven manipulation of the host.” *Current Opinion in Microbiology* 12(1): 117–24.

McKinney J D, zu Bentrup KH, Muñoz-Elías EJ, Miczak A, Chen B, Chan WT, Swenson D, Sacchettini JC, Jacobs WR and Russell DG. 2000. “Persistence of *Mycobacterium tuberculosis* in macrophages and mice requires the glyoxylate shunt enzyme isocitrate lyase.” *Nature* 406(6797): 735–8.

Memmi G, Filipe SR, Pinho MG, Fu Z and Cheung A. 2008. “*Staphylococcus aureus* PBP4 is essential for beta-lactam resistance in community-acquired methicillin-resistant strains.” *Antimicrobial Agents and Chemotherapy* 52(11): 3955–66.

Méresse S, Steele-Mortimer O, Finlay BB and Gorvel JP. 1999. “The rab7 GTPase controls the maturation of *Salmonella typhimurium*-containing vacuoles in HeLa cells.” *The EMBO Journal* 18(16): 4394–403.

Merkel T J, Dahl JL, Ebright RH and Kadner RJ. 1995. “Transcription activation at the *Escherichia coli uhpT* promoter by the catabolite gene activator protein.” *Journal of Bacteriology* 177(7): 1712–8.

Monk IR, Gahan CGM and Hill C. 2008. “Tools for functional postgenomic analysis of *Listeria monocytogenes*.” *Applied and Environmental Microbiology* 74(13): 3921–34.

Montgomery CP, Boyle-Vavra S, Adem PV, Lee JC, Husain AN, Clasen J, and Daum RS. 2008. “Comparison of virulence in community-associated methicillin-resistant *Staphylococcus aureus* pulsotypes USA300 and USA400 in a rat model of pneumonia.” *The Journal of Infectious Diseases* 198(4): 561–70.

Montgomery CP, Boyle-Vavra S, and Daum RS. 2010. “Importance of the global regulators Agr and SaeRS in the pathogenesis of CA-MRSA USA300 infection.” *PloS one* 5(12): e15177.

Nakamura N, Rabouille C, Watson R, Nilsson T, Hui N, Slusarewicz P, Kreis TE, and Warren G. 1995. “Characterization of a cis-Golgi Matrix Protein, GM130.” *Journal of Cell Biology* 131(6): 1715–1726.

Nanchen A, Schicker A, Revelles O and Sauer U. 2008. “Cyclic AMP-dependent catabolite repression is the dominant control mechanism of metabolic fluxes under glucose limitation in *Escherichia coli*.” *Journal of Bacteriology* 190(7): 2323–30.

Nimmo GR. 2012. “USA300 abroad: global spread of a virulent strain of community-associated methicillin-resistant *Staphylococcus aureus*.” *Clinical Microbiology and Infection : the official publication of the European Society of Clinical Microbiology and Infectious Diseases* 18(8): 725–34.

Novick R. 1967. “Properties of a cryptic high-frequency transducing phage in *Staphylococcus aureus*.” *Virology* 166: 155–166.

Novick RP, and Geisinger E. 2008. “Quorum sensing in staphylococci.” *Annual Review of Genetics* 42: 541–64.

Nuxoll AS, Halouska SM, Sadykov MR, Hanke ML, Bayles KW, Kielian T, Powers R, and Fey PD. 2012. “CcpA regulates arginine biosynthesis in *Staphylococcus aureus* through repression of proline catabolism.” *PLoS pathogens* 8(11): e1003033.

Pandey AK, and Sassetti CM. 2008. “Mycobacterial persistence requires the utilization of host cholesterol.” *PNAS* 105(11): 4376–4380.

Pang YY, Schwartz J, Thoendel M, Ackermann LW, Horswill AR and Nauseef WM. 2010. “*agr*-Dependent interactions of *Staphylococcus aureus* USA300 with human polymorphonuclear neutrophils.” *Journal of Innate Immunity* 2(6): 546–59.

Pao SS, Paulsen IANT and Saier MH. 1998. “Major Facilitator Superfamily.” *American Society for Microbiology* 62(1): 1–34.

Pizarro-Cerdá J and Cossart P. 2006. “Bacterial adhesion and entry into host cells.” *Cell* 124(4): 715–27.

Popovic M, Steinort D, Pillai S and Joukhadar C. 2010. “Fosfomycin: an old, new friend?” *European Journal of Clinical Microbiology & Infectious Diseases* 29(2): 127–42.

Postma PW, Lengeler JW and Jacobson GR. 1993. “Phosphoenolpyruvate : carbohydrate phosphotransferase systems of bacteria.” *Microbiological Reviews* 57(3): 543–94.

Premaratne RJ, Lin W and Johnson EA. 1991. “Development of an improved chemically defined minimal medium for *Listeria*.” *Applied and Environmental Microbiology* 57(10): 3046–3048.

Rabinovitch M. 1995. “Professional and non-professional phagocytes : an introduction.” *Trends in Cell Biology* 5: 85–87.

Rengarajan J, Bloom BR and Rubin EJ. 2005. “Genome-wide requirements for *Mycobacterium tuberculosis* adaptation and survival in macrophages.” *PNAS* 102(23): 8327–32.

Rice LB. 2006. “Antimicrobial resistance in gram-positive bacteria.” *American Journal of Infection Control* 34(5 Suppl 1): S11–19.

Richter SG, Elli D, Kim HK, Hendrickx APA, Sorg JA, Schneewind O and Missiakas D. 2013. “Small molecule inhibitor of lipoteichoic acid synthesis is an antibiotic for Gram-positive bacteria.” *PNAS* 110(9): 3531–6.

Ripio M T, Brehm K, Lara M, Suárez M, and Vázquez-Boland JA. 1997. “Glucose-1-phosphate utilization by *Listeria monocytogenes* is PrfA dependent and coordinately expressed with virulence factors.” *Journal of Bacteriology* 179(22): 7174–80.

Ripio M T, Domínguez-Bernal G, Lara M, Suárez M, and Vazquez-Boland JA. 1997. “A Gly145Ser substitution in the transcriptional activator PrfA causes constitutive overexpression of virulence factors in *Listeria monocytogenes*.” *Journal of Bacteriology* 179(5): 1533–40.

Ripio M T, Domínguez-Bernal G, Suárez M, Brehm K, Berche P, and Vázquez-Boland JA. 1996. “Transcriptional activation of virulence genes in wild-type strains of *Listeria monocytogenes* in response to a change in the extracellular medium composition.” *Research in Microbiology* 147(5): 371–84.

Robinson CG and Roy CR. 2006. “Attachment and fusion of endoplasmic reticulum with vacuoles containing *Legionella pneumophila*.” *Cellular Microbiology* 8(5): 793–805.

Runyen-Janecky LJ and Payne SM. 2002. “Identification of chromosomal *Shigella flexneri* genes induced by the eukaryotic intracellular environment.” *Infection and Immunity* 70(8): 4379–4388.

Sadykov MR, Mattes TA, Luong TT, Zhu Y, Day SR, Sifri CD, Lee CY and Somerville GA. 2010. “Tricarboxylic acid cycle-dependent synthesis of *Staphylococcus aureus* Type 5 and 8 capsular polysaccharides.” *Journal of Bacteriology* 192(5): 1459–62.

Sáenz JB, Sun WJ, Chang JW,Li J, Bursulaya B, Gray NS and Haslam DB. 2009. “Golgicide A reveals essential roles for GBF1 in Golgi assembly and function.” *Nature Chemical Biology* 5(3): 157–65.

Saka HA and Valdivia RH. 2010. “Acquisition of nutrients by *Chlamydiae*: unique challenges of living in an intracellular compartment.” *Current Opinion in Microbiology* 13(1): 4–10.

Salcedo SP, and Holden DW. 2003. “SseG, a virulence protein that targets *Salmonella* to the Golgi network.” *The EMBO Journal* 22(19): 5003–14.

Santillo M. 1997. “Role of the Small GTPase RAB7 in the Late Endocytic Pathway.” *Journal of Biological Chemistry* 272(7): 4391–4397.

Schär J, Stoll R, Schauer K, Loeffler DIM, Eylert E, Joseph B, Eisenreich W, Fuchs TM, and Goebel W. 2010. “Pyruvate carboxylase plays a crucial role in carbon metabolism of extra-and intracellularly replicating *Listeria monocytogenes*.” *Journal Of Bacteriology* 192(7): 1774–1784.

Schauer K, Geginat G, Liang C, Goebel W, Dandekar T and Fuchs TM. 2010. “Deciphering the intracellular metabolism of *Listeria monocytogenes* by mutant screening and modelling.” *BMC Genomics* 11(1): 573.

Schnaith A, Kashkar H, Leggio SA, Addicks K, Krönke M, and Krut O. 2007. “*Staphylococcus aureus* subvert autophagy for induction of caspase-independent host cell death.” *The Journal of Biological Chemistry* 282(4): 2695–706.

Schnappinger D, Ehrt S, Voskuil MI, Liu Y, Mangan JA, Monahan IM, Dolganov G, Efron B, Butcher PD, Nathan C and Schoolnik GK. 2003. “Transcriptional Adaptation of *Mycobacterium tuberculosis* within Macrophages: Insights into the Phagosomal Environment.” *The Journal of Experimental Medicine* 198(5): 693–704.

Scholing M, Schneeberger PM, van den Dries P, and Drenth JPH. 2007. “Clinical features of liver involvement in adult patients with listeriosis. Review of the literature.” *Infection* 35(4): 212–8.

Schröder A, Kland R, Peschel A, von Eiff C, and Aepfelbacher M. 2006. “Live cell imaging of phagosome maturation in *Staphylococcus aureus* infected human endothelial cells: small colony variants are able to survive in lysosomes.” *Medical Microbiology and Immunology* 195(4): 185–94.

Schwöppe C, Winkler HH, and Neuhaus HE. 2002. “Properties of the Glucose-6-Phosphate Transporter from *Chlamydia pneumoniae* (HPTcp) and the Glucose-6-Phosphate Sensor from *Escherichia coli* (UhpC)†.” *Journal of Bacteriology* 184(8): 2108–2115.

Scortti M, Lacharme-Lora L, Wagner M, Chico-Calero I, Losito P, and Vázquez-Boland JA. 2006. “Coexpression of virulence and fosfomycin susceptibility in *Listeria*: molecular basis of an antimicrobial *in vitro-in vivo* paradox.” *Nature Medicine* 12(5): 515–7.

Scortti M, Monzó HJ, Lacharme-Lora L, Lewis DA, and Vázquez-Boland JA. 2007. “The PrfA virulence regulon.” *Microbes and Infection* 9(10): 1196–207.

Seidl K, Müller S, François P, Kriebitzsch C, Schrenzel J, Engelmann S, Bischoff M, and Berger-Bächi B. 2009. "Effect of a glucose impulse on the CcpA regulon in *Staphylococcus aureus*." *BMC Microbiology* 9: 95.

Seto S, Tsujimura K and Koide Y. 2011. "Rab GTPases regulating phagosome maturation are differentially recruited to mycobacterial phagosomes." *Traffic (Copenhagen, Denmark)* 12(4): 407–20.

Sherwin R S. 1980. "Role of the liver in glucose homeostasis." *Diabetes Care* 3(2): 261–5.

Sinai AP and Joiner KA. 1997. "Safe haven: the cell biology of nonfusogenic pathogen vacuoles." *Annual Review of Microbiology* 51: 415–62.

Sinha B, François PP, Nüsse O, Foti M, Hartford OM, Vaudaux P, Foster TJ, Lew DP, Herrmann M, and Krause KH. 1999. "Fibronectin-binding protein acts as *Staphylococcus aureus* invasin via fibronectin bridging to integrin a5 b1." *Cellular Microbiology* 1(2): 101–17.

Sinha B and Fraunholz M. 2010. "*Staphylococcus aureus* host cell invasion and post-invasion events." *International Journal of Medical Microbiology : IJMM* 300(2-3): 170–5.

Somerville, GA, Chaussee MS, Morgan CI, Fitzgerald JR, Dorward DW, Reitzer LJ and Musser JM. 2002. "*Staphylococcus aureus* aconitase inactivation unexpectedly inhibits post-exponential-phase growth and enhances stationary-phase survival." *Infection and Immunity* 70(11): 6373–6382.

Stenmark H and Olkkonen VM. 2001. "Protein family review The Rab GTPase family." *Genome Biology* 2(5): 1–7.

Stoll R and Goebel W. 2010. "The major PEP-phosphotransferase systems (PTSs) for glucose, mannose and cellobiose of *Listeria monocytogenes*, and their significance for extra- and intracellular growth." *Microbiology* 156(4): 1069–1083.

Stryjewski ME and Chambers HF. 2008. "Skin and soft-tissue infections caused by community-acquired methicillin-resistant *Staphylococcus aureus*." *Clinical Infectious Diseases : an official publication of the Infectious Diseases Society of America* 46 Suppl 5(Suppl 5): S368–77.

Takahata S, Ida T, Hiraishi T, Sakakibara S, Maebashi K, Terada S, Muratani T, Matsumoto T, Nakahama C, and Tomono K. 2010. "Molecular mechanisms of fosfomycin resistance in clinical isolates of *Escherichia coli*." *International Journal of Antimicrobial Agents* 35(4): 333–7.

Tenover FC, Mcdougal LK, Goering RV, Killgore G, Projan SJ, Patel JB, Paul M, and Dunman PM. 2006. "Characterization of a Strain of Community-Associated Methicillin-Resistant *Staphylococcus aureus* Widely Disseminated in the United States." *Journal of Clinical Microbiology* 44(1): 108–118.

Thurlow LR, Joshi GS and Richardson AR. 2012. “Virulence strategies of the dominant USA300 lineage of community-associated methicillin-resistant *Staphylococcus aureus* (CA-MRSA).” *FEMS Immunology and Medical Microbiology* 65(1): 5–22.

Toledo-arana A, Merino N, Vergara-Irigaray M, Debarbouille M, Penades J and Lasa I. 2005. “*Staphylococcus aureus* Develops an Alternative , ica-Independent Biofilm in the Absence of the *arlRS* Two-Component System.” *Journal of Bacteriology* 187(15): 5318–5329.

Vázquez-Boland JA, Kuhn M, Berche P, Chakraborty T, Dominguez-Bernal G, Goebel W, Gonzalez-Zorn B, Wehand J and Kreft J. 2001. “*Listeria* pathogenesis and molecular virulence determinants.” *Clinical Microbiology Reviews* 14(3): 584–640.

Verhamme DT, Postma PW, Crielaard W and Hellingwerf C. 2002. “Cooperativity in signal transfer through the Uhp system of *Escherichia coli*.” *Journal Of Bacteriology* 184(15): 4205–4210.

Wammelink MMC, Struys EA and Jakobs C. 2008. “The biochemistry, metabolism and inherited defects of the pentose phosphate pathway: A review.” *Journal of Inherited Metabolic Disabilty*. 31:703-717.

Wang R, Braughton KR, Kretschmer D, Bach TL, Queck SY, Li M, Kennedy AD, Dorward DW, Klebanoff SJ, Peschel A, DeLeo FR, and Otto M. 2007. “Identification of novel cytolytic peptides as key virulence determinants for community-associated MRSA.” *Nature Medicine* 13(12): 1510–4.

Watkins RR, David MZ and Salata RA. 2012. “Current concepts on the virulence mechanisms of meticillin-resistant *Staphylococcus aureus*.” *Journal of Medical Microbiology* 61: 1179–93.

Wengender PA and Miller KJ. 1995. “Identification of a PutP proline permease gene homolog from *Staphylococcus aureus* by expression cloning of the high-affinity proline transport system in *Escherichia*.” *Applied and Environmental Microbiology* 61(1): 252–259.

Wesson CA, Liou LE, Todd KM, Bohach GA, Trumble WR, and Bayles KW. 1998. “*Staphylococcus aureus* Agr and Sar global regulators influence internalization and induction of apoptosis.” *Infection and Immunity* 66(11): 5238–43.

Wieland H, Ullrich S, Lang F and Neumeister B. 2005. “Intracellular multiplication of *Legionella pneumophila* depends on host cell amino acid transporter SLC1A5.” *Molecular Microbiology* 55(5): 1528–37.

Wilson GJ, Seo KS, Cartwright RA, Connelley T, Chuang-Smith ON, Merriman JA, Guinane CM, Park JY, Bohach GA, Schlievert PM, Morrison WI and Fitzgerald JR. 2011. “A novel core genome-encoded superantigen contributes to lethality of community-associated MRSA necrotizing pneumonia.” *PLoS pathogens* 7(10): e1002271.

Winkler HH. 1973. “Distribution of an inducible hexose-phosphate transport system among various bacteria.” *Journal of Bacteriology* 116(2): 1079–81.

Wright GD. 2005. “Bacterial resistance to antibiotics: enzymatic degradation and modification.” *Advanced Drug Delivery Reviews* 57: 1451–1470.

Yang J, Goldstein JL, Hammer RE, Moon YA, Brown MS, and Horton JD. 2001. “Decreased lipid synthesis in livers of mice with disrupted Site-1 protease gene.” *PNAS* 98(24): 13607–12.

Yang Z and Klionsky DJ. 2010. “Eaten alive: a history of macroautophagy.” *Nature Cell Biology* 12(9): 814–22.

Yasir M, Pachikara ND, Bao X, Pan Z and Fan H. 2011. “Regulation of chlamydial infection by host autophagy and vacuolar ATPase-bearing organelles.” *Infection and Immunity* 79(10): 4019–28.

Yimga MT, Leatham MP, Allen JH, Laux DC, Conway T and Cohen P. 2006. “Role of gluconeogenesis and the tricarboxylic acid cycle in the virulence of *Salmonella enterica* serovar Typhimurium in BALB/c mice.” *Infection and Immunity* 74(2): 1130–1140.

Yoshimori T. 2004. “Autophagy: a regulated bulk degradation process inside cells.” *Biochemical and Biophysical Research Communications* 313(2): 453–458.

Zhu Y, Weiss EC, Otto M, Fey PD, Smeltzer MS and Somerville GA. 2007. “*Staphylococcus aureus* biofilm metabolism and the influence of arginine on polysaccharide intercellular adhesin synthesis, biofilm formation, and pathogenesis.” *Infection and Immunity* 75(9): 4219–26.

Zhu Y, Xiong YQ, Sadykov MR, Fey PD, Lei MG, Lee CY, Bayer AS and Somerville GA. 2009. “Tricarboxylic acid cycle-dependent attenuation of *Staphylococcus aureus* in vivo virulence by selective inhibition of amino acid transport.” *Infection and Immunity* 77(10): 4256–64.

Appendix

Table A1. Bacterial strains used in this thesis.

Strain	Genotype / Characteristics	Reference/ source
Escherichia coli		
DH5α	Cloning host strain	Our laboratory
DH10β	Cloning host strain	Our laboratory
DH5α : pMAD-Cm	Carries shuttle vector for mutant construction	Wilson *et al.* 2011
DH10β :pTOPO UhpT REC	Carries the recombinant mutant *uhpT* allele (*S.aureus*)	This study
DH10β : pCR Blunt GlpT REC	Carries the recombinant mutant *glpT* allele (*S.aureus*)	This study
DH5α : pCR Blunt *uhpT* SA	Carries high fidelity *uhpT* gene (*S. aureus*)	This study
DH5α : pCR Blunt *glpT* SA	Carries high fidelity *glpT* gene (*S. aureus*)	This study
DH5α: pMAD-Cm UhpT	Carries shuttle vector construct for mutant *uhpT* allele	This study
DH5α: pMAD-Cm GlpT	Carries shuttle vector construct for mutant *glpT* allele	This study
DH10β: pMAD UhpT	Carries shuttle vector construct for mutant *uhpT* allele	This study
DH10β: pMAD GlpT	Carries shuttle vector construct for mutant *glpT* allele	This study
DH5α : pCR Blunt *hpt* LM	Carries high fidelity *hpt* gene (*L. monocytogenes* P14)	This study
DH5α: pPL2	Carries listerial integrative shuttle vector	Lauer *et al.* 2002
DH5α: pBC(*gfp*)P_{sod}	Carries fluorescence reporter plasmid	Köhler *et al*. 2000
DH5α: $pPL2_{(Psod)}$	Carries Listeria shuttle vector- *sod* promoter construct	This study

DH5α: pPL2$_{(Psod)}$ *hpt* LM	Carries pPL2-Psod complement construct for *hpt* gene (*L. monocytogenes* P14)	This study
DH5α: pPL2$_{(Psod)}$ *uhpT* SA	Carries pPL2-Psod complement construct for *uhpT* gene (*S. aureus*)	This study
DH5α: pPL2$_{(Psod)}$ *glpT* SA	Carries pPL2-Psod complement construct for *glpT* gene (*S. aureus*)	This study
DH5α : pCR Blunt PprfA	Carries *L. monocytogenes* PrfA promoter sequence for *hpt* gene	This study
DH10β: pPL2$_{(PpfrA)}$	Carries *Listeria* shuttle vector - PrfA promoter construct	This study
DH10β: pPL2$_{(PprfA)}$ *hpt* LM	Carries pPL2-PprfA complement construct for *hpt* gene *(L. monocytogenes* P14)	This study
DH10β: pPL2$_{(PprfA)}$ *uhpT* SA	Carries pPL2-PprfA complement construct for *uhpT* gene (*S. aureus*)	This study
DH10β: pPL2$_{(PprfA)}$ *glpT* SA	Carries pPL2-PprfA complement construct for *glpT* gene (*S. aureus*)	This study
Listeria monocytogenes		
P14	Wild type clinical isolate (Serovar 4b)	Our laboratory (Ripio *et al.* 1996)
P14-A	PrfA* mutant of P14. PrfA regulation is constitutively active	Our laboratory (Ripio *et al.* 1996, 1997)
P14-A *Δhpt*	In-frame deletion mutation of the *hpt* gene of P14-A	Our laboratory
Δhpt :pPL2$_{(Psod)}$ *hpt* LM AKA pPL2$_{(Psod)}$ *hpt*	P14-A *Δhpt* complemented with *L. monocytogenes* P14 *hpt* gene.	This study
Δhpt: pPL2$_{(Psod)}$ *uhpT* SA AKA. pPL2$_{(Psod)}$*uhpT*	P14-A *Δhpt* complemented with *S. aureus uhpT* gene.	This study

Δhpt: pPL2$_{(Psod)}$ glpT SA AKA. pPL2$_{(Psod)}$ *glpT*	P14-A *Δhpt* complemented with *S. aureus glpT* gene.	This study
Δhpt: pPL2$_{(PpfrA)}$ AKA. pPL2$_{(PpfrA)}$	P14-A *Δhpt* complemented with the empty vector (negative control)	This study
Δhpt: pPL2$_{(PprfA)}$ *hpt* LM AKA. pPL2$_{(PprfA)}$ *hpt*	P14-A *Δhpt* complemented with P14 *hpt* gene.	This study
Δhpt: pPL2$_{(PprfA)}$ *uhpT* SA AKA. pPL2$_{(PprfA)}$ *uhpT*	P14-A *Δhpt* complemented with *S. aureus uhpT* gene.	This study
Δhpt: pPL2$_{(PprfA)}$ *glpT* SA AKA. pPL2$_{(PprfA)}$ *glpT*	P14-A *Δhpt* complemented with *S. aureus glpT* gene.	This study
Staphylococcus aureus		
8325-4	Laboratory strain; a prophage cured derivative of a streptomycin resistant mutant of NCTC 8325	Novick 1967
USA300 LAC (WT)	Human clinical isolate. CA-MRSA. Pulsed field type USA300	Wilson *et al.* 2011
WT $^{(-pUSA03)}$	WT cured of the pUSA03 native plasmid	This study
ΔuhpT	In-frame deletion mutation of *uhpT* gene in USA300 LAC. Cured of pUSA03 native plasmid	This study
ΔglpT	In-frame deletion mutation of *glpT* gene in USA300 LAC. Cured of pUSA03 native plasmid	This study
ΔuhpTΔglpT	In-frame deletion mutation of *uhpT* & *glpT* genes in USA300 LAC. Cured of pUSA03 native plasmid	This study
Δagr::Tet	Insertion mutation spanning the entire *agr* locus of USA300 LAC	Benson *et al.* 2011
RN4220	Laboratory strain cloning intermediate. Restriction deficient derivative of RN450	Kreiswirth *et al.* 1983

RN4220: pMAD-Cm UhpT	Carries recombinant mutant *uhpT* allele (*S. aureus*)	This study
RN4220: pMAD-Cm GlpT	Carries recombinant mutant *glpT* allele (*S. aureus*)	This study
LAC: pMAD-Cm UhpT	Carries recombinant mutant *uhpT* allele (*S. aureus*)	This study
LAC: pMAD-Cm GlpT	Carries recombinant mutant *glpT* allele (*S. aureus*)	This study
LAC *ΔglpT:* pMAD-Cm UhpT	Mutant *glpT* strain carrying recombinant *uhpT* allele (*S. aureus*)	This study
LAC: pMAD-Cm UhpT (1^{st} REC)	USA300 LAC with UhpT construct integrated into chromosome	This study
LAC: pMAD-Cm GlpT (1^{st} REC)	USA300 LAC with GlpT construct integrated into chromosome	This study
LAC *ΔglpT:* pMAD-Cm UhpT (1^{st} REC)	Mutant *glpT* USA300 LAC strain with UhpT construct integrated into chromosome	This study

Table A2. Plasmids used in this thesis.

Plasmid	Description/ Use	Source /Reference
pMAD-Cm	Thermosensitive *E. coli -S. aureus* shuttle vector for generating *S. aureus* mutants. Ery^r Amp^r Cm^r *LacZ*	Memmi *et al.* 2008
pMAD-Cm UhpT	Contains recombinant mutant *uhpT* allele cloned in *BamHI -EcoRI* restriction sites	This study
pMAD-Cm GlpT	Contains recombinant mutant *glpT* allele cloned in *BamHI -EcoRI* restriction sites	This study
pPL2	Site specific integration vector for *L. monocytogenes.* Provides stable, single copy gene complementation. Cm^r	(Lauer *et al.* 2002)
$pPL2_{(Psod)}$	Allows constitutive gene expression via the listerial *sod* gene promoter cloned in *SalI – PstI* restriction sites	This study
$pPL2_{(Psod)}$ *hpt* LM	Contains *L. monocytogenes* P14 *hpt* gene cloned in *BamHI-SpeI* restriction sites	This study
$pPL2_{(Psod)}$ *uhpT* SA	Contains *S. aureus uhpT* gene cloned in *BamHI-SpeI* restriction sites	This study
$pPL2_{(Psod)}$ *glpT* SA	Contains *S. aureus glpT* gene cloned in *BamHI-SpeI* restriction sites	This study
$pPL2_{(PprfA)}$	Allows constitutive gene expression in *L. monocytogenes* via the *hpt* gene PrfA box promoter (*L. monocytogenes* P14) cloned in *KpnI – BamHI* restriction sites	This study
$pPL2_{(PprfA)}$ *hpt* LM	Contains *L.monocytogenes* P14 *hpt* gene cloned in *BamHI-SpeI* restriction sites	This study

pPL2$_{(PprfA)}$ *uhpT* SA	Contains *S. aureus uhpT* gene cloned in *BamHI-SpeI* restriction sites	This study
pPL2$_{(PprfA)}$ *glpT* SA	Contains *S. aureus glpT* gene cloned in *BamHI-SpeI* restriction sites	This study

Table A3. Oligonucleotides used in this thesis.

Primer	Sequence 5'-3'	Amplifies	DNA product Size (bp)	Use	Ref.
UhpT 1b_ EcoRI	GAATTCGTCACAATGGTCATAGA CACGAC	Upstream *uhpT* flanking sequence	900	*S. aureus* Mutagenesis	This study
UhpT 2	AACATCTGTCCATCCACGTTGTA CCGATAATGGAATGCC				
UhpT 3	TTATCGGTACAACGTGGATGGAC AGATGTTTTCATCGTC	Downstream *uhpT* flanking sequence	836		
UhpT 4b_ BamHI	GGATCCGCTTAGCATCTTGTCAT GATGCC				
UhpT C1	TGCATATGTCGCCAAGCC	Chromasomal region encompassing UhpT1b to UhpT4b.	WT 3216 Δ*uhpT* 1904	*S. aureus* Mutagenesis	This study
UhpT C2b	ACCAGTAAGACCATGCACAA				
GlpT 1b_EcoRI	GAATTCGGGCAAGGTCGTGGTG CTACAA	Upstream *glpT* flanking sequence	1036	*S. aureus* Mutagenesis	This study
GlpT 2	CGATGCCGGCATTGCGCAGCTG GCACAGCAGCTGGA				
GlpT 3	TGCTGTGCCAGCTGCGCAATGC CGGCATCGCTAACG	Downstream *glpT* flanking sequence	1119		
GlpT 4b_BamHI	GGATCCTAACCTCGTCCAGGTCT TTCACG				
GlpT C1b	AGGCCGTATGAAAGACGTTA	Chromasomal region encompassing GlpT1b to GlpT4b.	WT 3541 Δ*glpT* 2546	*S. aureus* Mutagenesis	This study
GlpT C2c	AGGCGCTTCAGTCGC				
LM hpt F1_BamHI	CGGGATCCAATGAAAATTACACT TGAAAGGAA	*L. monocytogenes* P14 *hpt* gene	1708	pPL2 complementation	This study
LM hpt R2_SpeI	GACTAGTTAGCGAACAAGGTCG GA				
SA UhpT F1_BamHI	CGGGATCCGCTTAACGAAAATG ATTGAGG	*S. aureus* USA300 *uhpT* gene	1756	pPL2 complementation	This study
SA UhpT R2_SpeI	GACTAGTACTAATGATTATGGCG CCTCCA				
SA GlpT F1_BamHI	CGGGATCCAAATGCATATAAATA CATATTAAGGAGGA	*S. aureus* USA300 *glpT* gene	1694	pPL2 complementation	This study
SA GlpT R2_SpeI	GACTAGTTGGTTGAACTTATAAGA GATGAATATATCA				
MR2 KpnI	CTAGGGTACCCAACTAACATATA TTATTCCT	*L. monocytogenes* P14 *prfA* gene	1113	Strain confirmation	Deshayes *et al.* 2012
MR10 SpeI	CTAG ACTAGT CTTGGTGAAGCAATCGTACGC				
PL95	ACATAATCAGTCCAAAGTAGATG C	*L. monocytogenes* chromosome - pPL2 plasmid integration site	499	Complemented strain confirmation	Lauer *et al.* 2002
NC16	GTCAAAACATACGCTCTTATC				

Psod 1F (SalI) Psod 5R (PStI)	ACGC GTCGAC AGCTCTTCCAGAAGCGTTTA CG CTGCAGTTTTACGTGAAAAGAAAT	*Sod* promoter	309	Complement plasmid construction	This study
PprfA _ KpnI F PprfA_Bam HI R	GGGGTACCCCCCAAGATAATTC CTGCTT CGGGATCCTATTTCCCCTTTTGC GCTG	*L.monocytogenes* P14 *hpt* gene PrfA promoter site	202	Complement plasmid construction	This study
T3	ATTAACCCTCACTAAAGGGA	Upstream of pPL2 MCS towards pPL2 1R	-	Forward sequencing of pPL2 constructs	Monk *et al.* 2008
pPL2 1R	CTGCGATGAGTGGCAGGGCGG	Downstream of pPL2 MCS towards T3	-	Reverse seqencing of pPL2 constructs	This lab
M13 Forward	GTAAAACGACGGCCAG	Upstream of pTOPO/pCRBLUNT MCS	-	Forward sequencing of pTOPO/pCRBlunt constructs	Invitrogen
M13 Reverse	CAGGAAACAGCTATGAC	Downstream of pTOPO/pCRBlunt MCS	-	Reverse sequencing of pTOPO/pCRBlunt constructs	Invitrogen

*All primers amplify with an annealing temperature within the range 55-60^{o}C.

**All primers designed in this study were purchased from Sigma.

Table A4. Composition of BHI medium.

BHI	
Composition	**Concentration (g/L)**
Beef heart	5 (infusion from 250g)
Calf brains	12.5 (infusion from 200g)
Disodium hydrogen phosphate	2.5
D(+) Glucose	2
Peptone	10
Sodium chloride	5

Table A5. Composition of LB medium.

LB	
Composition	**Concentration (g/L)**
Tryptone	10
Yeast extract	5
Sodium chloride	10

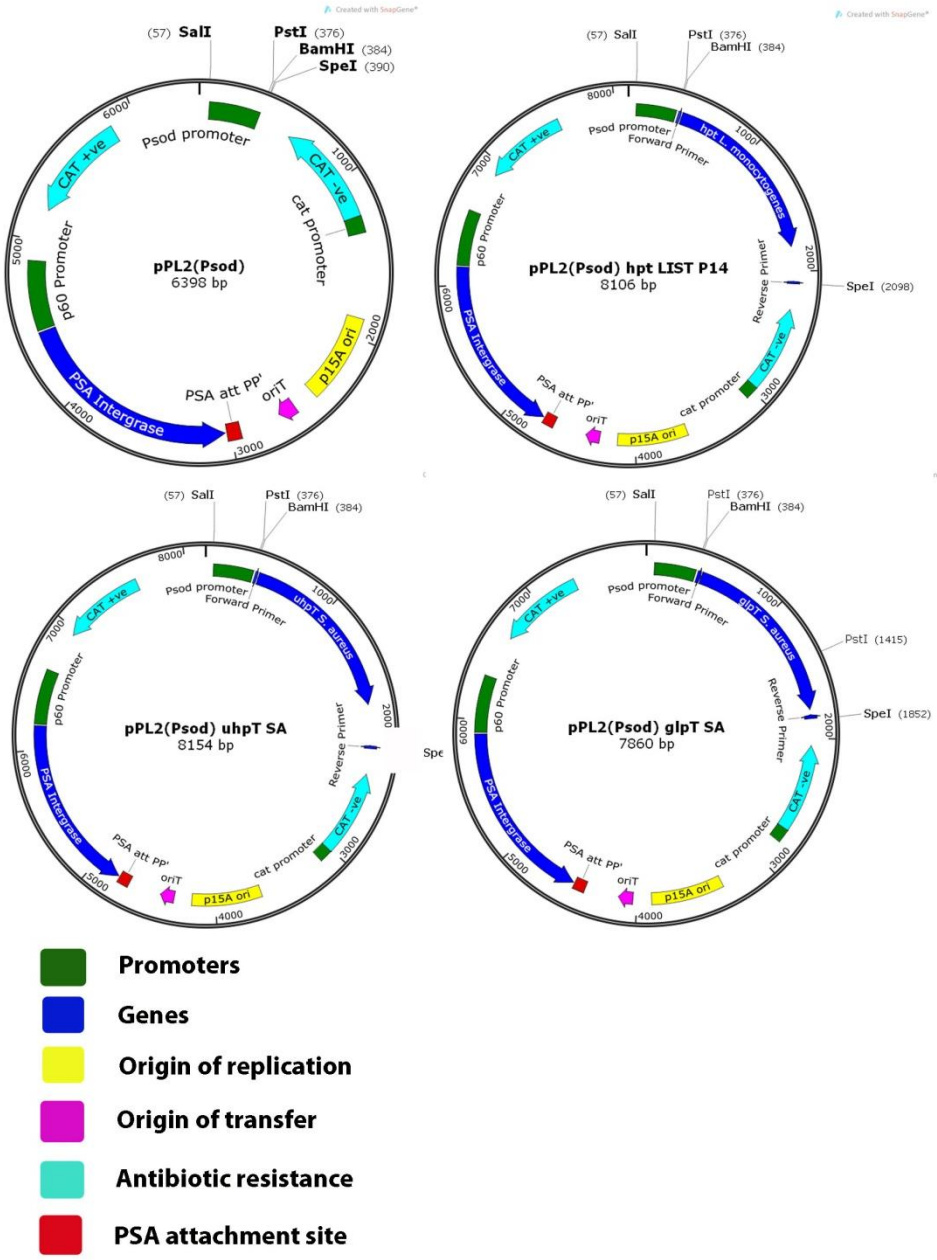

Figure A1. pPL2$_{(Psod)}$ plasmid constructs. Plasmid constructs show relevant components used for integrative complementation of *Listeria*. Restriction sites used for cloning sugar phosphate permease genes and *sod* promoter are noted.

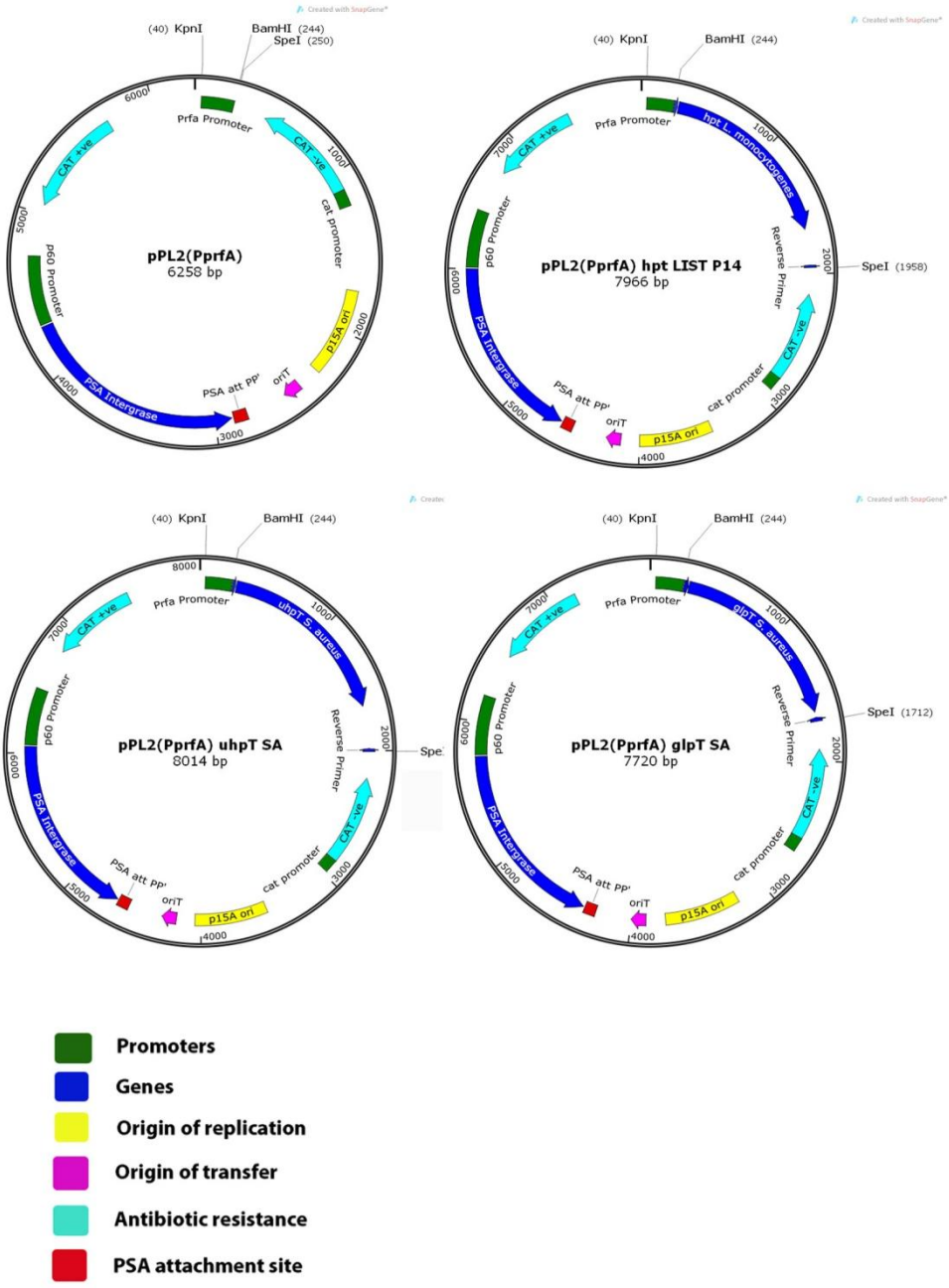

Figure A2. pPL2$_{(PprfA)}$ plasmid constructs. Plasmid constructs show relevant components used for integrative complementation of *Listeria*. Restriction sites used for cloning sugar phosphate permease genes and *hpt* PrfA promoter are noted.

***sod* Promoter**

5′ AGCTCTTCCAGAAGCGTTTAAAAATATTCATTCTTTTTTCAACACCTCGCCTAATG
GTTTAACTTTTGAGTTTCAGGGAAAAAGATACATGTATGTGCAAAAGAGCGTACT
TTTCCACCTAAACTTAATCATAGCTTGAAATGGTCGCAAAATCAATGTTGAAACA
TCAATGAGCAGAAAAATTGCAAGCATTTCGGGAGCATGGTAGGCTAAATGGTGT
AAGAAGAAACTGTTTTTAAGGTTGATAGTAGTTCTATTGAAATAGGACATGAAA
CTTTTGCCTTATACGTCATTTCTTTTCACGTAAAA

3′

Listerial *hpt* PrfA promoter sequence

5′
CCCCAAGATAATTCCTGCTTTTTTGTTTTCTGCATGATAACAAGTGTTAATGACGG
AAATAGAATTTCTGTTTTATATTTTTAGCAGCGCAAAAGGGGAAATAAAGCATTT
GGACAGCAGAGGTGATTGCTTTAGAAAAATTGATAGACTTTATATGGAAACGTT
TGCGTAATAATGCTCATCGCATTCTAAATTTGGAATG

3′

Figure A3. Promoter DNA sequences used to ensure expression of sugar phosphate permeases in *Listeria monocytogenes*

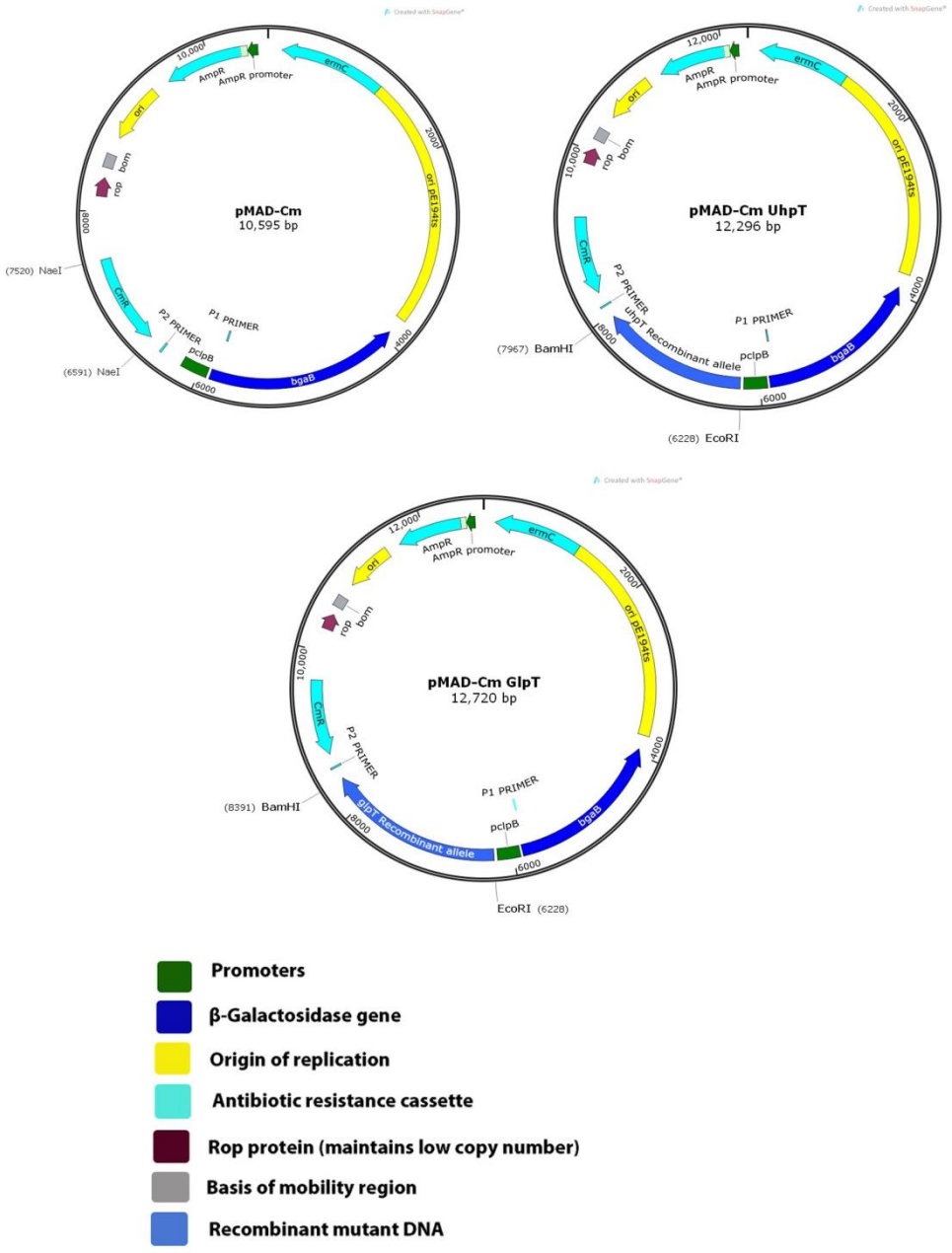

Figure A4 . pMAD-Cm plasmid constructs. Plasmid constructs show relevant components used for allelic replacement of metabolism genes in *S. aureus*. Restriction sites used for cloning recombinant mutant alleles are noted.